TABLE DES MATIÈRES

LISTE DES FIGURES

LISTE DES TABLEAUX

LISTE DES ABRÉVIATIONS, DES SIGLES ET DES ACRONYMES

^{14}C	Radiocarbone
AICc	Critère d'information d'Akaike de second ordre
Al	Aluminium
ANOVA	Analyse de variance
BC	Carbon pyrogénique
C	Carbone
C_{AI}	Carbone insoluble à l'acide
C_{BioR}	Carbone bioréactif
C_{fast}	Réservoir de carbone bioréactif
CO_2	Dioxyde de carbone
COS	Carbone organique du sol
CQT	Hypothèse de dépendance entre la qualité du carbone et la température pour la décomposition
C_{slow}	Réservoir de carbone insoluble à l'acide
C_{tot}	Réservoir total de carbone
DAG	Graphe acyclique directionnel
Fe	Fer
FH	Horizon organique fragmenté et humifié
GDD5	Degré-jours de croissance supérieurs à 5°C
IMD	Indice de dominance des mousses
MAP	Précipitations annuelles moyennes
MAT	Température annuelle moyenne
MIN	Horizon minéral du sol

MIN015	Horizon minéral du sol de 0 à 15 centimètres de profondeur
MIN1535	Horizon minéral du sol de 15 à 35 centimètres de profondeur
Mn	Manganèse
MOS	Matière organique du sol
Mpy	Métaux extractibles au pyrophosphate de sodium
n	Nombre
pc	Coefficient de chemin standardisé
pc_{avg}	Coefficient de chemin moyen
pc_i	Coefficient de chemin indirect
pH	Potentiel d'hydrogène
SOC	Carbon organique du sol
TDF	Temps écoulé depuis le dernier feu
TSF	Temps écoulé depuis le dernier feu
WB	Equilibre hydrique
WHC	Capacité de rétention en eau

LISTE DES SYMBOLES ET UNITÉS

%	Pourcent
Δ	Variation
°C	Degré Celsius
°N	Degré de latitude Nord
°W	Degré de longitude Ouest
cm	Centimètre
cm^2	Centimètre carré
g	Gramme
$g.kg^{-1}$	Gramme par kilogramme
Gt	Milliard de tonnes
GtC	Milliard de tonnes de carbone
h	Heure
ha	Hectare
k yrs	Millier d'années
M	Concentration molaire
m	Mètre
m^2	Mètre carré
mg $CO2\text{-}C.d^{-1}$ jour	Milligramme de dioxyde de carbone équivalent carbone par
mg $CO2\text{-}C.g^{-1}C_{org}$	Milligramme de dioxyde de carbone équivalent carbone par gramme de carbone organique initial
$MgC.ha^{-1}$	Mégagramme ou tonne de carbone par hectare
$MgC.ha^{-1}.yr^{-1}$	Mégagramme ou tonne de carbone par hectare et par année
mL	Millilitre

$ml.min^{-1}$	Millilitre par minute
mm	Millimètre
Pg	Pétagramme ou milliard de tonnes
ø	Diamètre
Tg	Téragramme ou milliard de kilogrammes
year cal. BP	Années étalonnées avant 1950 *anno domini*
yr	Année

RÉSUMÉ

Les forêts boréales renferment d'importantes quantités de carbone organique, principalement dans leurs sols. Elles constituent ainsi une composante critique du cycle du carbone terrestre et jouent, par là-même, un rôle de premier plan dans la régulation du climat planétaire. Accroître les stocks de carbone dans les écosystèmes terrestres, et particulièrement dans les sols des forêts boréales, est une des stratégies proposées pour atténuer le réchauffement climatique à moindre coût. L'amplitude et la direction du développement des réservoirs de carbone du sol qui surviendra en lien avec des modifications environnementales, induits par le réchauffement climatique, sont néanmoins incertaines. Les sols pourraient accumuler davantage de carbone avec l'accroissement de la productivité de l'écosystème, ce qui améliorerait la chimie de l'atmosphère et atténuerait le réchauffement climatique. A l'inverse, si la décomposition du carbone par les microorganismes du sol est stimulée avec l'augmentation des températures, les sols pourraient accélérer le réchauffement climatique en retournant du carbone vers l'atmosphère. Comprendre les variabilités spatiale et temporelle des stocks de carbone dans les sols, ainsi que les processus qui régissent sa séquestration à long terme apparaissent ainsi être des clés essentielles pour adapter des pratiques d'aménagement du territoire raisonnées pour participer aux efforts d'atténuation du réchauffement climatique.

L'objectif général de nos travaux était ainsi d'approfondir notre compréhension des processus de stockage du carbone dans les sols forestiers, avec l'étude de cas des sols à drainage modéré de la pessière à mousses au Québec. En se basant sur l'échantillonnage des sols dans 72 sites d'étude, répartis le long d'une chronoséquence après feu (de 2 à 314 ans) et dans un vaste territoire caractérisé par une variabilité climatique, nos travaux visaient à déterminer les principaux facteurs de contrôle et les mécanismes rattachés aux processus de stockage du carbone dans les sols. Pour chacun des sites étudiés, nous avons analysé la quantité et la qualité des réservoirs de carbone du sol. La quantité de carbone du sol à l'échelle du peuplement a été calculée à partir des données récoltées au terrain et de la concentration des échantillons en carbone déterminée en laboratoire. La qualité du carbone a été déterminée avec une méthode d'incubation des sols en atmosphère contrôlée pour évaluer la réactivité biologique du carbone, et avec l'hydrolyse acide des échantillons pour évaluer la récalcitrance du carbone. Nous avons aussi déterminé certaines propriétés physico-chimiques des sols par des analyses standardisées.

D'abord, nos résultats ont montré que seules les variables climatiques liées à la disponibilité en eau, et non pas aux températures, n'exerçaient qu'un contrôle indirect sur l'accumulation du carbone dans le sol. L'effet indirect du climat s'exprimait au travers de l'influence directe des variables liées à la disponibilité en eau sur la strate des mousses, qui elle-même avait une influence directe sur l'accumulation ou indirecte sur la réactivité biologique du carbone dans le sol. Le climat influençait aussi la complexation organométallique. Le temps écoulé depuis le dernier feu était le principal déterminant de l'accumulation de carbone dans l'horizon organique développé en surface du sol. Le temps depuis le dernier feu déterminait aussi le stock de carbone dans le sol minéral et la réactivité biologique du carbone dans l'horizon organique au travers de son influence sur le pH du sol. En limitant l'activité microbienne, le pH du sol a été identifié comme étant un facteur majeur de contrôle direct du stock de carbone dans le sol minéral, de la réactivité biologique du carbone dans l'horizon organique et dans le sol minéral. Le pH du sol modulait aussi les processus de complexation organométallique et influençait la quantité d'aluminium échangeable. Or la complexation organométallique influençait directement le stock et la réactivité biologique du carbone et l'aluminium échangeable influençait directement la réactivité biologique du carbone dans le sol minéral.

Les résultats de la thèse remettent en question le postulat de base utilisé dans les exercices de modélisation pour projeter l'évolution du climat futur, fondé sur la dépendance de la décomposition microbienne aux températures. Dans leur ensemble, nos travaux montrent que la dynamique du carbone organique du sol est contrôlée par des interactions complexes entre plusieurs facteurs bio-physicochimiques et que les conditions physico-chimiques du sol, tel que l'acidité, propres aux forêts anciennes sont favorables à l'accumulation du carbone dans le sol. Sur la base de nos résultats et pour séquestrer davantage de carbone en forêt boréale, nous préconisons de maintenir des attributs de forêts anciennes au sein du territoire, tout en conservant les mécanismes responsables de la séquestration de carbone dans les sols. Pour ce faire, il faudrait créer davantage d'aires naturelles protégées, augmenter la durée des rotations et adopter les coupes partielles dans les pratiques d'aménagement sylvicoles.

Mots-clés : réchauffement climatique, changement global, aménagement forestier durable, forêt boréale, feux, dynamique du carbone, stock de carbone, carbone du sol, séquestration du carbone, bioréactivité du carbone, épinette noire.

INTRODUCTION GÉNÉRALE

0.1 Prolégomènes

Le cycle du carbone (C) comprend tous les processus d'échanges biogéochimiques de C entre les différents compartiments fonctionnels du système terrestre (i.e. atmosphère, hydrosphère, géosphère, pédosphère et biosphère). Fondamentalement partie intégrante de la biosphère et donc du cycle du C, le genre *Homo* et notre dernière espèce *sapiens* peuplant actuellement le globe terrestre pourrait avoir influencé significativement le cycle naturel du C planétaire depuis plusieurs milliers d'années (Ruddiman, 2007; Ruddiman *et al.*, 2011; Sanderman *et al.*, 2017). L'altération du cycle du C attribuée à l'humanité préindustrielle est sans commune mesure comparée à l'amplitude des changements survenus depuis l'essor de la machine à vapeur au XVIII^{e} siècle (Ciais *et al.*, 2013). L'humanité est désormais considérée comme une force géologique majeure à l'échelle planétaire (Crutzen, 2002; Zalasiewicz *et al.*, 2011).

Les émissions massives de gaz à effet de serre dans l'atmosphère, tels que le méthane (CH_4) et le dioxyde de C (CO_2) liées aux activités humaines, sont indubitablement responsables du réchauffement climatique (Cook *et al.*, 2016; Harlos *et al.*, 2016). Les émissions de CO_2 anthropogéniques s'élevaient à 10.7 GtC.an^{-1} (engendrées à 88% par la combustion d'énergies fossiles et l'industrie, et à 12% par des changements dans l'utilisation des terres) durant la dernière décennie, engendrant un accroissement annuel de 4.7 GtC sous forme de CO_2 dans l'atmosphère (Le Quéré *et al.*, 2018). Une

partie du CO_2 émis vers l'atmosphère est ainsi capté par les grands puits de C planétaires, à savoir les océans qui emmagasinent le C par dissolution dans l'eau et les écosystèmes terrestres qui stockent le C dans la biomasse vivante et morte par le biais de la photosynthèse (Frontier *et al.*, 2008; Schimel *et al.*, 2001).

Le genre humain vit ainsi sous sa dette de C, telle une « épée de Damoclès » qui menace les équilibres dynamiques planétaires et par-là même la sécurité de sa population et la pérennité de ses activités (Steffen *et al.*, 2018). Reconnaître dorénavant l'ensemble du globe terrestre comme unique œkoumène – espace de vie des Hommes – dans sa dimension holistique implique un nouveau paradigme dans lequel l'humanité doit, pour se perpétuer dans le temps, s'investir de l'intendance de la planète (Ellis et Haff, 2009; Steffen *et al.*, 2018). La convention-cadre des Nations Unies sur les changements climatiques adoptée en 1992 est un des moteurs d'envergure internationale annonçant la volonté de comprendre et de lutter contre le réchauffement climatique. Les accords du protocole de Kyoto, ratifiés en 1997 par les Parties, constituent un accord non contraignant et un engagement des pays membres dans la mise en œuvre de stratégies nationales visant à limiter et diminuer les émissions de gaz à effet de serre (Nations Unies., 1998). La protection et l'accroissement des puits naturels de C sont préconisés par le Protocole de Kyoto. La séquestration du C dans les écosystèmes forestiers - et notamment dans les sols de la forêt boréale - est dès lors considérée être une avenue prometteuse pour compenser les émissions de CO_2 d'origine humaine (Lal, 2005).

La forêt boréale forme une ceinture circumpolaire aux hautes latitudes de l'hémisphère Nord, et englobe le tiers des surfaces forestières (920 Mha) de la planète (Kuusela, 1992). L'étendue des surfaces occupées par la forêt boréale combinée à la densité élevée des sols en C (Batjes, 2016) lui confèrent, avec 174 GtC emmagasiné dans les sols (Pan *et al.*, 2011), le statut du plus important réservoir de C organique du sol (COS) parmi les forêts de tous les biomes terrestres. Malgré les nombreuses études ayant porté

sur le sujet, les incertitudes persistent quant au comportement du COS des écosystèmes boréaux en réponse aux changements climatiques (Conant *et al.*, 2011; Kirschbaum, 2006). Même des changements infimes dans la quantité de COS pourrait avoir des répercussions importantes sur la chimie atmosphérique, aboutissant soit à l'accélération des changements climatiques - si les sols émettent du C dans l'atmosphère, soit à l'atténuation des changements climatiques - si la séquestration du COS est augmentée (Davidson et Janssens, 2006). Comprendre les variabilités spatiale et temporelle des stocks de COS, ainsi que les processus qui engendrent la séquestration du COS à long terme apparaissent ainsi être des clés essentielles dans l'adaptation de pratiques d'aménagement du territoire pour participer aux efforts d'atténuation du réchauffement climatique (Jandl *et al.*, 2007; Scharlemann *et al.*, 2014).

0.2 Équilibre et facteurs de contrôle du carbone dans les sols

Milieu situé à l'interface entre l'atmosphère, l'hydrosphère, la géosphère et la biosphère, le sol (pédosphère) constitue foncièrement un système dynamique caractérisé par d'importants flux d'énergies et de matières. L'équilibre du réservoir de COS reflète grossièrement la différence entre les flux entrants (apports de C) et sortants (pertes de C) du système sol (Chapin *et al.* (2006) ; Figure 0.1). La productivité de l'écosystème détermine les apports en C issus de la transformation du CO_2 par les voies biologiques de la photosynthèse, alors que le COS peut être perdu par lessivage du C dissout en solution, la suppression de biomasse ou encore le retour vers l'atmosphère au travers de la respiration microbienne (Clarke *et al.*, 2015; Jandl *et al.*, 2007; von Lützow et Kögel-Knabner, 2009).

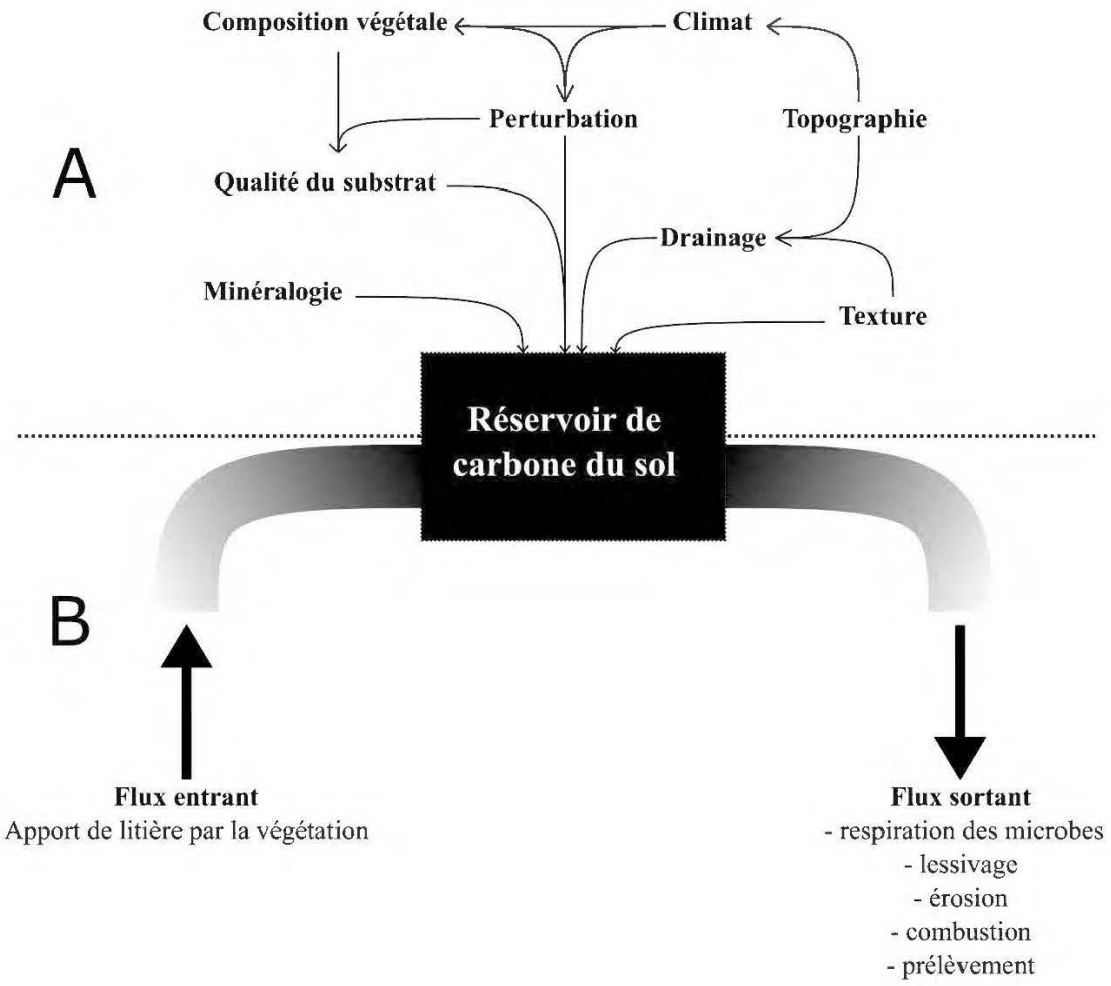

Figure 0.1 Schéma synthétique résumant les interactions entre les facteurs exerçant une influence sur le réservoir de carbone du sol (A) et contrôle des flux de carbone (B).

Longtemps considéré comme étant issu du processus de décomposition de la matière organique morte déposée au sol par la végétation, l'approvisionnement du sol en C provient surtout d'apports souterrains par les racines (exsudats racinaires et renouvellement des racines fines) et les champignons symbiotiques qui leurs sont associés (Clemmensen *et al.*, 2013; Rasse *et al.*, 2005; Rumpel et Kögel-Knabner, 2011). En plus des apports racinaires, les mousses et lichens qui peuplent le sous-bois

contribuent significativement à enrichir en C l'horizon organique développé en surface du sol (Preston *et al.*, 2006).

Additionnée aux pertes nettes de C engendrées par les perturbations de grande envergure (incendies, épidémies d'insectes ou encore coupes), l'élimination de la végétation vivante ampute le sol d'un de ses apports majeurs en C. Dépendamment du type de perturbation, les émissions de C associées à la décomposition de la matière organique morte résiduelle sont compensées par l'activité photosynthétique de la végétation en régénération dans un horizon de 5 à 30 ans, délai à partir duquel un peuplement source redevient un puit de C atmosphérique (Kurz *et al.*, 2013). Liées aux traits fonctionnels des végétaux, des différences de quantité et de distribution du COS dans la colonne de sol existent entre certaines espèces (De Deyn *et al.*, 2008; Laganière *et al.*, 2017; Laganière *et al.*, 2013), mais restent à démontrer à l'échelle des types fonctionnels (i.e. groupes d'espèces qui partagent des fonctions similaires ; Augusto *et al.* (2015)).

A l'échelle globale, les espèces végétales sont géographiquement restreintes à une enveloppe climatique par leurs optimums écologiques, obscurcissant la contribution relative du climat et de la végétation sur le contrôle du stockage de COS (Jobbagy et Jackson, 2000). En modulant l'activité des organismes décomposeurs, la température et la disponibilité en eau influencent néanmoins l'un des plus importants flux de C sortant du système sol (Allison et Treseder, 2008; Prescott, 2010; Zhang *et al.*, 2008). La saturation en eau dans les sols est impropice à l'activité des organismes décomposeurs alors limités par la disponibilité en oxygène. Associés au processus d'entourbement (Fenton *et al.*, 2005), les sols hydromorphes présentent des densités en C par unité de surface parfois décuplées comparés aux sols mieux drainés (Tremblay *et al.*, 2002; Yu, 2012). La température module la vitesse de réaction entre les enzymes sécrétées par les microbes dans leur environnement immédiat et la matière organique

environnante (Frey *et al.*, 2013). La distribution annuelle du CO_2 émis par les microbes hétérotrophes du sol se superpose ainsi avec l'évolution saisonnière des températures (Laganière *et al.*, 2012).

Le type de substrat est aussi un facteur de contrôle du stockage de COS. Par leur nature chimique, certains matériaux organiques – dits récalcitrants ou de faible qualité – requièrent davantage d'étapes enzymatiques et donc d'énergie pour être décomposés (Bosatta et Ågren, 1999; Craine *et al.*, 2010). Le statut d'altération de la phase minérale du sol détermine aussi le temps de recyclage du COS (Torn *et al.*, 1997). De plus, la distribution en taille des particules minérales régule la capacité de stockage en COS, avec les sols à texture fine présentant un seuil de saturation en COS plus élevé comparés aux sols à texture grossière (Castellano *et al.*, 2015; Six *et al.*, 2002).

Les interactions complexes entre les nombreux facteurs impliqués dans le contrôle du stockage de COS (Prescott, 2010) induisent une grande variabilité spatiale et temporelle dans les stocks de COS à l'échelle du paysage. Sachant que ces facteurs varient à différentes échelles spatiales et temporelles, il est important de considérer l'équilibre du COS comme une composante dynamique de l'écosystème. Comprendre comment les sols pourraient emmagasiner davantage de C implique une connaissance suffisante des mécanismes responsables de la stabilisation du COS à long terme (Dungait *et al.*, 2012; Schmidt *et al.*, 2011).

0.3 Protection et stabilisation du carbone dans les sols

Mis en place à la suite au retrait glaciaire il y a moins de 10000 ans, les sols de la forêt boréale sont relativement jeunes. Leur profil d'altération minérale est peu évolué (Minasny *et al.*, 2008) et le stock de C des sols minéraux considéré en équilibre (Deluca

et Boisvenue, 2012; Harden *et al.*, 1992; Seedre *et al.*, 2011). Combiné à des conditions fraîches et humides, auxquelles s'ajoute l'effet acidifiant de la végétation, le substrat acide favorise la formation de sols acides, souvent caractérisés par des processus de podzolisation (Sanborn *et al.*, 2011). Les podzols accumulent en surface une épaisse couche de matière organique dont le recyclage, surtout dominé par l'activité des champignons, est lent et contient peu de nutriments disponibles (Prescott *et al.*, 2000). Il s'agit d'un humus de type mor (Weetman, 1980). Dans l'horizon d'éluviation (horizon Ae) au sommet du sol minéral, les minéraux sont altérés sous l'action des acides organiques contenus dans l'humus. Lessivés avec l'infiltration des eaux gravitaires, les particules fines, la matière organique et les produits d'altération comme les oxydes de fer et d'aluminium s'accumulent plus en profondeur dans l'horizon B d'illuviation (Buurman et Jongmans, 2005).

Essentiellement liés à des raisons pratiques pour expliquer le budget C des sols, trois réservoirs fonctionnels ont historiquement été utilisés pour définir le taux de recyclage – ou persistance dans le temps - du COS (Amundson, 2001) : les réservoirs labile (ou actif), intermédiaire (ou lent) et réfractaire (ou passif, stable). Simpliste et abondamment utilisée, cette classification présuppose une préservation sélective des composés les plus difficilement biodégradables au détriment des composés naturellement décomposables (Cotrufo *et al.*, 2013). Cependant, elle peine à refléter la diversité des processus à l'œuvre dans la protection et la stabilisation du COS, ainsi que l'hétérogénéité des réservoirs structuraux du sol (von Lützow *et al.*, 2007). La stabilisation biochimique due à la composition intrinsèque des composés considérés comme récalcitrants, n'explique pas à elle seule la persistance du COS (Cotrufo *et al.*, 2013; Marschner *et al.*, 2008; Prescott, 2010). Dans la nature, la matière organique est par essence décomposable. Appliquée à la matière organique, le concept de récalcitrance est « une catégorie de commodité sémantique et non pas une classification utile de la propriété des matériaux » (traduit de Kleber (2010)). Regroupant deux

mécanismes primordiaux, un paradigme émergent postule que la stabilisation à long terme de la matière organique du sol (MOS) s'effectue d'abord par un contrôle microbien des flux de C et d'azote entre la litière et la MOS, puis ultimement par les interactions entre la MOS et la phase minérale des sols (Cotrufo *et al.*, 2013).

Les sols en forêt boréale sont nativement dépourvus d'organismes anéciques (e.g. lombriques) ou autres animaux fouisseurs impliqués dans le mélange de la MOS de surface et en profondeur. L'incorporation de COS dans les horizons minéraux s'effectue par la percolation de C dissout dans l'eau dont les flux suivent des voies préférentielles le long des racines (Rumpel et Kögel-Knabner, 2011). C'est pourquoi la stabilisation physico-chimique du COS par interactions avec la phase minérale intervient surtout en profondeur (Rasse *et al.*, 2005).

L'adsorption est un mécanisme par lequel les charges électroniques négatives de la MOS se lient aux charges négatives des particules d'argiles et de limons, *via* des ponts cationiques polyvalents chargés positivement tels que les ions fer, aluminium, manganèse ou encore calcium (Cotrufo *et al.*, 2013; Paul, 2016). Globalement, le temps de résidence du COS associé à la fraction fine des limons et des argiles est plus long que celui du COS associé aux particules de sable (von Lützow *et al.*, 2007) et similaire à la fraction de COS non-hydrolysable (Paul, 2016). En forêt boréale, la stabilisation du COS par adsorption sur les particules fines pourrait néanmoins être limitée par rapport à d'autres mécanismes, comme les associations organométalliques (Ziegler *et al.*, 2017).

Comparé aux sols neutres et alcalins, les propriétés acides (pH bas) des podzols favorisent les mécanismes de complexation organométallique (Rasmussen *et al.*, 2018). La quantité de COS augmente avec la quantité d'oxydes métalliques, mais la stabilité des complexes organométalliques pourrait dépendre des conditions d'acidité

puisque des conditions très acides rendent solubles les composés métalliques (Porras *et al.*, 2017). Toutefois, l'indice du degré de chélation entre le COS et les oxydes métalliques, appliqué aux sols de la forêt boréale, indique que la complexation organométallique est très probable et efficiente (Laganière *et al.*, 2015; Ziegler *et al.*, 2017). La rétention préférentielle des matériaux récalcitrants sur la phase minérale a été proposée pour expliquer le stockage du COS à long terme (Kramer *et al.*, 2012).

Outre les interactions entre COS et la phase minérale du sol qui le préserve d'une décomposition microbienne rapide, son accessibilité spatiale est un autre mécanisme de protection. Selon le modèle mathématique du mouvement de marche aléatoire (*random walk movement*), le recyclage du COS dépend de la probabilité de rencontre entre les enzymes d'un microbe décomposeur et une particule de substrat et donc le temps de résidence du COS devrait dépendre de sa concentration (Don *et al.*, 2013). C'est sans doute le cas dans les sols peu structurés, i.e., dont les particules minérales sont faiblement associées à l'humus et aux éléments échangeables. Les végétaux et certains de leurs microbes associés sécrètent un mucilage aux propriétés colloïdales qui favorisent la cohésion entre les phases minérales et organiques du sol, formant ainsi différents types d'agrégats structurant le sol par ces complexes dits argilo-humiques (Gobat *et al.*, 2010). Les agrégats contiennent généralement davantage de C par rapport à la matrice qui les contient, puisque le COS intra-agrégat est protégé physiquement de la décomposition par les microbes. Ces environnements sont également pauvres en oxygène et donc défavorables aux réactions enzymatiques oxydantes (Rasse *et al.*, 2005; Six *et al.*, 2002).

En plus de comprendre leurs diversité, évaluer la part relative de chacun des mécanismes qui favorisent la protection et la stabilisation du COS offrirait des opportunités majeures pour optimiser la séquestration du COS dans les territoires aménagés (Dungait *et al.*, 2012).

0.4 L'aménagement des forêts boréales et la séquestration du carbone dans les sols

La forêt boréale abrite essentiellement des forêts naturelles secondaires post-perturbation. A l'échelle mondiale, l'aménagement des forêts natives présente l'un des plus grands potentiels pour atténuer le réchauffement climatique à moindre coût (Griscom *et al.*, 2017). La capacité théorique d'accroissement des stocks de C des forêts natives est évaluée entre 921 à 8224 Tg équivalent CO_2 (soit 0.9 à 8.2 Gt) à l'horizon 2030 (Griscom *et al.*, 2017). Selon ces chiffres qui n'incluent pas les stocks de COS, près de 128 Tg équivalent CO_2 et 245 Tg équivalent CO_2 pourraient être séquestrés dans les forêts au Canada et en Russie, respectivement, en adaptant des pratiques sylvicoles adéquates.

Du fait de la diversité et des spécificités des pratiques et des spécificités variables des sites aménagés, l'impact des opérations sylvicoles sur les stocks de COS est difficilement généralisable (Clarke *et al.*, 2015; Johnson et Curtis, 2001). Les travaux les plus récents tendent néanmoins à montrer une diminution des stocks de COS après intervention sylvicole (James et Harrison, 2016), davantage prononcée dans les podzols. Le temps de rétablissement du réservoir de COS après perturbation est néanmoins tributaire de la sévérité de la perturbation appliquée (Fu *et al.*, 2017a). En minimisant l'impact écologique des récoltes et en réduisant leurs impacts sur les sols, les opérations de coupe permettraient d'éviter les pertes de COS, entre autres avantages (Marchi *et al.*, 2018). Les pertes de COS peuvent aussi être rapidement compensées par une gestion de la régénération après récolte, avec par exemple des opérations de reboisement (Ryan *et al.*, 2010).

Favoriser certaines essences dans les systèmes sylvicoles pourrait aussi améliorer la séquestration du COS. Augmenter la proportion d'espèces feuillues au détriment

d'espèces conifériennes au feuillage plus inflammable est une stratégie proposée pour réduire le risque d'incendies (Girardin et Terrier, 2015). Cette stratégie présente également l'avantage d'atténuer indirectement le réchauffement climatique par une modification de l'albédo de surface (Astrup *et al.*, 2018). Bien que l'influence de la composition végétale sur les mécanismes menant à un partitionnement des stocks de COS entre l'horizon organique et le sol minéral restent à explorer, le contrôle des essences forestières pourrait aussi permettre de moduler le réservoir de C dans la colonne de sol (Vesterdal *et al.*, 2013). Par exemple, alors que les forêts de peupliers faux-trembles (*Populus tremuloides* [Michx.]) emmagasinent moins de COS que les forêts de conifères, la grande partie du réservoir de COS y est distribué dans le sol minéral, ce qui lui confère une plus grande stabilité (Laganière *et al.*, 2011; Laganière *et al.*, 2017). En plus de ces facteurs biotiques liés à la végétation, les facteurs abiotiques pourraient avoir une importance majeure dans la séquestration du COS, mais nécessitent encore un examen approfondi pour comprendre l'influence de la composition végétale sur le stockage du COS à grande échelle (Laganière *et al.*, 2017; Vesterdal *et al.*, 2013).

0.5 Problématique générale

Les perturbations naturelles de grande envergure sont caractéristiques de la dynamique des écosystèmes en forêt boréale (Gauthier *et al.*, 2015; Rogers *et al.*, 2015) et ont une influence majeure sur l'équilibre du C (Bond-Lamberty *et al.*, 2007; Kurz *et al.*, 2008). Les incendies de grandes superficies (> 200 ha) sont, par exemple, responsables de 98 % des surfaces forestières annuellement brûlées au Canada (Stocks *et al.*, 2002; Weber et Stocks, 1998). Basé sur le régime des perturbations naturelles, l'aménagement écosystémique est le paradigme selon lequel le maintien des caractéristiques de la forêt dans ses limites de variabilités naturelles permet de répondre à certains critères de

l'aménagement forestier durable (Attiwill, 1994; Bergeron *et al.*, 2007; Cyr *et al.*, 2009). Transcrit le 1er avril 2013 dans la *Loi sur l'aménagement durable du territoire forestier* encadrant la gestion des forêts au Québec, l'aménagement écosystémique est l'approche préconisée pour aménager durablement la forêt. La gestion et l'exploitation durable des forêts doit ainsi être raisonnée à partir de connaissances suffisantes des patrons naturels de perturbations et des dynamiques forestières (Burton *et al.*, 2006).

Alors que les écosystèmes boréaux possèdent la plus grande partie de leur réservoir de C dans les sols, la comptabilisation du C forestier au Québec est uniquement effectuée à partir des tiges marchandes en croissance et des produits forestiers (Bureau du forestier en chef, 2015). Des 71 unités d'aménagement de la province en 2015, seulement 18 présentaient assez de données pour les calculs d'inventaires des stocks de carbone. A l'heure actuelle, les données concernant les sols sont sporadiques (Beguin *et al.*, 2017; Mansuy *et al.*, 2014). Le manque de données quantifiées sur les caractéristiques des sols, nécessaires pour comprendre les patrons de stockage du COS à différentes échelles spatiales, est un problème global. La base de données mondiale *World Soil Information System* (Batjes *et al.*, 2017), la plus à jour actuellement qui regroupe différentes caractéristiques physico-chimiques des sols à travers le monde, montre un biais d'échantillonnage prégnant (Figure 0.2). Sur les 94441 pédons regroupés dans cette base de données, seulement 148 sont enregistrés au Canada (principalement en sols agricoles), contre 50361 aux USA ou encore 12223 au Mexique, pour ne mentionner que l'Amérique du Nord. Notre compréhension des processus de stockage du COS est ainsi fortement biaisée par le manque de données et la non-uniformité de leur distribution spatiale. Pour exemple, Crowther *et al.* (2016) inféraient avec l'étude de 49 sites expérimentaux que les stocks de COS diminueraient en réponse au réchauffement climatique, particulièrement aux hautes latitudes. La même analyse, réalisée en ajoutant 94 sites supplémentaires à ces données, apportait des conclusions très différentes (van Gestel *et al.*, 2018). Il existe ainsi aujourd'hui un

besoin urgent d'amasser des données quantifiées et géoréférencées pour comprendre les patrons spatiaux en lien avec les processus de stockage du COS et ses facteurs de contrôle, qu'ils soient climatiques ou non climatiques. Renforcer les bases de données par un échantillonnage en forêt naturelle permettrait d'intégrer une dimension supplémentaire et non négligeable à l'aménagement écosystémique du territoire forestier, à savoir le stockage du COS. Au Québec, ce type de données pourrait compléter le registre des états de référence (Boucher *et al.*, 2011) - aujourd'hui cantonné à la végétation arborescente – et servir de base comparative pour évaluer les écarts entre les forêts naturelles et aménagées quant aux caractéristiques des stocks de COS.

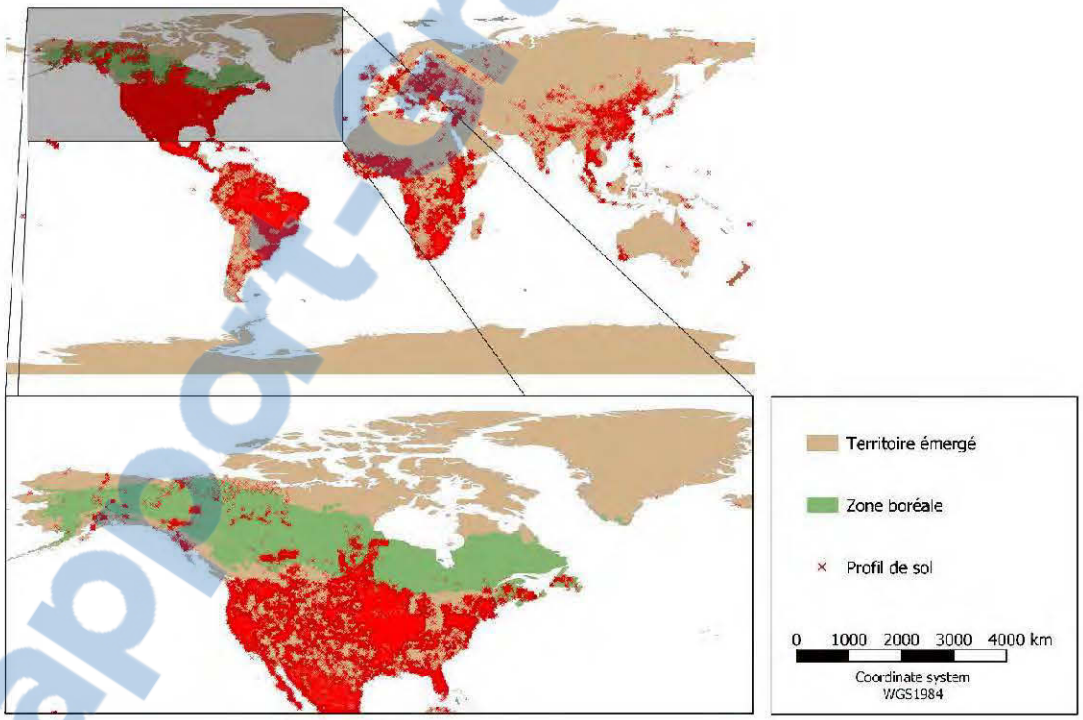

Figure 0.2 Distribution mondiale des profils de sol regroupés dans la base de données *World Soil Information System*. Seule la zone boréale d'Amérique du Nord est montrée. Données récupérées en Août 2018 sur les sites data.isric.org/ et rncan.gc.ca/forets/boreale/14476.

Aussi parfois restreints aux sols plus fertiles des régions agricoles, les modèles associés à notre compréhension des processus de stockage du COS (Jenkinson *et al.*, 1990; Paul *et al.*, 1997) biaisent fortement les projections des réservoirs forestiers de COS boréaux en réponse au réchauffement climatique. Pour mieux anticiper l'impact des changements climatiques, la communauté scientifique doit développer de nouvelles lignes de recherches et de modélisation pour comprendre la manière dont le C est recyclé dans l'écosystème (Bradford *et al.*, 2016; Schmidt *et al.*, 2011).

Globalement, l'objectif des travaux que je présente ici est d'approfondir notre compréhension des processus de stockage du COS, avec l'étude de cas des sols à drainage modéré de la pessière à mousses au Québec. Les trois chapitres de cette thèse reposent sur un échantillonnage inédit qui est utilisé dans les trois chapitres qui suivent. Compte-tenu des relations étroites entre l'équilibre du C et la dynamique d'incendies dans les écosystèmes étudiés, le premier chapitre (Chapitre I) se focalise essentiellement sur les caractéristiques du COS (stock, récalcitrance et bioréactivité) en fonction des régimes de feux comparés aux échelles régionale et locale. De nombreux facteurs sont impliqués dans le contrôle des stocks de COS (voir Chapitre 0.2). Dans le second chapitre (Chapitre II), nous nous intéressons aux interactions entre certains de ces facteurs – climatiques et non-climatiques - ainsi qu'à leur contribution relative pour expliquer, sur des bases mécanistiques, comment les stocks de COS se constituent. A la manière du second chapitre et pour comprendre ici comment ces stocks pourraient évoluer en lien avec des changements environnementaux, le troisième chapitre (Chapitre III) de cette thèse se concentre sur les facteurs contrôlant la facilité de décomposition du COS. Dans le quatrième et dernier chapitre, nous mettons en avant les contributions de la thèse à l'avancement des connaissances et nous soulevons plusieurs pistes de recherche à développer. Enfin, nous concluons sur les solutions qui doivent être adoptées pour maximiser la séquestration de COS dans les territoires aménagés.

CHAPITRE I

DOES CLIMATE OR FIRE REGIME CONTROL THE CARBON STORAGE IN BOREAL FOREST SOILS?

(LE STOCKAGE DU CARBONE DANS LES SOLS DE LA FORÊT BORÉALE EST-IL DÉTERMINÉ PAR LE CLIMAT OU LE RÉGIME DE FEUX ?)

Benjamin Andrieux[1,2,*], David Paré[2], Yves Bergeron[1]

[1]NSERC-UQAT-UQAM Chaire industrielle en aménagement forestier durable, Institut de Recherche sur les Forêts, Université du Québec en Abitibi-Témiscamingue, Rouyn-Noranda, QC, Canada ; [2]Ressources Naturelles Canada, Centre canadien sur la fibre du bois, Québec, QC, Canada.

*Auteur correspondant : benjamin.andrieux.etu@gmail.com

Manuscrit en préparation en date du dépôt de la thèse.

1.1 Abstract

With respect to the biogeochemical carbon (C) cycle, exploring the legacies of past fire regime on ecosystem C dynamic over long-time frames is a way toward understanding the potential effect that global change may have on state change of future ecosystem resilience with global warming. Our study aimed to assess the soil C stock and soil C stabilization variability in relation with fire regimes in eastern North America, first at the regional scale with fire cycle, and secondly at the plot scale with Holocene fire history. By comparing four regions with different fire cycles, our study shows general patterns of the soil C storage process. All regions had similar C stock in the FH horizon that turned over more rapidly in regions experiencing intermediate fire cycles, compared with the ones experiencing the shortest and the longest fire cycle. Also, the C stock of the mineral soil and the amount of organic-mineral associations increased with increasing fire cycle, whereas the recycling of C was similar among regions. We cannot downplay the importance of fire regime on the soil C processes, but as the fire cycle being controlled by climate parameters, it is most likely that these patterns depended more on the regional climate than on the fire cycles. Interestingly, about half of the mineral soils showed a C saturation deficit on the metal oxides. The soil C variables showed high variability around means. Together with the small sample size of our "local" study, this could explain why we were not able to link soil C process with Holocene fire history. Overall and considering fire cycle and climate commutable, our findings support the idea that ecosystem-based management based on the natural fire regime is an appropriate strategy to keep the soil C storage processes into their natural range of variability at the regional scale. Further research is needed to investigate how forest management practices could compensate for the C saturation deficit of some natural soils to increase the soil C reservoir.

1.2 Résumé

Au regard du cycle biogéochimique du carbone (C), explorer l'héritage du régime de feux passé sur la dynamique de l'écosystème à long terme est un moyen pour comprendre l'effet potentiel du changement global sur la modification de la résilience future des écosystèmes. Notre étude visait à évaluer la variabilité dans le stock de C ainsi que la stabilisation du C dans les sols en relation avec les régimes de feu à l'Est de l'Amérique du Nord, d'abord à l'échelle régionale avec le cycle de feu, puis à l'échelle locale avec l'historique de feux holocènes. En comparant quatre régions aux cycles de feux différents, notre étude montre des patrons généraux dans le stockage du C des sols. Toutes les régions avaient des stocks de C dans l'horizon FH qui étaient recyclés plus rapidement dans les régions aux cycles de feux intermédiaires, en comparaison avec les régimes dont les cycles de feux étaient le plus court ou le plus long. Le stock de C dans l'horizon minéral du sol et la quantité d'associations organo-minérales augmentaient avec l'accroissement du cycle de feu, alors que le recyclage du C était similaire entre les régions. Nous ne pouvons pas minimiser l'importance du régime des feux sur les processus de stockage du C dans les sols, mais comme le cycle de feu est contrôlé par des paramètres climatiques, il est plus probable que les patrons décrits ici dépendaient davantage du climat régional plutôt que du cycle des feux. Un fait intéressant est qu'environ la moitié des sols minéraux présentaient un déficit de saturation en C sur les oxydes métalliques. Les variables de C du sol montraient aussi une grande variabilité autour de leurs moyennes. Combiné à la petite taille d'échantillonnage de notre étude « locale », cela pourrait expliquer pourquoi nous n'avons pas trouvé de relation entre les processus de C du sol et l'historique des feux holocènes. Dans l'ensemble, et compte-tenu de la permutabilité du cycle de feux avec le climat, nos résultats supportent l'idée selon laquelle l'aménagement écosystémique de la forêt basé sur le régime des feux naturels est une stratégie propice pour conserver les processus de stockage du C dans leurs gammes de variabilités naturelles à l'échelle

régionale. Des recherches additionnelles sont nécessaires pour déterminer comment les pratiques d'aménagement forestier pourraient compenser le déficit de saturation identifié pour certains sols en forêt naturelle, afin d'augmenter le réservoir de C du sol.

1.3 Introduction

Wildfires are a major disturbance impacting terrestrial ecosystems worldwide (Bond *et al.*, 2005). In the boreal forest, wildfires shape the structure, composition and dynamics of the vegetation (Bergeron, 2000; Cyr *et al.*, 2012; Rogers *et al.*, 2015), as well as several soil processes influencing forest productivity and the carbon (C) cycle (Deluca et Boisvenue, 2012; Fu *et al.*, 2017a; Oris *et al.*, 2014; Wardle, Walker, *et al.*, 2004). Depending on the available fuel load (Rowe et Scotter, 1973; Stocks *et al.*, 2002), climate and meteorological parameters (Ali *et al.*, 2012; Le Goff *et al.*, 2007), increasing wildfire activity is expected in response to global warming (Bergeron *et al.*, 2010; Le Goff *et al.*, 2009; Wotton *et al.*, 2017).

Effects of global change on forest ecosystem C stocks may not be straightforward (Abbott *et al.*, 2016; Girardin *et al.*, 2016; Hui *et al.*, 2017). The potential compensation of soil C losses (Crowther *et al.*, 2016) through enhanced productivity promoted by CO_2 fertilization, atmospheric nitrogen deposition or enhanced nutrient mineralization (Houghton *et al.*, 1998; Hui *et al.*, 2017) remains highly uncertain (Girardin *et al.*, 2016). Nevertheless, Kurz *et al.* (2013) warn that carbon uptake from enhanced boreal ecosystems productivity will likely be insufficient to compensate large emissions from future disturbed areas, particularly if increasing fire frequency exceeds the recovery time of aboveground and belowground C stocks (Fu *et al.*, 2017a; Irulappa Pillai Vijayakumar *et al.*, 2016). Hence, exploring the legacies of past fire regime on ecosystem C dynamic over long time frames is a way toward understanding the

potential effect that global change may have on state change of future ecosystem resilience, with respect to the biogeochemical C cycle, with global warming (McLauchlan *et al.*, 2014).

Only few studies explored the relationships between long-term fire frequency and the ecosystem C cycle. Based on charcoal preserved in lake sediments, Bremond *et al.* (2010) quantified the Holocene C emissions from biomass burning in eastern Canada. Also based on charcoals preserved in lake sediments, a novel approach using paleo-informed modelling of ecosystem C dynamic is ongoing at the watershed scale (Hudiburg *et al.*, 2017; Kelly *et al.*, 2015). Altogether, these studies showed a prevalent control of fire frequency on ecosystem C balance, suggesting that forecasted increasing fire frequency might lead to ecosystem C losses to the atmosphere, and ultimately reinforcing global warming.

Nevertheless, boreal forest mostly store C in soils (Pan *et al.*, 2011) and models do not fully capture the complex processes acting belowground (Bradford *et al.*, 2016). Thus, improved understanding how fire frequency controls soil C storage processes might be raised from field-based studies. In this regard, the pioneering work of Czimczik *et al.* (2005) showed that increasing fire frequency lead to increasing mineral soil C stock in Siberian boreal forests. While organo-mineral interactions occur in mineral soil as a C stabilizing mechanism (Han *et al.*, 2016), it appears essential to investigate how fire frequency impacts together the soil C stock and the soil C stabilization potential.

Thus, the aim of this study was to explore the soil C stock and soil C stabilization variability in relation with fire regimes in the spruce-feather moss domain of Quebec province (Canada). First, we studied regional trends by comparing four regions characterized by their respective fire cycle. On the other hand, we studied local variations at the plot scale by reconstructing long-term local fire histories. We first

hypothesized that soil C stocks increase with long fire cycle or low fire frequency, but that the stable C fraction increase with short fire cycle or high fire frequency. If so, increasing fire frequency with global warming would lead to short-term soil C losses, but long-term soil C stabilization.

1.4 Materials and methods

1.4.1 Sampling sites

Our aim was first to identify regional trends in soil C storage in relation to the variability of the regional fire characteristics. Hence, we selected 72 comparable stands in terms of vegetation composition (black spruce dominance), surficial deposits (glacial tills) and mesic drainage conditions across the study area (Figure 1.1; for a description of the study area, see Andrieux *et al.* (2018b)). Prior to field works, stand were selected using numeric eco-forest maps (third and fourth decadal programs) produced by the Ministère des Forêts, de la Faune et des Parcs of Quebec together with published information about regional fire characteristics (see Figure 1.1 description).

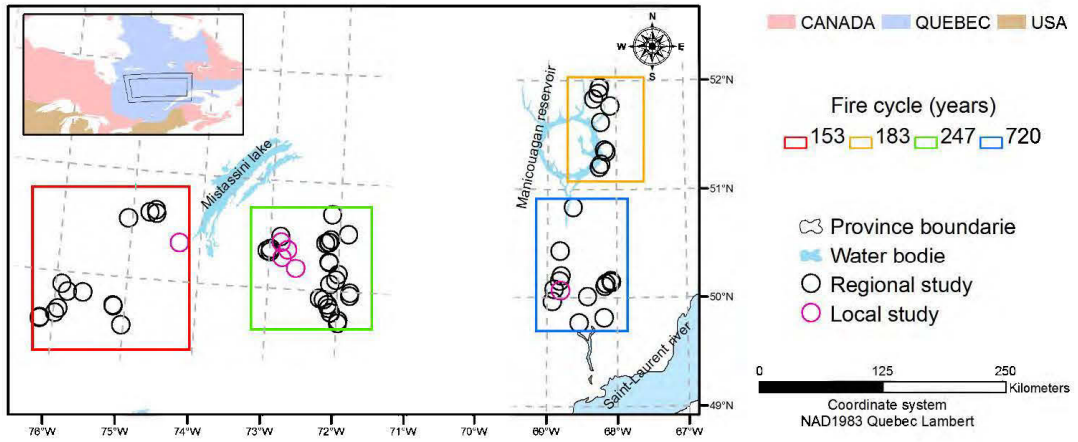

Figure 1.1 Map of the study area showing plot samples encompassed in homogeneous fire cycle zones. Fire cycle zones were delimited according to: (red) Le Goff *et al.* (2007); (green) Belisle *et al.* (2011); (orange and blue) Portier *et al.* (2016). Long-term fire history has been reconstructed at the stand scale in six plots (violet circles). Soil carbon data were gathered in all plots (black and violet circles).

For soil sampling, we followed the Canadian national forest inventory (NFI, 2016). Briefly, we established a 400 m² circular plot within each selected stands. We measured the thickness of the FH horizon every 2 meters along two orthogonal transects intersecting at the plot center, to get 20 depth records per plot. We selected three representative 20x20 cm² microplots at the edge of the plot to collect the litter and living mosses that were bagged apart, and the bulk FH horizon overlying the mineral soil. Thence, we used a metallic cylinder (ø = 4.7 cm; height = 15 cm) to sample the upper 15 cm mineral soil in the same three microplots. At the same location of one of the microplots, a soil pit was dug to sample the mineral soil from 15 to 35 cm and the diagnostic B horizon top 15 cm with a metallic cylinder (ø = 4.7 cm; height = 20 cm or 15 cm, respectively).

To investigate the impact of fire frequency might have on soil C storage at the plot scale, we selected six of the sampling plots (Figure 1.1) to reconstruct the local long-term fire history, according to the protocol of Payette *et al.* (2012). We chose 5 plots to take advantages of previous studies using similar protocols, by sampling of charcoal particles buried in soil horizons. Then, we used four plots published in the study of Frégeau *et al.* (2015) and one plot we published elsewhere (Remy *et al.*, 2018). For one plot where no data was available, we established three 50 meters-long parallel transects, each separated from 10 meters. Along the two outer transects, we sampled soil layers every 5 meters for a total of 10 microplots per transect. For the inner transect, soil samples were gathered at 12.5, 25 and 37.5 meters. In each microplot, we first collected a 20x20 cm^2 organic soil sample beneath the mineral soil. We then used a metallic corer (750 cm^3) to sample the mineral soil. All samples were further processed in lab for stand-scale long-term fire history reconstruction.

1.4.2 Fire history reconstructions

1.4.2.1 Fire cycle

Fire frequency estimations at the regional scale, expressed here as fire cycle, i.e., the time required to burn an entire area of pre-defined size (Li, 2002; Van Wagner, 1978), were not part of this study. We rather took advantages of previous published works using similar methodologies, from which we gathered these estimations. In each area, the fire cycle estimation was based on the distribution of time since fire inferred from dendrochronological analyses (see Belisle *et al.* (2011), Le Goff *et al.* (2007) and Portier *et al.* (2016) for further details). Hence, fire cycle is here an estimation of the recent (< 300 years) fire frequency.

1.4.2.2 Local fire frequency

Following the procedure developed in Payette *et al.* (2012) and Payette *et al.* (2016), we determined long-term past fire events based on the comparative analysis of all calibrated radiocarbon (^{14}C) dates. For five of the sampling plots (Figure 1.1), we used the published ^{14}C dates, and for the unpublished one (Figure 1.1, western plot), Accelerator Mass Spectrometry dating was done on randomly selected 30 (15 from the mineral soil and 15 from the organic layer-mineral soil boundary) charcoal fragments from the forest soil. We calibrated all the conventional ^{14}C dates with 2-sigma confidence intervals using the R package 'clam' v2.2 (Blaauw, 2010) together with the dendrochronological data curve for Northern hemisphere *IntCal13* (Reimer *et al.*, 2016). In this study, we only used the maximum probability distribution of the calibrated date for each charcoal fragment. To account for the inherent uncertainties on the ^{14}C dating, we considered that the charcoal dates with overlapping calendar years originate from the same fire event. Thus, several overlapping dates increased the age interval corresponding to a fire event, whereas for non-overlapping dates the age interval of the calibrated date corresponded to a single fire event.

Based on the sum of probabilities of all dates within each site, we attributed a unique date for each fire event as the age (year cal. BP) with the maximum sum of probabilities within each of the age interval corresponding to a fire event.

Nevertheless, one cannot be sure to detect all fires with the random sampling of soil charcoals. We used an indirect method developed by de Lafontaine et Payette (2011) and Frégeau *et al.* (2015) to estimate the number of fire events, accounting for the ones missing due to the sampling design, by computing the asymptotic accumulation curve from the ^{14}C dating data as follows:

$$F_n = F_{max}(1 - e^{Kn})$$

where F_n is the observed number of fire events, F_{max} is the estimated expected number of fire events (i.e. the asymptote), n is the number of charcoal fragments radiocarbon dated and K is a fitted constant controlling the shape of the accumulation curve. We used means of the 95% bootstrapped (n = 1000) dates of fire events from 1 to x (x being the number of dated charcoal fragments) to construct the mean accumulation curve. The parameters F_{max} and K were determined with non-linear least-squares using the 'nls' function implemented in R v3.0.2 software.

Finally, we calculated the estimated mean fire interval (I_{me}) based on the parameter F_{max}, as follows:

$$I_{me} = \frac{P}{F_{max} - 1}$$

where P is the fire period (corresponding, for each chronology, to the time elapsed between the younger and the oldest fire).

1.4.3 Laboratory work

First, we formed mean composite samples by mixing FH samples and mineral soil top 15 cm samples originating from the same plot and layer. Then, we oven-dried the FH samples at 60°C before sieving at 6 mm, whereas mineral soil samples (composite top 15 cm and mineral soil from 15 to 35 cm) were sieved through a 2 mm mesh before air-drying. We weighted the dried samples to estimate their bulk density, assuming no coarse fragments for the FH horizon and corrected from coarse fragments (> 2 mm) for

the mineral soil. For C content determination, metal oxide content and acid hydrolysis, we finely ground (0.5 mm) the dried soil samples after sub-sampling 9 g and 50 g of the FH horizon and mineral soil, respectively, that we incubated for the determination of the bioreactive soil C.

We analyzed the C concentration of each sample by dry combustion (Skjemstad et Baldock, 2007), using a Leco TruMac (Leco Corp., St. Joseph, MI, USA). We computed the carbon stock by multiplying the C concentration by bulk density and thickness for each sample. Metal oxides organically complexing C (Mpy) in the illuvial horizon were quantified by extracting in a $Na_4P_2O_7$ 0.1N solution before analyzing by ICP-AES (Courchesne et Turmel, 2007) with an Optima 7300 DV (Pelrkin Elmer Inc., Waltham, MA, USA). Rescaling C concentration and Mpy on the same unit, we calculated the C:Mpy ratio as an index of the degree of chelation between the two compounds. C:Mpy < 2 indicates potential for additional C storage, whereas C:Mpy > 10 indicates organometallic complexation limited by Mpy amounts (Masiello *et al.*, 2004).

We used acid-insoluble C as an index of soil C resistance to biological degradation (von Lützow *et al.*, 2007; Xu *et al.*, 1997). We carried out acid hydrolysis by refluxing 2 g of soil in HCl 6M for 2 hours (Silveira *et al.*, 2008). We rinsed acid-insoluble residues three times with 50 mL purified water in inert filter papers before drying, weighting and analyzing for C concentration by dry combustion. According to Plante *et al.* (2006), we calculated the acid-insoluble fraction (%) of each of the samples as follows:

$$C_{AI} = \frac{[C_{AI}] \times M_{AI}}{[C_i] \times M_i} \times 100$$

where C_{AI} is the acid-insoluble C fraction (%) in the sample, $[C_{AI}]$ is the C content (%) of the acid-insoluble residues, $[C_i]$ is the C content (%) of the sample before processing by acid hydrolysis, M_{AI} is the mass (g) of the acid-insoluble residues and M_i is the initial sample mass (g).

To determine the bioreactivity of soil C, a relative measure of the overall C lability (Laganière *et al.*, 2015; Xu *et al.*, 1997), we incubated soil samples separately for each layer (FH horizon, mineral soil top 15 cm and mineral soil from 15 to 35 cm) for approximately 1 year, according to Paré *et al.* (2011). We placed the samples in bottom-perforated plastic containers that were pre-filled with glass wool and pre-washed with HCl 1M. We saturated each of the samples with purified water and let them equilibrate for 24 h in a cooler at 2°C before weighting to determine their water holding capacity. Then, we placed each of the samples in a 500 mL glass Mason jar that were left in a growth chamber under constant temperature and air moisture conditions at 26°C and 100% humidity, respectively, during the experiments. Periodically, we measured the CO_2 production in each of the microcosms. For this, we first hermetically closed the jar with a metal lid, on which a rubber septum was installed, before measuring the CO_2 concentration of the jar headspace (initial CO_2 concentration, CO_{2i}). We measured again the CO_2 concentration of the jar headspace after 4h – 24h, depending on the soil layer and the progress of the experiment (final CO_2 concentration, CO_{2f}). We used a LI-6400 portable photosynthesis system (LI-COR®, Lincoln, NE, USA) to measure the CO_2 concentration. Briefly, we used a 2.5 mL and 10 mL (for FH horizon and mineral soils, respectively) syringe to sample an air volume from the jar head space through the rubber septum, that we injected in the LI-6400 infrared analyzer through a N_2 carrier gas (LI-COR® Application Note # 134) maintained at 100 mL.min^{-1} flow rates using a FMA1812A gas flow meter (Omega Engineering, INC, Norwalk, CO, USA). By doing so, the measured CO_2 concentration constitutes a dilution of the gas from the jar headspace. To obtain the real CO_2 concentration of the jar headspace, we regressed the

measured CO_2 peak of the sample against CO_2 peaks of benchmark gas (800 and 3000 ppm). To account solely for the CO_2 produced by the microcosm, we subtracted CO_{2i} from CO_{2f}. Then, we applied the gas law to calculate the specific respiration rate that was scaled on a 24h basis to obtain the daily specific respiration rate (R_t). Derived from the calculation of the cumulative respiration in Paré *et al.* (2006), we calculated the soil bioreactive C fraction in each of the samples as followed:

$$C_{BioR} = M_{t-1} + \frac{(R_t + R_{t-1})}{2} \times (t - t_{-1}) \times k$$

where C_{BioR} is the percent initial C lost through microbial respiration (%) at time t, M_{t-1} is the cumulative CO_2-equivalent C mass mineralized at time $t\text{-}1$ (mg CO_2-C.d^{-1}), R_t and R_{t-1} are the daily specific respiration rate (mg CO2-C.g^{-1}Corg) at t and $t\text{-}1$, respectively, t is the Julian day and k is a scaling factor (0.1).

Hereafter, we use the value of C_{BioR} considering all the computed values gathered during the entire period of incubations and C_{BioR} expressed the cumulative percent initial C lost through microbial respiration to the end of the experiments.

1.4.4 Statistical analysis

Our first objective was to compare the soil C stock, the acid-insoluble soil C fraction and the soil C_{BioR} at the regional fire cycle scale. Based on Levene's test, equality of variance could not be assumed between groups of homogeneous fire cycle for each of the response variables. Then, we compared differences between groups' mean using Welsh's one-way ANOVA that is not affected by unequal variances. When Welsh's ANOVA was found to be significant, we performed post-hoc pairwise comparisons

using Games-Howell test to account for our unbalanced design (Games et Howell, 1976).

The second objective was to investigate relationships between local variations in soil C characteristics with stand-scale fire frequency. Because of our small sample size (n = 6), we used Spearman rank correlation between soil C variables and the estimated mean fire return interval, testing for monotonic relationships between covariates with a test robust to outliers.

All calculations and statistical analyses were performed with R v.3.4.3 software (R Core Team, 2017). ANOVAs and post-hoc tests were computed using the package '*userfriendlyscience*' (Peters, 2018). All statistics were considered significant at $p < 0.05$.

1.5 Results

1.5.1 Soil C characteristics as a function of regional fire regime

To investigate the role that fire regime might have on soil C characteristics at the regional scale, we compared four fire cycles by using three soil C variables (Figure 1.2). For the FH horizon (Figure 1.2A), the C stock values varied from 26 $MgC.ha^{-1}$ and 217 $MgC.ha^{-1}$ (mean = 80 ± [SD] 36 $MgC.ha^{-1}$) and the means did not differ between groups ($F_{3,29.54} = 0.63$, $p = 0.60$). The acid-insoluble C fraction (C_{AI}) of the FH horizon ranged from 48% to 91% (mean = 73 ± 5 %) and was significantly different among groups ($F_{3,29.10} = 3.51$, $p = 0.03$). Post-hoc Games-Howell pairwise comparisons revealed that the 183-years fire cycle group had the lowest C_{AI} mean (mean = 69.59 ± 2.80 %), significantly different from the 247-years fire cycle one (mean = 73.00 ± 3.31

%, $p = 0.02$), whereas the 153- and 720-years fire cycle groups have similar C_{AI} compared to all other groups (mean = 72.09 ± 2.99 % and mean = 74.23 ± 9.19 %, respectively). Despite that the C_{BioR} of the FH horizon was found to be different for some groups ($F_{3,27.90} = 3.20$, $p = 0.04$), post-hoc test considered all groups to have a similar mean ($p > 0.05$), underlining the conservative nature of the test. For the mineral soil (Figure 1.2B), the C stock varied with the fire cycle ($F_{3,27.96} = 9.31$, $p < 0.001$) and generally increased with increasing fire cycle, when differences were found to be significant between the 153-years fire cycle (mean = 47 ± 15 $MgC.ha^{-1}$) and the 247- and 720-years fire cycles (mean = 83 ± 41 $MgC.ha^{-1}$ and mean = 74 ± 24 $MgC.ha^{-1}$, respectively). The C_{BioR} of the mineral soil ranged from 2% to 11% and was not significantly different between groups ($F_{3,55.24} = 0.39$, $p = 0.76$). By summing FH horizon and mineral soil C stocks, the total soil C stock showed differences among groups ($F_{3,52.20} = 3.25$, $p = 0.03$), with the 153-years fire cycle group having the lowest C stock (mean = 123 ± 43 $MgC.ha^{-1}$) and the 247-years fire cycle having the highest one (mean = 167 ± 51 $MgC.ha^{-1}$), whereas the mean C stocks of the 183- and the 720-years fire cycles were not significantly different from other groups.

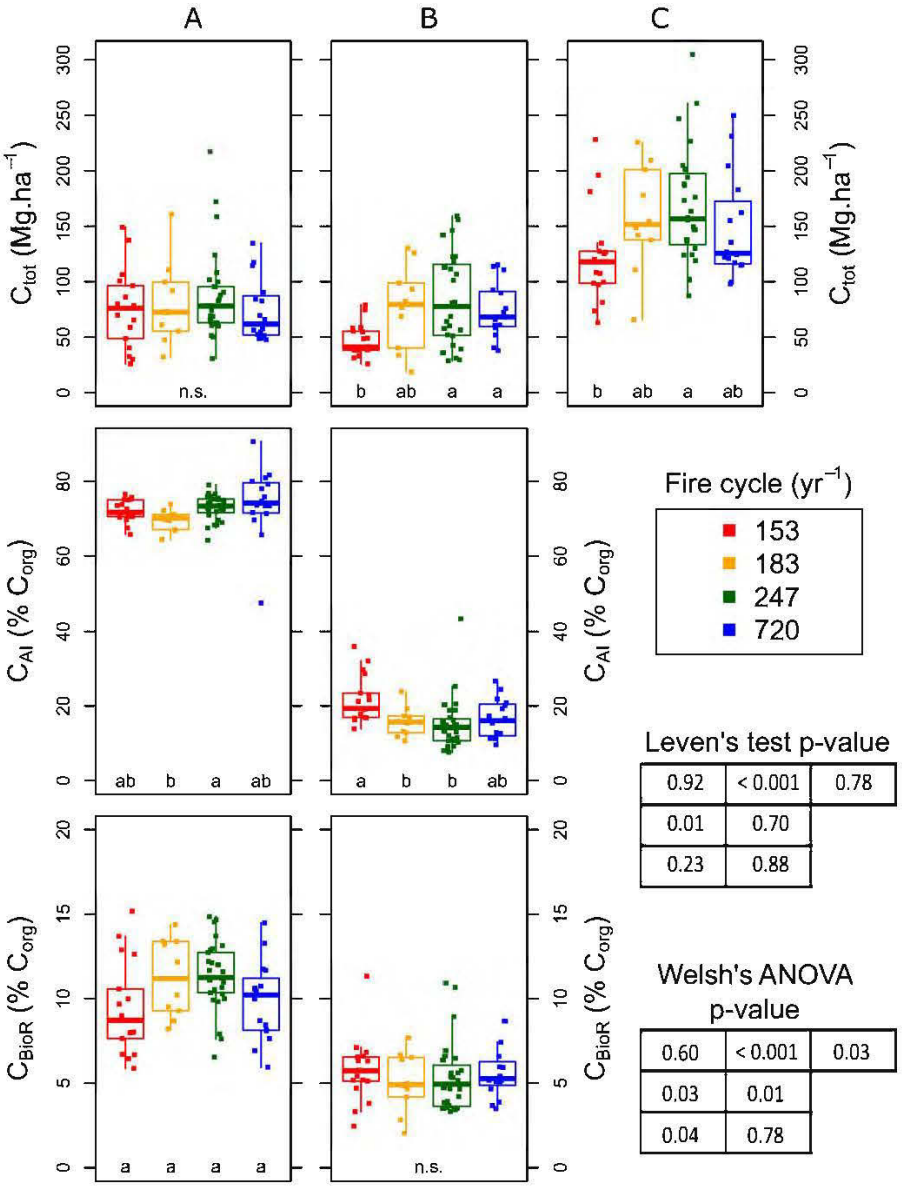

Figure 1.2 Regional-scale soil C characteristics by groups of homogeneous fire cycle. A: FH horizon; B: mineral soil top 35 cm; C: all soil column (A + B). When Welch's ANOVA was found to be significant ($p < 0.05$), pairwise differences were tested using Games-Howell post-hoc test (lowercase letters). C_{tot}: total carbon stock; C_{Al}: acid-insoluble C fraction; C_{BioR}: bioreactive soil C. *n.s.*: not significant ($p > 0.05$). Note: positions of the Leven's tests and Welsh's ANOVA tables correspond, for each cell, to the position of each graph.

Trends about changes in soil C characteristics with fire cycle appeared to be more straightforward for the B horizon (Figure 1.3). Metal oxides organically-complexing C (Mpy) were found to be significantly different between groups ($F_{3,31.02} = 5.31$, $p = 0.004$) and increased with increasing fire cycle, the 153-years fire cycle group having the lowest Mpy content (mean = 10.45 ± [SD] 5.51 $g.kg^{-1}$) and the 247- and 720-years fire cycle groups having the highest ones (mean = 17.53 ± 10.02 $g.kg^{-1}$ and mean = 20.15 ± 10.34 $g.kg^{-1}$, respectively). The C concentration of the B horizon followed the same trend as Mpy with significant differences among groups ($F_{3,29.70} = 6.06$, $p = 0.002$), the 153-years fire cycle group having the lowest C concentration (mean = 2.05 ± 1.04 %) and the 247- and 720-years fire cycle groups having the highest ones (mean = 3.78 ± 2.14 % and mean = 4.04 ± 2.41 %, respectively). The C:Mpy ratio ranges from 0.64 to 9.75 (mean = 2.23 ± 1.16) and did not show differences by groups ($F_{3,31.35} = 2.27$, $p = 0.10$).

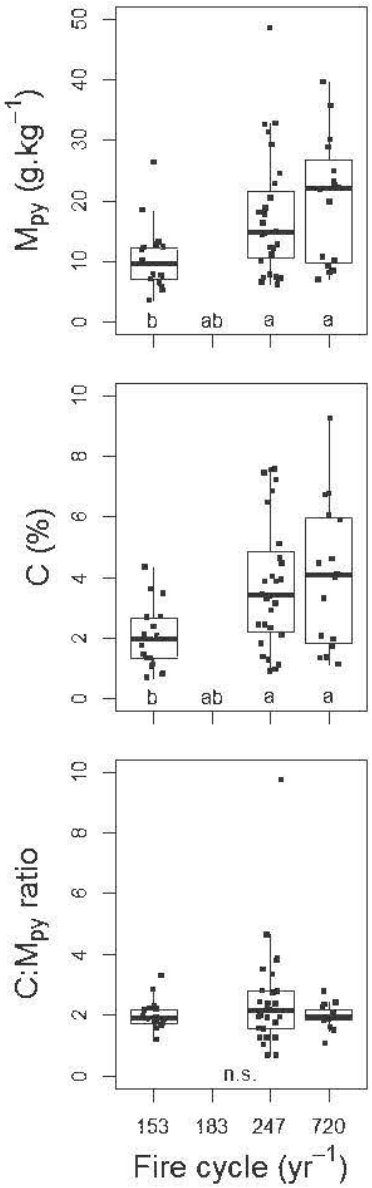

Figure 1.3 Regional-scale illuvial (B) horizon C characteristics by groups of homogeneous fire cycle. *M_{py}*: pyrophosphate extractable metals; *C*: carbon concentration; *C:M_{py} ratio*: ratio calculated by rescaling variables on the same unit.

1.5.2 Soil C characteristics as a function of stand-scale fire frequency

To investigate the role that fire regime might have on soil C characteristics at the stand scale, we compared six sites for which we reconstructed the local long-term fire history (Annexe A, Figure S1.1), by using three soil C variables (Figure 1.4) and the local estimated mean fire interval. Whether considering the C stock, the acid-insoluble C fraction or the C_{BioR} of the FH horizon and of the mineral soil, there were no significant statistical relationships between soil C variables and Holocene mean fire interval (Spearman's correlation $p > 0.05$). Likewise, there were no significant statistical relationships between soil C variables of the illuvial horizon and Holocene mean fire interval (Figure 1.5).

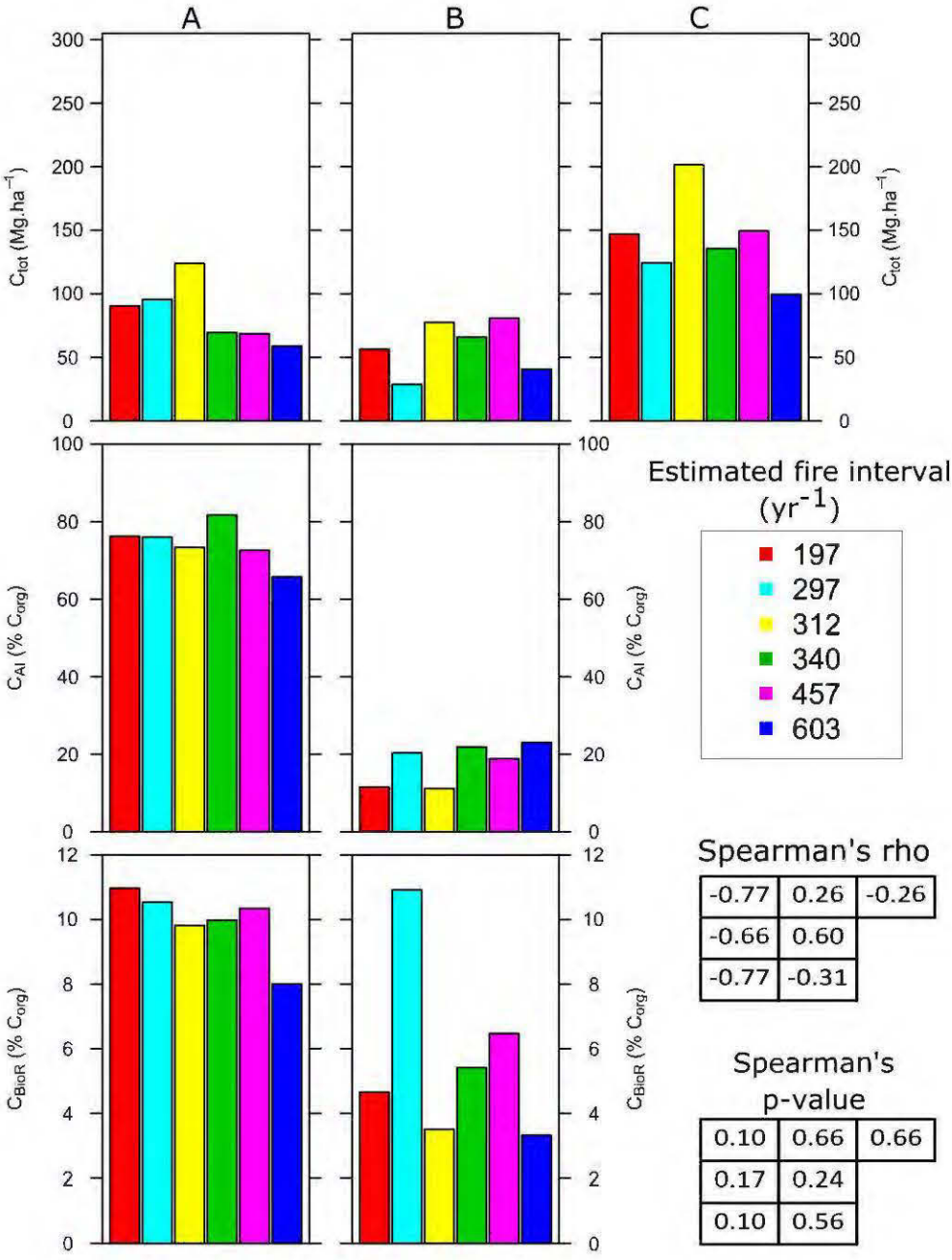

Figure 1.4 Stand-scale soil C characteristics sorted by decreasing mean fire interval (from the left to the right) and correlation tests. A: FH horizon; B: mineral soil top 35 cm; C: all soil column. C_{tot}: total carbon stock; C_{Al}: acid-insoluble C fraction; C_{BioR}: bioreactive soil C. Note: positions of the Spearman's tests tables correspond, for each cell, to the position of each graph.

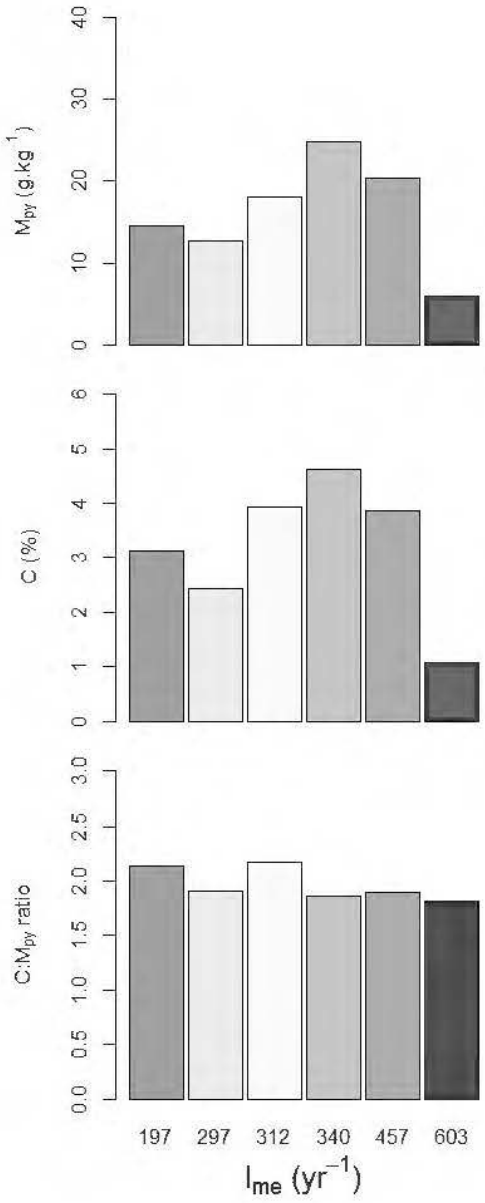

Figure 1.5 Stand-scale illuvial (B) horizon carbon characteristics sorted by decreasing mean fire interval (from the left to the right). M_{py}: pyrophosphate extractable metals (g/kg); *C*: carbon concentration (%); *C*:M_{py} *ratio*: ratio calculated by rescaling variables on the same unit. I_{me}: estimated mean fire interval (yr).

1.6 Discussion

In this study, we explored the soil C stock and soil C stabilization variability in relation with fire regimes, by comparing soil C characteristics at the regional scale with recent (decadal to centennial) fire cycle and at the stand scale with long term (Holocene) fire frequency. Because no pattern in soil C characteristics was found to be significant at the stand scale, likely due to our small sample size, we focus our analysis on trends observed at the regional scale hereafter.

1.6.1 Does fire cycle control the C turnover and not the C stock of the FH horizon?

In this study, C stocks of the FH horizon were found to be comparable among all the fire cycle groups (Figure 1.2A), which is consistent with the results of Czimczik *et al.* (2005). These results contrast with the findings of Lecomte *et al.* (2006), where the density of soil organic matter in the unburnt part of the FH horizon increased mostly from about 270 years following fire, bringing these authors to conclude that increasing fire cycle might lead to increase ecosystem carbon stocks. The sites studied by Lecomte *et al.* (2006) had poor soil drainage conditions, whereas the soils we studied here were mesic environments. This suggests that soil C storage processes are quite variable and depend on soil drainage conditions (Trumbore et Harden, 1997; Wang, C. *et al.*, 2003).

In our study, differences in C_{BioR} were found not to be significant among fire cycle groups (Figure 1.2A), likely due to the conservative nature of the statistic tests. Nevertheless, the variation of C_{BioR} and of C_{AI} with fire cycle groups showed reversed patterns (Figure 1.2A). This imply that the use of acid hydrolysis and the use of soil incubations together are complementary methods to study the soil C cycling (Paul *et al.*, 2006). Overall, the results of our study with comparable C stocks in the FH horizon

among the different fire cycle groups and reversed patterns between C_{AI} and C_{BioR} with fire cycle groups suggest that the fire cycle controls the C turnover without changing the C stock of the FH horizon.

We found lower C_{AI} and higher C_{BioR} both with the shortest and the longest fire cycles. This implies that the C of the FH horizon in regions experiencing intermediate fire cycles is rapid in comparison with shortest or longest ones. Black carbon (BC) is a by-product of organic matter processed by thermal oxidation which is resistant to biological degradation (Santin *et al.*, 2016). Re-burning of BC is not a major process of BC loss in the FH horizon (Santín *et al.*, 2013). In our study, it is possible that the high C_{AI} concentration and the low C_{BioR} of the FH horizon in the region with a short fire cycle resulted from the accumulation of BC. But this assumption is inconsistent with the high C_{AI} concentration and low C_{BioR} of the FH horizon we found for the longest fire cycle group, because amounts of BC tend to decrease with time in the absence of fire disturbance (Preston *et al.*, 2017; Santín *et al.*, 2013). Rather, a plausible explanation could be that the fire regime being very dependant on climatic conditions (Chaste *et al.*, 2018), the pattern in soil C characteristics we found in our study could be a direct expression of the regional climate in the C storage process of the FH horizon, and particularly the regime of precipitation more than to be a direct effect of the fire cycle (Annexe A, Figure S1.3).

1.6.2 Organo-mineral association controls the size of the mineral soil C reservoir but not its turnover

As a mechanism of soil organic C stabilization, metallic complexation mostly occur in acidic soil conditions (Rasmussen *et al.*, 2018). In our study, the index of chelation (C:Mpy ratio) always was below 10 (Figure 1.3), suggesting that the complexation of

C with metal oxides was effective (Masiello *et al.*, 2004) and that the soil capacity to retain C is strongly linked to the amount of iron and aluminum species (Annexe A, Figure S1.2).

Both the Mpy content and the C content of the illuvial horizon and the C stock of the mineral soil increased with increasing fire cycle. This suggest that the longer is the fire cycle and the more the soil store metal oxide that can bind C, increasing the mineral soil C reservoir. Here, organometallic complexation did not likely result from heating of soil during wildfire, as previously described (Fernández *et al.*, 1997). In theory, areas characterized by long fire cycle have higher proportion of old-growth forests (Bergeron *et al.*, 2002). So, it is possible that old-growth forests own attributes favoring the release of metal oxide, and indirectly enhancing soil C sequestration. Alternatively, the observed increase of both Mpy content and C content with increasing fire cycle could be the direct expression of climate conditions that control the regional fire regime (Chaste *et al.* (2018); Annexe A, Figure S1.3). Both explanations agree with our previous findings (Andrieux *et al.*, 2018b).

One could expect a decreasing C_{BioR} with increasing fire cycle, as regards to the organometallic stabilization pattern found in our study. Interestingly, C_{BioR} of the mineral soil did not vary significantly between fire cycle groups (Figure 1.2). This suggest that organometallic complexation is not necessarily a factor of long-term C sequestration in these soils and that stabilization of soil C by association with soil mineral phase could be modulated by other soil parameters. So, Mpy content is a strong predictor of soil C concentration and not soil C turnover, agreeing with Porras *et al.* (2017), who also showed that associations between organic and metal species is less stable in the most acidic soils. Hence, the local soil pH conditions in our case study, more than the amount of metal oxides, could have modulated the soil C turnover (Andrieux *et al.*, 2018b).

Interestingly, the index of chelation C:Mpy was under a value of 2 for 49% of our sampling sites (Figure 1.3 and Figure 1.6). As these soils had more metal ion charges than organic carbon charges (Masiello *et al.*, 2004), it implies that additional C could be bound to metals. Overall, half of our sampling soils were C under-saturated, with some regional variations (Figure 1.6) remaining to be further investigated.

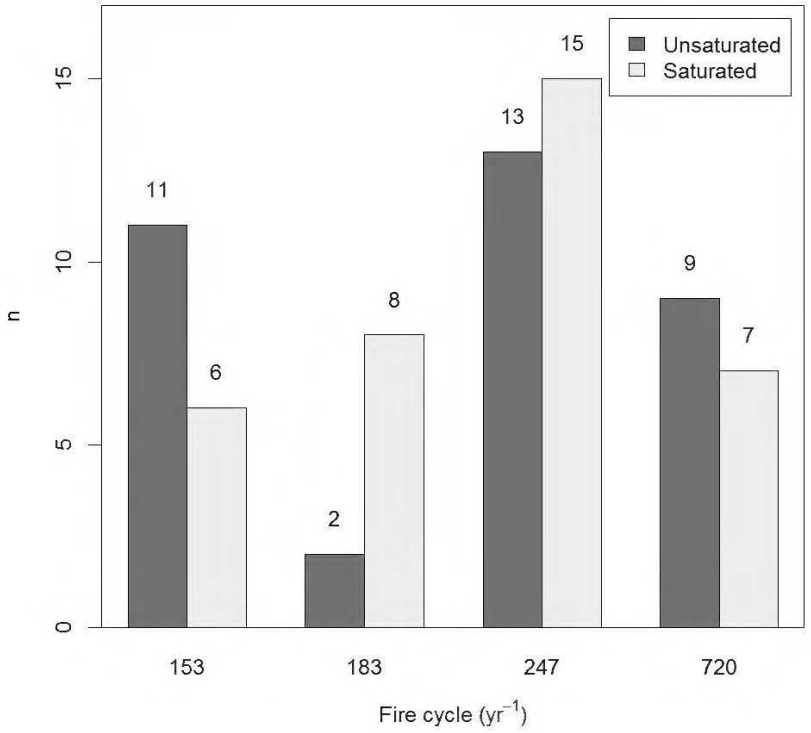

Figure 1.6 Number of soils with an efficient organometallic complexation (light grey) or with an additional potential for binding more carbon on metal oxides (dark grey), by homogeneous fire cycle zone. Soil with a carbon to pyrophosphate extractable metals ratio (C:Mpy) less than 2 where considered unsaturated, or saturated when C:Mpy ranged between 2 and 10 (Masiello *et al.*, 2004).

1.6.3 Needs for research

Our study aimed to assess the impact of fire regime on soil C characteristics. Our design involved sampling plots grouped by regional fire cycle, in a vast territory with climate variability. Based on our findings, it is more likely that the regional variations in soil C characteristics mirrored the variations in climate conditions, rather than fire regime ones. Although we found regional trends in soil C storage processes, high variabilities characterized the observed soil C variables. Moreover, the absence of recognizable patterns in soil C characteristics with long term fire frequency at the local scale could have resulted from large variabilities in unmeasured factors of soil condition. This indicates that several local environmental properties could modulate the soil C storage processes. Clearly, further research is needed to account for both the relative contribution of climate or fire regime and local environment factors involved in the control of the soil C storage processes.

Nevertheless, our study brings some important implications about ecosystem-based management of boreal forests, first thought as regards to the natural fire disturbance (Bergeron *et al.*, 2007; Bergeron *et al.*, 2002; Harvey *et al.*, 2002). Currently limited to the aboveground biomass, we assume that this strategy could be expand to the soil system with respect to the soil C cycle. Indeed, our results suggest that, considering climate and fire cycle to be commutable, integrating knowledge about fire cycles in ecosystem-based management is appropriate to keep the soil C storage processes into their natural range of variability at the regional scale. Moreover, further understanding about how forest management practices could compensate for the C saturation deficit of some soils would participate to increase the soil C reservoirs. For achieving a target of increasing C sequestration in boreal forests, we urgently need to develop further research to disentangle both the role of climate and fire cycle on soil C storage process, advance methodological fire history reconstructions, comprehensive analyses on the

soil C storage capacity and better understanding on the local controlling factors of soil C storage.

1.7 Acknowledgements

This study was funded by the Mitacs Acceleration grant IT05018. We acknowledge all our field assistants (Eric Beaulieu, Catherine Bruyère, Cécile Remy and Arnaud Guillemard). We thank Danielle Charron and Pierre Clouâtre for the support with field logistic. Véronique Poirier and Jean Noël helped with digital data, and we are also grateful to Serge Rousseau for the laboratory analyses. The authors declare no conflict of interest.

CHAPITRE II

DRIVERS OF POST-FIRE SOIL ORGANIC CARBON ACCUMULATION IN THE BOREAL FOREST

(DÉTERMINANTS DE L'ACCUMULATION DU CARBONE ORGANIQUE DES SOLS APRÈS FEU EN FORÊT BORÉALE)

Benjamin Andrieux[1,2,*], Julien Beguin[3], Yves Bergeron[1], Pierre Grondin[4], David Paré[2]

[1]NSERC-UQAT-UQAM Chaire industrielle en aménagement forestier durable, Institut de Recherche sur les Forêts, Université du Québec en Abitibi-Témiscamingue, Rouyn-Noranda, QC, Canada ; [2]Ressources Naturelles Canada, Service Canadien des Forêts, Centre de Foresterie des Laurentides, Québec, QC, Canada ; [3]Ressources Naturelles Canada, Centre canadien sur la fibre du bois, Québec, QC, Canada; [4]Direction de la recherche forestière, Ministère des Forêts, de la Faune et des Parcs du Québéc, Québec, QC, Canada.

*Auteur correspondant : benjamin.andrieux.etu@gmail.com

Article publié dans Global Change Biology, 2018. doi : 10.1111/gcb.14365

2.1 Abstract

The accumulation of soil carbon (C) is regulated by a complex interplay between abiotic and biotic factors. Our study aimed to identify the main drivers of soil C accumulation in the boreal forest of eastern North America. Ecosystem C pools were measured in 72 sites of fire origin that burned 2 to 314 years ago over a vast region with a range of Δ mean annual temperature of 3°C and one of Δ 500 mm total precipitation. We used a set of multivariate *a priori* causal hypotheses to test the influence of time since fire (TSF), climate, soil physico-chemistry and bryophyte dominance on forest soil organic C accumulation. Integrating the direct and indirect effects among abiotic and biotic variables explained as much as 50% of the full model variability. The main direct drivers of soil C stocks were: TSF > bryophyte dominance of the FH layer and metal oxide content > pH of the mineral soil. Only climate parameters related to water availability contributed significantly to explaining soil C stock variation. Importantly, climate was found to affect FH layer and mineral soil C stocks indirectly through its effects on bryophyte dominance and organo-metal complexation, respectively. Soil texture had no influence on soil C stocks. Soil C stocks increased both in the FH layer and mineral soil with TSF and this effect was linked to a decrease in pH with TSF in mineral soil. TSF thus appears to be an important factor of soil development and of C sequestration in mineral soil through its influence on soil chemistry. Overall, this work highlights that integrating the complex interplay between the main drivers of soil C stocks into mechanistic models of C dynamics could improve our ability to assess C stocks and better anticipate the response of the boreal forest to global change.

2.2 Résumé

L'accumulation du carbone (C) dans les sols est régulée par des interactions complexes entre des facteurs biotiques et abiotiques. Notre étude visait à identifier les principaux facteurs d'accumulation du C dans les sols de la forêt boréale à l'Est de l'Amérique du Nord. Les réservoirs de C de l'écosystème ont été mesurés dans 72 sites originaires d'incendies naturels qui ont brûlé il y a 2 à 314 ans, dans une vaste région présentant une variabilité des températures moyennes de 3°C et 500 mm de précipitations totales. Nous avons utilisé un ensemble d'hypothèses causales *a priori* pour évaluer l'influence du temps écoulé depuis le dernier feu (TSF), du climat, de la physico-chimie du sol et de la dominance des bryophytes sur l'accumulation du C organique des sols forestiers. L'intégration des effets directs et indirects parmi les variables biotiques et abiotiques a permis d'expliquer jusqu'à 50% de la variabilité totale du modèle. Les principaux déterminants directs des stocks de C étaient : TSF > dominance des bryophytes pour la couche organique FH et la concentration en oxydes métalliques > pH pour le sol minéral. Seuls les paramètres climatiques liés à la disponibilité de l'eau contribuaient significativement à expliquer la variation dans les stocks de C du sol. Il est important de noter que le climat n'affectait qu'indirectement les stocks de C dans la couche FH et le sol minéral, au travers de ses influences sur la dominance des bryophytes et sur la complexation organométallique, respectivement. La texture du sol n'a pas eu d'influence sur les stocks de C du sol. Le stock de C du sol augmentait à la fois dans la couche FH et dans le sol minéral avec le TSF, et cet effet était lié à une diminution du pH avec l'augmentation du TSF dans le sol minéral. Le TSF était un facteur majeur du développement du sol et de la séquestration de C dans le sol minéral, au travers de ses influences sur la chimie du sol. Dans l'ensemble, ce travail met en lumière que l'intégration des interactions complexes entre les principaux facteurs déterminant les stocks de C du sol dans les modèles mécanistiques de la dynamique du C pourrait

améliorer notre capacité à évaluer les stocks de C et mieux anticiper la réponse de la forêt boréale au regard des changements globaux.

2.3 Introduction

One third of the global forest carbon (C) is stored in boreal ecosystems (Dixon *et al.*, 1994; Pan *et al.*, 2011). Due to the slow rate of organic matter decomposition (Hobbie *et al.*, 2000), boreal forests accumulate C mostly in their soil (Deluca et Boisvenue, 2012). Understanding the processes involved in organic C storage in soils at high latitudes is a prerequisite to appreciate the potential of C sequestration in terrestrial sinks as a strategy to mitigate global warming (Jandl *et al.*, 2007; Lal, 2005). Thus far, soil C pool has remained the major source of uncertainty in forest C stock predictions (Shaw *et al.*, 2014), underlining that the complexity of soil systems is not fully pictured in models of C dynamics. By focusing on the complex interplay between climate, fire, vegetation attributes and soil geochemistry regulating soil C pools, empirical studies should help improving the mechanistic understanding of soil C accumulation (Schmidt *et al.*, 2011).

Climate drives forest ecosystem C stocks by affecting forest growth and decomposition processes. It also affects C stocks through changes in wildfire regime (frequency and severity). Following fire and in the absence of other major disturbance, aboveground biomass accumulates over time until it stabilizes (Bormann et Likens, 1979; Ward *et al.*, 2014) or decreases (Wardle, Walker, *et al.*, 2004). Similar responses have been observed in the forest floor wherein organic matter accumulates following time since disturbance (Nave *et al.*, 2011) until it either levels off (Ward *et al.*, 2014) or continues to increase over time such as observed in soils undergoing paludification (Simard *et al.*, 2007). Regarding mineral soil C stocks, the effect of time since fire (TSF) on the

shape of C accumulation curves over time is not as well documented and most theoretical models simply assume a steady state or a very slow accumulation (Deluca et Boisvenue, 2012; Harden *et al.*, 1992; Seedre *et al.*, 2011) with increasing TSF. Total ecosystem C is generally thought to reach a maximum in forest ecosystems after the living vegetation aggradation phase (Bormann et Likens, 1979; Ward *et al.*, 2014), and possibly retrogresses (Wardle, Walker, *et al.*, 2004) in the absence of any other major disturbance event. However, it has been argued that total ecosystem C might slowly continue to accumulate in old-growth forests (Luyssaert *et al.*, 2008), especially in dead organic matter pools (Kurz *et al.*, 2013; Zhou *et al.*, 2006). All such divergent patterns and conflicting ideas highlight the gaps that exist in our comprehension of the processes that regulate C dynamics in boreal forest ecosystems.

Recent findings point out climate as a secondary predictor of soil C stocks, weaker than soil geochemistry (Doetterl *et al.*, 2015). Indeed, mineral surface reactivity has long been recognized as a strong determinant of soil C storage capacity (Castellano *et al.*, 2015; Six *et al.*, 2002). In the boreal region, acidic parent material typically results in podsolization, which is characterized by organic matter accumulation in the illuvial (B) horizon, where organic matter is associated to different degrees with aluminum and iron oxides (Sanborn *et al.*, 2011). Whereas podsolization occurs over long time scales, the changes and processes controlling mineral soil C accumulation over shorter periods of time following the years since the last fire event are poorly understood. Vegetation is another driver that can exert a profound effect on soil C cycling (Laganière *et al.*, 2017). In the boreal black spruce forest, changes in the composition of the tree canopy with TSF are limited as pure black spruce stands are typical of old-growth successional stages and are able to regenerate quickly after fire (Harper *et al.*, 2003). Changes in the vegetation mostly occur in the understory, particularly in the moss layer (Fenton et Bergeron, 2008), where moss species dominance is known to change over time after fire disturbances. Nevertheless, simple effects of climate and vegetation on soil C

stocks may prove to be difficult to disentangle as vegetation types often equilibrate within their optimal climatic envelope (Jobbagy et Jackson, 2000).

The objective of this study is to fill these knowledge gaps by quantifying changes in boreal forest C pools with TSF (from 2 to 314 years) and to disentangle the role played by soil physical (texture) and chemical (pH and metal oxide contents) properties, local biotic conditions (bryophyte dominance) and climate on soil C accumulation across the spruce feathermoss bioclimatic domain in eastern North America. Using a set of *a priori* causal hypotheses with direct and indirect effects, we addressed the following questions: i) Does the ecosystem reach a maximum C storage after the living vegetation aggradation phase following disturbance? and ii) To which extent do interdependent relationships among TSF, climate, physical and chemical soil properties and bryophyte dominance influence soil organic C accumulation in both the FH layer and the mineral soil? Our study is framed within the state factor model of ecosystems (Amundson et Jenny, 1997). Thus, we start with the assumption that once site factors such as overstory composition, surficial deposits and soil drainage are accounted for, dynamic-ecosystem C pools (i.e. aboveground biomass, downed coarse woody debris and FH layer) are mostly controlled by TSF (Seedre *et al.*, 2011), whereas mineral soil C pools are mostly controlled by climate and soil chemistry (Doetterl *et al.*, 2015).

In boreal ecosystems, the accumulation and maintenance of soil organic matter in the forest floor are driven by the primary fungal decomposition of plant residues. This humification process is governed by the incomplete decomposition of litter, notably resulting from a great biological competition for limited nitrogen, that favors an immobilization and a blockage of the nitrogen cycle (Prescott *et al.*, 2000). Following the Soil Classification Working Group (1998), we use the term FH layer in reference to the partially decomposed (fragmented, F) and decomposed (humified, H) soil organic matter accumulated in a thick layer at the soil surface, also defined as mor

humus (Weetman, 1980), in distinction with the mineral soil layers beneath. The FH layer is equivalent to the Oi and Oe/Oa layers.

2.4 Materials and methods

2.4.1 Study area

This study was carried out in sites distributed across the managed portion of the boreal forest of eastern Canada, a forest dominated by evergreen conifer species and located roughly between 49°N and 52°N and from 68°W to 76°W (Figure 2.1).

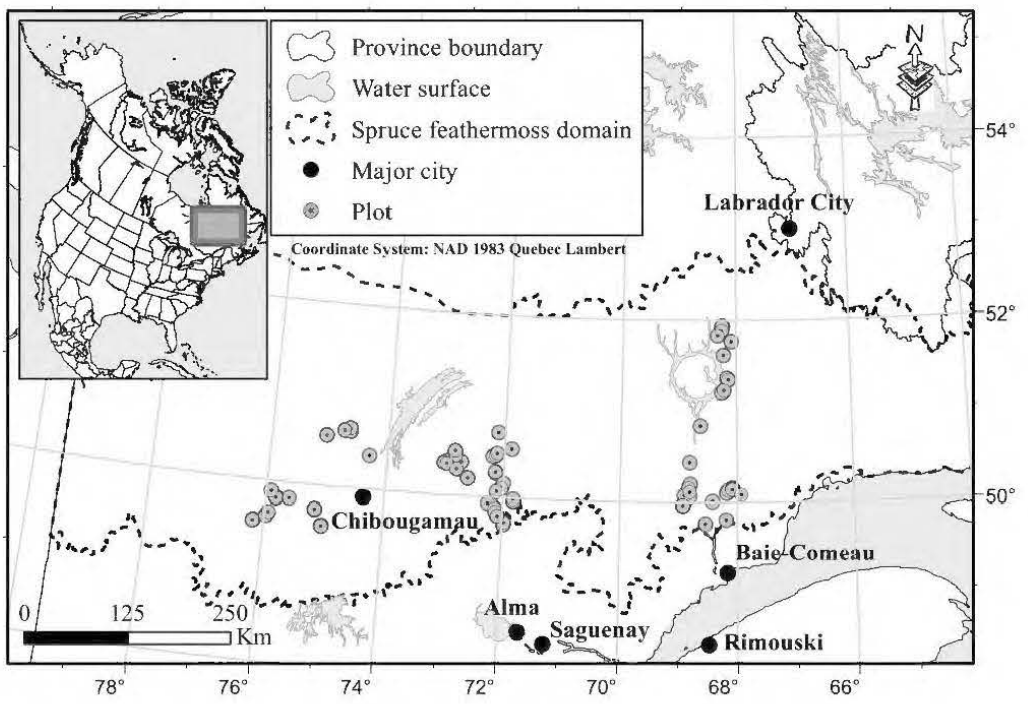

Figure 2.1 Map of the study area showing the spatial distribution of the sample plots (N = 72).

In this study region, the Canadian Shield bedrock is mainly composed of igneous (granitoïds) and metamorphic (gneiss, migmatites) materials formed during the

Precambrian, covered by glacial tills and localized fluvio-glacial deposits (Robitaille et Saucier, 1998). Topography is flat in the west and undulated with more pronounced slopes in the center and in the east. Regional climate is sub-polar sub-humid with mean annual temperatures ranging south to north from 0°C to -5°C. Mean annual precipitations ranges from west to east from 800 mm to 1300 mm (Robitaille et Saucier, 1998), reflecting continental climate and maritime influences on the regional climate (Ecological Stratification Working Group, 1996). The landscapes are dominated by black spruce (*Picea mariana* [Mill.] B.S.P) stands associated with ericaceous understory and feathermoss ground layers. The length of fire cycles typically increases north to south and west to east (Portier *et al.*, 2016). As a result, within a general matrix of black spruce, fire resistant jack pine (*Pinus banksiana* [Lamb.]) and fire intolerant balsam fir (*Abies balsamea* [L.] Mill.) exchange co-dominance across this fire gradient. In this territory where human density is very low, fires are naturally ignited by lightning strikes. Large and stand-replacing crown wildfires are common in these black spruce forests (Bergeron *et al.*, 2004; Rogers *et al.*, 2015). In burnt areas, as a result of crowning most trees are left dead following fire in pure black spruce stands (Kafka *et al.*, 2001; Fig.2). The thick forest floor layer developing under the black spruce canopy develop a thick organic layer that can be reduced by 60% with burning (Greene *et al.*, 2007), depending on its bulk density and its moisture content (Miyanishi et Johnson, 2002).

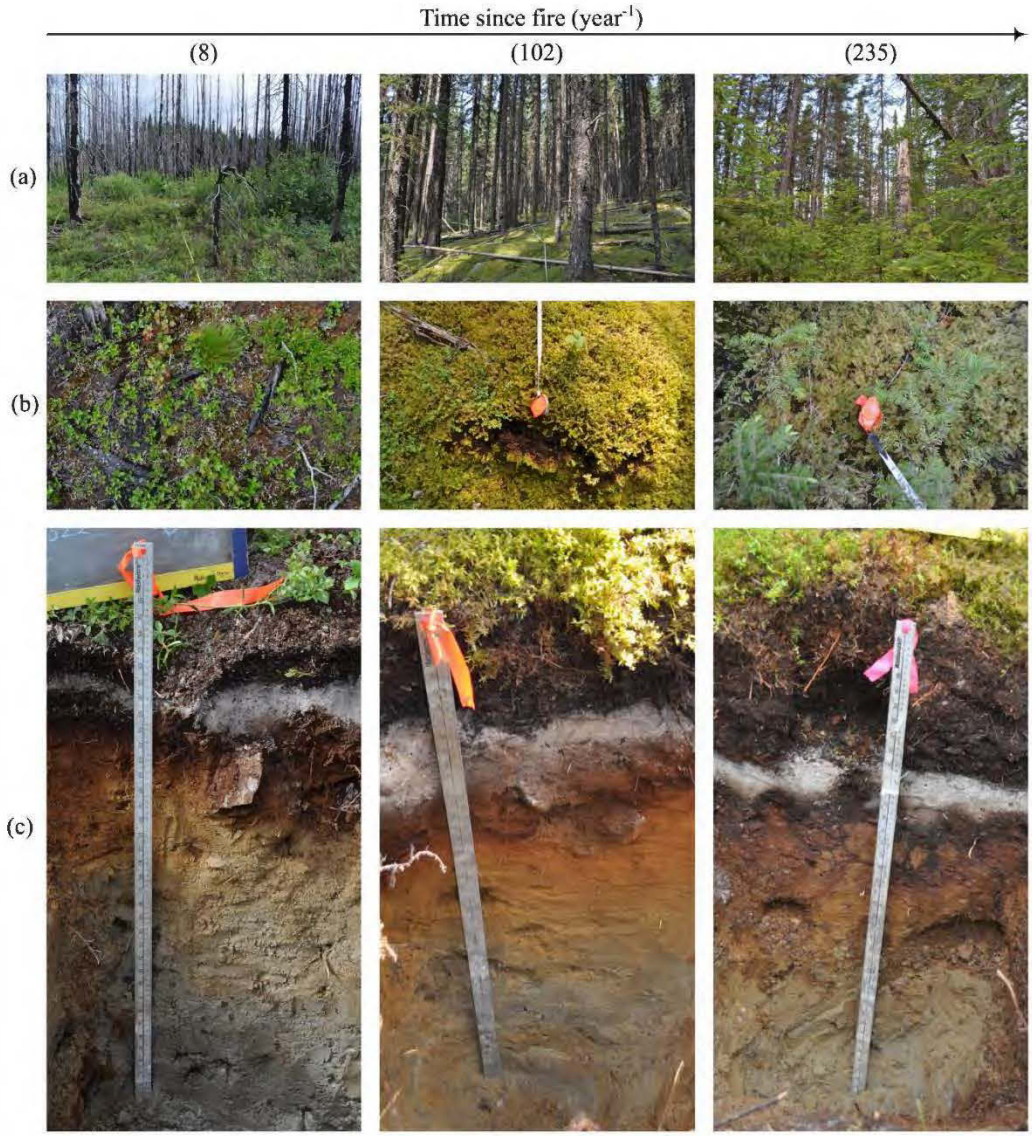

Figure 2.2 Set of field photos. Horizontal overall plan of the stand from the plot centre (a) shows the transition from dead trees to single age structure toward a more complex age-class structure with several cohorts and senescent trees when the stand gets older. View from above (b) captured the ground layers, with charred twigs and mosses after fire toward a dense moss carpet in mature stands, with seedlings benefiting from canopy opening in older stands. Soil pits (c) exhibit the organic layer depth and the podzolized mineral soil horizons (scale = 1 m).

2.4.2 Stand selection and field sampling design

Our goal was to establish sample plots across a chronosequence of time since fire (TSF). We used digital forest inventory maps produced between 1990-2000 and 2000-2010 by the ministère des Forêts, de la Faune et des Parcs du Québec (MFFPQ) to ensure that stands were as similar as possible in terms of canopy composition, surficial deposits and mesic drainage conditions. We used *ArcGIS* v10.2 to overlay these forest inventory maps with fire maps compiled by the MFFPQ and other published dendrochronological survey (Belisle *et al.*, 2011; Bouchard *et al.*, 2008; Cyr *et al.*, 2012; Frégeau *et al.*, 2015; Le Goff *et al.*, 2007; Portier *et al.*, 2016) in order to implement our chronosequence. When in doubt, stand age was verified in the field by coring 2-3 dominant trees, although none of these verifications came up with ages that were significantly different from those of the digital maps. The sampling effort thus planned covered 72 sites and was carried out in 2015.

Field inventory and soil sampling mostly followed Canada's National Forest Inventory ground plot guidelines (NFI (2016); Annexe B, Figure S2.1). In each stand, we established a single 314 m^2 circular plot (10 m radius) for biophysical descriptions and soil sampling. Slope was measured from the center of the plot with a clinometer, aspect with a compass, and stand basal area using a factor-2 prism. FH layer depth was measured every 2 m with a soil auger along two orthogonal transects following main cardinal directions, for a total of 20 measurements per plot. At the same point locations where FH layer depth was recorded, we identified the dominant moss at the genus level using 400 cm^2 microplots, for a total of 20 microplots per 314 m^2. We also recorded tree species, diameter and decay class of all downed coarse woody debris ($\geq$ 3 cm in diameter) crossing the two orthogonal transects. For the FH layer sampling, we selected three 400 cm^2 microplots, each separated by a minimum distance of 15 m. In these microplots, we first gathered the litter and the green living mosses layer separately. We

then collected volumetric samples of the FH layer down to the mineral soil (Preston *et al.*, 2006). After FH layer was carefully extracted, we sampled the mineral soil (top 15 cm) using volumetric samples with a metallic cylinder (height = 15 cm, inner diameter = 4.7 cm) in each of the three microplots. Finally, a soil pit was dug down to the illuvial (B) horizon or to the bedrock when possible. One wall of the pit was cleaned and the entire soil profile was described. Then, we collected samples from 15 to 35 cm under the FH layer-mineral soil boundary and in the illuvial horizon (top 15 cm) using volumetric samples with a metallic cylinder (inner diameter = 4.7 cm). Because of the stoniness in one site, we could not sample the mineral soil. Thereafter, this site was discarded from the analyses of soil C stocks. Soil samples were maintained at 2°C in a cooler before processing for analyses.

2.4.3 Laboratory analyses

For soil analyses, we used mean composite samples for each of the 72 sample plots where soil materials obtained from every microplot were pooled and mixed by plot and soil layer (FH layer or top 15 cm of mineral soil). FH layer was sieved at 6 mm and oven dried (60°C), whereas mineral soil samples were air dried and sieved through a 2-mm mesh. Dried samples were weighted to estimate bulk density before processing for physicochemical analyses.

All samples were finely ground (0.5 mm) for C content or Fe and Al (illuvial horizon only) determination. Carbon concentration was analyzed by dry combustion (Skjemstad et Baldock, 2007) using a Leco TruMac (Leco Corp., St. Joseph, MI, USA). Organically-complexed Fe and Al (Mpy), hereafter defined as metal oxides, were extracted with a tetrasodium pyrosphosphate solution ($Na_4P_2O_7$ 0.1 N) and analyzed by inductively coupled plasma atomic emission spectroscopy (Courchesne et Turmel,

2007) with an Optima 7300 DV (Perkin Elmer Inc., Waltham, MA, USA). FH layer and mineral soil potential of hydrogen (pH) was determined in a soil:water solution of 1:10 and 1:2 (Hendershot et Lalande, 2007), respectively, with a pH meter (Orion 2 Star) and soil texture was assessed by a standard hydrometer method (Kroetsch et Wang, 2007). Because bedrocks are acidic and soil pH is low (3.3 < FH layer pH < 4.2; 4.4 < illuvial horizon pH < 5.7), we did not expect any carbonates in soil samples, and total C is considered here as organic C (Strand *et al.*, 2016).

All laboratory analyses were carried out at the Laurentian Forestry Center in Québec, QC, Canada.

2.4.4 Carbon pool calculations

We calculated C stock in aboveground tree biomass separately for each plot using basal area field measurements and the allometric equation of Paré *et al.* (2013), assuming half C in the total biomass:

$$C_{ABG} = \frac{1}{2}\sum(a \times B_S^b \times B_T^c)$$

where C_{ABG} is the aboveground C density (MgC.ha^{-1}), B_S is the basal area for a species S (m².ha^{-1}), B_T is the total basal area (m².ha^{-1}), and a, b and c are parameters whose values are species-specific.

We calculated C stock in coarse woody debris according to the line intersect method of Van Wagner (1968) assuming total biomass contains half C (Wang, C. *et al.*, 2003), as follows:

$$C_{CWD} = \left(\frac{\pi^2 \sum(d^2 D_{WS})}{8L}\right) \times 0.5$$

where C_{CWD} is the C density in coarse woody debris (kgC.ha^{-1}), d is piece diameter (cm), D_{WS} is the wood density (kg.m^{-3}) for a species S and for a given decay class (unpublished internal database: National Forest Inventory Project Office), and L is the total measured transect length (m).

We calculated soil C content for each sample by multiplying its C concentration with its respective bulk density and depth (here, equals to mean depth based on 20 measurements for the FH layer), assuming there were no coarse fragments in FH layer, and corrected for coarse fragments (> 2 mm) in the mineral soil horizons.

Because of some very stony mineral soils, some samples (samples 15-35 cm, n = 8; samples 0-15 cm in the illuvial horizon, n = 5) had to be extracted in a non-volumetric manner. Based on the other samples of our database, we estimated their bulk density using a nonlinear organic density model developed by Federer *et al.* (1993) and successfully used by Périé et Ouimet (2008) in soils of eastern North America:

$$D_b = \frac{D_{bm}\, D_{bo}}{(F_o\, D_{bm}) + (1 - F_o)\, D_{bo}}$$

where D_b is the bulk density, D_{bm} is the bulk density of "pure" mineral soil material (i.e. soil without any organic fraction), D_{bo} is the bulk density of "pure" organic soil (i.e. soil without any mineral fraction), and F_o is the organic mass fraction of the sample. Whereas only C concentration was analyzed here, we assumed a conversion factor of 2 (Pribyl, 2010) to estimate the value of F_o.

Mineral soil C stocks were summed across horizons (top 15 cm and 15 to 35 cm deep) and other mineral soil explanatory variables were transformed with a weighted mean by depth for subsequent statistical analysis. For this study, we did not use the litter plus green living mosses carbon pool because this C reservoir was very small (Taylor *et al.*, 2014). All C stocks are reported in tons per hectare ($MgC.ha^{-1}$) hereafter.

2.4.5 Climatic data

Climatic data were generated using BioSIM v10.3.2 (Régnière *et al.*, 2013). Based on current knowledge and *a priori* hypotheses, we selected mean annual temperature (MAT), mean annual precipitation (MAP), annual growing degree-days above 5°C (GDD5) and water balance (WB, i.e. annual precipitation minus potential evapotranspiration) as the main possible climatic drivers of soil C stocks in our analyses. We used the 1981-2010 climate normals (http://climat.meteo.gc.ca/) to interpolate these climatic drivers at the plot level from the eight nearest surrounding weather stations, considering local field-measured slope attributes as correcting factors (for more details, see Régnière (1996)). The Canadian climate normals used in this study are meteorological daily records of weather stations across the national territory. Following the World Meteorological Organization standards, normals are computed with the arithmetic mean for each month within a year, over a 30-year period.

2.4.6 Ground layer dominance

To discriminate the importance of *Sphagnum* spp. from that of feathermoss species holding different ecophysiological characteristics (Bisbee *et al.*, 2001), we calculated an index of moss dominance (IMD) inspired by Nalder et Wein (1999) as follows:

$$IMD = \frac{O_{sph}}{O_{sph} + O_{pl} + O_h + O_{pt}}$$

where O is the sum of occurrence for a species in the 20 (20 x 20 cm²) microplots, *sph*: *Sphagnum* spp., *pl*: *Pleurozium schreberi* (Brid.) Mitt., *h*: *Hylocomium splendens* (Hedw.) Schimp., and *pt*: *Ptilium crista-castrensis* (Hedw.).

When the IMD tends towards 1, the moss stratum is dominated by *Sphagnum* spp., whereas when the IMD tends towards 0, other moss species dominate the moss stratum. For plots where fire was recent and no moss species were observed (n = 5), the IMD was set to 0. We detected no significant changes in the results when excluding or including these plots in our analyses.

2.4.7 Ecological a priori hypotheses

The chronosequence approach used in our study implies the existence of a single successional trajectory (Kenkel *et al.*, 1997). In black spruce-dominated forests of eastern North America, Frégeau *et al.* (2015) inferred from paleological data that the local vegetation has developed under recurrent dynamics (i.e., the cyclic return to a black spruce dominance after fire) for several millennia. Thus, we assumed there were no changes in canopy composition with time and that the current vegetation has developed from similar vegetation. Also, the low vegetation diversity in the study area together with the single and cyclic successional trajectory make space-for-time inferences suitable (Walker *et al.*, 2010).

The following environmental variables were considered as important drivers of soil C storage within boreal forest ecosystems and were included in our analyses: climate

(temperature and water supply), soil texture, TSF, dominance of the moss functional type, soil pH and concentration in metal oxides. Based on our overall dataset, preliminary results showed that carbon stocks in the FH layer and in the mineral horizons were uncorrelated (Annexe B, Figure S2.2). Moreover, numerous studies have already shown that C storage patterns in the FH layer and mineral soil are often governed by different processes (Fierer, Noah *et al.*, 2003; Salomé *et al.*, 2010; Ziegler *et al.*, 2017). We therefore built, for each of these two C pools, separate sets of *a priori* ecological hypotheses using direct acyclic graphs (DAGs) representing different causal relationships among environmental variables and C stocks (Figure 2.3). This led us to test the validity of six competing *a priori* ecological hypotheses, each being represented by a DAG. We used a hypothetico-deductive approach in which each *a priori* hypothesis was coherent with ecological knowledge and represented an alternative causal explanation that could be falsified as regards the underlying mechanisms of soil C storage in the two main C pools. The first two hypotheses, one for each C pool (hypothesis FH0 and B0 in Figure 2.3), assume direct relationships between variables and C stocks, as well as statistical independence among variables. These two hypotheses were used as baseline for comparisons since they mirror the dominant approach with only direct effects used in the literature to assess the effect of environmental variables on soil C stocks (for example, see Marty *et al.* (2015); Nalder et Wein (1999); Strand *et al.* (2016)), which uses Jenny's factor model of soil formation (Jenny, 1994). We also formulated a set of *a priori* competing hypotheses involving indirect effects among variables and C stocks (hypotheses FH1, FH2, B1 and B2 in Figure 2.3).

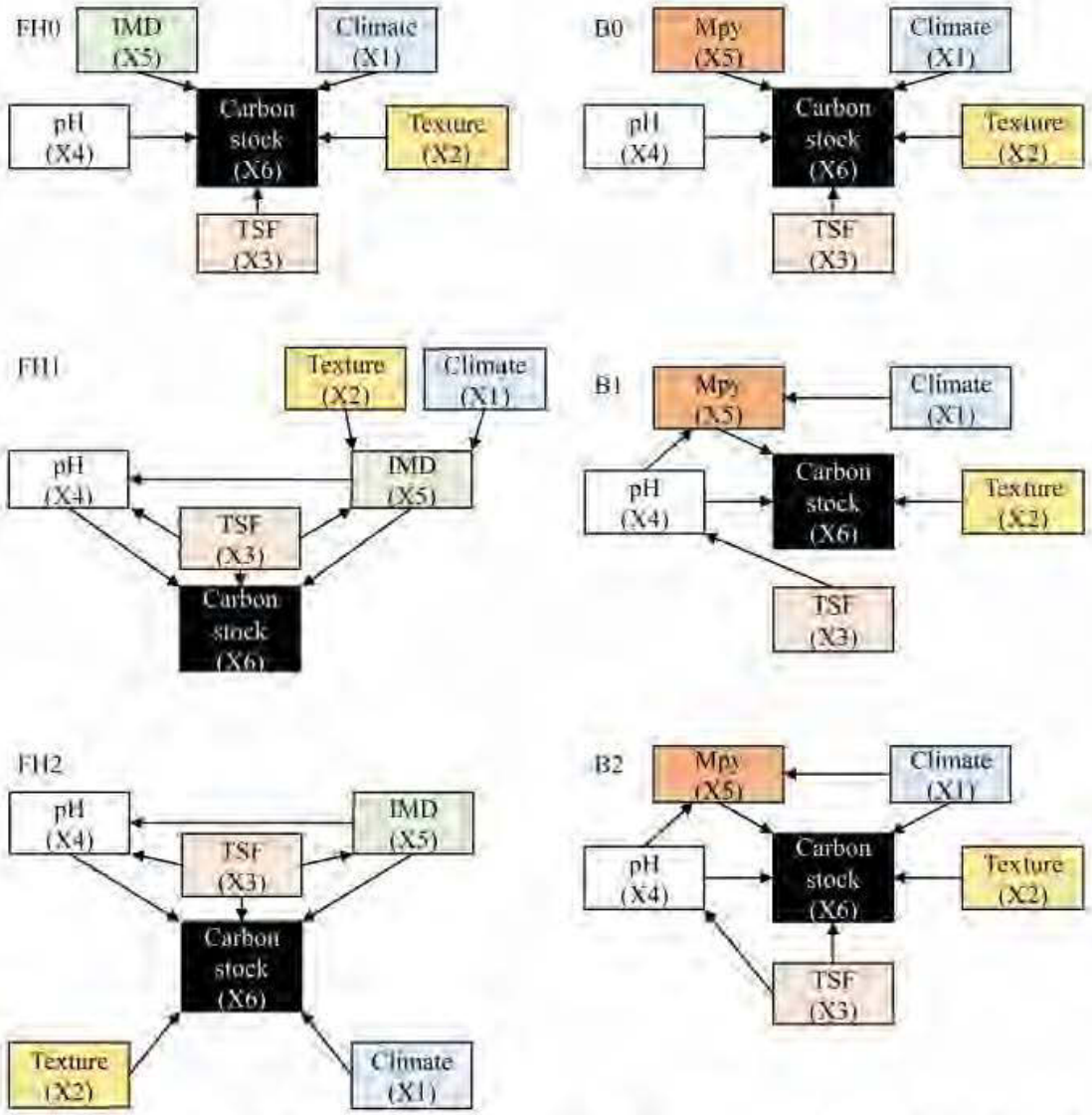

Figure 2.3 Path models for multivariate causal hypotheses testing FH layer C stocks (FH0, FH1 and FH2) and illuvial horizon C stocks (B0, B1 and B2). Arrows indicate direct causal effects. *Climate*: climate variable; *Texture*: texture of the mineral soil (top 35 cm); *TSF*: time since fire; *pH*: potential of hydrogen in the FH layer (FH models) or illuvial horizon (B models); *IMD*: index of moss dominance; *Mpy*: pyrophosphate extractable metals in the illuvial horizon.

Ecological justification for each *a priori* hypothesis represented by a different DAG (Figure 2.3) is given below:

Baseline hypothesis for the FH layer, FH0. In this hypothesis, fire directly affects FH layer pool size through direct combustion and FH layer buildup with TSF (Harden *et al.*, 2012; Knicker, 2007). Climatic conditions and pH both have direct effects on C accumulation because they are key determinants of the decomposition process (Prescott *et al.*, 2000; Zhang *et al.*, 2008). Climate and pH also are important drivers of the substrate use efficiency of soil microbes (Cotrufo *et al.*, 2013), but their relative contributions remain unknown. Several studies have reported that the dominance of the ground layer vegetation also influences C accumulation processes (Bisbee *et al.*, 2001; Bona *et al.*, 2013). Feathermosses have a higher decomposability (Fenton *et al.*, 2010; Lang *et al.*, 2009) and lesser productivity (Bisbee *et al.*, 2001) than sphagna, so we expected more C accumulation in the FH layer with the increasing dominance of sphagna. Finally, waterlogged conditions are known to promote anoxic environment impeding microbial decomposition, so rapid draining on coarse-textured soils may favor faster soil organic matter decomposition (Bauhus *et al.*, 1998; Trumbore et Harden, 1997).

Alternative hypothesis for the FH layer, FH1. In this hypothesis, as in hypothesis FH0, fire has a direct effect on C stocks through changes in FH layer pool size with TSF. However, contrary to hypothesis FH0, hypothesis FH1 postulates that TSF also has indirect effects on C stocks through direct effects on pH conditions and on the moss dominance, as supported by empirical studies (Simard *et al.*, 2007; Ward *et al.*, 2014). FH1 hypothesis also postulates that climate conditions and soil texture influence C stocks only indirectly through their direct and synergic effects on the change of dominance in the ground layer from feathermosses to sphagnum species. Fire can modify soil pH through organic acid denaturation and neutralization of acidity by base-

saturated ash materials (Certini, 2005; Gonzalez-Perez *et al.*, 2004; Knicker, 2007). In addition, FH layer pH has been shown to decrease with TSF in the mesic black spruce forests of eastern Quebec (Ward *et al.*, 2014), as well as in most aggrading forests, due to the imbalance of charge in nutrient uptake (Driscoll et Likens, 1982). More specifically, protons are exchanged by roots when cations are taken up by growing vegetation in excess compared to anions. When the vegetation maintains physiological electroneutrality, it leads to soil acidification. Simard *et al.* (2007) reported a shift in ground layer dominance with TSF on poorly-drained fine textured soil, suggesting that under these conditions, an increasing dominance of sphagnum species may be expected in the ground layer with increasing TSF. The IMD may have a direct effect on pH because sphagnum mosses have distinct physiological characteristics (release of polyuronic, humic and fulvic acids during decomposition, and hyaline cells retaining water) involved in the acidification of their environment relative to feathermosses (Lavoie *et al.*, 2005) and the drawing of water from the water table (Bisbee *et al.*, 2001), which create conditions that favor the maintenance and spread of sphagnum colonies. Hence, contrary to hypothesis FH0, hypothesis FH1 postulates that climate has a direct effect on the IMD because we expected that feathermosses would be more dependent on water availability than sphagna.

Alternative hypothesis for the FH layer, FH2. This hypothesis is a combination of FH0 and FH1. In this hypothesis, TSF is predicted to have both direct and indirect effects on C stocks according to the same causal relationships as in hypothesis FH1. However, hypothesis FH2 differs from hypothesis FH1 in that climate conditions and soil texture only have direct effects on C stocks, irrespective of the dominance of feathermoss versus sphagnum species. Sphagnum spp. occurrence is mostly related to local hydraulic parameters and available light (Bisbee *et al.*, 2001), and because we controlled for drainage conditions in our study, we could expect ground layer dominance to be independent of soil texture and climate.

Baseline hypothesis for the illuvial horizon, B0. In this hypothesis, variables are assumed to have only direct and independent effects on C stocks in the illuvial horizon. Metal oxides and fine mineral particles are known to bind C in mineral soils (organometallic complexation and adsorption) (Kaiser *et al.*, 2002; Rumpel et Kögel-Knabner, 2011; Soucémarianadin *et al.*, 2014). This suggests that C stocks in the mineral soil will increase with concentrations of metal oxides or fine mineral particles. Acidity slows the activity of decomposers (see hypothesis FH0), whereas a wetter and a warmer climate enhances C accumulation in the mineral soil (Buurman et Jongmans, 2005; Liski et Westman, 1997; Sanborn *et al.*, 2011; Strand *et al.*, 2016). This is supposedly due to an above- and belowground litter production that is imbalanced with the activity of decomposers in well-drained soils (Callesen *et al.*, 2003), which allows for larger organic matter inputs to the mineral soil that can potentially be stabilized through complexation and adsorption on the inorganic mineral phase. The effect of fire on C stocks in the mineral soil is still ambiguous in the literature and is often assumed to be negligible (Deluca et Boisvenue, 2012; Knicker, 2007; Seedre *et al.*, 2011). Nevertheless, we assumed a direct effect of TSF on C stocks in the illuvial horizon as some studies have shown that C stocks in the mineral soil were larger in old forests compared with adjacent burnt stands (Smith *et al.*, 2000), or that they accumulated slightly with TSF (Johnson et Curtis, 2001; Pregitzer et Euskirchen, 2004).

Alternative hypothesis for the illuvial horizon, B1. In this hypothesis, climate exerts an indirect control only on C stocks (Doetterl *et al.*, 2015) through its direct effect on mineral weathering and on the amounts of metal oxides leached from the upper horizons (Egli *et al.*, 2009). Soil pH is hypothesized to have both a direct effect on C stocks through changes brought to the decomposition process and an indirect effect on C stocks through changes occurring in the creation of organometallic complexes (Buurman et Jongmans, 2005; Porras *et al.*, 2017). Time since fire exerts an indirect effect on C stocks by influencing soil pH through the liming effect within the first few

years after fire (see FH1), whereas over the long term, mineral soil acidifies through a charge imbalance in the nutrient uptake with vegetation growth (Driscoll et Likens, 1982).

Alternative hypothesis for the illuvial horizon, B2. This hypothesis is a combination of B0 and B1. In this hypothesis, climate and TSF are predicted to have both direct and indirect effects on C stocks according to the same causal relationships as in hypotheses B0 and B1. The direct effect of TSF on illuvial horizon C stocks arises from the slow incorporation of charcoal and hydrophobic organic matter into the mineral soil following fire (Johnson and Curtis, 2001). The indirect effect of TSF on illuvial horizon C stocks is attributed to changes in the mineral soil pH with TSF (see FH1). Climate has a direct effect on illuvial horizon C stocks through its direct effect on litter inputs and on the decomposition process (see B0). Climate also has an indirect effect on illuvial horizon C stocks through its direct effect on mineral weathering and leaching (see B1).

2.4.8 Statistical analyses

First, we evaluated post-fire C dynamics using linear regression of C pools with TSF. When a curvature in the relationship was observed, we used a piecewise regression with the R package *'segmented'* (Muggeo, 2008) to extract breakpoint coordinates. Second, we used confirmatory path analysis with directional separation tests (*d-separation* or *d-sep*; Shipley (2000a)) to quantify direct and indirect causal relationships between variables and C stocks according to the set of alternative *a priori* ecological hypotheses described above (Figure 2.3). We used path analysis together with Fisher's *C* test (Shipley, 2000b) as a simultaneous test of independence for a model basis set (i.e. all non-adjacent pairs of variables defined as claims of

independence) in order to assess how each hypothetical DAG was supported by our data and to identify which hypothesis could be rejected or not based on a robust statistical test (Shipley, 2009). Fisher's *C* statistic was compared to a chi-squared distribution with 2k degrees of freedom (where k is the number of independence claims in a model basis set). We chose the significance level of 0.05 to decide when to reject a causal model (rejected when $p < 0.05$). All variables were standardized (i.e., centered on the mean and divided by the standard deviation) prior to analyses to quantify their relative contributions to C stocks variability.

We compared the fit of each DAG within each C pool using a model selection approach (Shipley, 2013) together with the second order Akaike's information criterion (AICc) in order to account for finite sample size (N = 71). Model selection was based on relative AICc difference with the 'best model' or relative weight (Symonds et Moussalli, 2010). As we had no *a priori* knowledge about which specific climate and texture variables should be used for testing the validity of each hypothesis/DAG, we used the cross-product of four climatic (MAT, MAP, GDD and WB) and three soil texture (sand %, silt % and clay %) variables, which yielded a total of 12 model combinations to be tested for each hypothesis/DAG. As we had three different hypotheses in both C pools, the model selection procedure resulted in the comparison of 36 candidate DAG models for each C pool. We calculated model-averaged estimates by multiplying each estimate within each model by the corresponding Akaike weight and by summing the resulting values across all models. By doing so, we avoided making arbitrary decisions about which model should be considered by allowing all models to influence model-averaged estimates. Path analyses were conducted using the *'ggm'* package (Marchetti *et al.*, 2015) and all calculations and statistical analyses were made with *R* software version 3.0.2 (R Core Team, 2017). All data presented in this paper can be retrieved online for free (Andrieux *et al.*, 2018a).

2.5 Results

2.5.1 Post-fire carbon dynamics

Across our plots, carbon (C) accumulated with increasing time since fire (TSF), but the shape of this accumulation varied by pool (Figure 2.4). Total ecosystem C stock tended to increase linearly (Figure 2.4a), ranging from 83 $MgC.ha^{-1}$ to 356 $MgC.ha^{-1}$ for TSF values of 2 years and 283 years, respectively. Aboveground tree C stock (Figure 2.4b) was negligible in the first decades after fire, peaked at 90 ± 9 years, and showed a significant ($p = 0.02$) but minor decrease in older stands. The maximum observed aboveground tree C stock was 105 $MgC.ha^{-1}$ in a 91-year-old stand. The C stock in coarse woody debris first decreased until 51 ± 11 years, and then increased until TSF reached 237 ± 25 years. The maximum observed C stock in coarse woody debris was 19 $MgC.ha^{-1}$ in a 10-year-old stand. Values of C stocks in coarse woody debris were negligible for values of TSF between 48 and 91 years. Coarse woody debris was found to be the smallest of all ecosystem C pools (Figure 2.4c). FH layer C stock generally increased linearly with TSF, but showed a very high variability around this trend. The lowest and highest values of 26 $MgC.ha^{-1}$ and 217 $MgC.ha^{-1}$ were found in plots with TSF values of 102 years and 91 years respectively (Figure 2.4d). Mineral soil (top 35 cm) C stock also increased linearly with TSF and also showed a high variability in measured values. The lowest and highest values of 19 $MgC.ha^{-1}$ and 159 $MgC.ha^{-1}$ were found in plots with TSF values of 171 years and 314 years, respectively (Figure 2.4e).

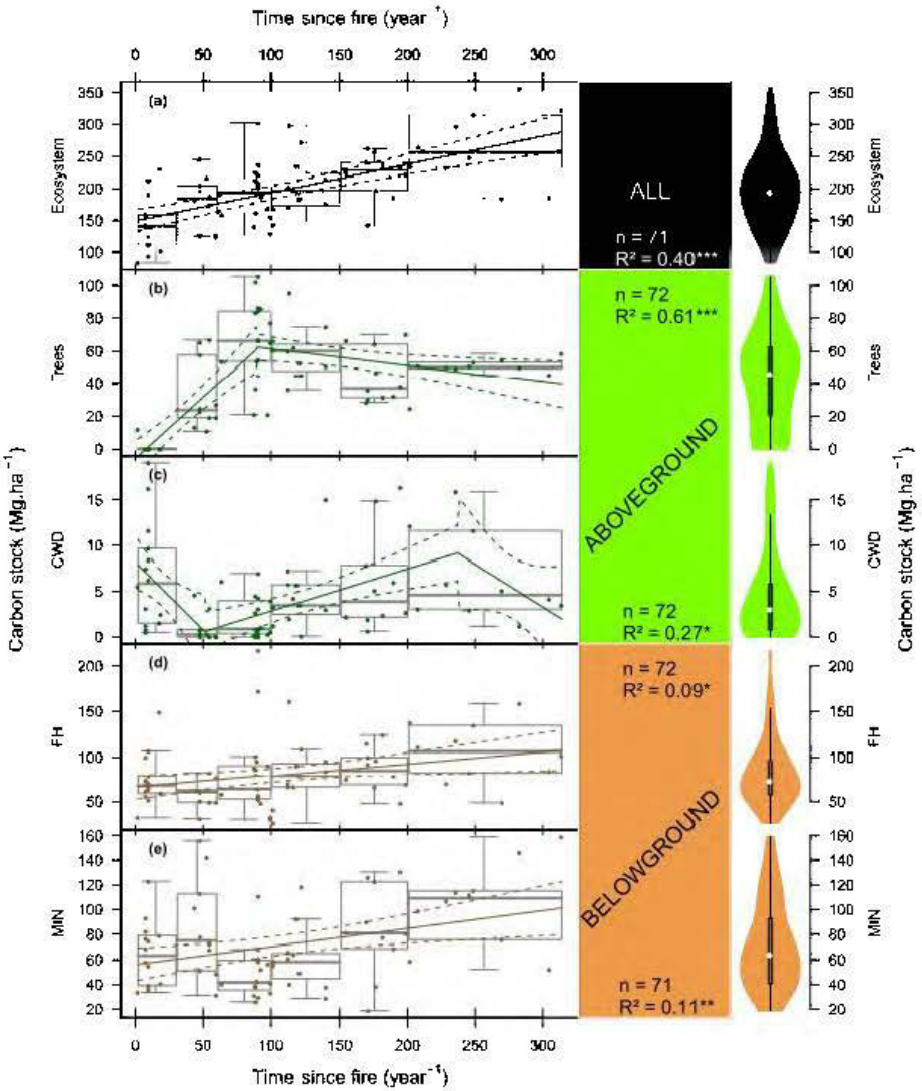

Figure 2.4 Observed (points) and predicted (plain lines) post-fire carbon stocks with 95% confidence interval (dashed lines) as a function of time since fire and the type of aboveground (green) or belowground (maroon) carbon pool, with boxplots representing age-class carbon stock distribution (limits at 2, 30, 60, 100, 150, 200 and 314 years; see Annexe B, Figure S2.3 for the number of plots per age-class) (left panel). Violin plots show the kernel density of observed carbon stocks within each carbon pool (right panel). *Ecosystem (a)*: sum of all carbon pools; *Trees (b)*: aboveground trees; *CWD (c)*: lying coarse woody debris; *FH (d)*: FH layer; *MIN (e)*: top 35 cm of mineral soil. (*) $p \leq 0.05$; (**) $p \leq 0.01$; (***) $p \leq 0.001$.

The simple linear functions using TSF as sole explanatory variable explained 40% (for ecosystem), 61% (for aboveground tree biomass), 27% (for coarse woody debris), 9% (for FH layer) and 11% (for mineral soil) of C stock variability. According to these simple linear models, the ecosystem accumulated 0.44 $MgC.ha^{-1}.yr^{-1}$ ($p < 0.001$) (Table 2.1). In the first 90 ± 9 years following fire, aboveground tree showed the greatest C accumulation rate, followed by FH layer and mineral soil (Table 2.1).

Table 2.1 Equation parameters and statistics in linear trends of carbon stocks ($MgC.ha^{-1}$) changes with time since fire (yr^{-1}) for the main ecosystem carbon pools.

Carbon pool ($MgC.ha^{-1}$)	Number of breakpoints	Breakpoint (years ± sd)	Equation before breakpoint	Equation after breakpoint	R^2	p-value
Ecosystem						
	0	-	149.20 + 0.44 (TSF)	-	0.40	< 0.001
Aboveground trees						
	1	90 ± 9	-5.93 + 0.75 (TSF)	71.57 - 0.10 (TSF)	0.61	< 0.001
Coarse woody debris						
	2	51 ± 12 237 ± 25	8.17 - 0.15 (TSF) -1.78 + 0.05 (TSF)	-1.78 + 0.05 (TSF) 31.94 - 0.10 (TSF)	0.27	0.012
FH layer						
	0	-	66.00 + 0.13 (TSF)	-	0.09	0.011
Mineral soil (top 35 cm)						
	0	-	56.05 + 0.14 (TSF)	-	0.11	0.004

2.5.2 FH layer path analysis and model selection

The first hypothesis (FH0) testing for direct effects of variables on FH layer C stocks was rejected based on Fisher's *C* statistic ($p < 0.01$), whereas most models related to FH1 and FH2 were not (Table 2.2). According to the model selection procedure, the two competing path models that best explained the data ($\Delta AICc < 2$; Table 2.2), both belonged to hypothesis FH1 with water availability (MAP or WB) as climate variable and clay content as texture variable. Together, these two path models accounted for 74% of the Akaike weight and explained 44% and 46% of the variation between covariables and FH layer C stocks (FH1 with WB and clay % and FH1 with MAP and clay %, respectively; Figure 2.5 and Annexe B, Table S1.1). We therefore concentrated our analyses on these two FH1-based path models.

Table 2.2 Model comparisons for alternative *a priori* hypotheses, each testing for different causal relationships among variables and carbon stocks in the FH layer of the boreal forest of eastern North America (see Figure 2.3 for details about the Directed Acyclic Graph (DAG) associated with each hypothesis). The two competing path models that best explain the data ($\Delta AICc \leq 2$) are in bold font.

Hypothesis	Climate	Texture	C statistic (df, p)	K	AICc	ΔAICc	W
FH1	**WB**	**Clay %**	**8.956 (14, 0.83)**	**11**	**35.43**	**0**	**0.40**
FH1	**MAP**	**Clay %**	**9.294 (14, 0.81)**	**11**	**35.77**	**0.34**	**0.34**
FH1	GDD5	Clay %	11.996 (14, 0.61)	11	38.47	3.04	0.09
FH1	GDD5	Silt %	14.009 (14, 0.45)	11	40.48	5.05	0.03
FH2	WB	Clay %	14.643 (14, 0.40)	11	41.12	5.69	0.02
FH2	GDD5	Clay %	15.103 (14, 0.37)	11	41.58	6.15	0.02
FH1	MAT	Clay %	15.248 (14, 0.36)	11	41.72	6.29	0.02
FH1	WB	Sand %	15.416 (14, 0.35)	11	41.89	6.46	0.02
FH1	GDD5	Sand %	15.422 (14, 0.35)	11	41.90	6.47	0.02

Table 2.2 (suite)

Hypothesis	Climate	Texture	C statistic (df, p)	K	AICc	ΔAICc	W
FH2	GDD5	Silt %	16.357 (14, 0.29)	11	42.83	7.4	0.01
FH2	GDD5	Sand %	16.629 (14, 0.28)	11	43.10	7.67	0.01
FH1	WB	Silt %	16.710 (14, 0.27)	11	43.18	7.75	0.01
FH2	MAP	Clay %	17.517 (14, 0.23)	11	43.99	8.56	0.01
FH1	MAP	Sand %	18.166 (14, 0.20)	11	44.64	9.21	0
FH1	MAT	Silt %	18.572 (14, 0.18)	11	45.05	9.62	0
FH2	MAT	Clay %	18.874 (14, 0.17)	11	45.35	9.92	0
FH1	MAP	Silt %	19.175 (14, 0.16)	11	45.65	10.22	0
FH2	WB	Sand %	19.202 (14, 0.16)	11	45.68	10.25	0
FH1	MAT	Sand %	19.214 (14, 0.16)	11	45.69	10.26	0
FH2	MAT	Sand %	20.939 (14, 0.10)	11	47.41	11.98	0
FH2	MAT	Silt %	21.438 (14, 0.09)	11	47.91	12.48	0
FH2	WB	Silt %	21.637 (14, 0.09)	11	48.11	12.68	0
FH2	MAP	Sand %	24.487 (14, 0.04)	11	50.96	15.53	0
FH0	GDD5	Clay %	37.746 (20, 0.01)	6	51.06	15.63	0
FH0	WB	Clay %	38.410 (20, 0.01)	6	51.72	16.29	0
FH0	GDD5	Silt %	39.458 (20, 0.01)	6	52.77	17.34	0
FH0	GDD5	Sand %	39.727 (20, 0.01)	6	53.04	17.61	0
FH2	MAP	Silt %	26.637 (14, 0.02)	11	53.11	17.68	0
FH0	MAP	Clay %	42.112 (20, < 0.01)	6	55.42	19.99	0
FH0	WB	Sand %	43.425 (20, < 0.01)	6	56.74	21.31	0
FH0	MAT	Clay %	43.895 (20, < 0.01)	6	57.21	21.78	0
FH0	WB	Silt %	45.863 (20, < 0.01)	6	59.18	23.75	0
FH0	MAT	Sand %	46.416 (20, < 0.01)	6	59.73	24.3	0
FH0	MAT	Silt %	46.917 (20, < 0.01)	6	60.23	24.8	0
FH0	MAP	Sand %	49.539 (20, < 0.01)	6	62.85	27.42	0
FH0	MAP	Silt %	51.691 (20, < 0.01)	6	65.00	29.57	0

MAT, mean annual temperature; *MAP*, mean annual precipitation; *GDD5*, growing degree-days above 5°C; WB, water balance; *C statistic* (df: degree of freedom, p: probability of compliance of the basis set with the conditions of independence testing the hypothesized causal structure of the DAG); *K*, number of free parameters; *AICc*, second order Akaike's information criterion; *ΔAICc*, relative AICc difference with the 'best model'; *W*: Akaike weight.

Overall, in the FH1 hypothesis, TSF showed the greatest direct effect on FH layer C stocks (standardized path coefficient, pc = 0.37, $p < 0.01$), followed by moss layer dominance (pc = 0.31, $p < 0.01$). The value of pH decreased with TSF (pc = -0.32, $p < 0.01$), but increased with IMD (pc = 0.31, $p < 0.01$). The index of moss dominance significantly decreased with increasing values of WB or MAP (pc = -0.27, $p < 0.05$ or pc = -0.33, $p < 0.01$, respectively), suggesting that either WB or MAP have an indirect effect on FH layer C accumulation (indirect path coefficient, $pc_i = -0.08$ or $pc_i = -0.10$) through their influence on moss dominance. When accounting for the effect of other variables, the direct effects of pH on FH layer C stocks, of TSF on moss dominance, and of clay content on moss dominance all became non-significant in the FH1 hypothesis ($p > 0.05$).

When averaging path coefficients (Annexe B, Table S2.1), the most important variables exerting a direct control on FH layer C stocks were found to be, in decreasing order of importance, TSF (model-averaged estimator, $pc_{avg} = 0.37$) and moss dominance ($pc_{avg} = 0.32$). Direct effects of pH ($pc_{avg} = 0.13$), climate ($pc_{avg} = 0$) and soil texture ($pc_{avg} = -0.01$) were either non-significant or negligible.

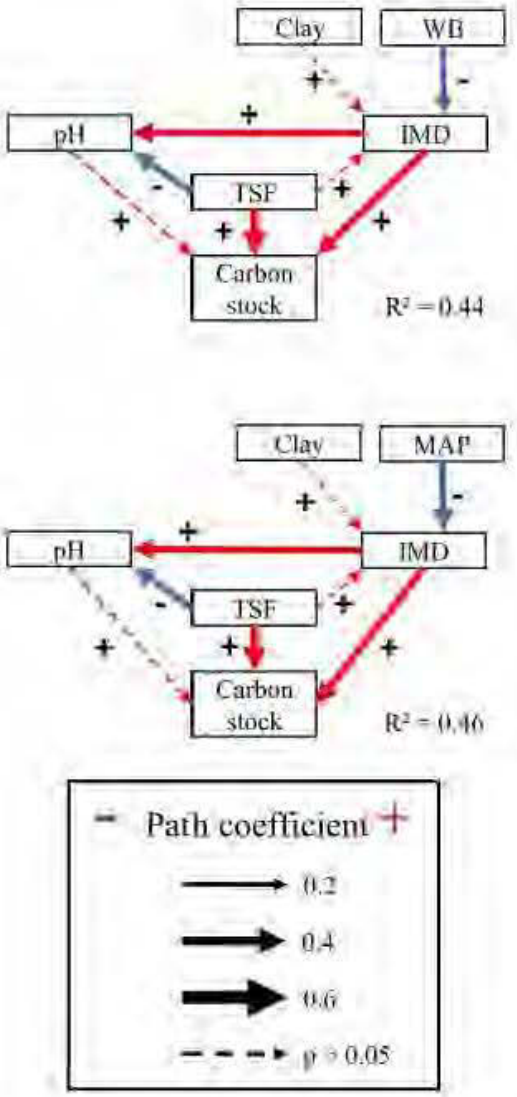

Figure 2.5 The two minimum adequate path models based on the FH1 hypothesis that best fit the data to explain FH layer carbon stock variability. Arrows indicate direct causal relationships between variables. Arrow widths are proportional to path coefficients. Red or blue arrows show positive or negative path coefficients, respectively. Plain or dashed arrows depict significant ($p \leq 0.05$) or non-significant ($p > 0.05$) causal relationships between variables, respectively. *WB*, water balance; *MAP*, mean annual precipitation; *Clay*, mineral soil (top 35 cm) clay content; *TSF*, time since fire; *pH*, FH layer potential of hydrogen; *IMD*, index of moss dominance.

2.5.3 Mineral soil path analysis and model selection

The first hypothesis (B0) testing for direct effects of variables on illuvial horizon carbon stocks was rejected based on Fisher's *C* statistic ($p < 0.01$), whereas most models related to B1 and B2 hypotheses were not (Table 2.3). Six path models best explained the data ($\Delta AICc < 2$; Table 2.3) and all included clay content as texture variable. For climate variables, the two best path models belonging to hypothesis B1 had WB or MAT as the best climate explanatory variables. The four other best path models belonging to hypothesis B2 had GDD5 and MAP in addition to WB and MAT as the best climate explanatory variables. Together, those six path models accounted for 83% of the Akaike weight.

Table 2.3 Model comparisons for alternative *a priori* hypotheses, each testing for different causal relationships among variables and carbon stocks in the illuvial (B) horizon of the boreal forest of eastern North America (see Figure 2.3 for details about the Directed Acyclic Graph (DAG) associated with each hypothesis). The six competing path models that best explain the data ($\Delta AICc \leq 2$) are in bold font.

Hypothesis	Climate	Texture	C statistic (df, p)	K	AICc	ΔAIC	W
B2	**WB**	**Clay %**	**14.554 (14, 0.41)**	**12**	**43.93**	**0**	**0.18**
B1	**MAT**	**Clay %**	**20.528 (18, 0.30)**	**10**	**44.19**	**0.26**	**0.16**
B2	**MAT**	**Clay %**	**14.918 (14, 0.38)**	**12**	**44.3**	**0.37**	**0.15**
B1	**WB**	**Clay %**	**20.684 (18, 0.30)**	**10**	**44.35**	**0.42**	**0.14**
B2	**GDD5**	**Clay %**	**15.585 (14, 0.34)**	**12**	**44.96**	**1.03**	**0.11**
B2	**MAP**	**Clay %**	**15.944 (14, 0.32)**	**12**	**45.32**	**1.39**	**0.09**
B1	GDD5	Clay %	22.766 (18, 0.20)	10	46.43	2.50	0.05
B1	MAP	Clay %	22.885 (18, 0.20)	10	46.55	2.62	0.05
B1	MAT	Sand %	25.143 (18, 0.12)	10	48.81	4.88	0.02
B2	MAT	Sand %	19.461 (14, 0.15)	12	48.84	4.91	0.02
B2	GDD5	Sand %	19.498 (14, 0.15)	12	48.88	4.95	0.01
B2	WB	Sand %	20.663 (14, 0.11)	12	50.04	6.11	0.01
B1	WB	Sand %	26.579 (18, 0.09)	10	50.25	6.32	0.01
B1	GDD5	Sand %	26.859 (18, 0.08)	10	50.53	6.60	0.01

Table 2.3 (suite)

Hypothesis	Climate	Texture	C statistic (df, p)	K	AICc	ΔAIC	W
B2	GDD5	Silt %	21.884 (14, 0.08)	12	51.26	7.33	0
B1	MAT	Silt %	28.406 (18, 0.06)	10	52.07	8.14	0
B2	MAT	Silt %	22.731 (14, 0.06)	12	52.11	8.18	0
B1	GDD5	Silt %	29.308 (18, 0.04)	10	52.98	9.05	0
B2	MAP	Sand %	24.802 (14, 0.04)	12	54.18	10.25	0
B1	MAP	Sand %	31.568 (18, 0.02)	10	55.23	11.30	0
B2	WB	Silt %	26.506 (14, 0.02)	12	55.89	11.96	0
B1	WB	Silt %	32.376 (18, 0.02)	10	56.04	12.11	0
B2	MAP	Silt %	30.479 (14, 0.01)	12	59.86	15.93	0
B1	MAP	Silt %	37.245 (18, < 0.01)	10	60.91	16.98	0
B0	MAT	Clay %	49.722 (20, < 0.01)	7	65.50	21.57	0
B0	GDD5	Clay %	50.158 (20, < 0.01)	7	65.94	22.01	0
B0	WB	Clay %	50.597 (20, < 0.01)	7	66.37	22.44	0
B0	MAP	Clay %	50.809 (20, < 0.01)	7	66.59	22.66	0
B0	GDD5	Sand %	52.583 (20, < 0.01)	7	68.36	24.43	0
B0	MAT	Sand %	52.686 (20, < 0.01)	7	68.46	24.53	0
B0	WB	Sand %	56.056 (20, < 0.01)	7	71.83	27.90	0
B0	GDD5	Silt %	56.902 (20, < 0.01)	7	72.68	28.75	0
B0	MAT	Silt %	57.776 (20, < 0.01)	7	73.55	29.62	0
B0	MAP	Sand %	58.680 (20, < 0.01)	7	74.46	30.53	0
B0	WB	Silt %	63.082 (20, < 0.01)	7	78.86	34.93	0
B0	MAP	Silt %	65.421 (20, < 0.01)	7	81.20	37.27	0

MAT, mean annual temperature; *MAP*, mean annual precipitation; *GDD5*, growing degree-days above 5°C; *WB*, water balance; *C statistic* (df: degree of freedom, p: probability of compliance of the basis set with the conditions of independence testing the hypothesized causal structure of the DAG); *K*, number of free parameters; *AICc*, second order Akaike's information criterion; *ΔAICc*, relative AICc difference with the 'best model'; *W*: Akaike weight.

The best DAG under hypotheses B1 and B2 explained 56% and 61% of the variation between covariates and illuvial horizon C stocks, respectively (Figure 2.6 and Annexe B, Table S2.2). Carbon stocks were correlated positively with Mpy ($0.37 \leq pc \leq 0.41$, $p < 0.01$), but negatively with pH ($-0.32 \leq pc \leq -0.23$, $p < 0.05$, except for B2 with MAP and clay content where $p = 0.053$). Pyrophosphate extractable metals (Mpy) were found to depend on WB ($pc = 0.25$, $p < 0.05$) and MAP ($pc = 0.23$, $p < 0.05$) but not

on other climate variables ($p > 0.05$), and were negatively correlated with pH ($-0.52 \leq pc \leq -0.46$, $p < 0.001$), which was itself found to be negatively correlated with TSF ($pc = -0.28$, $p < 0.05$). Accounting for the effects of other variables, the direct effects of both clay content and TSF on illuvial horizon C stocks became non-significant ($p > 0.05$). Nevertheless, climate (WB and MAP variables only) was found to affect illuvial horizon C stocks through its effect on Mpy (indirect path coefficient, $pc_i = 0.1$ for hypotheses B1 and B2 with WB and clay content, and $pc_i = 0.09$ for hypothesis B2 with MAP and clay content). Also, TSF was found to be indirectly linked to illuvial horizon C stocks through its effect on pH, considering the effects of pH on C stock, of pH on Mpy, and of Mpy on C stock ($0.12 < pc_i < 0.15$).

When averaging path coefficients (Annexe B, Table S2.2), the most important variables exerting a direct control on illuvial horizon C stocks were Mpy (model-averaged estimator, $pc_{avg} = 0.39$) followed by pH ($pc_{avg} = -0.26$). The direct effect of TSF ($pc_{avg} = 0.19$) was not significant and direct effects of climate ($pc_{avg} = -0.1$) and texture ($pc_{avg} = -0.02$) were either not significant or negligible.

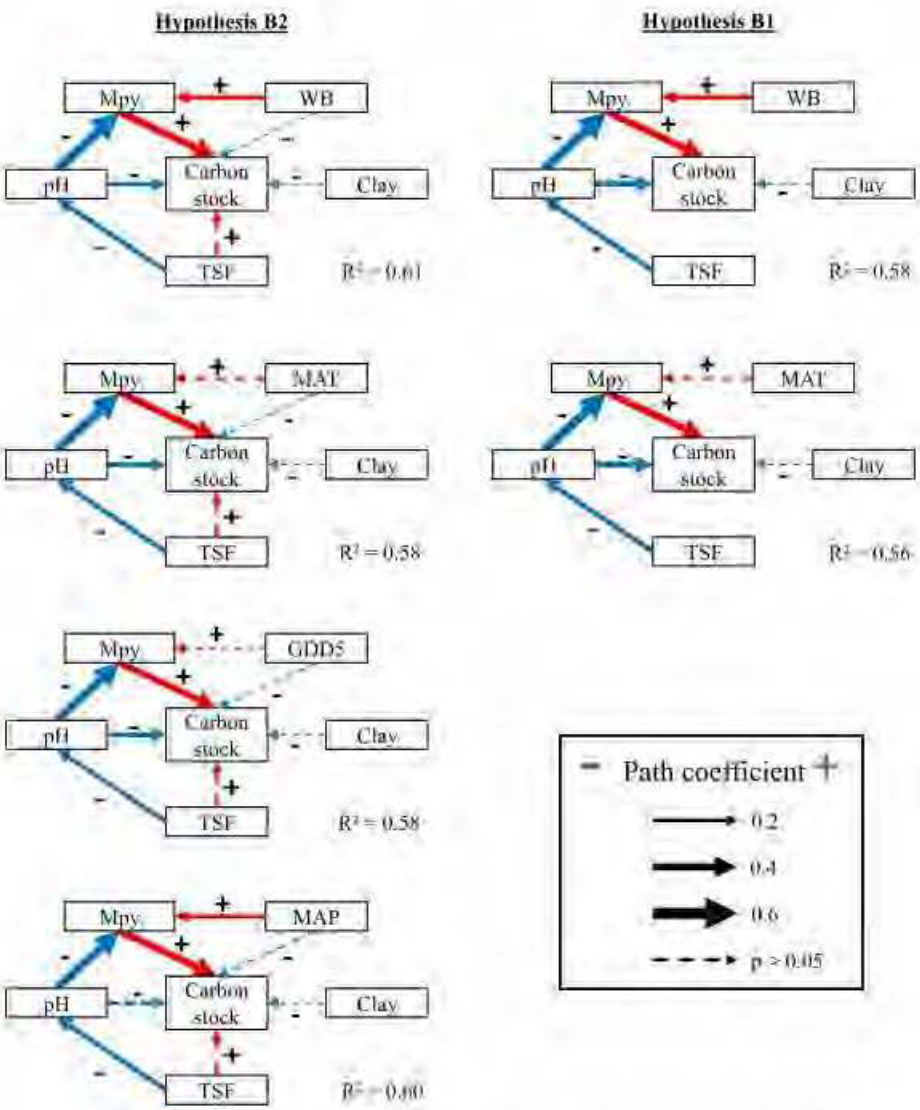

Figure 2.6 The five minimum adequate path models that best fit the data to explain illuvial (B) horizon carbon stock variability. Arrows indicate direct causal relationships between variables. Arrow widths are proportional to path coefficients. Red or blue arrows show positive or negative path coefficients, respectively. Plain or dashed arrows depict significant ($p \leq 0.05$) or non-significant ($p > 0.05$) causal relationships between variables, respectively. *WB*, water balance; *MAT*, mean annual temperature; *Clay*, mineral soil (top 35 cm) clay content; *TSF*, time since fire; *pH*, illuvial horizon potential of hydrogen; *Mpy*, pyrophosphate extractable metals in the illuvial horizon.

2.6 Discussion

Our results show that time since fire (TSF) is an important driver of the most dynamic ecosystem carbon (C) pools (Figure 2.4). Carbon stocks in live aboveground biomass (Figure 2.4b) and in coarse woody debris (Figure 2.4c) varied predictably with TSF in agreement with aggradation and stabilisation patterns (Bormann et Likens, 1979; Sturtevant *et al.*, 1997; Ward *et al.*, 2014), whereas C stocks in the FH layer increased linearly with TSF (Czimczik *et al.*, 2005; Nalder et Wein, 1999) in agreement with our hypothesis (see the description of FH0), although the latter relationship was weak. Contrary to our expectations, we also found a significant but weak positive correlation between TSF and mineral soil C stocks. Together these results indicate that the net C accumulation phase in the terrestrial pools of these forests goes beyond the aboveground aggradation phase, which is in agreement with Luyssaert *et al.* (2008) and Zhou *et al.* (2006), but in contradiction with Bormann et Likens (1979), Wardle, Walker, *et al.* (2004) and Gao *et al.* (2017). Soil C pools (FH layer and top 35 cm of mineral soil) were found to represent as much as 77% of total ecosystem C stocks (Figure 2.4), whereas still not accounting for deeper soil stocks (Jobbagy et Jackson, 2000). This percentage clearly indicates that better predictions of changes in boreal forest C stocks can only be achieved through a better understanding of the processes involved in soil C accumulation (Shaw *et al.*, 2014), in particular with respect to changes in disturbance patterns (Buma *et al.*, 2014; Fu *et al.*, 2017b) or climate.

2.6.1 Soil C stock predictability

When quantifying explicitly direct and indirect relationships among fire, climate, local biotic and abiotic variables involved in soil C storage, our study demonstrates that the overall model explained variability (i.e., accounted for all causal relationships among

variables, and between variables and soil C stocks) increases from 28% (model assumes only direct relationships between variables) to 46% (model with indirect relationships), and from 40% to 60% for FH layer and illuvial horizon, respectively (Annexe B, Table S2.1 and Table S2.2). In our study, the rejection of all hypotheses that assumed only direct relationships between environmental variables and soil C stocks supports the claim that the assumption of direct relationships associated with the dominant modeling approaches such as ANOVA, multiple regressions or machine learning algorithms may be an important limitation and a source of uncertainty in current soil organic C predictions. This result agrees with recent findings showing that complex direct and indirect relationships between climate, soil properties, C inputs and C pools regulate soil organic C dynamics in agricultural landscapes (Luo *et al.*, 2017). Our study goes a step further by using a confirmatory approach with a set of *a priori* hypotheses and a low number of variables (climate, soil texture, TSF, pH, moss dominance and metal oxide concentrations) that are readily interpretable from an ecological point of view and readily comparable in terms of their relative contribution. With only five variables, our best path models explained as much as 46% and 61% of the overall variation among environmental variables and C stocks in the FH layer and illuvial horizon, respectively.

2.6.2 Climate is an indirect driver of soil C stocks

When accounting explicitly for direct and indirect relationships between climate and C stocks, our results indicate that the influence of water availability – i.e., the main climatic predictor in our study – on soil C stocks is only indirect through changes in vegetation dominance (i.e., moss layer composition, which, when dead, is the primary source of FH layer mass in our study system) or through changes in metal oxide contents (illuvial horizon). This result is in agreement with previous findings showing

that accounting for sphagnum- and feathermoss-derived C reduces errors in black spruce C stock estimates (Bona *et al.*, 2013). Relationships between climate and bryophyte vegetation justify the use of climate parameters to predict moss species distribution at the landscape scale (Gignac, 2001). Our results indicate that water availability is more important than temperature in explaining moss layer dominance, as bryophyte species often tolerate a wide range of temperatures and are dependent on the water content of their habitat (Gignac, 2001). The index of moss dominance used in our study is a gross index that discriminates between Sphagnum spp. and feathermosses and that does not account for all the diversity of species or functional traits in the ground layer vegetation. Nevertheless, the indirect effect of climate on soil C stocks through changes in bryophyte dominance indicates that considering water availability (i.e. bryophyte dominance) – FH layer C stock relationships should improve our ability to predict soil C stocks with changes in climate.

In our study, metal oxide content exerted a primary control on illuvial horizon C stocks, indicating that binding of organic matter on the mineral phase is a major direct process of C sequestration (Kramer *et al.*, 2012; Mikutta *et al.*, 2006; Porras *et al.*, 2017). Doetterl *et al.* (2015) argue that over a wide climatic gradient soil C stocks primarily evolve with climate-driven mineral weathering and release of reactive mineral surfaces. In our study, we also found an indirect control of climate on illuvial horizon C stocks through metal oxide contents rather than a direct relationship between climate and illuvial horizon C stocks. Our findings corroborate the view that climate-mediated mineral weathering is important for C sequestration. Indeed, the faster podsolization process favored by increased eluviation (Sanborn *et al.*, 2011) has been shown to occur under wetter and warmer climate compared with a dryer and colder one (Egli *et al.*, 2009; Protz *et al.*, 1988).

At the global scale, soil C stocks have been shown to decrease with rising temperatures (Crowther *et al.*, 2016). In our study, it is noteworthy that temperature factors (MAT and GDD5) did not significantly contribute to soil C stocks once direct and indirect relationships with other biotic and abiotic factors were accounted for. Our data encompass a range of mean annual temperatures of about 3.5°C (Annexe B, Figure S2.4), which could be insufficient to detect a temperature gradient effect. Moreover, we used the most recent 30-year climate data that does not span the range of the TSF studied here (314 years). This evidently brings some uncertainties in interpreting the role played by climate in soil C accumulation. Nevertheless, our results suggest that contrary to water availability, soil C stocks do not vary quantitatively with temperature (Annexe B, Figure S2.4), which implies that under a raise of mean annual temperature of 2°C, global warming would be unlikely to have a net direct effect on boreal soil C stocks at the scale of our study area. Increasing temperature at the regional scale has been showed to accelerate boreal forest ecosystem C fluxes without changing soil C stocks (Ziegler *et al.*, 2017).

2.6.3 Distinct mechanisms of C stock change with TSF in FH layer and mineral soil

Our results support previous findings that TSF is an important direct driver of C stocks in the organic layer (Czimczik *et al.*, 2005; Harden *et al.*, 2012; Nalder et Wein, 1999; Pellegrini *et al.*, 2018). Indeed, the organic layer is consumed in part or in whole during fire (Greene *et al.*, 2007; Harden *et al.*, 2012), depending on fire severity (Lecomte *et al.*, 2006) and pre-fire organic layer depth (Kane *et al.*, 2007). However, in the illuvial horizon, our results demonstrate that TSF is mostly an indirect driver that alters pH conditions, which in turn influence both C stocks directly or indirectly through changes in metal oxide contents. To our knowledge, this study is the first to simultaneously document and quantify these complex relationships among TSF, pH, metal oxides and

C stocks in the illuvial horizon of forest ecosystems; previous studies mainly focused on separate elements of these complex relationships. Interestingly, we found that pH was the strongest driver of metal oxide contents, and that metal oxides increased when pH decreased. This result supports the view that organo-metal complexation reactions in acidic environments depend on soil pH (Heckman *et al.*, 2009; Porras *et al.*, 2017). In addition, soil pH largely controls the weathering of minerals (Drever, 1994; Drever et Stillings, 1997); thus, we assume that enhanced organo-metal complexation could arise from the increased availability of metal ions released by mineral weathering when pH decreases (Porras *et al.*, 2017). In other words, the potential of organo-metal complex formation at the scale of our study could reflect the synergistic effect of soil pH with microbial decomposition process and mineral weathering. As the soil substrate becomes more acidic, greater amounts of undecomposed organic materials can bind to the overload of metal ions released from enhanced weathering.

2.6.4 Insignificant role of soil texture

Surprisingly, we found no direct or indirect effect of soil texture on both FH layer and illuvial horizon C stocks, indicating that once the effects of other factors are controlled, soil texture does not contribute quantitatively to C sequestration. This result contrasts with the wide use of soil texture in models of soil organic matter (Six *et al.*, 2002; Soucémarianadin *et al.*, 2014). One explanation could lie in the low Nordic soil data availability. Indeed, most of our knowledge on the control of soil C stocks by soil texture comes from warm agricultural regions (Rasmussen *et al.*, 2018). Also, it is possible that the weathering of the granitic bedrock of the Canadian Shield did not produce reactive surface silt and clay particles considering that the studied soils are young and have been developing since the end of the last glaciation (< 10 k yrs; Minasny *et al.* (2008)). It is also possible that our results are limited to the short range

of mineral soil clay content contained in these boreal soils (Annexe B, Figure S2.5), and that on fine textured boreal soils, silt and clay contents could have a significant influence on soil C stocks.

2.6.5 Research avenues

In this study, TSF and climate only had indirect effects on mineral soil C stocks. This finding brings some important implications. First, it may help solving discrepancies found in the literature where mineral soil C stocks either decrease, increase, or do not change with TSF (Johnson et Curtis, 2001; Knicker, 2007; Nave *et al.*, 2011; Pregitzer et Euskirchen, 2004; Seedre *et al.*, 2011). Indeed, the effects of TSF on mineral soil C stocks in these studies may be the reflection of unevaluated complex interrelationships between local site conditions defined by conditions such as pH and metal oxide content. The second main implication about the prevalence of indirect climatic and fire-mediated effects on mineral C stocks is that it questions the underlying assumption of forecasting exercises projecting the effect of global changes on future soil C stocks, and especially how forecast models account for the important role played by local variation in vegetation and chemical soil properties. Eastern North America is projected to receive about 10% more precipitation by the end of this century (IPCC, 2013). According to our results, increasing the water supply through greater amounts of precipitation could increase mineral soil C stocks through enhanced mineral weathering and leaching, releasing metal oxides that can bind to organic matter (Doetterl *et al.*, 2015; Mikutta *et al.*, 2006; Porras *et al.*, 2017; Rumpel et Kögel-Knabner, 2011). Otherwise, the projected increase in fire frequency suggested by models (Kloster et Lasslop, 2017; Wang, X. *et al.*, 2017; Wotton *et al.*, 2017) could weaken the C capture function of boreal forests (Genet *et al.*, 2018; Pan *et al.*, 2011). Integrating direct and indirect effects of abiotic and biotic factors on C storage

processes, as presented here through mechanistic models of C dynamics in boreal forest ecosystems, could improve our ability to account for C stocks and anticipate the response of boreal forests to global change. Assessing the sensitivity of global change forecast models to local variation in biotic and abiotic conditions is a key challenge that will need to be addressed and integrated in future studies.

2.7 Acknowledgements

This research was supported by grants from the Mitacs Acceleration program. The authors warmly thank Véronique Poirier and Jean Noël (MFFP) for help with geomatic data, Eric Beaulieu, Catherine Bruyère, Cécile Remy and Arnaud Guillemard for help in the field, Danielle Charron and Pierre Clouâtre (MFFP) for logistic support, and Serge Rousseau (NRCan – CFS – LFC) for laboratory analyses. We are grateful to Pierre Bernier for his comments on the initial version of this text and for his precious advices. The authors declare no conflict of interest.

CHAPITRE III

BOREAL FOREST SOIL CHEMISTRY AS MORE CONTROL OVER THE SIZE OF THE POST-FIRE BIOREACTIVE SOIL ORGANIC CARBON RESERVOIR THAN CLIMATE

(LA CHIMIE DES SOLS EN FORÊT BORÉALE EXCERCE UN PLUS GRAND CONTRÔLE QUE LE CLIMAT SUR LA TAILLE DU RÉSERVOIR DE CARBONE ORGANIQUE BIORÉACTIF DU SOL APRÈS FEU)

Benjamin Andrieux[1,2], David Paré[2], Julien Beguin[3], Pierre Grondin[4], Yves Bergeron[1]

[1]NSERC-UQAT-UQAM Chaire industrielle en aménagement forestier durable, Institut de Recherche sur les Forêts, Université du Québec en Abitibi-Témiscamingue, Rouyn-Noranda, QC, Canada ; [2]Ressources Naturelles Canada, Service Canadien des Forêts, Centre de Foresterie des Laurentides, Québec, QC, Canada ; [3]Ressources Naturelles Canada, Centre canadien sur la fibre du bois, Québec, QC, Canada; [4]Direction de la recherche forestière, Ministère des Forêts, de la Faune et des Parcs du Québéc, Québec, QC, Canada.

Article soumis pour révision dans la revue *Soil Biology and Biochemistry*.

3.1 Abstract

Large uncertainties remain as to how the vast boreal soil carbon (C) reservoirs will respond to environmental changes and global warming. Therefore, we characterized soil organic C (SOC) and edaphic factors along a chronosequence of time since fire (TSF, from 2 to 314 years) and along a climatic gradient in a large area of black spruce forests in the boreal region of Quebec, Canada. We used long-term incubation and acid hydrolysis studies to answer two main questions: i) Does soil C bioreactivity (C_{BioR}) change with the SOC accumulation observed with TSF? and ii) To what extent do interdependent relationships among TSF, climate, physico-chemical soil properties and bryophyte dominance influence soil C_{BioR}? We found that all soil C pools increased linearly with TSF. The bioreactive and acid-insoluble soil C pools increased at a rate of 0.02 $MgC.ha^{-1}.yr^{-1}$ and 0.12 $MgC.ha^{-1}.yr^{-1}$, respectively, and their proportions relative to total soil C stock remained constant with TSF (8% and 46%, respectively). In our study, the physico-chemical soil properties of Podzolic soils that characterize the study area were the best direct predictors of soil C_{BioR}, both in the organic (FH) horizon and in the mineral soil, with pH being the main driver of all properties tested. The direct effects of TSF and pH on C_{BioR} in the FH horizon were significant, but much more so for pH than for TSF, indicating that acidic soil conditions in post-fire old-growth forests favor the accumulation of labile C by limiting the activity of decomposers. We showed that higher amounts of exchangeable manganese, which plays a role in lignin degradation, enhanced C_{BioR} in the FH horizon. We also showed that exchangeable aluminum had the greatest direct and negative effect on the C_{BioR} in the mineral soil and act as a medium for the indirect effect of clay content. Our analyses showed that the amount of pyrophosphate extractable metals also had a direct and negative effect on C_{BioR} in the mineral soil, suggesting that organo-metallic complexation is an efficient mechanism of soil C sequestration. Of the four climate factors examined in this study (mean annual temperature, growing degree-days above

5°C, and mean annual precipitation and water balance; MAT, GDD5, MAP, WB) only those related to water availability, and not to temperature, had an indirect effect on soil C_{BioR}. The indirect effect of climate on C_{BioR} in the FH horizon, being mediated by moss vegetation, which itself has a direct effect on pH, was found to be very small. By disentangling the complex interplay among the direct and indirect effects of TSF, climate, physico-chemical soil properties and bryophyte dominance through mechanistic models of soil C_{BioR}, our study stresses the need to revise the common assumptions associated with Earth System Models, based on the carbon quality-temperature hypothesis, to forecast the response of boreal soils to global warming. The antagonistic effects of exchangeable elements on FH horizon and mineral soil C_{BioR} found in our study imply that global change might lead to responses that are different in the mineral soil from those in the FH horizon. Focusing on the amplitude of changes in soil chemistry is a key challenge that remains to be addressed in future works to improve the understanding of soil C dynamics in the response to global change.

3.2 Résumé

De grandes incertitudes demeurent quant à la manière dont les vastes réservoirs de carbone (C) du sol en forêt boréale répondront aux changements environnementaux et au réchauffement planétaire. Nous avons caractérisé le C organique du sol sur une chronoséquence de temps depuis feu (TSF, de 2 à 314 ans) établie sur un grand territoire englobant une variabilité climatique dans une grande aire forestière de la région boréale du Québec, Canada. Nous avons utilisé l'incubation et l'hydrolyse acide des sols pour répondre à deux questions principales : i) la bioréactivité du C du sol change-t-elle avec l'accumulation de C organique du sol observée avec le TSF ? Et ii) Dans quelles mesures les relations d'interdépendance entre le TSF, le climat, les propriétés physico-chimiques du sol et la dominance des bryophytes influencent-elles

la réactivité biologique du C des sols ? Nous avons constaté que les réservoirs de C du sol augmentaient de façon linéaire avec le TSF. Les réservoirs de C bioréactif et insoluble à l'acide augmentaient de 0.02 $MgC.ha^{-1}.an^{-1}$ et de 0.12 $MgC.ha^{-1}.an^{-1}$, respectivement, et leurs proportions par rapport au stock total de C dans les sols demeuraient constante avec le TSF (8% et 46%, respectivement). Dans notre étude, les propriétés physico-chimiques des sols podzoliques qui caractérisent la région d'étude étaient les meilleurs prédicteurs de la réactivité biologique du C, tant dans l'horizon FH que dans le sol minéral, avec le pH comme principal déterminant de toutes les propriétés testées. L'effet direct et positif du TSF sur la réactivité biologique de l'horizon FH était compensé par un effet médiateur du pH, ce qui indique que les conditions d'acidité dans les forêts anciennes originaires d'un incendie favorisent l'accumulation de C labile en limitant l'activité des décomposeurs. Nous avons montré qu'une quantité plus élevée de manganèse échangeable, qui joue un rôle dans la dégradation de la lignine, augmentait la bioréactivité du C dans l'horizon FH. Nous avons aussi montré que l'aluminium échangeable avait l'effet direct et négatif le plus important sur la bioréactivité du C du sol minéral, et qu'il était un médiateur de l'effet indirect de la quantité d'argiles granulométriques. Nos analyses ont montré que la quantité de métaux extractibles au pyrophosphate avaient aussi un effet direct et négatif sur la bioréactivité du C dans le sol minéral, ce qui suggère que la complexation organométallique est un des mécanismes efficaces de la séquestration du C dans le sol. Parmi les quatre facteurs climatiques examinés dans notre étude (température annuelle moyenne, degré jour de croissance supérieur à 5°C, précipitation annuelle moyenne et équilibre hydrique ; MAT, GDD5, MAP, WB) seuls les facteurs reliés à la disponibilité en eau, et non pas aux températures, avaient un effet indirect sur la bioréactivité du C du sol. Le climat avait un effet direct sur la végétation muscinale qui, elle, avait un effet direct sur le pH. C'est pourquoi le climat n'avait qu'un petit effet indirect sur la bioréactivité du C dans l'horizon FH. En démêlant les interactions complexes entre le TSF, le climat, les propriétés physico-chimiques du sol à travers des modèles mécanistiques de la bioréactivité du C des sols, notre étude souligne le besoin de réviser

les postulats communs aux modèles numériques du système Terre fondés sur l'hypothèse de la dépendance entre la qualité du C et la température pour la décomposition, afin de mieux prévoir la réponse des sols boréaux au réchauffement climatique. Les effets antagonistes des éléments échangeables sur l'horizon FH et sur le sol minéral que nous avons trouvés dans notre étude impliquent que le changement global pourrait entraîner des réponses différentes parmi les couches du sol. Considérer l'amplitude de ces changements dans la chimie du sol est donc un défi d'envergure qui reste à être élucidé dans les futurs travaux pour améliorer notre compréhension de l'équilibre du C des sols en lien avec les changements globaux.

3.3 Introduction

About 20% (174.5 Pg) of the global forest carbon (C; 861 Pg) is stored in boreal forest soils (Pan *et al.*, 2011). The maintenance of this vast soil C reservoir is partly under microbial control and could respond to variations of environmental conditions. The C quality-temperature hypothesis (CQT), based on the enzymatic kinetic theory, predicts a greater enzymatic activity and a lesser activation energy of the decomposition process as a result of increasing temperature (Craine *et al.*, 2010; Fierer, Noah *et al.*, 2005). According to this hypothesis, even a small change in soil C pools with a rise in temperature could increase atmospheric CO_2 concentrations under global warming, generating a positive feedback loop (Davidson, 2016; Davidson et Janssens, 2006). This is especially important to boreal biomes (Carey *et al.*, 2016) where a rise of 3.2°C in mean annual temperature (MAT) is forecasted by the end of this century (IPCC, 2013). Despite the numerous studies that have investigated the temperature dependence of the decomposition process, no consensus has emerged about the direction and amplitude of the response of soil organic C (SOC) stocks to global warming (Conant *et al.*, 2011; Kirschbaum, 2006). This lack of agreement underpins the need for

reviewing our mechanistic understanding of soil C processes to better anticipate the effects of global change on soil C reservoirs (Bradford *et al.*, 2016; Schmidt *et al.*, 2011).

Bioreactivity is defined as a relative measure of soil C lability (Laganière *et al.*, 2015; Xu *et al.*, 1997), hereafter defined as the proportion of C mineralized in CO_2 by microbes at constant temperature and water content over a long period (see Methods). Using soil C bioreactivity (C_{BioR}) is a way to overcome the confusing concept of lability and recalcitrance currently attributed to organic matter chemical properties (Kleber, 2010). We assumed that soil C_{BioR} is an overall index of degradability once the constraints of temperature and water content are standardized across samples rather than assuming C organic compounds are resistant to decomposition due to their inherent chemical recalcitrance *per se*. Understanding soil C_{BioR} is key to anticipating how boreal forest soil C reservoirs could respond to environmental variations inherent to global warming. According to the CQT hypothesis, a chronic increase in temperature will likely enhance microbial decomposition in the soil C reservoir. In cases where soil C_{BioR} builds up with time since fire (TSF) because of cold conditions limiting decomposition, the CQT hypothesis suggests massive soil C losses might result from global warming. However, in cases where soil C_{BioR} saturates and stabilizes, soil C builds up with TSF and soil C losses to the atmosphere due to global warming might be limited. Global warming might also enhance soil physico-chemical reactions, thus favoring soil C stabilization (Thornley et Canell, 2001).

Climate influences vegetation distribution which, in turn, influences soil C storage through differences in the quality of litter inputs (Augusto *et al.*, 2015; Jobbagy et Jackson, 2000). In boreal ecosystems, climate also affects C cycle through its control over disturbance regimes (type, frequency and severity; Kurz *et al.* (2013); van Bellen

et al. (2010)). North American forests are prone to crown wildfires that induce tree mortality (Rogers *et al.*, 2015) and burn part of the forest floor (Greene *et al.*, 2007; Miyanishi et Johnson, 2002), leading to C release into the atmosphere. Soil C quantity and quality change after fire (Gonzalez-Perez *et al.*, 2004; Knicker, 2007). The time since the last major disturbance, including TSF, and the age-class structure determine the C source-sink potential of a forest from the plot to the landscape scale (Kurz *et al.*, 2013). Besides its direct role in C cycling, climate has been shown to be an indirect predictor of soil C storage, through its effects on geochemistry (Andrieux *et al.*, 2018b; Doetterl *et al.*, 2015). Bound soil C on reactive mineral surfaces is a mechanism that stabilizes C from microbial decomposition (Davidson, 2015; Porras *et al.*, 2017). Although many of these relationships have been investigated separately, we are not aware of any empirical study so far that has quantified all of these processes simultaneously and assessed the relative contribution of climate, TSF, vegetation attributes and soil physico-chemistry on soil C_{BioR}.

The objectives of this study are to address this gap by investigating changes in boreal forest soil C_{BioR} with TSF (from 2 to 314 years) and to disentangle the relative contribution of climate, moss dominance, soil particle size distribution and soil chemical properties (pH, exchangeable Mn and Al, and metal oxides) to soil C_{BioR} across the spruce-feather moss bioclimatic domain in eastern North America. Focusing on the complex interplay between climatic and non-climatic factors and their influence on soil C_{BioR}, we addressed the following questions: i) Does soil C_{BioR} change with SOC accumulation observed with TSF? and ii) To what extent do interdependent relationships among TSF, climate, physico-chemical soil properties and bryophyte dominance influence soil C_{BioR}? We framed our study within the state factor model of ecosystems (Amundson et Jenny, 1997), which emphasizes soil physico-chemical properties understood to be important to the pedogenesis of Podzolic soils (Schaetzl et Anderson, 2005) that occur on the sampled sites. From there, we hypothesize that once

site factors such as overstory composition, surficial deposits and soil drainage are accounted for as in the present study: 1) the proportion of soil C_{BioR} increases as forest stands get older, leading to a buildup of soil C_{BioR} under the cold conditions of the boreal forest; 2) alternatively, if the soil C_{BioR} saturates because its turnover is rapid, the proportion of bioreactive C should decline as soil C stocks increase with TSF; and 3) soil C_{BioR} is primarily controlled by TSF and moss dominance in the FH horizon, and by soil physico-chemistry in the mineral soil.

3.4 Material and methods

3.4.1 Site selection, sampling design and fieldwork

To account for the effects of TSF and climate on soil C pools, we established sample plots across both a chronosequence and a climosequence (Figure 3.1; see Andrieux *et al.* (2018b) for a description of the study area). Based on digital forest inventory maps compiled by the Ministère des Forêts, de la Faune et des Parcs du Québec (MFFPQ), we selected stands as similar as possible in terms of canopy composition (black spruce [*Picea mariana*] stands), surficial deposits (thick till) and mesic drainage conditions. The soils that develop under these conditions typically belong to the Podzolic order (Table 3.1). It is important to note that within the mesic drainage conditions, soil texture was quite variable (Table 3.1). These stands were overlaid with fire maps produced by the MFFPQ and other published dendrochronological surveys (Belisle *et al.*, 2011; Bouchard *et al.*, 2008; Cyr *et al.*, 2012; Frégeau *et al.*, 2015; Le Goff *et al.*, 2007; Le Goff *et al.*, 2008; Portier *et al.*, 2016) to set up the chronosequence. We assumed that the black spruce canopy composition did not change significantly with time and that the forest cyclically returned to a black spruce dominance after fire, in so-called recurrent dynamics, as previously described for these forests in a paleological survey (Frégeau *et al.*, 2015). Then, while studying this ecosystem with a single and cyclic

successional trajectory and a low vegetation diversity, and by carefully selecting stable permanent site conditions, we controlled most pitfalls associated with space-time substitutions when using a chronosequence approach (Kenkel *et al.*, 1997; Walker *et al.*, 2010).

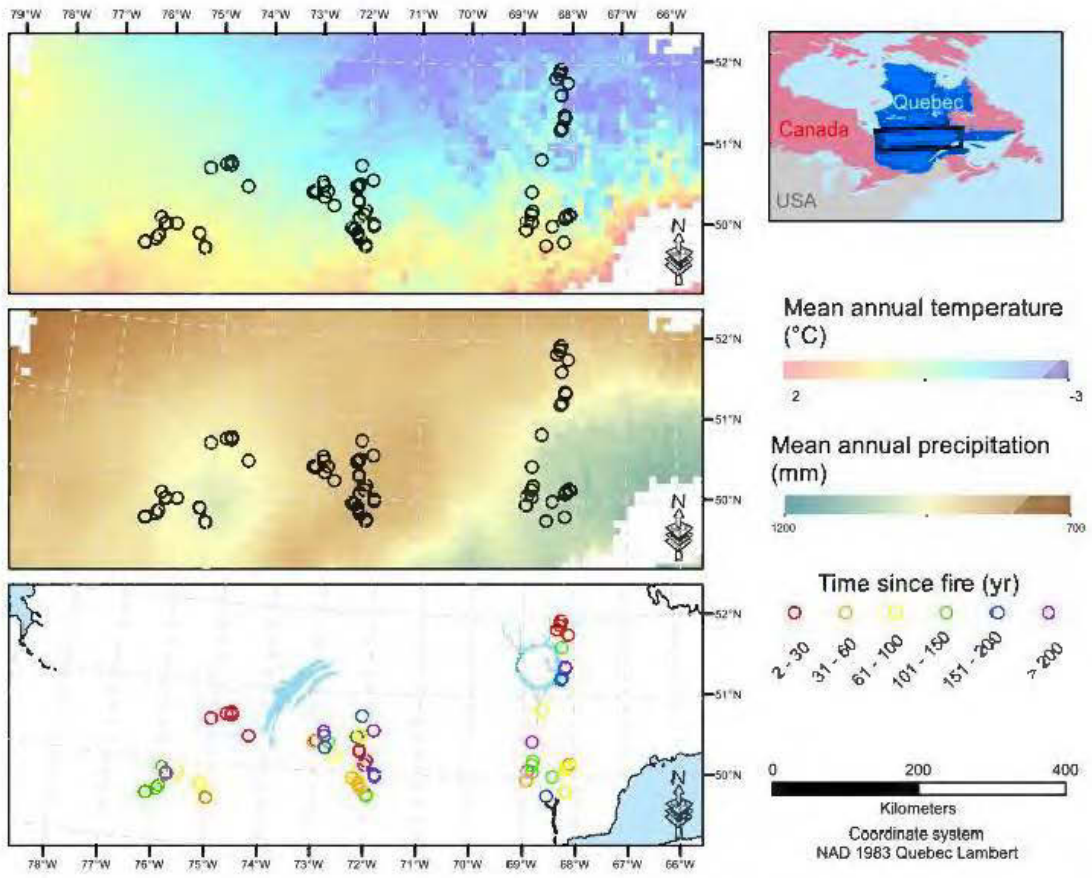

Figure 3.1 Map of the study area showing the location of the sample plots. Mean annual temperature (upper panel) and mean annual precipitation (middle panel) are interpolations from the 1981–2010 Canadian climate normals on a 10 x 10 km pixel grid (Chaste et al. 2018). The lower panel presents the location of the sample plots in relation to TSF.

For field inventory and soil sampling, we followed Canada's National Forest Inventory ground plot guidelines (NFI, 2016). Stand biophysical description and soil sampling took place in a single 314 m² circular plot (10 m radius) in each stand. Slope inclination and orientation were recorded from the center of each plot with a clinometer and a compass, respectively. Every 2 m along two orthogonal transects oriented following the main cardinal directions, and for a total of 20 records per plot, the thickness of the O layer (FH horizon) was measured on a sample taken with a soil auger and the dominant moss types (*Sphagnum* spp. or feather mosses) were identified using three 400 cm² microplots. After litter and green living mosses were removed and bagged separately, the FH was sampled at the edge of the plot in three 400 cm² microplots that were spaced 15 m from each other, in which we extracted volumetric mineral soil samples (top 15 cm) with a metallic cylinder (ø = 4.7 cm, height = 15 cm). One soil pit was dug at the plot edge, down to the podzolic B horizon or to the bedrock when possible, for soil description, and to collect the mineral soil from 15 to 35 cm under the forest floor-mineral soil boundary as well as the top 15 cm B horizon with a metallic cylinder (ø = 4.7 cm). The abundant stoniness in one site did not allow to sample the mineral soil from 15 to 35 cm and was thus discarded from analyses. Before being processed for physico-chemical analyses, soil samples were maintained at 2°C in a cooler.

The fieldwork was conducted in 2015, from June 15 to September 8. The sampling effort covered 72 sites in stands of fire origin that burned 2 to 314 years ago. Climate data were interpolated at the plot level using BioSim v10.3.2 (Régnière *et al.*, 2013) together with 1981–2010 climate normal series (http://climat.meteo.gc.ca/) from surrounding weather stations, and considering local slope attributes measured in the field as correcting factors (Régnière, 1996). Soil characteristics are summarized below (Table 3.1).

Table 3.1 General characteristics of the sampling sites.

Variable		Min	Max	Mean (± sd)
MAT (°C)		-2.8	0.7	-0.5 (± 0.8)
GDD5 (°C)		838	1290	1110 (± 110)
MAP (mm)		861	1027	934 (± 52)
WB (mm)		493	660	558 (± 46)
FH depth (cm)		9.8	49.3	22.6 (± 8.4)
A_e depth (cm)		1	40	9.4 (± 6.3)
Soil thickness (cm)		10	103	39 (± 15)
pH	FH	3.3	4.2	3.7 (± 0.2)
	MIN015	4.2	5.6	4.7 (± 0.2)
	MIN1535	4.5	5.9	5.2 (± 0.3)
Particle size (%)	Sand	26	92	70 (± 11)
	Silt	5	63	24 (± 10)
	Clay	2	22	6 (± 3)
Reference Soil Group[a]		Podzol (n = 73)		

[a] According to IUSS Working Group WRB (2015). *MAT: mean annual temperature; GDD5: growing degree-days above 5°C; MAP: mean annual precipitation; WB: water balance (i.e., precipitation minus potential evapotranspiration); Ae: eluvial horizon; MIN015: top 15 cm of mineral soil; MIN1535: mineral soil, from 15 to 35 cm. Particle size of the mineral soil.*

3.4.2 Laboratory analyses

3.4.2.1 Soil preparation

First, we composited soil materials obtained from every sampled microplot (N = 3) by plot and soil layer (FH or top 15 cm of mineral soil) to create representative samples

for each layer in each of the 72 sample plots. FH was sieved through a 6-mm mesh before oven drying (60°C), whereas mineral soil samples were air dried and passed through a 2-mm sieve. Bulk density was determined after weighing the dried samples, assuming there were no coarse fragments in the FH horizon, and corrected for fragments > 2 mm for the mineral soil. A part of each sample was retained for soil incubation. We used the < 2 mm fraction to determine pH, exchangeable cation and texture (mineral soil only). Finely ground sub-samples (< 0.5 mm) were used for C concentration, extractable Fe and Al (B horizon only) and acid hydrolysis analyses.

3.4.2.2 Soil physico-chemistry

C concentration of each sample was analyzed by dry combustion (Skjemstad et Baldock, 2007) using a Leco TruMac (Leco Corp, St. Joseph, MI, USA). Exchangeable cations were extracted using a Mehlich-3 solution and were analyzed by inductively coupled plasma atomic emission spectroscopy (Ziadi et Sen Tran, 2007) with an Optima 7300 DV (Perkin Elmer Inc., Waltham, MA, USA). Pyrophosphate extractable Fe and Al (i.e. organically complexed metals; Mpy, hereafter defined as metal oxides) were extracted with a 0.1N $Na_4P_2O_7$ solution before analysis with the Optima 7300 DV (Courchesne et Turmel, 2007). FH horizon and mineral soil pH were determined in a soil:water solution of 1:10 and 1:2 (Hendershot et Lalande, 2007), respectively, using a pH meter (Orion 2 Star). Particle size distribution of the mineral soil was assessed using a standard hydrometer method (Kroetsch et Wang, 2007).

3.4.2.3 Incubation settings

Soil incubation followed the method described in Paré *et al.* (2011). We prepared a total of 215 microcosms (72 sites x 3 soil layers minus one sample in the 15-35 cm mineral soil). We used 9 g of oven-dried FH and 50 g of air-dried mineral soil. Dried soil was used to ensure that initial incubation moisture conditions were similar. Soil samples were placed in 100 mL bottom-perforated plastic containers. The containers were previously filled with glass wool (to avoid material losses during moisture adjustments) and pre-washed with HCl (0.1 M) followed by deionized water. The microcosms were saturated with deionized water, drained for 24 h at 2°C in a cooler, and weighed to determine their water-holding capacity (WHC). Over approximately 50 weeks of experiment, microcosms were placed under constant air temperature (26°C) and humidity (100%) in a growth chamber and, when necessary, deionized water was periodically added to adjust soil moisture to 85% of the WHC. Except during CO_2 production measurements, each microcosm was stored in a 500 mL Mason jar kept open to maintain aerobic conditions and to prevent CO_2 accumulation to toxic levels. A rubber septum was installed on the metal lid for gas sampling when measuring CO_2 production.

3.4.2.4 CO_2 production measurements

Carbon dioxide produced by each microcosm was measured periodically (at day 20, 26, 48, 64, 108, 126, 154, 227, 264, 340 for the FH horizon and at day 8, 14, 21, 29, 36, 43, 51, 57, 72, 79, 86, 101, 113, 140, 203, 238, 358 for mineral soil layers; Figure S1) with a LI-6400 portable photosynthesis system (LI-COR®, Lincoln, NE, USA) connected to a N_2 carrier gas (LI-COR® Application Note # 134). The flow rate of the carrier gas was set to 100 $mL.min^{-1}$ using the gas flow meter FMA1812A (Omega

Engineering, INC., Norwalk, CO, USA). Initial (directly after hermetically sealing a jar with a metal lid) and final (after 4 h to 24 h, depending on the soil layer and the progress of the experiment) CO_2 measurements were done using a 2.5 mL or 10 mL (for FH horizon or mineral soil, respectively) air volume, extracted from the jar headspace with a syringe through the rubber septum. This gas sample was injected through the carrier gas into the LI-6400 infrared analyzer. Carbon dioxide concentration ($\mu mol.mol^{-1}$) was predicted using the linear regression of a sample's measured CO_2 peak against calibration curves obtained from a benchmark gas (CO_2 at 800 ppm and 3000 ppm). The first measurement (initial CO_2 concentration) accounted for the CO_2 concentration of the ambient air when closing the jars. This value was subtracted from the final CO_2 concentration to account solely for the CO_2 produced by the microcosm.

All data were standardized to a 24 h period to provide a daily respiration rate and for cumulative C mineralization calculations (Figure S1), following Paré *et al.* (2006). Briefly, we applied the gas law to convert CO_2 concentration ($\mu mol.mol^{-1}$) to a C mass basis, using a constant pressure at 101.3 kPa and the specific head space volume of each sample (total volume of the jar minus soil volume and container). Cumulative respiration was calculated according to the following equation:

$$M_t = M_{t-1} + \frac{(R_t + R_{t-1})}{2} \times (t - t_{-1})$$

where M_t (mg CO_2-C) is the cumulative mass of C mineralized at time t, R_t (mg CO_2-$C.d^{-1}$) is the daily respiration rate at time t, and t is the Julian day (d). M_t was divided by the initial C mass (g) of each sample to compute the specific respiration (R_S; mg

CO_2-C.$g^{-1}C_{org}$). Then, dividing R_s by 10 gave the percentage of initial mass of soil C lost through microbial respiration, or C_{BioR}.

3.4.2.5 Acid hydrolysis

We used acid hydrolysis as an index of biologically recalcitrant soil C (von Lützow *et al.*, 2007), which is the slow cycling soil C pool (Paul *et al.*, 2006). Hydrolysis was carried out by refluxing 2 g of soil with 50 mL HCl (6M) brought to the boiling point on a hot plate. We used a 2 h reaction time because the majority of soil organic matter is hydrolyzed during the first 2 h and longer reaction times do not significantly change C release (Silveira *et al.*, 2008; Xu *et al.*, 1997). Acid-insoluble residues were separated from hydrolyzates by filtering the solution on inert paper filters, rinsed three times with 50 mL deionized water to remove any chlorine residues, oven-dried at 60°C over night, and weighed before C concentration analysis by dry combustion (see section 2.3.2). Based on the total C concentration of the acid-insoluble residues and mass loss of the samples during the treatments, the hydrolysability (Plante *et al.*, 2006) of a sample was calculated following the equation:

$$C_{AI} = \left(\frac{[C_{AI}] \times M_{AI}}{[C_i] \times M_i}\right) \times 100$$

where C_{AI} is the percentage of the acid-insoluble C (%), $[C_{AI}]$ and $[Ci]$ are the C concentration of the acid-insoluble residues and of the initial soil (%), M_{AI} and M_i are the mass of acid-insoluble residues and of initial soil sample (g).

3.4.3 Ecological a priori hypotheses

To address the complex interplay among climatic and non-climatic factors, we first selected the following environmental variables documented in the literature as being important drivers of soil C_{BioR} and pedogenesis of Podzolic soils: climate (temperature and water supply), soil texture, TSF, dominance of the moss functional type, soil pH, and concentration of metal oxides and of exchangeable elements (Mn and Al). As in other ecosystems (Fierer, Noah *et al.*, 2003; Salomé *et al.*, 2010), the boreal forest soil microbial community differentiates with depth (Clemmensen *et al.*, 2013; Hynes et Germida, 2013), suggesting different decomposition processes in FH and mineral soil layers. Hence, for each of the FH and mineral soil layers, we built separate sets of *a priori* ecological hypotheses expressed as direct acyclic graphs (DAGs) that represented different causal relationships among environmental variables and soil C_{BioR} (Figure 3.2). Therein, we tested the validity of four competing *a priori* ecological hypotheses represented by a DAG. This hypothetico-deductive approach, in which each *a priori* hypothesis was supported by ecological knowledge, represented an alternative causal explanation that could be falsified as regards to the underlying mechanisms of soil C_{BioR} in the two soil layers. For each soil layer, the first hypothesis assumed only direct relationships between environmental variables and soil C_{BioR} (hypotheses FH1 and MIN1 in Figure 3.2), such that they mirrored the widespread assumptions used in soil C prediction models based on multiple regression or ANOVA analyses. Also, framed within Jenny's factor model of soil formation (Jenny, 1994), these baseline hypotheses assumed independence among environmental variables. Alternatively, we formulated *a priori* competing hypotheses in which both direct and indirect effects among variables and soil C_{BioR} were explicit (hypotheses FH2 and MIN2 in Figure 3.2). Justifications for each *a priori* ecological hypothesis are listed below.

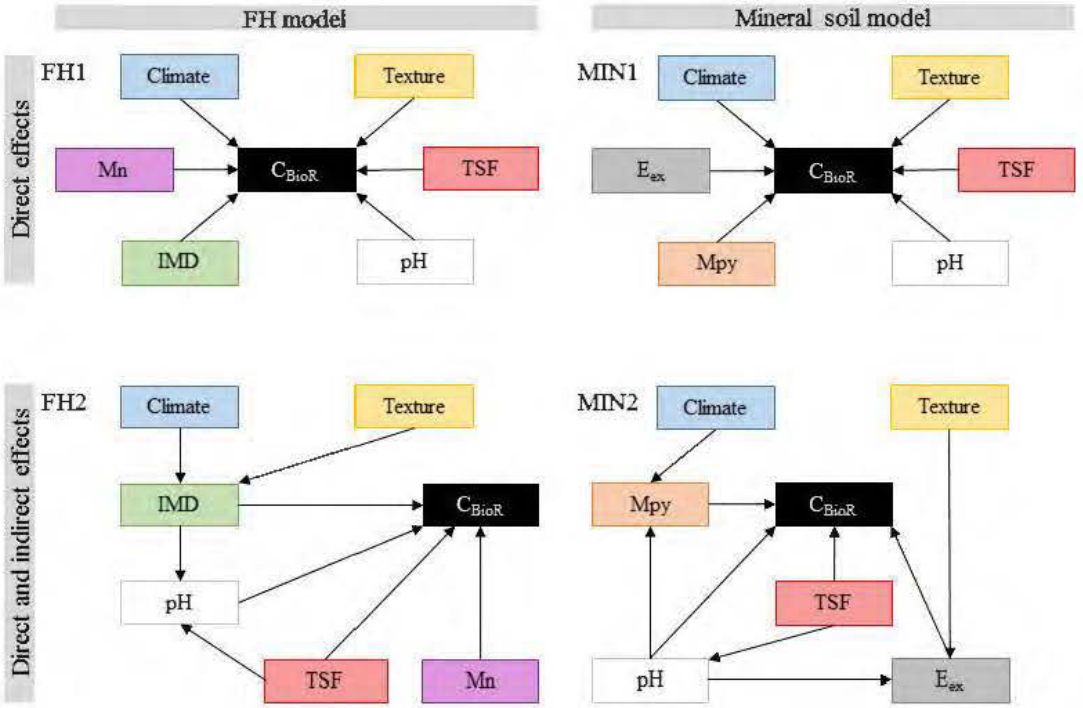

Figure 3.2 Path models for each of the multivariate causal hypotheses. Arrows indicate direct causal relationships. *Climate*: climate variable; *Texture*: texture variable; *TSF*: time since fire; *pH*: pH of the FH horizon (FH1 and FH2) or of the top 35 cm of mineral soil (MIN1 and MIN2); *IMD*: index of moss dominance; *Mn*: exchangeable manganese of the FH horizon; *Mpy*: pyrophosphate extractable metals; E_{ex}: exchangeable element (Al or Mn) of the mineral soil.

Baseline hypothesis for the FH horizon, FH1. In this hypothesis, according to enzyme kinetics, soils that have developed under cooler conditions that limit microbial activity should have a greater C_{BioR} (Laganière *et al.*, 2015). In addition, the microbial decomposition process is slowed by the waterlogged conditions of the soil environment, and rapid drainage on coarse-textured soils might favor less C_{BioR} accumulation (Bauhus *et al.*, 1998; Trumbore et Harden, 1997). Water limited

conditions may limit decomposition and favor the buildup of a C_{BioR} pool (Allison et Treseder, 2008). Overall, these results tend to support the hypothesis that climate has direct effects on soil C_{BioR}. On the other hand, wildfires induce polymerization and polycondensation of organic compounds, resulting in residues that are more resistant to biological degradation (Certini, 2005; Gonzalez-Perez *et al.*, 2004; Knicker, 2007). TSF was expected to have a direct positive effect on C_{BioR} and thus C_{BioR} was anticipated to increase with TSF. Soil pH also had a direct effect on soil bioreactivity because it regulates the microbial community (Fierer, N. et Jackson, 2006) and is a key determinant of the decomposition process (Prescott *et al.*, 2000; Zhang *et al.*, 2008). We expected decreasing C_{BioR} with more acidic soil conditions. Compared to *Sphagnum* spp., feather mosses decompose faster and have a lower productivity (Fenton *et al.*, 2010; Lang *et al.*, 2009), so we expected lower C_{BioR} reservoir with more *Sphagnum*. Also, manganese (Mn) availability has been shown to be a good predictor of boreal soil C stocks (Stendahl *et al.*, 2017); hence, Mn being a co-metabolic compound of lignin degradation, we assumed that Mn had a direct positive effect on C_{BioR}.

Alternative hypothesis for the FH horizon, FH2. As in hypothesis FH1, TSF, pH, moss functional type and Mn had direct effects on C bioreactivity. However, this hypothesis differed from FH1 in that TSF and moss dominance also had indirect effects on C_{BioR} through changes in pH conditions. We expected decreasing pH with increasing *Sphagnum* spp. dominance because some physiological characteristics of these organisms lead to environment acidification (Andrus, 1986). Also, in the short term, fire modifies pH through the liming effect (Gonzalez-Perez *et al.*, 2004; Knicker, 2007). In the long term, soils acidify as a result of vegetation regrowth, which implies the exchange of protons against cations to maintain the physiological electro-neutrality of the vegetation (Driscoll et Likens, 1982). Contrary to hypothesis FH1, which postulated climate and soil texture had direct effects on C_{BioR}, hypothesis FH2 assumed

these drivers only had indirect effects on C_{BioR} through their influence on moss dominance.

Baseline hypothesis for the mineral soil, MIN1. This hypothesis assumes there are only direct effects of environmental variables on C_{BioR} in the mineral soil. Climate and pH directly control the decomposition process (see FH1). Organic matter that bound with the mineral phase has been recognized has an important mechanism of C protection against decomposition (Doetterl *et al.*, 2015; Kaiser *et al.*, 2002; Porras *et al.*, 2017). We then assumed there are direct effects of soil texture and metal oxide contents on C_{BioR}. Following fire, the slow incorporation of charred residues from upper soil layers into the mineral soil could decrease the organic matter quality (Johnson et Curtis, 2001); therefor, C_{BioR} might decrease with increasing TSF. Mn availability could directly modulate C_{BioR} (see FH1), and exchangeable Al could impede microbial decomposition when in excess (Kunito *et al.*, 2016).

Alternative hypothesis for the mineral soil, MIN2. As an alternative to hypothesis MIN1, this hypothesis only assumes that TSF, pH, metal oxides and Mn/Al have direct effects on C_{BioR}. Additionally, pH is assumed to decrease with TSF because of the imbalance in nutrient uptake caused by aggrading vegetation (see FH2). Also, exchangeable cations are dependent on pH (Sanborn *et al.*, 2011) and the decrease in pH favors the creation of organometallic complexes impeding microbial decomposition (Buurman et Jongmans, 2005; Porras *et al.*, 2017). Contrary to hypothesis MIN1, which assumed direct effects of climate and soil texture on C_{BioR}, this hypothesis assumes that climate and soil texture only have indirect effects on C_{BioR}. The indirect effect of climate on C_{BioR} is mediated through its effect on mineral weathering (Doetterl *et al.*, 2015) and the quantity of metal oxides leached from the upper soil layers (Egli *et al.*, 2009). Compared to coarse-textured soils, fine-textured soils have more reactive surface sites that can bind additional Mn and Al ions (Six *et al.*, 2002).

3.4.4 Calculations and data analyses

3.4.4.1 Moss dominance index

In order to account for the effects of moss functional traits on C_{BioR} of the FH horizon, we discriminated between *Sphagnum* spp. and feather mosses, since they have different ecophysiological characteristics (Bisbee *et al.*, 2001). Based on Nalder et Wein (1999), we calculated an index of moss dominance (IMD) as follows:

$$IMD = \frac{O_{sph}}{O_{sph} + O_{pl} + O_h + O_{pt}}$$

where O is the sum of occurrence for a species in the 20 microplots (see section 2.1), *sph*: *Sphagnum* spp.; *pl*: *Pleurozium schreberi* (Brid.) Mitt.; *h*: *Hylocomium splendens* (Hedw.) Schimp.; *pt*: *Ptilium crista-castrensis* (Hedw.).

Feather mosses dominate the moss stratum when the IMD tends toward 0, whereas *Sphagnum* spp. dominate the moss stratum when the IMD tends toward 1. Some sites (n = 5) that recently burnt did not have any moss species regrowth at the time of the fieldwork. For these sites, we set the IMD to 0.

3.4.4.2 Soil C quality and bioreactivity

First, we wanted to estimate variation in the size of the soil C pools (bioreactive and recalcitrant) with TSF. For each soil layer (FH, top 15 cm of mineral soil and 15 to 35

cm of mineral soil), we scaled up to the plot scale the cumulative proportion of C mineralized at the end of the incubations and the proportion of acid-insoluble C as follows:

$$C_{fast} = C_{BioR} \times D_B \times h$$

$$C_{slow} = C_{AI} \times D_B \times h$$

where C_{fast} and C_{slow} are the bioreactive and recalcitrant soil C pools (Mg.ha^{-1}), C_{BioR} *is* the percentage of initial mass of soil C lost through microbial respiration (%), D_B is the bulk density (g.cm^{-3}), h is the soil depth (i.e., mean depth based on 20 measurements per plot for FH; cm) and C_{AI} is the acid-insoluble C fraction (%). Hereafter, the total C stock (C_{tot}), C_{fast} or C_{slow} pool size represent, within each plot, the sum of each C pool across all soil layers.

Second, to express the qualitative (relative) changes in soil C in relation to environmental variables, we used the proportion of initial mass of soil C lost through microbial respiration as an index of C_{BioR} (see section 2.2.4). In the statistical analyses, we considered the whole mineral soil (top 15 cm and 15 to 35 cm) as a unique soil layer by calculating the weighted mean by depth for all mineral soil variables.

3.4.4.3 Statistical analyses

First, we evaluated post-fire C stocks changes in functional reservoirs (bioreactive versus recalcitrant) using the linear regression of C stocks against TSF. Preliminary analyses with generalized additive models and piecewise regressions did not show any significant non-linear or segmented relationships. Second, we quantified direct and indirect causal relationships among variables and C_{BioR} using confirmatory path analysis with directional separation tests (d-separation or d-sep; Shipley (2000a)), according to the set of alternative *a priori* hypotheses (Figure 2). Path analysis was used together with Fisher's C test (Shipley, 2000b) as a simultaneous test of independence for a model basis set (i.e., all non-adjacent pairs of variables defined as claims of independence). This led us to quantify how our data supported each hypothetical DAG and to identify whether some hypotheses would be rejected based on a robust statistical test (Shipley, 2009). Fisher's C statistic was compared with a χ^2 distribution with 2k degrees of freedom (where k is the number of claims of independence in a model basis set). We rejected a causal model at the significance level $\alpha = 0.05$ when $p < \alpha$. Prior to analyses, we standardized (reduced centered) all variables to quantify their relative contribution to the variability of soil C_{BioR}.

The fit of each DAG within each soil layer (FH and mineral soil) was compared using a model selection approach together with the second order Akaike information criterion (AICc) in order to account for small sample size (Shipley, 2013). For model selection, we used the relative AICc difference with the 'best' model or relative weight (Symonds et Moussalli, 2010). To avoid having latent variables in the models, and because we had no *a priori* knowledge about which specific climate, texture or exchangeable elements should be used for testing the validity of each hypothesis, we used the cross-product of four climatic variables (MAT, GDD5, MAP, WB), three soil texture

variables (sand %, silt % and clay %), and two exchangeable elements (Al and Mn, only for mineral soil). Therefore, we tested a total of 12 and 24 model combinations for each hypothesis/DAG for the FH horizon and the mineral soil, respectively. Each soil layer having two alternative causal hypotheses, we then compared 24 and 48 candidate DAG models using a model selection procedure for FH and mineral soil, respectively. Model-averaged estimates were calculated by multiplying each estimate within each model by the corresponding Akaike weight and by summing the resulting values across all models; this allowed all models to influence model-averaged estimates. By doing so, we guarded against making arbitrary decisions about which model should be considered. We used the '*ggm*' package to compute Fisher's *C* statistic (Marchetti *et al.*, 2015). All calculations and statistics were made using the *R* software version 3.4.3 (R Core Team, 2017). All data presented in this paper can be accessed online for free (to be determined).

3.5 Results

3.5.1 Post-fire soil carbon pool size

Total soil C stock (C_{tot}), the size of the recalcitrant C pool or the size of C_{BioR} pool (C_{slow} and C_{fast}, respectively) all increased linearly with TSF (Figure 3.3A). A minimum C_{tot} value of 63 MgC.ha^{-1} was observed for a 100-years-old stand, which is close to the C_{tot} value of 66 MgC.ha^{-1} of the youngest (2-years-old) stand. A maximum C_{tot} value of 305 MgC.ha^{-1} was observed for a 283-years-old stand. On average, C_{slow} size was 6-fold bigger than C_{fast} size. C_{fast} values ranged from 5 MgC.ha^{-1} to 25 MgC.ha^{-1} for a 100-year-old stand and for a 91-year-old stand, respectively. C_{slow} values were 29 MgC.ha^{-1} and 175 MgC.ha^{-1} for the 2-year-old stand and for a 91-year-old stand, respectively.

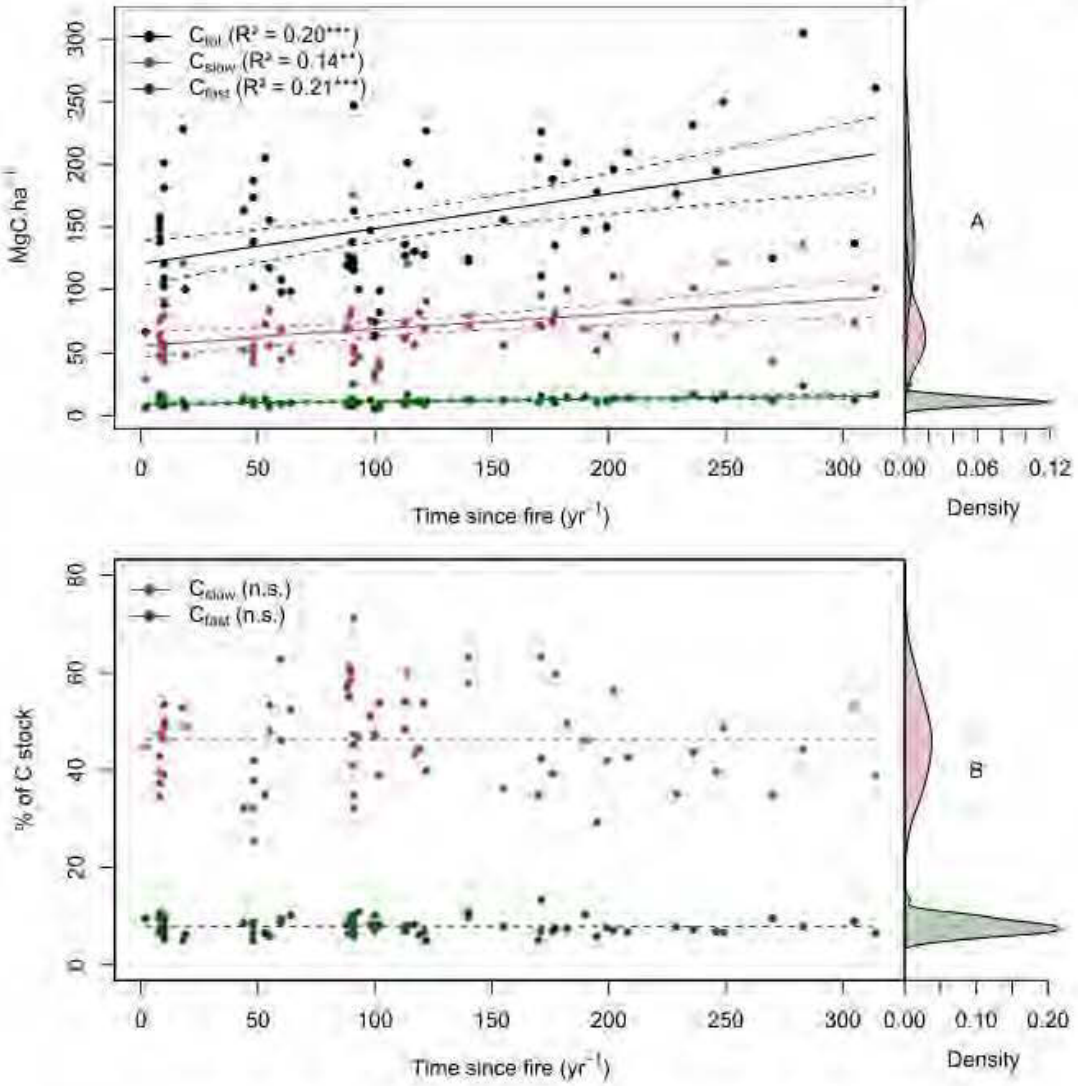

Figure 3.3 Carbon quality as a function of time since fire (TSF). The upper panel shows the total soil C reservoir (C_{tot}), the recalcitrant C pool (C_{slow}) and the C_{BioR} pool (C_{fast}) sizes as a function of TSF (A, on the left), and the kernel density for each pool (A, on the right). The lower panel shows the proportion of C_{slow} and C_{fast} relative to C_{tot} as a function of TSF (B, on the left), and their kernel density (B, on the right).

Using these simple linear trends, C_{tot} accumulated faster than C_{slow} and C_{fast}, and C_{fast} showed the lowest accumulation rate (Table 2 and Figure 3A). Surprisingly, the

proportion of C_{slow} and C_{fast} remained constant over the timespan of the fire chronosequence (Figure 3B), implying that overall soil C quality does not vary quantitatively with TSF ($R^2 < 0.01$, $p \geq 0.81$ for both C pools; Table 2).

Table 3.2 Post-fire soil C pool size and accumulation rates.

		Mean (± sd)	Equation	R^2	p-value
C_{tot}	$MgC.ha^{-1}$	150.80 (± 49.91)	120.32 + 0.280*(TSF)	0.20	**< 0.001**
C_{slow}	$MgC.ha^{-1}$	69.01 (± 25.79)	56.16 + 0.118*(TSF)	0.14	**0.002**
	% of C_{tot}	46.40 (± 9.35)	46.74 - 0.003*(TSF)	< 0.01	0.808
C_{fast}	$MgC.ha^{-1}$	11.47 (± 3.59)	9.25 + 0.020*(TSF)	0.21	**< 0.001**
	% of C_{tot}	7.85 (± 1.67)	7.87 – 0.0002*(TSF)	<0.01	0.935

3.5.2 FH path analysis and model selection

The causal structure of the baseline hypothesis FH1, which assumes there are only direct effects of covariates on C_{BioR} in the FH horizon, was rejected based on Fisher's *C* statistic ($p < 0.05$; Figure 3.4 and Table S3.1). Instead, the causal structure of the alternative hypothesis FH2 was supported by the data, which indicates that indirect effects among covariates and C_{BioR} in the FH horizon need to be accounted for to properly assess the variation structure in the data. The model selection procedure revealed that one model best fitted the data (hereafter, 'best' model; Figure 3.4 and Table S3.1); this model belonged to FH2, with MAP as the climate variable and clay content as the texture variable. The Akaike weight for this model (68%) was about eight times greater than the weight of the second most supported model (8%). Thereafter, we focused our analysis on the 'best' FH2-based path model.

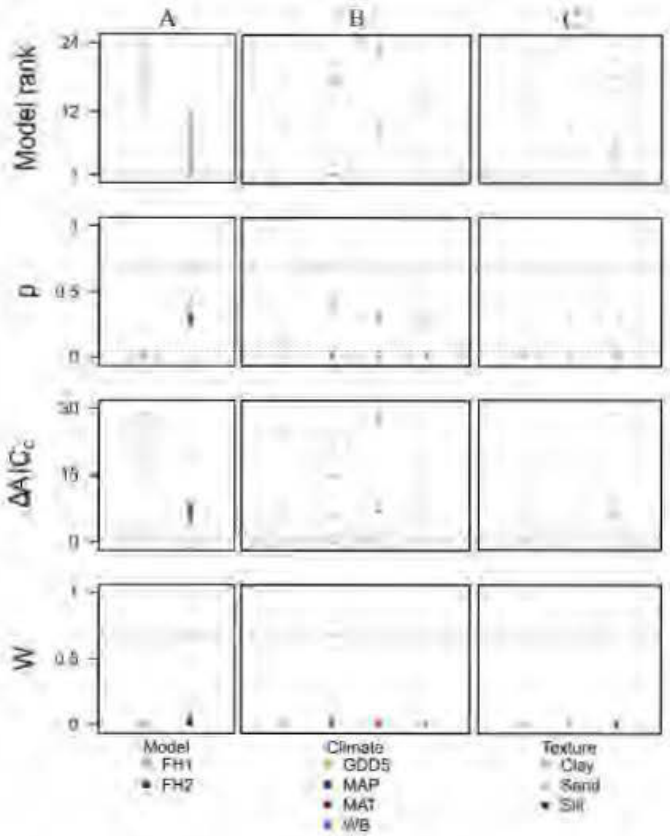

Figure 3.4 Model comparison for the two hypotheses testing for C_{BioR} in the FH horizon. The left panel (A) shows the comparison between models FH1 and FH2. The central panel (B) shows the climate variables corresponding to each model. The right panel (C) shows the texture variables corresponding to each model. *Model rank*: rank based on the second order Akaike criterion (AIC_c); *p*: p-value of Fisher's *C* statistic, with p = 0.05 (dashed line); *ΔAICc*: AIC_c difference with the 'best' model, with $\Delta AIC_c = 2$ (dashed line); *W*: Akaike weight. *FH1*: baseline model considering only the direct effects of covariates on the C_{BioR} in the FH horizon; *FH2*: alternative model considering the direct and indirect effects of covariates on the C_{BioR} in the FH horizon; *GDD5*: growing-degree days above 5°C; *MAP*: mean annual precipitation; *MAT*: mean annual temperature; *WB*: water balance; *Clay*: clay content in the top 35 cm of mineral soil; *Sand*: sand content in the top 35 cm of mineral soil; *Silt*: silt content in the top 35 cm of mineral soil. The model that best fits the data is highlighted with a red banner.

When accounting for all covariables together, exchangeable Mn and pH of the FH horizon showed the greatest direct and positive effects on C_{BioR} of the FH horizon (both with a path coefficient, pc = 0.34, $p < 0.01$; Figure 3.5 and Table S3.2). TSF was the second most important relative driver with a significant direct and positive effect on C_{BioR} (pc = 0.25, $p < 0.05$). Moss dominance had no significant direct effect on C_{BioR} (pc = 0.08, p = 0.46). In addition, TSF and moss dominance had indirect effects on C_{BioR} through their effects on pH (TSF: pc = -0.33, $p < 0.01$; moss dominance: pc = 0.31, $p < 0.01$; Figure 3.5). Also, the model contained an indirect effect of climate (MAP) on C_{BioR} through its direct and negative effect on moss dominance (pc = -0.33, $p < 0.01$). Texture (clay content) of the mineral soil had no significant effect on moss dominance (pc = 0.06, p = 0.62). When accounting for the direct relationships of covariates on C_{BioR}, the hypothesis FH2 explained 30% of the variation in C_{BioR}.

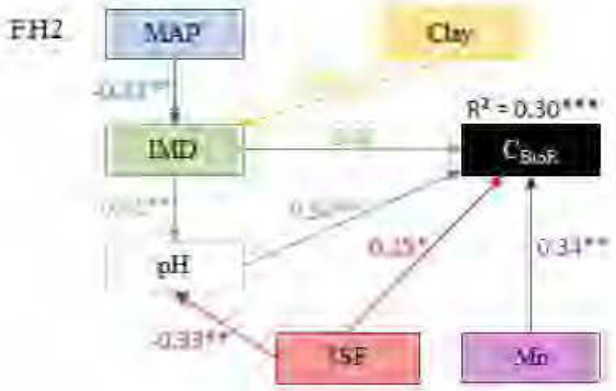

Figure 3.5 Model that best fitted the data to explain carbon bioreactivity (C_{BioR}) in the FH horizon. Arrows indicate direct causal relationships. The numbers are standardized path coefficients. *MAP*: mean annual precipitation; *Clay*: clay content in the top 35 cm of mineral soil; *Mn*: exchangeable manganese; *pH*: pH of the FH horizon; *TSF*: time since fire; *IMD*: index of moss dominance. (*) $p < 0.05$; (**) $p < 0.01$; (***) $p < 0.001$.

By allowing all the models (FH1 and FH2) to influence estimates, the model-averaging procedure indicated that the most important variables exerting a direct control over C_{BioR} of the FH horizon were, by decreasing importance: pH and Mn, TSF, and moss dominance (Figure 3.6 and Table S3.2). According to the model-averaging procedure, the direct effect of climate and texture on C_{BioR} was null.

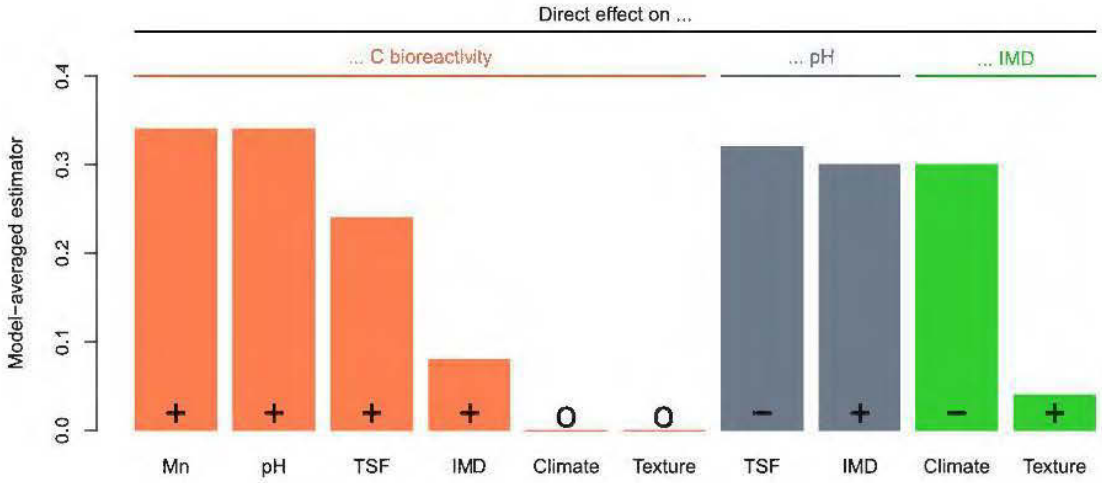

Figure 3.6 Normalized and weighted estimates of the direct effects according to the model-averaging procedure for the FH horizon, accounting for all the models' Akaike weights. Orange: direct effect on C_{BioR}; Grey: direct effect on pH of the FH horizon; Green: direct effect on moss dominance. Symbols on the bars represent positive effects (+), negative effects (-), or null effects (o). *Mn*: exchangeable manganese; *pH*: pH of the FH horizon; *TSF*: time since fire; *IMD*: index of moss dominance; *Climate*: climate variable; *Texture*: texture variable.

3.5.3 Mineral soil path analysis and model selection

The causal structure of the baseline hypothesis MIN1, which assumed only that the direct effects of covariates on the C_{BioR} of the mineral soil, was rejected based on Fisher's *C* statistic ($p < 0.05$; Figure 3.4 and Table S3.3). Instead, the causal structure of the alternative hypothesis MIN2 was supported by the data indicating that indirect effects among covariates need to be accounted for assessing properly the variation in the C_{BioR} stock of the mineral soil. The model selection procedure revealed that one model best fitted the data (hereafter, 'best' model; Figure 3.7 and Table S3.3). This model belonged to MIN2, with WB as the climate variable, clay content as the texture variable, and Al as the exchangeable element variable. The Akaike weight for this model (47%) was about three times greater than for the second most supported model (14%). Thereafter, we focused our analysis on the 'best' MIN2-based path model.

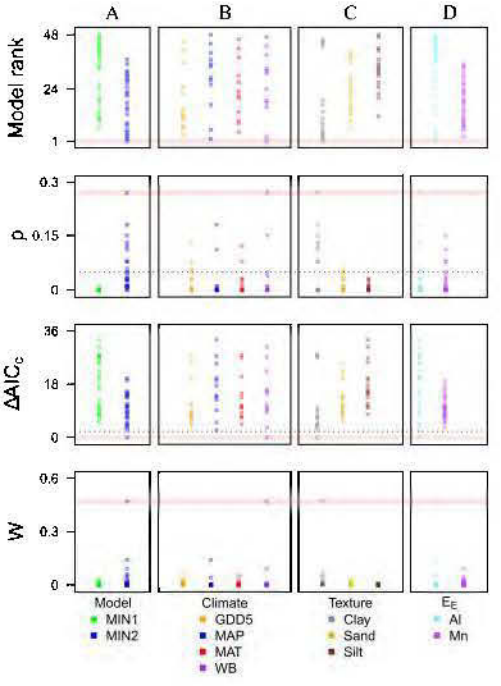

Figure 3.7 Model comparison for the two hypotheses testing for the C_{BioR} in the top 35 cm of mineral soil. From left to right: comparison between models MIN1 and MIN2 (A); climate variables corresponding to each model (B); texture variables corresponding to each model (C); exchangeable elements corresponding to each model (D). *Model rank*: rank based on the second order Akaike criterion (AIC_c); *p*: p-value of Fisher's *C* statistic, with p = 0.05 (dashed line); *ΔAIC$_c$*: AIC_c difference with the 'best' model, with ΔAIC_c = 2 (dashed line); *W*: Akaike weight. *MIN1*: baseline model considering only the direct effects of covariates on C_{BioR} in the top 35 cm of mineral soil; *MIN2*: alternative model considering the direct and indirect effects of covariates on C_{BioR} in the top 35 cm of mineral soil; *GDD5*: growing-degree days above 5°C; *MAP*: mean annual precipitation; *MAT*: mean annual temperature; *WB*: water balance; *Clay*: clay content in the top 35 cm of the mineral soil; *Sand*: sand content in the top 35 cm of the mineral soil; *Silt*: silt content in the top 35 cm of the mineral soil; *Al*: exchangeable aluminum in the top 35 cm of the mineral soil; *Mn*: exchangeable manganese in the top 35 cm of the mineral soil. The model that best fits the data is highlighted with a red banner.

When accounting for all covariables together, exchangeable Al showed the greatest direct and negative effect on the C_{BioR} of the mineral soil (pc = -0.43, $p < 0.001$; Figure 3.8 and Table S3.4). Metal oxide content and pH were the second most influential drivers with significant and negative direct effects on the C_{BioR} of the mineral soil (both with a path coefficient, pc = -0.27, $p < 0.05$). TSF had a small positive direct effect on the C_{BioR} of the mineral soil, but this relationship was not significant (pc = 0.09, p = 1). In addition, pH had two indirect effects on the C_{BioR} of the mineral soil, i.e., through its negative and direct effects on Al and Mpy (Al: pc = -0.33, $p < 0.01$; Mpy: pc = -0.38, $p < 0.01$). Interestingly, clay content had an indirect effect on the C_{BioR} of the mineral soil, through its direct and positive effect on exchangeable Al (pc = 0.24, $p < 0.05$). Also, climate (here, WB) had a weak indirect effect on the C_{BioR} of the mineral soil through its direct effect on Mpy (pc = 0.21, p = 0.07). When accounting for the direct relationships of covariates on C_{BioR}, the hypothesis MIN2 explained 22% of the variation in C_{BioR} in the mineral soil.

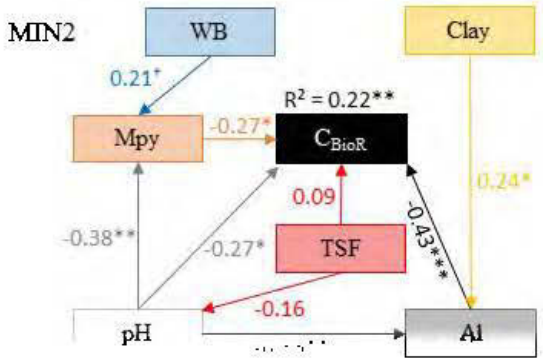

Figure 3.8 Model that best fitted the data to explain the carbon bioreactivity (C_{BioR}) in the top 35 cm of the mineral soil. Arrows indicate direct causal relationships. The numbers are standardized path coefficients. *Al*: exchangeable aluminum in the top 35 cm of the mineral soil; *pH*: pH of the top 35 cm of the mineral soil; *TSF*: time since fire; *Mpy*: metal oxide content in the top 15 cm of the B horizon; *WB*: water balance; *Clay*: clay content the top 35 cm of the mineral soil. (†) $p < 0.10$; (*) $p < 0.05$; (**) $p < 0.01$; (***) $p < 0.001$.

By allowing all the models (MIN1 and MIN2) to influence estimates, the model-averaging procedure indicated that the most important variables exerting a direct control over the C_{BioR} of the mineral soil were, by decreasing importance: exchangeable elements, metal oxide contents, pH, TSF, and climate (Figure 3.9 and Table S3.4). According to the model-averaging procedure, the direct effect of mineral soil texture on C_{BioR} was null.

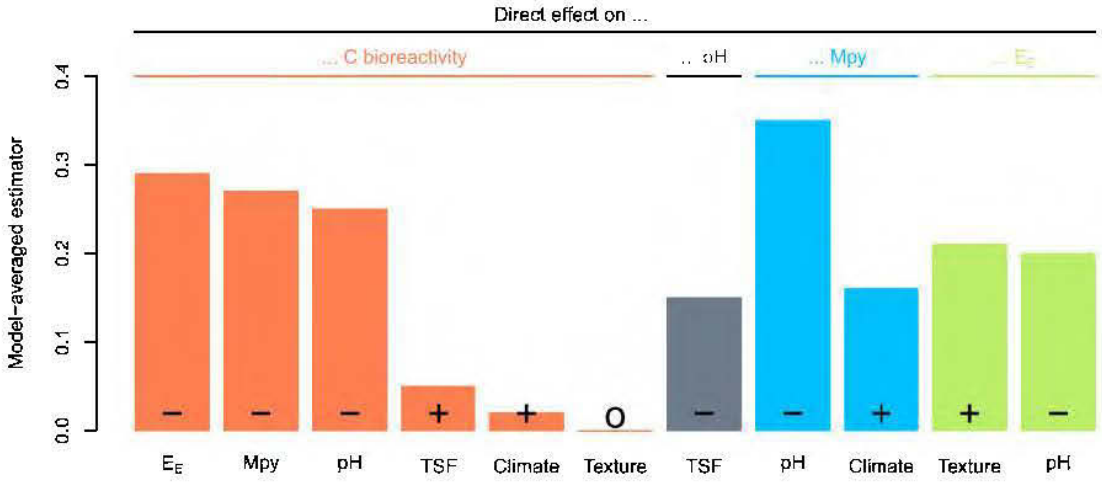

Figure 3.9 Normalized and weighted estimates of the direct effects according to the model-averaging procedure for the top 35 cm of the mineral soil, accounting for all the models' Akaike weights. Orange: direct effect on C_{BioR}; Grey: direct effect on pH of the mineral soil; Blue: direct effect on metal oxide content in the B horizon; Green: direct effect on echangeable elements. Symbols on the bars represent positive effects (+), negative effects (-) or null effects (o). *E_E*: exchangeable elements in the top 35 cm of the mineral soil; *pH*: pH of the top 35 cm of the mineral soil; *TSF*: time since fire; *Mpy*: metal oxide content of the top 15 cm of the B horizon; *Climate*: climate variable; *Texture*: texture variable.

3.6 Discussion

3.6.1 Post-fire soil C quality and bioreactivity

Most of the studies on post-fire soil C have focused on immediate- or short-term responses and found that fire affects soil C quality by creating profound changes in the structure of soil organic matter compounds through thermal oxidation (Certini, 2005; Gonzalez-Perez *et al.*, 2004). By using a long-term chronosequence of TSF ranging from 2 to 314 years, our study was able to provide important insights into the understanding of the trajectory of soil C quality following fire, over hundreds of years. Our results indicate that both fast- and slow-cycling soil C pools accumulate with TSF, and that the proportion of each C pool remains constant with TSF relative to total soil C stock (Figure 3.2 and Table 3.1). This does not necessarily imply that fire has no effect on soil C functional pools, because our chronosequence has a low resolution for the first years following fire, but rather that these changes, if present, may not be long lasting.

Our results also challenge the concept that the amount of C that soil can accumulate is fixed and determined by soil physical properties such as clay content (Abramoff *et al.*, 2017; Castellano *et al.*, 2015). Instead, our study suggests that in a humid and acidic environment that favors the development of Podzolic soils, other soil properties related to stabilization mechanisms (Rasmussen *et al.*, 2018) should be considered to better predict soil C dynamics. Specifically, we found that the accumulation process of C_{BioR} does not saturate, at least not in the first three centuries following fire, as an equilibrium between C input and decay was not achieved. Alternatively, environmental conditions limiting decomposition, such as cold temperatures under a thickening FH horizon developed with TSF, protect labile C and allow its accumulation (Kane *et al.*, 2005).

3.6.2 Control mechanisms of the soil C bioreactivity

This study shows that C_{BioR} of the FH horizon and of the mineral soil is affected by different climatic and non-climatic variables, which suggest that different mechanisms control the decomposition process in the FH horizon and in the mineral soil (Shaw *et al.*, 2015; Ziegler *et al.*, 2017).

3.6.2.1 C_{BioR} in the FH horizon

As found in other ecosystems, soil C_{BioR} in the FH horizon was lower in warm site conditions compared with cold ones in boreal forests (Laganière *et al.*, 2015). In contradiction with these results, we did not detect any direct effect of climate on soil C_{BioR} in the FH horizon. Consequently, our results do not support the CQT hypothesis. This indicates that at the regional scale of the boreal forest studied, soils that experience different temperature conditions are unlikely to show any greater susceptibility to C losses through decomposition with global warming, at least in the range of climate conditions experienced over the last three centuries. This finding agrees with the results of unchanged soil C stocks with *in situ* experimental warming worldwide (van Gestel *et al.*, 2018). Also, when synthesizing data of *in situ* experimental warming, Carey *et al.* (2016) found no change in the temperature sensitivity of soil respiration at the global biome scale, while changes were found to be significant for the boreal biome. The cumulative soil C mineralization in our study was not modulated by temperature, which supports the results of Carey *et al.* (2016) for their whole dataset, but not for the boreal biome-restricted dataset. However, Carey *et al.* (2016) did not study soils from the Canadian Boreal Shield, as in our study. Our contradictory results suggest potential intra-biome regional variations in the susceptibility to soil C losses, and that Podzolic

soil properties and other temperature-independent factors predispose the response of soil C dynamics as regards climate change.

As discussed above, C_{BioR} in the FH horizon increased with TSF. Additionally, TSF had an indirect effect on C_{BioR} in the FH horizon, mediated by pH. In contradiction with our hypotheses FH1 and FH2 and with results showing a direct effect of moss dominance on C stock in the FH horizon (Andrieux *et al.*, 2018b), moss dominance had no direct effect on C_{BioR} in the FH horizon. Instead, we found an indirect effect of moss dominance on C_{BioR} in the FH horizon, which was also mediated by pH. Hence, pH appears to be a key factor regulating C_{BioR} in the FH horizon. Changes in pH conditions as a function of TSF confirm our hypothesis (see hypothesis FH2 in section 3.4.3).

Our results also show that C_{BioR} in the FH horizon increased with increasing concentrations of exchangeable Mn. In our study, we did not normalize Mn to C contents (Stendahl *et al.*, 2017) to avoid potentially erroneous conclusions arising from "spurious" correlations between Mn and C_{BioR} (Berges, 1997; Brett, 2004). As mirrored by the high acid-insoluble fraction contained in our FH horizon samples (73 ± 5% of acid-insoluble C, data not shown), boreal evergreen coniferous species generate high lignin contents in litters and forest floors (Laganière *et al.*, 2017). Thus, soil C cycling in this ecosystem should depend on the capacity of microbes to depolymerize lignin. Microorganisms in the acidic soils of this ecosystem are dominated by fungi that use metalloenzymes – such as Mn peroxidases – to metabolize lignin (Pollegioni *et al.*, 2015), or are white-rot fungi (Basidiomycota) equipped with enzymes that oxidize lignin (Cragg *et al.*, 2015). Additionally, there is increasing evidence of enhanced bacterial lignin degradation in the presence of exchangeable Mn through pathways that are less efficient than those used by fungi (de Gonzalo *et al.*, 2016). Our study provides

a new insight about the role of soil chemistry as a controlling mechanism of C_{BioR} in the FH horizon, where pH limits the activity of soil microbes and exchangeable Mn is a mediator of decomposition in lignin-rich environments.

3.6.2.2 C_{BioR} in the mineral soil

As in the FH horizon, pH was found to be a key factor regulating C_{BioR} in the mineral soil. In addition to having a direct effect, pH was found to have two indirect effects: the first one is metal oxide contents mediation. Low pH conditions in the mineral soil are conducive to enhanced metal oxide contents, which in turn decreases C_{BioR} in the mineral soil. This result is consistent with our previous findings about mineral soil C stock and strengthens our previous assumptions about the role played by pH in mineral weathering and the preservation of C from decomposition through organo-metal complexation (Andrieux *et al.*, 2018b). The second indirect effect of pH on C_{BioR} in the mineral soil is mediation by exchangeable Al only; not Mn (Table S3.4). Microbes are, in general, vertically stratified within the soil column (Clemmensen *et al.*, 2013; Ekschmitt *et al.*, 2008; Hynes et Germida, 2013), with fungi populating the upper soil layers because of their greater need for metabolic oxygen compared with bacteria, which can more easily dwell in the less-oxygenated deeper soil layers. Our results suggest that oxidative depolymerization of lignin compounds mediated by Mn peroxidases may not be a major process for C cycling in the mineral soil, contrary to the FH horizon (see above). Instead, the negative effect of pH on Al together with the negative effect of Al on C_{BioR} in the mineral soil indicate that low pH conditions favor a greater Al abundance, which in turn impedes C decomposition. These findings are consistent with the mechanism of pH-dependent Al toxicity on microbial degradation that has been described for acidic forest soils in Japan (Kunito *et al.*, 2016) and in laboratory experiments (Wood, 1995). However, our study goes one step further in that

we showed that Al content is directly related to soil texture (especially clay content). This supports the hypothesis that exchangeable Al bound to fine mineral particles, such as clay might act as a source of stored Al that can be mobilized and complexed with C to impede decomposition.

3.6.3 Research needs

The results of this study identified new pathways for the control mechanisms of soil C_{BioR} that could help to predict the response of boreal forest soils to global change. While earth system models (ESMs) commonly assume a temperature dependence of soil C decomposition according to the CQT hypothesis for the last two decades (Bradford *et al.*, 2016), our study focusing on Podzolic boreal forest soils showed that the current approach of ESMs for modeling soil C should be re-evaluated to account for ecosystem-specific C processes. In particular, our study shows that predictive models need to include the direct effects of soil chemistry and the indirect effects of climate and soil texture on soil C_{BioR}. Moreover, while some processes were found to affect soil C_{BioR} (this study) and soil C stocks (Andrieux *et al.*, 2018b), other processes did not. For example, moss dominance had a direct effect on C sotck of the FH horizon (Andrieux *et al.*, 2018b), but not on FH horizon C_{BioR} (this study). ESMs that would consider the drivers of soil C stock as well as the drivers of soil C_{BioR} would build confidence in the forecasted role of the boreal forest to act as a C source or a C sink in response to global warming.

The path analyses and model selection procedure used in our study have made it possible to distinguish direct from indirect effects of factors on soil C dynamics. We conclude that the effect of climate on soil C_{BioR} is indirect and that of the four climatic variables examined, only the variables related to water supply – and not temperature –

were found to have a significant indirect effect on soil C_{BioR}. This suggests that the forecasted increase of 11% precipitation by the end of this century in eastern North America (IPCC, 2013) would indirectly modulate soil C stocks (Andrieux *et al.*, 2018b) and soil C_{BioR} (this study), together with the direct effects of climate on the mechanisms of soil C stock and bioreactivity. How the boreal ecosystem C balance will evolve in the context of global change might be assessed through further research focusing on the changes in soil physico-chemical reactions pertaining to the mechanisms of soil organic matter decomposition and stabilization (Thornley et Canell, 2001) in Podzolics soils, as well as in other soil types that commonly occur in the boreal biome where the physico-chemical control over decomposition and stabilization may differ from Podzols.

3.7 Conclusion

The bioreactivity of the large C reservoirs in boreal forest soils is a key factor regulating future global C cycle in the context of global warming. Our study provides new insights into the complex interplay between climatic and non-climatic factors controlling soil C_{BioR}. We showed that soil chemistry plays a dominant role in controlling soil C_{BioR}, with exchangeable elements (Mn or Al) and soil pH being the main drivers both in the FH horizon and in the mineral soil. The increasing C_{BioR} of the FH horizon with TSF was outbalanced by the mediating effect of pH, which implies that acidic soil conditions in post-fire old-growth forests favor the accumulation of labile C by limiting the activity of soil decomposers. However, the antagonist effects of exchangeable elements on the FH horizon and on the mineral soil found in this study imply that global change might lead to different responses in mineral soil and organic (FH) soil layers. Therefore, focusing on the amplitude of these changes in soil chemistry is a key

challenge that remains to be addressed in future works to improve our understanding of soil C balance with global change.

We showed that climate, expressed here as temperature and water availability factors, has no direct effect on soil C_{BioR}. Moreover, the indirect effects of climate on soil C_{BioR} are limited to water supply factors, not to temperature. Thus, our results reinforce the need to revise the concepts of soil C dynamics commonly used by ESMs, especially when applied to boreal ecosystems, so that the predicted responses of terrestrial ecosystems to climate change may be specific to ecosystems. Our results are in agreement with Davidson et Janssens (2006) and Davidson (2015), who suggest that improvements to ESMs may arise from integrating the long-term effect of climate on soil properties with the environmental constraints on microbiological degradation of soil organic matter.

3.8 Acknowledgements

This project was funded by Mitacs Acceleration grants IT05018 (FR11062 to FR11067). We thank Catherine Bruyère, Cécile Remy, Arnaud Guillemard and Eric Beaulieu for field assistance. We are grateful to Danielle Charron and Pierre Clouâtre for helping with field logistics. We warmly thank Véronique Poirier, Jean Noël and Emeline Chaste for help with geomatic work and Serge Rousseau for laboratory analyses as well as Cindy Shaw for insightful comments. We declare no conflicts of interest.

CONCLUSION GÉNÉRALE

L'objectif général des travaux effectués dans le cadre de cette thèse de doctorat était d'approfondir les connaissances associées aux processus de stockage du carbone dans les sols mésiques en pessière à mousses au Québec. Le domaine de la pessière à mousses au Québec comprend les plus grandes étendues forestières exploitables à l'échelle de la province. Bien que défini comme unité homogène du territoire, ce domaine englobe néanmoins une mosaïque forestière aux caractéristiques biotiques et abiotiques parfois hétérogènes (Ministère des Ressources Naturelles du Québec, 2013; Saucier *et al.*, 1998). Dans nos travaux, les plans d'échantillonnage ont été réfléchis pour refléter les caractéristiques dominantes à l'échelle du paysage. Les nouvelles connaissances générées par nos travaux pourraient donc être transposables à la plus grande partie de ce territoire.

4.1 Contributions à l'avancement des connaissances

4.1.1 Considérations spatiales des processus de stockage du COS

La taille des réservoirs de COS et leurs vitesses de recyclage sont largement associés aux conditions spatiales de température et de précipitations (Carey *et al.*, 2016; Stockmann *et al.*, 2015), ainsi qu'aux caractéristiques de la végétation (Laganière *et al.*, 2017). La distribution zonale et/ou altitudinale des types végétaux amène ainsi une confusion à propos de la contribution relative du climat sur les processus de stockage du COS (Jobbagy et Jackson, 2000; Marty *et al.*, 2015). Circonscrits aux peuplements d'épinettes noires, nos travaux s'affranchissent ainsi de l'effet de la composition

végétale arborescente et permettent de mieux comprendre l'influence des patrons climatiques sur les processus spatiaux liés au stockage du COS.

Les travaux de cartographie prédictive effectués à l'échelle du Canada montrent que la concentration du COS est presque exclusivement expliquée par des variables climatiques, relativement aux variables topographiques (Mansuy *et al.*, 2014). La localisation géographique ou les conditions de précipitations se sont aussi révélées être des prédicteurs des stocks de COS à l'échelle du Québec (Marty *et al.*, 2015; Tremblay *et al.*, 2002). Les travaux réalisés dans le cadre de cette thèse supportent les résultats obtenus par les études antérieures. En effet, des tendances régionales observées pour les caractéristiques du COS ont surtout été attribuées aux régimes climatiques (Chapitre I). De plus, les résultats obtenus dans nos travaux ont aussi montré que les variables climatiques liées aux conditions hydriques, seules, avaient une influence sur les processus rattachés au stockage du COS et non pas les variables de température (Chapitre II et Chapitre III). En quantifiant la taille des réservoirs de COS et en déterminant les facteurs qui facilitent leur décomposition, nos travaux apportent néanmoins un regard nouveau sur les influences relatives du climat et des autres facteurs non-climatiques dans le contrôle des processus liés au stockage du COS. En effet, nos résultats montrent que le régime hydrique n'a qu'une influence indirecte sur les stocks de COS (Chapitre II) ou leur bioréactivité (Chapitre III), au travers de leurs influences sur d'autres facteurs bio-physicochimiques. Ces résultats obtenus en forêt boréale sont par ailleurs cohérents avec les observations effectuées dans d'autres types d'écosystèmes (Doetterl *et al.*, 2015).

Parmi les faits majeurs mis en évidence par nos travaux, on peut également souligner l'importance du temps depuis le dernier feu (TDF) sur le contrôle des processus de stockage du COS. Le TDF avait des effets direct et indirect sur les stocks et la bioréactivité du COS de l'horizon organique (Chapitre II et Chapitre III), et un effet

indirect sur le stock de COS de l'horizon minéral d'accumulation (Chapitre II). Dans leur ensemble, nos résultats suggèrent que la structure de classes d'âges des peuplements, dépendante en grande partie du TDF dans ces écosystèmes sujets aux incendies récurrents (Bergeron *et al.*, 2001), pourrait être un prédicteur notable des processus de stockage du COS à l'échelle du paysage (Kurz *et al.*, 2013). Les effets du TDF sur les processus de stockage du COS restent mal compris, particulièrement en ce qui a trait au sol minéral (Chapitre II). C'est sans doute la raison pour laquelle les travaux de cartographie prédictive des propriétés du sol n'intègrent pas le TDF en covariable (Beguin *et al.*, 2017; Mansuy *et al.*, 2014; Tremblay *et al.*, 2002).

En somme, nos résultats impliquent que les prédictions spatiales des stocks de COS et de leur évolution potentielle pourraient être améliorées en intégrant à la fois la structure de classes d'âges des peuplements ou le TDF, ainsi que les variables bio-physicochimiques qui varient de concert avec le climat et le TDF. Affiner de telles prédictions spatiales apporterait une base robuste pour quantifier les stocks de COS et permettrait de réduire les incertitudes liées aux exercices de projection dans le temps.

4.1.2 Temporalités des processus liés au stockage du COS

L'évolution temporelle des processus de stockage du COS ont été abordés, dans nos travaux, au moyen d'une chronoséquence après feu dans un horizon de 314 ans. Les résultats obtenus par cette méthode nous ont permis de mettre en évidence que, même si l'accumulation du C dans la végétation arborescente atteignait un seuil de saturation avec le TDF aux environs de 90 ans après feu, les stocks de C dans l'écosystème continuaient d'augmenter et que cette augmentation était due à l'accumulation constante de C dans les réservoirs du sol (Chapitre II). En contradiction avec certaines études (Gao *et al.*, 2017; Wardle, Walker, *et al.*, 2004), nos résultats supportent

néanmoins l'idée que les forêts anciennes continuent d'accumuler du C (Carey *et al.*, 2001; Curtis et Gough, 2018; Luyssaert *et al.*, 2008), essentiellement dans les sols (Zhou *et al.*, 2006). En plus d'apporter une nouvelle preuve descriptive de ce phénomène, nos travaux ont permis de mettre en évidence l'un des mécanismes associés à ce processus, au moins propre à l'écosystème étudié. Si seul l'effet direct du TDF sur la bioréactivité du COS dans l'horizon organique avait été considéré, d'aucuns en seraient venus à la conclusion que le réservoir de COS diminuerait avec l'augmentation du TDF (Annexe C, Tableau S3.2). Confirmant ce qui a été préalablement observé dans cet écosystème (Ward *et al.*, 2014), le pH de l'horizon organique diminue avec le TDF. Or, nos données suggèrent que l'effet direct et négatif du pH sur la bioréactivité du COS dans l'horizon organique est plus important que l'effet direct et positif du TDF. Le stock de COS dans l'horizon organique s'accumulait ainsi avec le TDF (Chapitre II) – en principe sous une forme facile à décomposer, en raison de l'inhibition de l'activité des microbes décomposeurs par acidification du substrat (Chapitre III). La modification de paramètres chimiques du sol, comme ici le pH qui contrôle directement l'activité des microbes du sol et donc les flux de C sortants du système, s'opère donc à l'échelle décennale à centennale de la régénération et de la maturation végétale arborescente.

Le pH du sol minéral était aussi un prédicteur de la quantité d'oxydes métalliques associés à la matière organique (Chapitre II-III). Or, la quantité d'oxydes métalliques exerçait une influence directe sur le stock et sur la bioréactivité du COS. Encore une fois, comme le pH variait avec le TDF, nos résultats impliquent que la formation des complexes organométalliques dans les sols s'opère dans un horizon temporel décennal à centennal.

Ces observations revêtent une importance capitale dès lors qu'on considère la dizaine et centaine d'années comme étant l'échelle opérante des changements climatiques

(IPCC, 2013). Pour comprendre comment les processus de stockage du COS pourraient évoluer avec les variations des conditions environnementales liées au réchauffement climatique, il est donc nécessaire de tenir compte des interactions complexes entre les facteurs qui les contrôlent (Bradford *et al.*, 2016).

4.1.3 Dynamique du COS intégrée à la complexité de l'écosystème

Le modèle factoriel *scorpan* (McBratney *et al.*, 2003) est une généralisation du modèle des facteurs d'état de la formation des sols (Jenny, 1994), ou plus globalement du modèle des facteurs d'état des écosystèmes (Amundson et Jenny, 1997). D'après cette conception, un attribut du sol est mathématiquement représenté comme une fonction de la somme et/ou des interactions entre sept facteurs d'état (McBratney *et al.*, 2003) : sol, climat, organismes, topographie ou attributs du paysage, matériel parent, âge, espace ou position spatiale. Largement utilisée pour les prédictions spatiales des propriétés du sol, cette approche ne permet pas de comprendre les processus déterminant un attribut du sol, puisque les relations de dépendances entre les facteurs ne sont pas explicitement formulées. Pourtant, les relations entre ces facteurs, exprimées sur des bases mécanistiques, représentent le cœur des modèles numériques du système Terre. Ces modèles pourraient être améliorés en intégrant les connaissances adossées aux processus de stockage du COS pour projeter et mieux anticiper la dynamique du COS en réponse aux changements environnementaux liés au réchauffement climatique (Schmidt *et al.*, 2011).

Un des résultats saillants de nos travaux, qui s'appuient sur une méthode d'analyse de pistes, réside dans la représentation mécanistique des processus rattachés aux stockage du COS (Chapitre II-III). Les analyses de piste sont généralement utilisées pour explorer les relations de dépendance entre les facteurs impliqués dans les processus de

stockage du COS (e.g. Zhang *et al.* (2008); Luo *et al.* (2017)). L'approche développée dans nos travaux, basée sur l'examen d'hypothèses *a priori* fondées sur les connaissances issues de la littérature scientifique, va encore plus loin dans le sens où elle est confirmatoire et non exploratoire. En plus d'offrir la possibilité de falsification des hypothèses, cette approche nous a permis de déterminer l'importance relative des facteurs de contrôle des stocks de COS (Chapitre II) et de leur bioréactivité (Chapitre III). A ma connaissance, il n'existe pas d'étude similaire en sciences des sols actuellement. Les nouvelles connaissances générées dans nos travaux, avec la quantification du poids relatif attribué aux facteurs de contrôle liés à la dynamique du COS, pourraient s'avérer utiles pour paramétrer les modèles mécanistiques intégrant le cycle du C, tels que les modèles numériques du système Terre.

Dans leur ensemble, nos travaux montrent que la dynamique du COS est contrôlée par des interactions complexes entre plusieurs facteurs bio-physicochimiques (Figure 4.1) et apportent de nouveaux éléments de compréhension au regard de l'impact des changements globaux sur les processus de stockage du COS en forêt boréale. Le régime hydrique du climat avait une influence sur la proportion relative des types fonctionnels de mousses, ainsi que sur la quantité d'oxydes métalliques en interaction avec la matière organique. Or, ces deux variables exerçaient un contrôle direct sur le stock et la bioréactivité du COS (Chapitre II-III). Ces résultats supportent l'idée selon laquelle l'augmentation de 11% des précipitations annuelles anticipées pour la fin du 21^{e} siècle au Canada (IPCC, 2013) aura des effets sur la dynamique du COS au travers de changements dans les processus biologiques et physico-chimiques du sol. Il est toutefois difficile de se prononcer sur l'ampleur et la direction des changements attendus, puisque certaines propriétés du sol et d'autres facteurs qui ne varient pas avec le climat ont des effets auxiliaires ou antagonistes sur les processus liés au stockage du COS. Néanmoins, les travaux développés dans cette thèse montrent que le statut des conditions pédologiques non altérées par le climat prédispose la réaction du système

au regard de variations climatiques. Nos travaux indiquent ainsi que le développement pédologique est un vecteur important du potentiel présenté par les sols de la forêt boréale pour atténuer la vitesse et l'ampleur des conséquences des changements climatiques sur les processus de stockage du COS. Le statut pédologique des sols devrait donc être pris en compte dans la conception de solutions propices à la séquestration du C dans les sols en forêt boréale. A la lumière de ces constats, il apparait nécessaire de replacer les sols au cœur des recherches futures qui traiteront du cycle du carbone, et en particulier dans les écosystèmes de la forêt boréale.

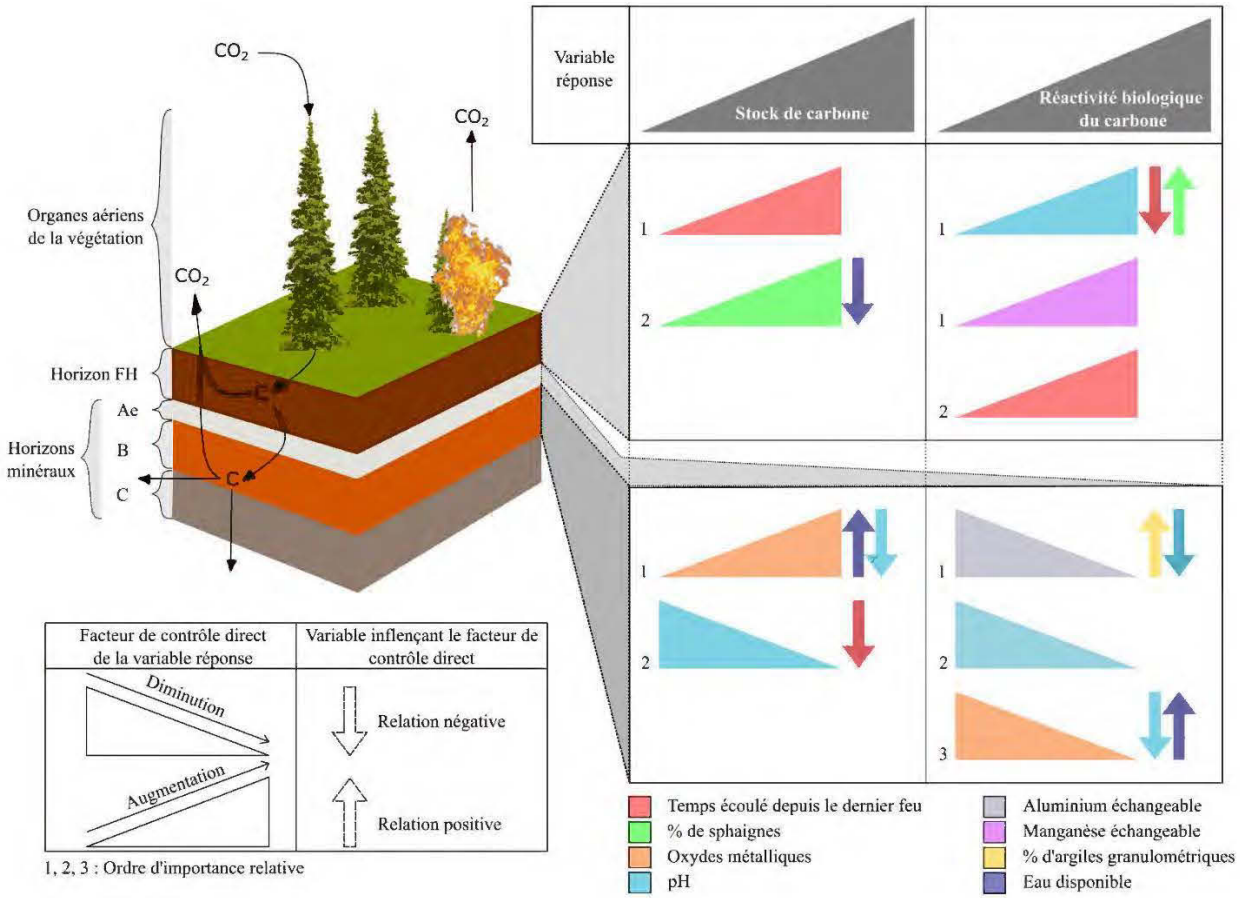

Figure 4.1 Schéma synthèse des résultats de la thèse. La grille d'interprétation est donnée par l'encadré du coin inférieur gauche.

4.2 Avenues pour la recherche

Notre étude est circonscrite à l'étude de cas des sols mésiques en pessière à mousses au Québec. A l'avenir, les résultats de nos travaux devront donc être validés avec des données indépendantes. Pour comprendre dans quelles mesures les processus de stockage du COS décrits dans cette thèse sont généralisables à différentes échelles spatio-temporelles et à d'autres écosystèmes, les futurs travaux devront se focaliser sur une plus grande gamme de valeurs observées dans les facteurs de contrôle de ces processus. Cependant, nos travaux amènent plusieurs pistes de recherches d'intérêts sur les plans théorique et pratique.

D'abord, nos travaux ont permis de remettre en question la validité des modèles numériques du système Terre (Chapitre II-III), largement utilisés pour projeter l'évolution du système climatique planétaire en lien avec le cycle du C. Une modification des modèles ou le développement d'une nouvelle génération de modèles, en tenant compte des processus de stockage du COS spécifiques à la forêt boréale, pourraient être une des solutions envisagées pour améliorer la confiance dans les projections climatiques (Bradford *et al.*, 2016).

Les processus de stockage du COS sont intimement liés aux incendies naturels (Chapitre I-II-III). Les recherches concentrées sur la dynamique des perturbations naturelles apparaissent ainsi essentielles pour apporter des connaissances suffisantes sur les patrons spatiaux et temporels des perturbations qui, intégrées dans les modèles du cycle du C, permettraient aussi de construire une meilleure confiance dans les projections climatiques.

Avec la canopée des forêts tropicales et les grands fonds océaniques, le sol est l'une des trois grandes frontières biotiques de notre planète. Pourtant, le sol abrite de nombreux microorganismes impliqués dans divers processus écologiques fondamentaux (WardleBardgett, *et al.*, 2004), comme le recyclage du COS (Chapitre III). De nombreuses avancées scientifiques centrées sur le microbio-fonctionnement des sols restent ainsi à venir. Pour comprendre comment la forêt boréale peut séquestrer davantage de COS, la recherche future devra s'orienter sur l'étude des facteurs qui limitent la décomposition du COS (Chapitre III), en relations avec le microbiome des sols dans les forêts naturelles ou aménagées (Cardenas *et al.*, 2015; Hynes et Germida, 2013).

Dans nos travaux, nous avons quantifié les stocks et la bioréactivité du COS ainsi que l'importance relative des facteurs qui les contrôlent en forêt naturelle. Nos données pourraient ainsi servir de base comparative pour évaluer les écarts entre les forêts naturelles et aménagées quant aux caractéristiques des stocks de COS. Une quantité suffisante de données, issues d'échantillonnages en forêts aménagées, serait nécessaire pour effectuer les comparaisons. Des études réalisées dans les systèmes après récolte permettront d'évaluer comment le pH du sol, la strate des mousses, la complexation organométallique et les éléments échangeables sont affectés par les opérations sylvicoles.

D'autres études en forêt aménagée devront aussi être développées pour comprendre comment les pratiques forestières pourraient pallier au déficit de saturation en COS qui a été identifié en forêt naturelle (Chapitre I). Ce type de connaissance apporterait de nouvelles pistes pour adapter des solutions adéquates afin de maximiser la séquestration de C dans les sols des territoires aménagés.

4.3 Solutions d'aménagements pour séquestrer le carbone dans les sols

Les résultats de nos recherches amènent plusieurs pistes de réflexions pour des solutions potentielles et inclusives, i.e. pouvant toutes être développées simultanément, menant à une optimisation de la séquestration du COS dans les territoires forestiers soumis à l'aménagement. D'après nos résultats, les conditions d'acidité du sol et de complexation organométallique propres aux forêts anciennes, ainsi que certaines conditions chimiques liées à la disponibilité d'éléments échangeables sont propices à l'accumulation et à la séquestration du C dans les sols (Chapitre II-III). Ces observations mènent à proposer deux stratégies principales pour optimiser la taille du réservoir de C du sol :

- augmenter la proportion de forêts anciennes à l'échelle du paysage ;

- adapter des pratiques de récoltes pour conserver les mécanismes responsables de la séquestration de C dans les sols.

Il existe plusieurs solutions pour augmenter la proportion de forêts anciennes à l'échelle du paysage (Bergeron *et al.*, 2017) :

- protéger les territoires forestiers : conserver une proportion des forêts productives, normalement attribuées à des fins de récolte, afin d'en faire des aires protégées dans lesquelles les opérations sylvicoles sont bannies ;

- augmenter la durée de révolution : accroître le temps entre les récoltes effectuées au sein d'un même territoire ;

- diversifier les systèmes de coupe : remplacer la coupe totale par des systèmes alternatifs raisonnés pour maintenir des attributs de forêts anciennes.

Augmenter la proportion de forêts anciennes dans le paysage est une stratégie que nous recommandons. Elle s'appuie sur la capacité des écosystèmes forestiers à atteindre leur maturité et à maintenir leur productivité en l'absence de perturbation majeure (Ward *et al.*, 2014). Or, les forêts anciennes sont plus susceptibles aux perturbations et donc aux pertes nettes de C (Kurz *et al.*, 2013). Pour pallier au risque de perturbation croissant avec l'âge de la forêt et pour s'assurer de maintenir les processus qui favorisent la séquestration de C dans l'écosystème, cette stratégie devrait être couplée à une surveillance accrue de l'écosystème pour intervenir rapidement en cas de perturbation, engendrant un coût financier et des enjeux de faisabilité pour les régions éloignées (Gauthier *et al.*, 2015). Un des autres inconvénients liés à cette stratégie réside dans la diminution de la possibilité forestière, ce qui soulève la question des effets collatéraux d'ordre socio-économiques. Une diminution de la possibilité forestière implique, par exemple, une baisse de l'activité et des bénéfices industriels et donc un besoin moindre en main-d'œuvre.

Le Québec représente un territoire qui s'étend sur 1667712 km². Parmi les 156709 km² d'aires protégées de la province, la superficie des écosystèmes forestiers au statut 'exceptionnel' bénéficiant d'un cadre légal de protection s'élève actuellement à 352 km² (Gouvernement du Québec, 2018), soit 0.2% du territoire total. La protection d'une plus grande proportion du territoire, afin d'augmenter la proportion de forêts anciennes, pourrait être envisagée. Cependant, compte-tenu des limitations mentionnées plus haut, la conservation d'une plus grande superficie de forêts naturelles ne pourrait être mise en place que sur une petite portion du territoire, dans le respect d'un développement socio-économique et écologique durable et intégré. Ces deux stratégies, conservation et augmentation de la durée des révolutions, sont néanmoins des options viables pour

maintenir un grand nombre de services écologiques rendus par les écosystèmes forestiers, et particulièrement ceux rattachés aux enjeux de biodiversité (Harper *et al.*, 2003; Peura *et al.*, 2018; Triviño *et al.*, 2017).

La coupe totale est le système le plus utilisé actuellement dans les pratiques sylvicoles en forêts boréales d'Amérique du Nord (Conseil canadien des ministres des forêts, 2018) et de Scandinavie (Gelman *et al.*, 2013; Siira-Pietikäinen *et al.*, 2001). Néanmoins, des options alternatives d'aménagement devraient être mises en place pour conserver une structure de classes d'âges dans les limites de variabilités naturelles de la mosaïque forestière, puisque cette pratique d'aménagement équien entraîne un rajeunissement des forêts (Bergeron, 2004; Bergeron *et al.*, 2002; Van Wagner, 1978). Les systèmes alternatifs de coupes, i.e. les coupes partielles, sont des outils variés et flexibles (Raymond *et al.*, 2009). Adaptables en fonction des besoins, les coupes partielles peuvent être utilisées localement pour gérer la compétition entre les arbres ou encore favoriser la présence et la croissance radiale d'essences à grand potentiel commercial, mais elles peuvent aussi être utilisées pour conserver ou restaurer une structure inéquienne des peuplements (Jandl *et al.*, 2007; Prévost et Raymond, 2012; Raymond *et al.*, 2009; Vesala *et al.*, 2005). Les coupes partielles sont aussi considérées comme des alternatives efficaces pour diminuer les impacts écologiques négatifs liés aux coupes totales, et notamment pour réduire les pertes de C (Jandl *et al.*, 2007; Keenan et Kimmins, 1993; Prescott, 1997). L'altération du microclimat et des cycles biogéochimiques à l'échelle du peuplement sont fonctions du degré d'ouverture de la canopée (Muscolo *et al.*, 2014; Schliemann et Bockheim, 2014). Les coupes partielles qui permettent une gestion à fine échelle du degré d'ouverture de la canopée pourraient donc être utilisées de manière raisonnée pour maintenir des attributs de pH du sol, de quantités d'éléments échangeables ou encore de complexation organométallique similaires aux forêts anciennes et/ou favorables à l'accumulation et la séquestration du COS. Le degré d'ouverture de la canopée influence aussi la couverture des mousses

terricoles (Pacé *et al.*, 2017). Alors que le type fonctionnel des mousses influence directement la taille du réservoir de COS (Chapitre II) ou indirectement sa bioréactivité (Chapitre III), une gestion à fine échelle du degré d'ouverture de la canopée permettrait de moduler l'accumulation du COS par une gestion de la strate des mousses.

En somme, nous préconisons d'utiliser davantage les coupes partielles au détriment des coupes totales, de manière raisonnée pour conserver les mécanismes favorables à la séquestration de COS sans altérer la productivité des peuplements, comme étant un compromis à envisager pour combiner le maintien des activités de récolte avec la séquestration de C dans les sols.

ANNEXE A

MATÉRIEL SUPPLÉMENTAIRE DU CHAPITRE I

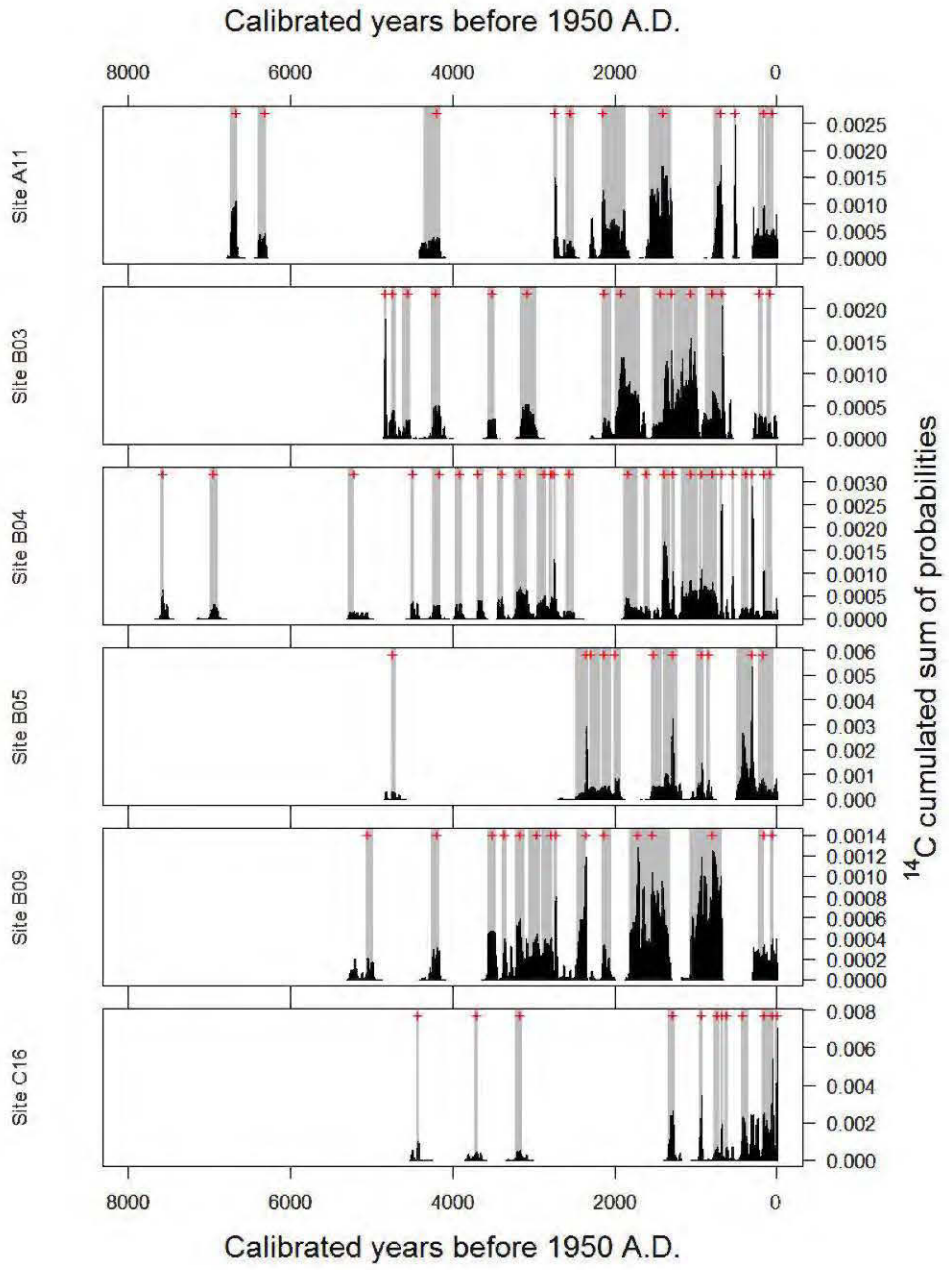

Figure S1.1 Holocene fire history reconstructions based on the comparative analysis of calibrated radiocarbon (^{14}C) dates of charcoal particles buried in soils. The probabilistic age interval of a fire event (grey shading) and the attributed age of fire event (+) are shown. B sites: Frégeau *et al.* (2015); C16 : Remy *et al.* (2018); A11: this study.

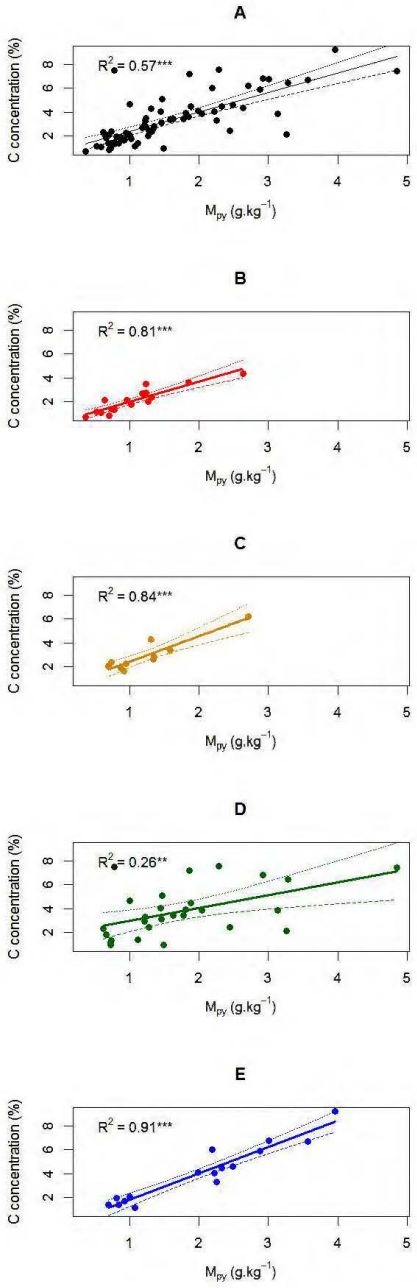

Figure S1.2 Carbon concentration as a function of the amount of pyrophosphate extractable metals in the illuvial horizon. A: all data; B: 153-years fire cycle; C: 183-years fire cycle; D: 247-years fire cycle; E: 720-years fire cycle. $p < 0.001$ (***); $p < 0.01$ (**).

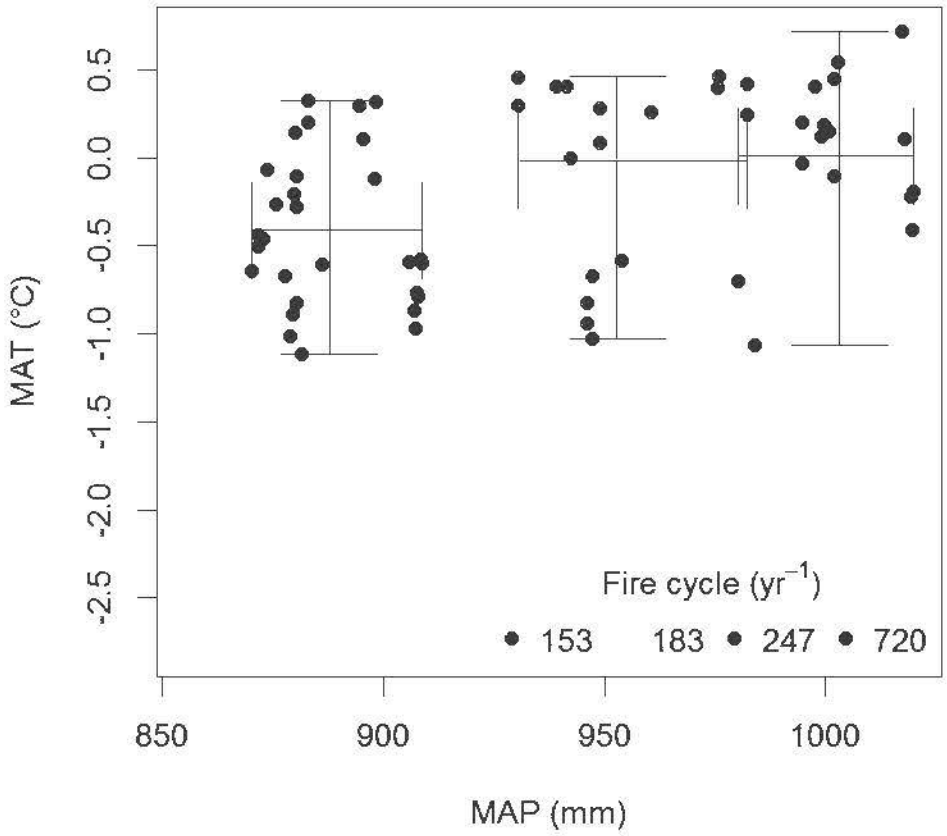

Figure S1.3 Ranges of mean annual precipitation (MAP, mm) and mean annual temperature (MAT, °C) by fire cycle groups. For further details about the climate data, see Andrieux *et al.* (2018b).

ANNEXE B

MATÉRIEL SUPPLÉMENTAIRE DU CHAPITRE II

Table S2.1 Model goodness-of-fit (R^2) and path coefficients (columns 5 to 14) for all FH hypothesis relationships. Based on the Akaike information criterion (AICc; see Tab.2), the hypotheses that best fit our data are shown in bold characters.

Model	Climate	Texture	R^2	X1→X6	X2→X6	X1→X5	X2→X5	X3→X6	X4→X6	X5→X6	X3→X4	X3→X5	X5→X4
FH0	MAT	Sand %	0.28	-0.02	0.19	-	-	0.37 **	0.10	0.30 **	-	-	-
FH0	MAT	Silt %	0.28	-0.02	-0.18	-	-	0.36 **	0.10	0.30 *	-	-	-
FH0	MAT	Clay %	0.26	-0.03	-0.11	-	-	0.38 **	0.12	0.32 **	-	-	-
FH0	MAP	Sand %	0.28	0.07	0.21	-	-	0.36 **	0.11	0.33 **	-	-	-
FH0	MAP	Silt %	0.28	0.07	-0.20	-	-	0.35 **	0.11	0.32 **	-	-	-
FH0	MAP	Clay %	0.26	0.02	-0.11	-	-	0.38 **	0.12	0.33 **	-	-	-
FH0	GDD5	Sand %	0.28	0.05	0.20	-	-	0.36 **	0.11	0.31 **	-	-	-
FH0	GDD5	Silt %	0.28	0.04	-0.19	-	-	0.36 **	0.11	0.31 **	-	-	-
FH0	GDD5	Clay %	0.26	0.03	-0.12	-	-	0.38 **	0.13	0.33 **	-	-	-
FH0	WB	Sand %	0.28	0.05	0.20	-	-	0.36 **	0.11	0.32 **	-	-	-
FH0	WB	Silt %	0.28	0.06	-0.19	-	-	0.35 **	0.11	0.31 **	-	-	-
FH0	WB	Clay %	0.26	0.01	-0.11	-	-	0.38 **	0.12	0.33 **	-	-	-
FH1	MAT	Sand %	0.43	-	-	-0.22	0.06	0.37 **	0.13	0.31 **	-0.32 **	0.01	0.31 **
FH1	MAT	Silt %	0.44	-	-	-0.22	-0.09	0.37 **	0.13	0.31 **	-0.32 **	0.00	0.31 **
FH1	MAT	Clay %	0.44	-	-	-0.24 *	0.08	0.37 **	0.13	0.31 **	-0.32 **	0.00	0.31 **
FH1	MAP	Sand %	0.46	-	-	-0.32 **	0.01	0.37 **	0.13	0.31 **	-0.32 **	0.01	0.31 **
FH1	MAP	Silt %	0.46	-	-	-0.31 *	-0.04	0.37 **	0.13	0.31 **	-0.32 **	0.01	0.31 **
FH1	MAP	Clay %	0.46	-	-	-0.33 **	0.06	0.37 **	0.13	0.31 **	-0.32 **	0.00	0.31 **
FH1	GDD5	Sand %	0.43	-	-	-0.19	0.05	0.37 **	0.13	0.31 **	-0.32 **	-0.02	0.31 **
FH1	GDD5	Silt %	0.43	-	-	-0.19	-0.09	0.37 **	0.13	0.31 **	-0.32 **	-0.03	0.31 **
FH1	GDD5	Clay %	0.43	-	-	-0.22	0.10	0.37 **	0.13	0.31 **	-0.32 **	-0.03	0.31 **
FH1	WB	Sand %	0.44	-	-	-0.26 *	0.04	0.37 **	0.13	0.31 **	-0.32 **	0.00	0.31 **
FH1	WB	Silt %	0.45	-	-	-0.26 *	-0.06	0.37 **	0.13	0.31 **	-0.32 **	0.00	0.31 **
FH1	WB	Clay %	0.44	-	-	-0.27 *	0.04	0.37 **	0.13	0.31 **	-0.32 **	0.00	0.31 **
FH2	MAT	Sand %	0.43	-0.02	0.19	-	-	0.37 **	0.10	0.30 **	-0.32 **	-0.03	0.31 **
FH2	MAT	Silt %	0.42	-0.02	-0.18	-	-	0.36 **	0.10	0.30 *	-0.32 **	-0.03	0.31 **
FH2	MAT	Clay %	0.41	-0.03	-0.11	-	-	0.38 **	0.12	0.32 **	-0.32 **	-0.03	0.31 **

Model	Climate	Texture	R^2	X1→X6	X2→X6	X1→X5	X2→X5	X3→X6	X4→X6	X5→X6	X3→X4	X3→X5	X5→X4
FH2	MAP	Sand %	0.43	0.07	0.21	-	-	0.36 **	0.11	0.33 **	-0.32 **	-0.03	0.31 **
FH2	MAP	Silt %	0.43	0.07	-0.20	-	-	0.35 **	0.11	0.32 **	-0.32 **	-0.03	0.31 **
FH2	MAP	Clay %	0.41	0.02	-0.11	-	-	0.38 **	0.12	0.33 **	-0.32 **	-0.03	0.31 **
FH2	GDD5	Sand %	0.43	0.05	0.20	-	-	0.36 **	0.11	0.31 **	-0.32 **	-0.03	0.31 **
FH2	GDD5	Silt %	0.43	0.04	-0.19	-	-	0.36 **	0.11	0.31 **	-0.32 **	-0.03	0.31 **
FH2	GDD5	Clay %	0.41	0.03	-0.12	-	-	0.38 **	0.13	0.33 **	-0.32 **	-0.03	0.31 **
FH2	WB	Sand %	0.43	0.05	0.20	-	-	0.36 **	0.11	0.32 **	-0.32 **	-0.03	0.31 **
FH2	WB	Silt %	0.43	0.06	-0.19	-	-	0.35 **	0.11	0.31 **	-0.32 **	-0.03	0.31 **
FH2	WB	Clay %	0.41	0.01	-0.11	-	-	0.38 **	0.12	0.33 **	-0.32 **	-0.03	0.31 **
Model-averaged estimator				0.00	-0.01	-0.26	0.04	0.37	0.13	0.32	-0.32	-0.01	0.31

MAT: mean annual temperature; *MAP*: mean annual precipitation; *GDD5*: growing degree-days above 5°C; *WB*: water balance; *Sand*, *Silt* and *Clay*: mineral soil (top 35 cm) sand, silt and clay content, respectively; *X1*: climate parameter; *X2*: texture parameter; *X3*: time since fire; *X4*: forest floor pH; *X5*: index of moss dominance; *X6*: forest floor carbon stock. Arrows indicate direct causal relationships between variables. (*) $p \leq 0.05$; (**) $p \leq 0.01$; (***) $p \leq 0.001$.

Table S2.2 Model goodness-of-fit (R^2) and path coefficients (columns 5 to 12) for all mineral soil (B horizon) model relationships. Based on the Akaike information criterion (AICc; see Tab.3), the hypotheses that best fit our data are shown in bold characters.

Model	Climate	Texture	R^2	X1→X6	X2→X6	X1→X5	X3→X6	X4→X6	X5→X6	X3→X4	X4→X5
B0	MAT	Sand %	0.41	-0.07	0.07	-	0.19	-0.24 *	0.39 ***	-	-
B0	MAT	Silt %	0.40	-0.07	-0.05	-	0.19	-0.24 *	0.38 ***	-	-
B0	MAT	Clay %	0.41	-0.07	-0.07	-	0.19	-0.26 *	0.39 ***	-	-
B0	MAP	Sand %	0.41	-0.12	0.05	-	0.20	-0.21	0.4 ***	-	-
B0	MAP	Silt %	0.41	-0.12	-0.04	-	0.19	-0.22	0.4 ***	-	-
B0	MAP	Clay %	0.42	-0.13	-0.08	-	0.20	-0.23	0.41 ***	-	-
B0	GDD5	Sand %	0.41	-0.11	0.05	-	0.18	-0.24 *	0.37 ***	-	-
B0	GDD5	Silt %	0.41	-0.12	-0.04	-	0.18	-0.24 *	0.37 **	-	-
B0	GDD5	Clay %	0.41	-0.11	-0.05	-	0.18	-0.26 *	0.37 ***	-	-
B0	WB	Sand %	0.41	-0.08	0.06	-	0.19	-0.23	0.40 ***	-	-
B0	WB	Silt %	0.40	-0.08	-0.05	-	0.19	-0.23	0.39 ***	-	-
B0	WB	Clay %	0.41	-0.09	-0.08	-	0.19	-0.25 *	0.41 ***	-	-
B1	MAT	Sand %	0.56	-	0.06	0.15	-	-0.30 **	0.40 ***	-0.28 *	-0.49 ***
B1	MAT	Silt %	0.56	-	-0.05	0.15	-	-0.30 *	0.39 ***	-0.28 *	-0.49 ***
B1	MAT	Clay %	0.56	-	-0.07	0.15	-	-0.32 **	0.40 ***	-0.28 *	-0.49 ***
B1	MAP	Sand %	0.58	-	0.06	0.23 *	-	-0.30 **	0.40 ***	-0.28 *	-0.52 ***
B1	MAP	Silt %	0.57	-	-0.05	0.23 *	-	-0.30 *	0.39 ***	-0.28 *	-0.52 ***
B1	MAP	Clay %	0.58	-	-0.07	0.23 *	-	-0.32 **	0.40 ***	-0.28 *	-0.52 ***
B1	GDD5	Sand %	0.55	-	0.06	-0.01	-	-0.30 **	0.40 ***	-0.28 *	-0.46 ***

Model	Climate	Texture	R^2	X1→X6	X2→X6	X1→X5	X3→X6	X4→X6	X5→X6	X3→X4	X4→X5
B1	GDD5	Silt %	0.55	-	-0.05	-0.01	-	-0.30 *	0.39 ***	-0.28 *	-0.46 ***
B1	GDD5	Clay %	0.55	-	-0.07	-0.01	-	-0.32 **	0.40 ***	-0.28 *	-0.46 ***
B1	WB	Sand %	0.58	-	0.06	0.25 *	-	-0.30 **	0.40 ***	-0.28 *	-0.51 ***
B1	WB	Silt %	0.58	-	-0.05	0.25 *	-	-0.30 *	0.39 ***	-0.28 *	-0.51 ***
B1	WB	Clay %	0.58	-	-0.07	0.25 *	-	-0.32 **	0.40 ***	-0.28 *	-0.51 ***
B2	MAT	Sand %	0.58	-0.07	0.07	0.15	0.19	-0.24 *	0.39 ***	-0.28 *	-0.49 ***
B2	MAT	Silt %	0.58	-0.07	-0.05	0.15	0.19	-0.24 *	0.38 ***	-0.28 *	-0.49 ***
B2	MAT	Clay %	0.58	-0.07	-0.07	0.15	0.19	-0.26 *	0.39 ***	-0.28 *	-0.49 ***
B2	MAP	Sand %	0.60	-0.12	0.05	0.23 *	0.20	-0.21	0.40 ***	-0.28 *	-0.52 ***
B2	MAP	Silt %	0.60	-0.12	-0.04	0.23 *	0.19	-0.22	0.40 ***	-0.28 *	-0.52 ***
B2	MAP	Clay %	0.60	-0.13	-0.08	0.23 *	0.20	-0.23	0.41 ***	-0.28 *	-0.52 ***
B2	GDD5	Sand %	0.58	-0.11	0.05	-0.01	0.18	-0.24 *	0.37 ***	-0.28 *	-0.46 ***
B2	GDD5	Silt %	0.58	-0.12	-0.04	-0.01	0.18	-0.24 *	0.37 **	-0.28 *	-0.46 ***
B2	GDD5	Clay %	0.58	-0.11	-0.05	-0.01	0.18	-0.26 *	0.37 ***	-0.28 *	-0.46 ***
B2	WB	Sand %	0.60	-0.08	0.06	0.25 *	0.19	-0.23	0.40 ***	-0.28 *	-0.51 ***
B2	WB	Silt %	0.60	-0.08	-0.05	0.25 *	0.19	-0.23	0.39 ***	-0.28 *	-0.51 ***
B2	WB	Clay %	0.61	-0.09	-0.08	0.25 *	0.19	-0.25 *	0.41 ***	-0.28 *	-0.51 ***
Model-averaged estimator				-0.10	-0.02	0.15	0.19	-0.26	0.39	-0.28	-0.49

MAT: mean annual temperature; *MAP*: mean annual precipitation; *GDD5*: growing degree-days above 5°C; *WB*: water balance; *Sand*, *Silt* and *Clay*: mineral soil (top 35 cm) sand, silt and clay content, respectively; *X1*: climate parameter; *X2*: texture parameter; *X3*: time since fire; *X4*: illuvial horizon pH; *X5*: pyrophosphate extractable metals in illuvial horizon; *X6*: illuvial horizon (top 15 cm) carbon stock. Arrows indicate direct causal relationships between variables. (*) $p \leq 0.05$; (**) $p \leq 0.01$; (***) $p \leq 0.001$.

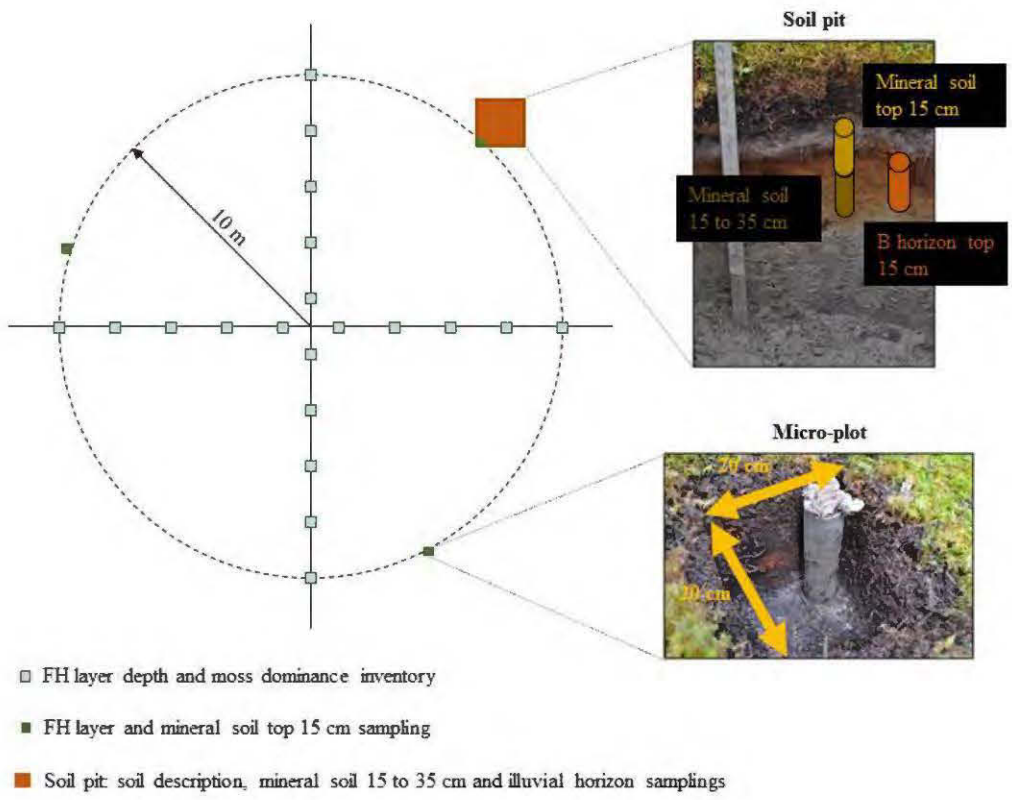

Figure S2.1 Diagram of the plot inventory and soil sampling.

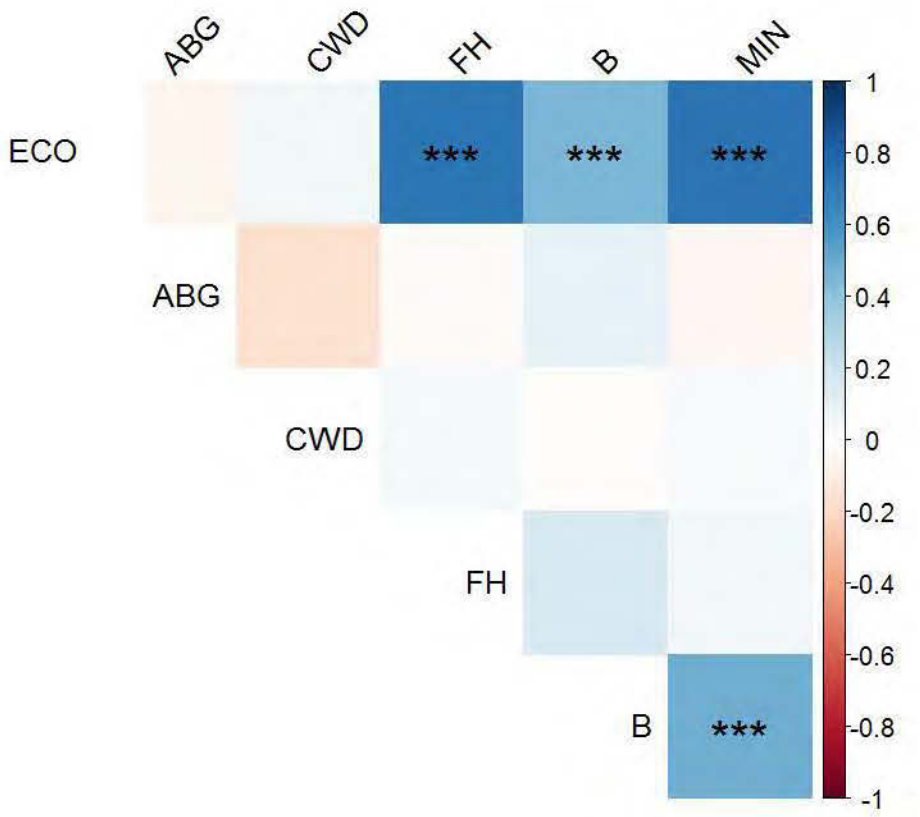

Figure S2.2 Pearson correlation between carbon pools. Only soil carbon pools correlate with the whole ecosystem carbon stock, indicating that soils are the major carbon reservoir in mesic black spruce forests. *ECO*: ecosystem carbon density; *ABG*: living tree carbon density; *FH*: FH layer carbon density; *B*: illuvial (B) horizon carbon density; *MIN*: mineral soil (top 35 cm) carbon density. (***) $p \leq 0.001$.

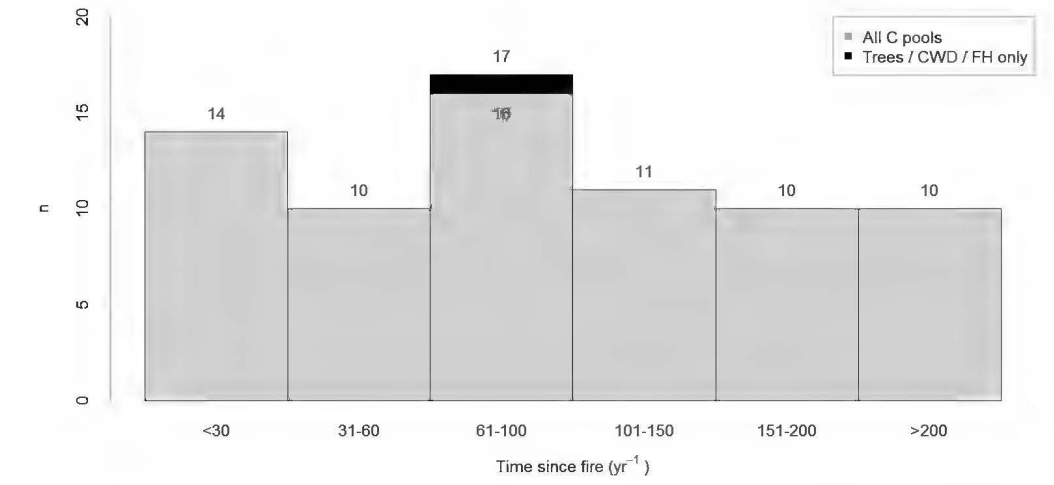

Figure S2.3 Number of sample plots per time since fire-class.

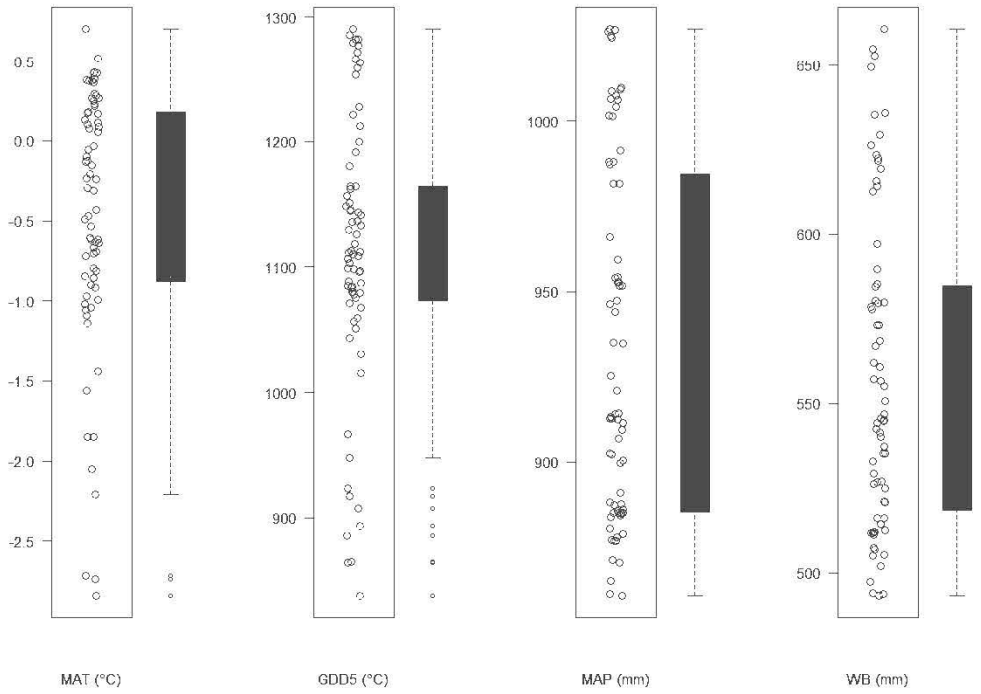

Figure S2.4 Ranges of values for temperature factors (red) and water availability factors (blue) used in this study.

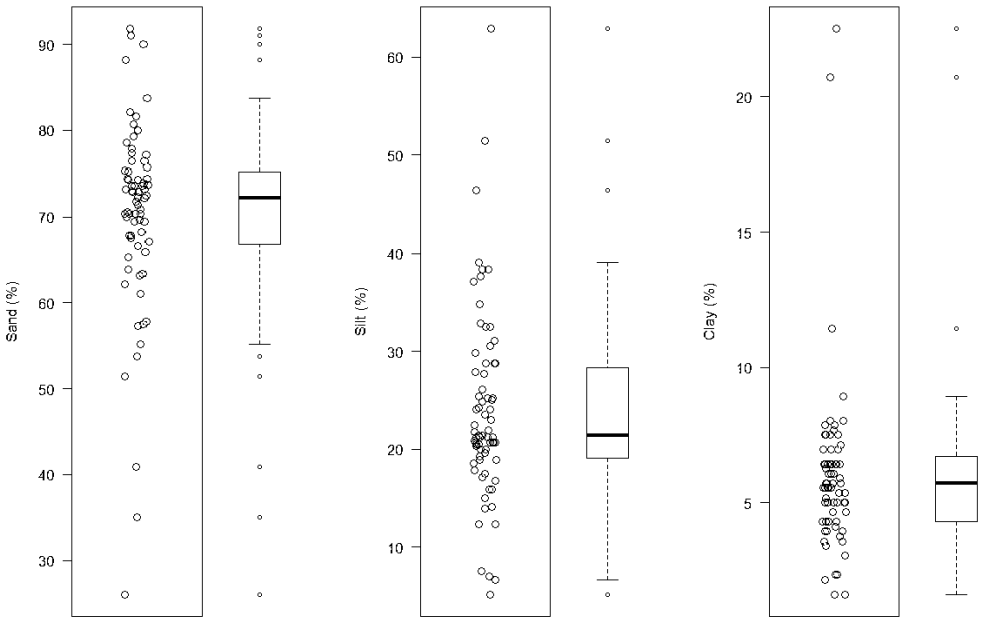

Figure S2.5 Ranges of values for texture factors in mineral soil (top 35 cm) used in this study.

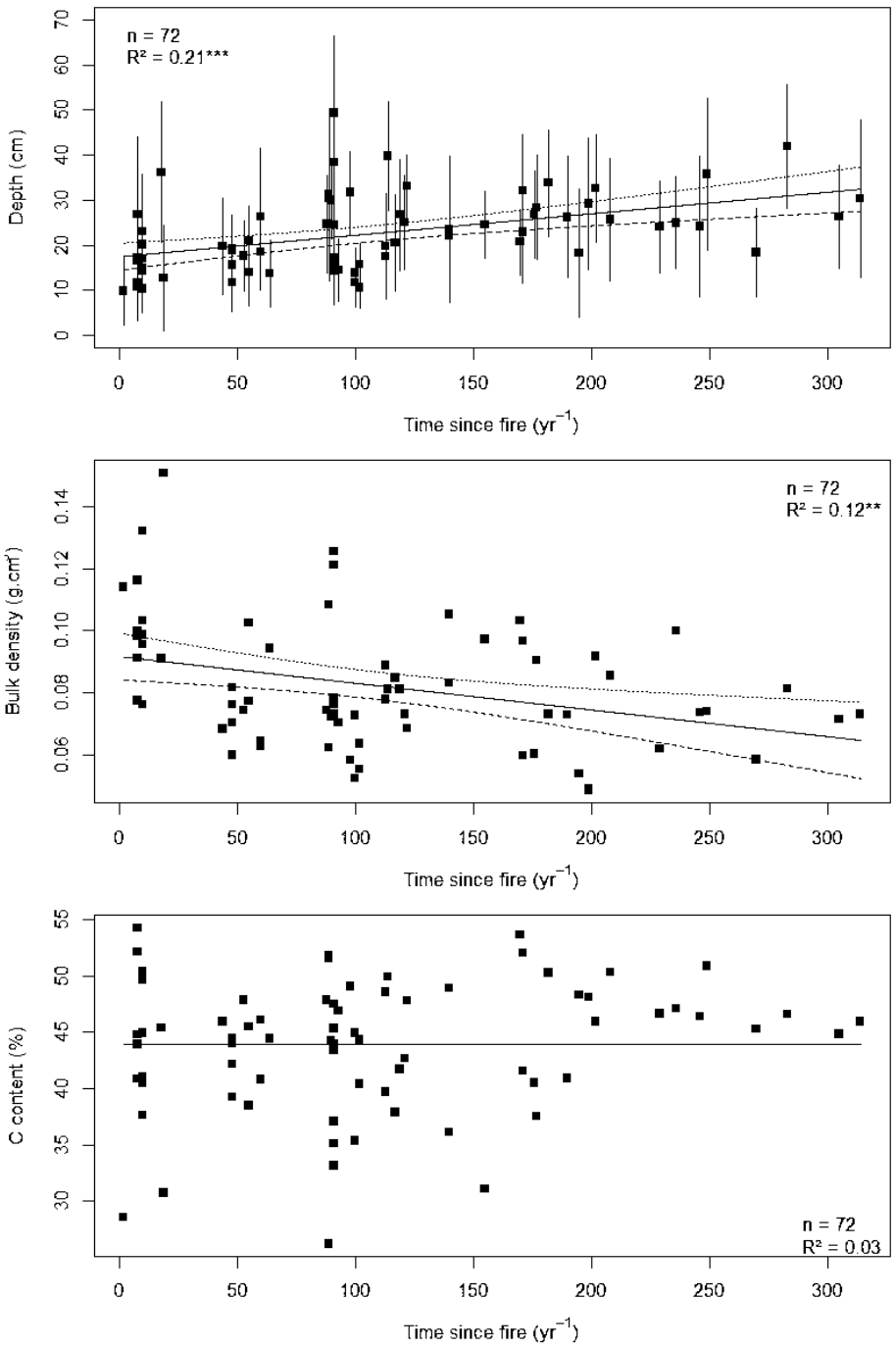

Figure S2.6 Observed (squares) and predicted (plain lines) values for post-fire FH variables used to compute the forest floor carbon stocks, with 95% confidence interval (dashed lines), as a function of time since fire. Error bars represent the standard deviation of the mean FH layer depth based on 20 records per plot. () n.s.; (**) $p \leq 0.01$; (***) $p \leq 0.001$.

ANNEXE C

MATÉRIEL SUPPLÉMENTAIRE DU CHAPITRE III

Table S3.1 Model fitness to the data for *a priori* hypotheses for the FH horizon. Models are sorted by increasing second order Akaike information criterion (AICc). *Model*: model name; *Climate*: climate variable; *Texture*: texture variable; *C statistic*: statistic of the Fisher's C test; *df*: degree of freedom; *p*: p-value of the Fisher's C test (when $p < 0.05$, the model is not supported by the data); *K*: number of free parameters; *AICc*: second order information criterion; $\Delta AICc$: relative AICc difference with the model that best fit the data (in bold); *W*: Akaike weight.

Model	Climate	Texture	C statistic	df	p	K	AICc	ΔAICc	W
FF2	**MAP**	**Clay**	**22.295**	**26**	**0.67**	**11**	**48.77**	**0.00**	**0.68**
FF2	WB	Clay	26.495	26	0.44	11	52.97	4.20	0.08
FF2	MAP	Sand	27.282	26	0.39	11	53.76	4.99	0.06
FF2	MAP	Silt	28.553	26	0.33	11	55.03	6.26	0.03
FF2	WB	Sand	28.934	26	0.31	11	55.41	6.64	0.02
FF2	MAT	Silt	29.029	26	0.31	11	55.50	6.73	0.02
FF2	GDD5	Silt	29.040	26	0.31	11	55.51	6.74	0.02
FF2	MAT	Clay	29.287	26	0.30	11	55.76	6.99	0.02
FF2	MAT	Sand	29.432	26	0.29	11	55.91	7.14	0.02
FF2	GDD5	Sand	30.118	26	0.26	11	56.59	7.82	0.01
FF2	WB	Silt	30.479	26	0.25	11	56.95	8.18	0.01
FF2	GDD5	Clay	30.556	26	0.25	11	57.03	8.26	0.01
FF1	WB	Clay	46.660	30	0.03	7	62.44	13.67	0.00
FF1	MAP	Clay	47.954	30	0.02	7	63.73	14.96	0.00
FF1	WB	Sand	50.525	30	0.01	7	66.30	17.53	0.00
FF1	WB	Silt	53.497	30	0.01	7	69.27	20.50	0.00
FF1	MAP	Sand	54.231	30	0.00	7	70.01	21.24	0.00
FF1	MAP	Silt	56.918	30	0.00	7	72.70	23.93	0.00
FF1	GDD5	Clay	57.791	30	0.00	7	73.57	24.80	0.00
FF1	GDD5	Sand	58.623	30	0.00	7	74.40	25.63	0.00

Model	Climate	Texture	C statistic	df	p	K	AICc	ΔAICc	W
FF1	GDD5	Silt	58.888	30	0.00	7	74.67	25.90	0.00
FF1	MAT	Clay	59.816	30	0.00	7	75.59	26.82	0.00
FF1	MAT	Sand	61.188	30	0.00	7	76.97	28.20	0.00
FF1	MAT	Silt	62.223	30	0.00	7	78.00	29.23	0.00

Table S3.2 Explained variability (R^2) in C_{BioR} for each model of the FH horizon, as well as path coefficients and model-averaged estimators for each of the *a priori* hypothesized causal relationship among variables (arrows). *Model*: model name; *Climate*: climate variable; *Texture*: texture variable; *TSF*: time since fire; *pH*: pH of the FH horizon; *Mpy*: pyrophosphate extractable metals; C_{BioR}: carbon bioreactivity of the FH horizon. The model that best fit the data is highlighted by bold font. (*) $p \leq 0.05$; (**) $p \leq 0.01$; (***) $p \leq 0.001$.

Model	Climate	Texture	R^2	Climate ↓ C_{BioR}	Texture ↓ C_{BioR}	Climate ↓ IMD	Texture ↓ IMD	TSF ↓ CBioR	pH ↓ CBioR	IMD ↓ CBioR	Mn ↓ CBioR	TSF ↓ pH	IMD ↓ pH
FF1	MAT	Sand	0.31	0.02	-0.11	-	-	0.25*	0.36**	0.09	0.35**	-	-
FF1	MAT	Silt	0.30	0.03	0.08	-	-	0.25*	0.36**	0.09	0.35**	-	-
FF1	MAT	Clay	0.31	0.02	0.11	-	-	0.24*	0.36**	0.08	0.34**	-	-
FF1	GDD5	Sand	0.31	-0.04	-0.11	-	-	0.25*	0.36**	0.08	0.33**	-	-
FF1	GDD5	Silt	0.30	-0.03	0.09	-	-	0.25*	0.35**	0.08	0.33**	-	-
FF1	GDD5	Clay	0.31	-0.05	0.12	-	-	0.24*	0.35**	0.06	0.31**	-	-
FF1	MAP	Sand	0.38	-0.29**	-0.17	-	-	0.28**	0.34**	0.00	0.35***	-	-
FF1	MAP	Silt	0.38	-0.29**	0.16	-	-	0.28**	0.34**	0.01	0.35***	-	-
FF1	MAP	Clay	0.37	-0.26*	0.12	-	-	0.26*	0.33**	0.00	0.34**	-	-
FF1	WB	Sand	0.39	-0.30**	-0.16	-	-	0.28**	0.35**	0.01	0.39***	-	-
FF1	WB	Silt	0.38	-0.31**	0.15	-	-	0.28**	0.34**	0.01	0.40***	-	-
FF1	WB	Clay	0.37	-0.26*	0.10	-	-	0.26*	0.34**	0.00	0.38***	-	-
FF2	MAT	Sand	0.30	-	-	-0.22	0.06	0.25*	0.34**	0.08	0.34**	-0.32**	0.30**
FF2	MAT	Silt	0.30	-	-	-0.22	-0.09	0.25*	0.34**	0.08	0.34**	-0.32**	0.30**
FF2	MAT	Clay	0.30	-	-	-0.24*	0.08	0.25*	0.34**	0.08	0.34**	-0.32**	0.30**
FF2	GDD5	Sand	0.30	-	-	-0.19	0.05	0.25*	0.34**	0.08	0.34**	-0.32**	0.30**

Model	Climate	Texture	R^2	Climate ↓ C_{BioR}	Texture ↓ C_{BioR}	Climate ↓ IMD	Texture ↓ IMD	TSF ↓ CBioR	pH ↓ CBioR	IMD ↓ CBioR	Mn ↓ CBioR	TSF ↓ pH	IMD ↓ pH
FF2	GDD5	Silt	0.30	-	-	-0.19	-0.09	0.25*	0.34**	0.08	0.34**	-0.32**	0.30**
FF2	GDD5	Clay	0.30	-	-	-0.22	0.09	0.25*	0.34**	0.08	0.34**	-0.32**	0.30**
FF2	MAP	Sand	0.30	-	-	-0.32**	0.01	0.25*	0.34**	0.08	0.34**	-0.32**	0.30**
FF2	MAP	Silt	0.30	-	-	-0.32*	-0.04	0.25*	0.34**	0.08	0.34**	-0.32**	0.30**
FF2	**MAP**	**Clay**	**0.30**	-	-	**-0.33****	**0.06**	**0.25***	**0.34****	**0.08**	**0.34****	**-0.32****	**0.30****
FF2	WB	Sand	0.30	-	-	-0.26*	0.04	0.25*	0.34**	0.08	0.34**	-0.32**	0.30**
FF2	WB	Silt	0.30	-	-	-0.26*	-0.06	0.25*	0.34**	0.08	0.34**	-0.32**	0.30**
FF2	WB	Clay	0.30	-	-	-0.27*	0.04	0.25*	0.34**	0.08	0.34**	-0.32**	0.30**
Model-averaged estimator				0.00	0.00	-0.30	0.04	0.24	0.34	0.08	0.34	-0.32	0.30

Table S3.3 Model fitness to the data for *a priori* hypotheses for the mineral soil. Models are sorted by increasing second order Akaike information criterion (AICc). *Model*: model name; *Climate*: climate variable; *Texture*: texture variable; E_E: exchangeable element variable ; *C statistic*: statistic of the Fisher's C test; *df*: degree of freedom; *p*: p-value of the Fisher's C test (when $p < 0.05$, the model is not supported by the data); *K*: number of free parameters; *AICc*: second order information criterion; $\Delta AICc$: relative AICc difference with the model that best fit the data (in bold); *W*: Akaike weight.

Model	Climate	Texture	E_E	C statistic	df	p	K	AICc	ΔAICc	W
MIN2	**WB**	**Clay**	**Al**	**27.757**	**24**	**0.27**	**14**	**63.26**	**0.00**	**0.47**
MIN2	MAP	Clay	Al	30.177	24	0.18	14	65.68	2.42	0.14
MIN2	WB	Clay	Mn	31.145	24	0.15	14	66.65	3.39	0.09
MIN2	GDD5	Clay	Al	31.781	24	0.13	14	67.28	4.02	0.06
MIN2	MAT	Clay	Al	32.209	24	0.12	14	67.71	4.45	0.05
MIN2	MAP	Clay	Mn	32.807	24	0.11	14	68.31	5.05	0.04
MIN1	GDD5	Sand	Mn	52.772	30	0.01	7	68.55	5.29	0.03
MIN2	GDD5	Clay	Mn	34.342	24	0.08	14	69.84	6.58	0.02
MIN2	MAT	Clay	Mn	34.572	24	0.08	14	70.07	6.81	0.02
MIN1	MAT	Sand	Mn	54.439	30	0.00	7	70.22	6.96	0.01
MIN1	GDD5	Clay	Mn	54.775	30	0.00	7	70.55	7.29	0.01
MIN1	GDD5	Silt	Mn	55.215	30	0.00	7	70.99	7.73	0.01
MIN2	GDD5	Sand	Al	35.514	24	0.06	14	71.01	7.75	0.01
MIN1	MAT	Clay	Mn	55.903	30	0.00	7	71.68	8.42	0.01
MIN2	GDD5	Sand	Mn	36.206	24	0.05	14	71.71	8.45	0.01
MIN2	WB	Sand	Al	36.261	24	0.05	14	71.76	8.50	0.01
MIN1	MAP	Clay	Mn	56.703	30	0.00	7	72.48	9.22	0.00
MIN2	WB	Sand	Mn	37.141	24	0.04	14	72.64	9.38	0.00
MIN1	WB	Clay	Mn	57.535	30	0.00	7	73.31	10.05	0.00
MIN1	MAT	Silt	Mn	57.653	30	0.00	7	73.43	10.17	0.00
MIN2	MAT	Sand	Al	38.058	24	0.03	14	73.56	10.30	0.00
MIN2	GDD5	Silt	Mn	38.188	24	0.03	14	73.69	10.43	0.00
MIN2	MAT	Sand	Mn	38.435	24	0.03	14	73.93	10.67	0.00
MIN1	WB	Sand	Mn	58.565	30	0.00	7	74.34	11.08	0.00
MIN2	GDD5	Silt	Al	39.035	24	0.03	14	74.53	11.27	0.00
MIN1	MAP	Sand	Mn	60.145	30	0.00	7	75.92	12.66	0.00
MIN2	MAT	Silt	Mn	41.318	24	0.02	14	76.82	13.56	0.00
MIN2	MAP	Sand	Al	41.490	24	0.01	14	76.99	13.73	0.00
MIN2	MAP	Sand	Mn	41.884	24	0.01	14	77.38	14.12	0.00
MIN2	MAT	Silt	Al	42.639	24	0.01	14	78.14	14.88	0.00

Model	Climate	Texture	E_E	C statistic	df	p	K	AICc	ΔAICc	W
MIN2	WB	Silt	Mn	42.635	24	0.01	14	78.14	14.88	0.00
MIN2	WB	Silt	Al	43.251	24	0.01	14	78.75	15.49	0.00
MIN1	WB	Silt	Mn	63.715	30	0.00	7	79.49	16.23	0.00
MIN1	MAP	Silt	Mn	65.010	30	0.00	7	80.79	17.53	0.00
MIN2	MAP	Silt	Mn	47.027	24	0.00	14	82.53	19.27	0.00
MIN1	GDD5	Sand	Al	67.221	30	0.00	7	83.00	19.74	0.00
MIN2	MAP	Silt	Al	47.772	24	0.00	14	83.27	20.01	0.00
MIN1	MAT	Sand	Al	68.014	30	0.00	7	83.79	20.53	0.00
MIN1	WB	Sand	Al	69.719	30	0.00	7	85.50	22.24	0.00
MIN1	MAP	Sand	Al	72.479	30	0.00	7	88.26	25.00	0.00
MIN1	GDD5	Silt	Al	72.851	30	0.00	7	88.63	25.37	0.00
MIN1	MAT	Silt	Al	74.414	30	0.00	7	90.19	26.93	0.00
MIN1	WB	Clay	Al	74.567	30	0.00	7	90.35	27.09	0.00
MIN1	MAP	Clay	Al	74.916	30	0.00	7	90.69	27.43	0.00
MIN1	GDD5	Clay	Al	75.104	30	0.00	7	90.88	27.62	0.00
MIN1	MAT	Clay	Al	75.357	30	0.00	7	91.13	27.87	0.00
MIN1	WB	Silt	Al	78.055	30	0.00	7	93.83	30.57	0.00
MIN1	MAP	Silt	Al	80.530	30	0.00	7	96.31	33.05	0.00

Table S3.4

Explained variability (R^2) in C_{BioR} for each model for the mineral soil, as well as path coefficients and model-averaged estimators for each of the *a priori* hypothesized causal relationship among variables. *Model*: model name; *Climate*: climate variable; *Texture*: texture variable; *TSF*: time since fire; *pH*: pH of the FH horizon; *Mpy*: pyrophosphate extractable metals; E_E: exchangeable element variable; C_{BioR}: carbon bioreactivity of the mineral soil. The model that best fit the data is highlighted by bold font. (*) $p \leq 0.05$; (**) $p \leq 0.01$; (***) $p \leq 0.001$.

Model	Climate	Texture	E_E	R^2	Climate ↓ C_{BioR}	Texture ↓ C_{BioR}	Climate ↓ Mpy	TSF ↓ C_{BioR}	pH ↓ C_{BioR}	Mpy ↓ C_{BioR}	E_E ↓ C_{BioR}	TSF ↓ pH	pH ↓ Mpy	pH ↓ E_E	Texture ↓ E_E
MIN1	MAT	Sand	Mn	0.18	0.25*	0.23	-	-0.11	-0.19	-0.32*	0.15	-	-	-	-
MIN1	MAT	Sand	Al	0.30	0.21	0.21	-	0.06	-0.27*	-0.30**	-0.42***	-	-	-	-
MIN1	MAT	Silt	Mn	0.18	0.24*	-0.22	-	-0.11	-0.18	-0.33*	0.14	-	-	-	-
MIN1	MAT	Silt	Al	0.31	0.21	-0.24*	-	0.06	-0.26*	-0.31**	-0.44***	-	-	-	-
MIN1	MAT	Clay	Mn	0.15	0.23	-0.14	-	-0.11	-0.25	-0.30*	0.17	-	-	-	-
MIN1	MAT	Clay	Al	0.26	0.18	-0.02	-	0.06	-0.31*	-0.29*	-0.42**	-	-	-	-
MIN1	GDD5	Sand	Mn	0.17	0.21	0.24*	-	-0.08	-0.16	-0.28*	0.15	-	-	-	-
MIN1	GDD5	Sand	Al	0.29	0.18	0.22	-	0.08	-0.25*	-0.26*	-0.42***	-	-	-	-
MIN1	GDD5	Silt	Mn	0.16	0.20	-0.22	-	-0.08	-0.15	-0.28*	0.14	-	-	-	-
MIN1	GDD5	Silt	Al	0.30	0.17	-0.24*	-	0.09	-0.23	-0.27*	-0.44***	-	-	-	-
MIN1	GDD5	Clay	Mn	0.14	0.20	-0.17	-	-0.09	-0.23	-0.26*	0.17	-	-	-	-
MIN1	GDD5	Clay	Al	0.24	0.14	-0.03	-	0.08	-0.29*	-0.26*	-0.42**	-	-	-	-
MIN1	MAP	Sand	Mn	0.18	0.24	0.25*	-	-0.09	-0.20	-0.33**	0.13	-	-	-	-
MIN1	MAP	Sand	Al	0.30	0.22	0.23*	-	0.07	-0.28*	-0.31**	-0.42***	-	-	-	-

Model	Climate	Texture	E_E	R^2	Climate ↓ C_{BioR}	Texture ↓ C_{BioR}	Climate ↓ Mpy	TSF ↓ C_{BioR}	pH ↓ C_{BioR}	Mpy ↓ C_{BioR}	E_E ↓ C_{BioR}	TSF ↓ pH	pH ↓ Mpy	pH ↓ E_E	Texture ↓ E_E
MIN1	MAP	Silt	Mn	0.18	0.25*	-0.26*	-	-0.09	-0.18	-0.34**	0.11	-	-	-	-
MIN1	MAP	Silt	Al	0.31	0.23*	-0.28*	-	0.07	-0.27*	-0.33**	-0.44***	-	-	-	-
MIN1	MAP	Clay	Mn	0.13	0.18	-0.12	-	-0.09	-0.24	-0.31*	0.14	-	-	-	-
MIN1	MAP	Clay	Al	0.25	0.16	0.00	-	0.07	-0.31*	-0.30*	-0.42**	-	-	-	-
MIN1	WB	Sand	Mn	0.15	0.16	0.22	-	-0.08	-0.17	-0.32*	0.12	-	-	-	-
MIN1	WB	Sand	Al	0.28	0.15	0.21	-	0.08	-0.27*	-0.31*	-0.42***	-	-	-	-
MIN1	WB	Silt	Mn	0.15	0.18	-0.23	-	-0.08	-0.16	-0.33*	0.11	-	-	-	-
MIN1	WB	Silt	Al	0.29	0.17	-0.26*	-	0.08	-0.25*	-0.32**	-0.44***	-	-	-	-
MIN1	WB	Clay	Mn	0.11	0.12	-0.11	-	-0.08	-0.22	-0.30*	0.14	-	-	-	-
MIN1	WB	Clay	Al	0.24	0.11	0.01	-	0.08	-0.30*	-0.30*	-0.43**	-	-	-	-
MIN2	MAT	Sand	Mn	0.09	-	-	0.14	-0.07	-0.18	-0.28*	0.12	-0.16	-0.37**	0.23	-0.07
MIN2	MAT	Sand	Al	0.22	-	-	0.14	0.09	-0.27*	-0.27*	-0.43***	-0.16	-0.37**	-0.37**	-0.02
MIN2	MAT	Silt	Mn	0.09	-	-	0.14	-0.07	-0.18	-0.28*	0.12	-0.16	-0.37**	0.24*	0.01
MIN2	MAT	Silt	Al	0.22	-	-	0.14	0.09	-0.27*	-0.27*	-0.43***	-0.16	-0.37**	-0.35**	-0.05
MIN2	MAT	Clay	Mn	0.09	-	-	0.14	-0.07	-0.18	-0.28*	0.12	-0.16	-0.37**	0.27*	0.21
MIN2	MAT	Clay	Al	0.22	-	-	0.14	0.09	-0.27*	-0.27*	-0.43***	-0.16	-0.37**	-0.33**	0.24*
MIN2	GDD5	Sand	Mn	0.09	-	-	-0.04	-0.07	-0.18	-0.28*	0.12	-0.16	-0.35**	0.23	-0.07
MIN2	GDD5	Sand	Al	0.22	-	-	-0.04	0.09	-0.27*	-0.27*	-0.43***	-0.16	-0.35**	-0.37**	-0.02
MIN2	GDD5	Silt	Mn	0.09	-	-	-0.04	-0.07	-0.18	-0.28*	0.12	-0.16	-0.35**	0.24*	0.01
MIN2	GDD5	Silt	Al	0.22	-	-	-0.04	0.09	-0.27*	-0.27*	-0.43***	-0.16	-0.35**	-0.35**	-0.05
MIN2	GDD5	Clay	Mn	0.09	-	-	-0.04	-0.07	-0.18	-0.28*	0.12	-0.16	-0.35**	0.27*	0.21
MIN2	GDD5	Clay	Al	0.22	-	-	-0.04	0.09	-0.27*	-0.27*	-0.43***	-0.16	-0.35**	-0.33**	0.24*
MIN2	MAP	Sand	Mn	0.09	-	-	0.18	-0.07	-0.18	-0.28*	0.12	-0.16	-0.39**	0.23	-0.07

Model	Climate	Texture	E_E	R^2	Climate ↓ C_{BioR}	Texture ↓ C_{BioR}	Climate ↓ Mpy	TSF ↓ C_{BioR}	pH ↓ C_{BioR}	Mpy ↓ C_{BioR}	E_E ↓ C_{BioR}	TSF ↓ pH	pH ↓ Mpy	pH ↓ E_E	Texture ↓ E_E
MIN2	MAP	Sand	Al	0.22	-	-	0.18	0.09	-0.27*	-0.27*	-0.43***	-0.16	-0.39**	-0.37**	-0.02
MIN2	MAP	Silt	Mn	0.09	-	-	0.18	-0.07	-0.18	-0.28*	0.12	-0.16	-0.39**	0.24*	0.01
MIN2	MAP	Silt	Al	0.22	-	-	0.18	0.09	-0.27*	-0.27*	-0.43***	-0.16	-0.39**	-0.35**	-0.05
MIN2	MAP	Clay	Mn	0.09	-	-	0.18	-0.07	-0.18	-0.28*	0.12	-0.16	-0.39**	0.27*	0.21
MIN2	MAP	Clay	Al	0.22	-	-	0.18	0.09	-0.27*	-0.27*	-0.43***	-0.16	-0.39**	-0.33**	0.24*
MIN2	WB	Sand	Mn	0.09	-	-	0.21	-0.07	-0.18	-0.28*	0.12	-0.16	-0.38***	0.23	-0.07
MIN2	WB	Sand	Al	0.22	-	-	0.21	0.09	-0.27*	-0.27*	-0.43***	-0.16	-0.38***	-0.37**	-0.02
MIN2	WB	Silt	Mn	0.09	-	-	0.21	-0.07	-0.18	-0.28*	0.12	-0.16	-0.38***	0.24*	0.01
MIN2	WB	Silt	Al	0.22	-	-	0.21	0.09	-0.27*	-0.27*	-0.43***	-0.16	-0.38***	-0.35**	-0.05
MIN2	WB	Clay	Mn	0.09	-	-	0.21	-0.07	-0.18	-0.28*	0.12	-0.16	-0.38***	0.27*	0.21
MIN2	**WB**	**Clay**	**Al**	**0.22**	-	-	**0.21**	**0.09**	**-0.27***	**-0.27***	**-0.43*****	**-0.16**	**-0.38*****	**-0.33****	**0.24***
Model-averaged estimator					0.02	0.00	0.16	0.05	-0.25	-0.27	-0.29	-0.15	-0.35	-0.20	0.21

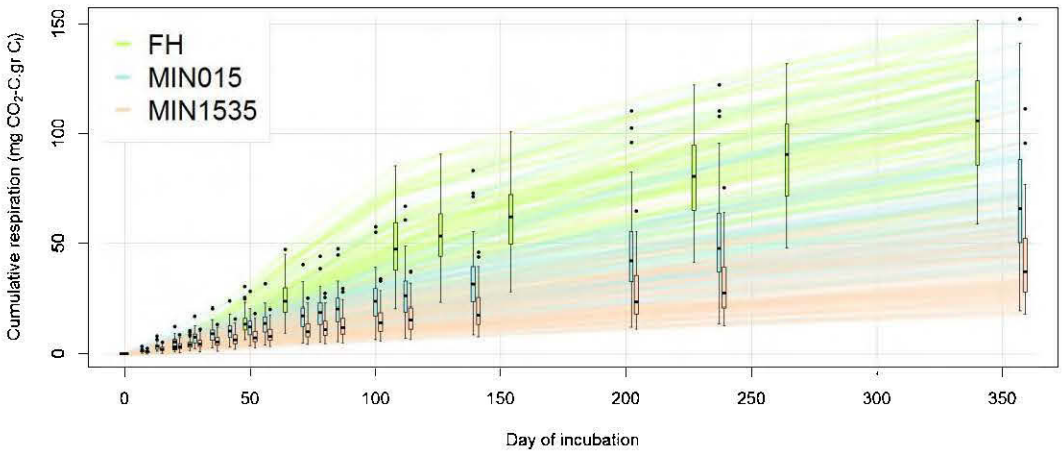

Figure S3.1 Cumulative specific respiration (R_S) as a function of the sampling Julian day. Boxplots represent the distribution of R_S values for each of the soil layers for each sampling day. Lines are drawn for each of the samples. *FH* (green): FH horizon; *MIN015* (blue): mineral soil top 15 cm; *MIN1535* (salmon): mineral soil from 15 to 35 cm.

RÉFÉRENCES

Abbott, B.W., Jones, J.B., Schuur, E.A.G., Chapin III, F.S., Bowden, W.B., Bret-Harte, M.S., Epstein, H.E., Flannigan, M.D., Harms, T.K., Hollingsworth, T.N., Mack, M.C., McGuire, A.D., Natali, S.M., Rocha, A.V., Tank, S.E., Turetsky, M.R., Vonk, J.E., Wickland, K.P., Aiken, G.R., Alexander, H.D., Amon, R.M.W., Benscoter, B.W., Bergeron, Y., Bishop, K., Blarquez, O., Ben, B.-L., Breen, A.L., Buffam, I., Cai, Y., Carcaillet, C., Carey, S.K., Chen, J.M., Chen, H.Y.H., Christensen, T.R., Cooper, L.W., Cornelissen, J.H.C., de Groot, W.J., DeLuca, T.H., Dorrepaal, E., Fetcher, N., Finlay, J.C., Forbes, B.C., French, N.H.F., Gauthier, S., Girardin, M.P., Goetz, S.J., Goldammer, J.G., Gough, L., Grogan, P., Guo, L., Higuera, P.E., Hinzman, L., Hu, F.S., Hugelius, G., Jafarov, E.E., Jandt, R., Johnstone, J.F., Jan, K., Kasischke, E.S., Kattner, G., Kelly, R., Keuper, F., Kling, G.W., Kortelainen, P., Kouki, J., Kuhry, P., Laudon, H., Laurion, I., Macdonald, R.W., Mann, P.J., Martikainen, P.J., McClelland, J.W., Molau, U., Oberbauer, S.F., Olefeldt, D., Paré, D., Parisien, M.-A., Payette, S., Peng, C., Pokrovsky, O.S., Rastetter, E.B., Raymond, P.A., Raynolds, M.K., Rein, G., Reynolds, J.F., Robards, M., Rogers, B.M., Schädel, C., Schaefer, K., Schmidt, I.K., Shvidenko, A., Sky, J., Spencer, R.G.M., Starr, G., Striegl, R.G., Teisserenc, R., Tranvik, L.J., Virtanen, T., Welker, J.M. et Zimov, S. (2016). Biomass offsets little or none of permafrost carbon release from soils, streams, and wildfire: an expert assessment. *Environmental Research Letters, 11*(3), 034014. doi: 10.1088/1748-9326/11/3/034014

Abramoff, R., Xu, X., Hartman, M., O'Brien, S., Feng, W., Davidson, E., Finzi, A., Moorhead, D., Schimel, J., Torn, M. et Mayes, M.A. (2017). The Millennial model: in search of measurable pools and transformations for modeling soil carbon in the new century. *Biogeochemistry, 137*(1-2), 51-71. doi: 10.1007/s10533-017-0409-7

Ali, A.A., Blarquez, O., Girardin, M.P., Hely, C., Tinquaut, F., El Guellab, A., Valsecchi, V., Terrier, A., Bremond, L., Genries, A., Gauthier, S. et Bergeron, Y. (2012). Control of the multimillennial wildfire size in boreal North America by spring climatic conditions. *Proc Natl Acad Sci U S A, 109*(51), 20966-20970. doi: 10.1073/pnas.1203467109 Récupéré de https://www.ncbi.nlm.nih.gov/pubmed/23213207

Allison, S.D. et Treseder, K.K. (2008). Warming and drying suppress microbial activity and carbon cycling in boreal forest soils. *Global Change Biology, 14*(12), 2898-2909. doi: 10.1111/j.1365-2486.2008.01716.x

Amundson, R. (2001). The Carbon Budget in Soils. *Annual Review of Earth and Planetary Sciences, 29*(1), 535-562. doi: 10.1146/annurev.earth.29.1.535

Amundson, R. et Jenny, H. (1997). On a state factor model of ecosystems. *BioScience, 47*(8), 536-543. doi: 10.2307/1313122

Andrieux, B., Beguin, J., Bergeron, Y., Grondin, P. et Paré, D. (2018a). *Carbon stocks in Quebec's spruce feathermoss forest (Canada)*. 1. Québec, QC, Canada : Natural Ressources Canada.

Andrieux, B., Beguin, J., Bergeron, Y., Grondin, P. et Paré, D. (2018b). Drivers of post-fire organic carbon accumulation in the boreal forest. *Global Change Biology*. doi: 10.1111/gcb.14365

Andrus, R.E. (1986). Some aspects of Sphagnum ecology. *Canadian Journal of Botany, 64*(2), 416-426. doi: 10.1139/b86-057

Astrup, R., Bernier, P.Y., Genet, H., Lutz, D.A. et Bright, R.M. (2018). A sensible climate solution for the boreal forest. *Nature Climate Change, 8*(1), 11.

Attiwill, P.M. (1994). The disturbance of forest ecosystems: the ecological basis for conservative management. *Forest Ecology and Management, 63*(2-3), 247-300. doi: 10.1016/0378-1127(94)90114-7

Augusto, L., De Schrijver, A., Vesterdal, L., Smolander, A., Prescott, C. et Ranger, J. (2015). Influences of evergreen gymnosperm and deciduous angiosperm tree species on the functioning of temperate and boreal forests. *Biol Rev Camb Philos Soc, 90*(2), 444-466. doi: 10.1111/brv.12119 Récupéré de https://www.ncbi.nlm.nih.gov/pubmed/24916992

Batjes, N.H. (2016). Harmonized soil property values for broad-scale modelling (WISE30sec) with estimates of global soil carbon stocks. *Geoderma, 269*, 61-68. doi: 10.1016/j.geoderma.2016.01.034

Batjes, N.H., Ribeiro, E., van Oostrum, A., Leenaars, J., Hengl, T. et Mendes de Jesus, J. (2017). WoSIS: providing standardised soil profile data for the world. *Earth System Science Data, 9*(1), 1-14. doi: 10.5194/essd-9-1-2017

Bauhus, J., Paré, D. et Côté, L. (1998). Effects of tree species, stand age and soil type on soil microbial biomass and its activity in a southern boreal forest. *Soil Biology and Biochemistry, 30*(8-9), 1077-1089. doi: 10.1016/s0038-0717(97)00213-7

Beguin, J., Fuglstad, G.-A., Mansuy, N. et Paré, D. (2017). Predicting soil properties in the Canadian boreal forest with limited data: Comparison of spatial and non-spatial statistical approaches. *Geoderma, 306*, 195-205. doi: 10.1016/j.geoderma.2017.06.016

Belisle, A.C., Gauthier, S., Cyr, D., Bergeron, Y. et Morin, H. (2011). Fire regime and old-growth boreal forests in central Quebec, Canada: An ecosystem management perspective. *Silva Fennica, 45*(5), 889-908.

Bergeron, Y. (2000). Species and stand dynamics in the mixed woods of Quebec's southern boreal forest. *Ecology, 81*(6), 1500-1516. doi: Doi 10.1890/0012-9658(2000)081[1500:Sasdit]2.0.Co;2

Bergeron, Y. (2004). Is regulated even-aged management the right strategy for the Canadian boreal forest? *Forestry Chronicle, 80*(4), 458-462. doi: 10.5558/tfc80458-4

Bergeron, Y., Cyr, D., Girardin, M.P. et Carcaillet, C. (2010). Will climate change drive 21st century burn rates in Canadian boreal forest outside of its natural variability: collating global climate model experiments with sedimentary charcoal data. *International Journal of Wildland Fire, 19*(8), 1127-1139. doi: 10.1071/wf09092

Bergeron, Y., Drapeau, P., Gauthier, S. et Lecomte, N. (2007). Using knowledge of natural disturbances to support sustainable forest management in the northern Clay Belt. *Forestry Chronicle, 83*(3), 326-337.

Bergeron, Y., Gauthier, S., Flannigan, M. et Kafka, V. (2004). Fire regimes at the transition between mixewood and coniferous boreal forest in northwestern Quebec. *Ecology, 85*(7), 1916-1932. doi: 10.1890/02-0716

Bergeron, Y., Gauthier, S., Kafka, V., Lefort, P. et Lesieur, D. (2001). Natural fire frequency for the eastern Canadian boreal forest: consequences for sustainable forestry. *Canadian Journal of Forest Research, 31*(3), 384-391. doi: 10.1139/cjfr-31-3-384

Bergeron, Y., Irulappa Pillai Vijayakumar, D.B., Ouzennou, H., Raulier, F., Leduc, A. et Gauthier, S. (2017). Projections of future forest age class structure under the influence of fire and harvesting: implications for forest management in the boreal forest of eastern Canada. *Forestry: An International Journal of Forest Research, 90*(4), 485-495. doi: 10.1093/forestry/cpx022

Bergeron, Y., Leduc, A., Harvey, B.D. et Gauthier, S. (2002). Natural fire regime: a guide for sustainable management of the Canadian boreal forest. *Silva fennica, 36*(1), 81-95.

Berges, J.A. (1997). Ratios, regression statistics, and "spurious" correlations. *Limnology and Oceanography, 42*(5), 1006-1007. doi: 10.4319/lo.1997.42.5.1006

Bisbee, K., Gower, S., Norman, J. et Nordheim, E. (2001). Environmental controls on ground cover species composition and productivity in a boreal black spruce forest. *Oecologia, 129*(2), 261-270. doi: 10.1007/s004420100719

Blaauw, M. (2010). Methods and code for 'classical' age-modelling of radiocarbon sequences. *Quaternary Geochronology, 5*(5), 512-518. doi: 10.1016/j.quageo.2010.01.002

Bona, K.A., Fyles, J.W., Shaw, C. et Kurz, W.A. (2013). Are mosses required to accurately predict upland black spruce forest soil carbon in national-scale forest

C accounting models? *Ecosystems, 16*(6), 1071-1086. doi: 10.1007/s10021-013-9668-x

Bond-Lamberty, B., Peckham, S.D., Ahl, D.E. et Gower, S.T. (2007). Fire as the dominant driver of central Canadian boreal forest carbon balance. *Nature, 450*(7166), 89-92. doi: 10.1038/nature06272 Récupéré de http://www.ncbi.nlm.nih.gov/pubmed/17972883

Bond, W.J., Woodward, F.I. et Midgley, G.F. (2005). The global distribution of ecosystems in a world without fire. *New Phytologist, 165*(2), 525-537. doi: 10.1111/j.1469-8137.2004.01252.x

Bormann, F.H. et Likens, G.E. (1979). *Pattern and process in a forested ecosystem: disturbance, development and the steady state based on the Hubbard Brook ecosystem study*. New York, NY : Springer-Verlag.

Bosatta, E. et Ågren, G.I. (1999). Soil organic matter quality interpreted thermodynamically. *Soil Biology and Biochemistry, 31*(13), 1889-1891. doi: 10.1016/s0038-0717(99)00105-4

Bouchard, M., Pothier, D. et Gauthier, S. (2008). Fire return intervals and tree species succession in the North Shore region of eastern Quebec. *Canadian Journal of Forest Research, 38*(6), 1621-1633. doi: 10.1139/x07-201

Boucher, Y., Bouchard, M., Grondin, P. et Tardif, P. (2011). Le registre des états de référence : intégration des connaissances sur la structure, la composition et la dynamique des paysages forestiers naturels du Québec méridional. *Mémoire de recherche forestière, 161*, 40.

Bradford, M.A., Wieder, W.R., Bonan, G.B., Fierer, N., Raymond, P.A. et Crowther, T.W. (2016). Managing uncertainty in soil carbon feedbacks to climate change. *Nature Climate Change, 6*(8), 751-758. doi: 10.1038/nclimate3071

Bremond, L., Carcaillet, C., Favier, C., Ali, A.A., Paitre, C., Begin, Y., Bergeron, Y. et Richard, P.J.H. (2010). Effects of vegetation zones and climatic changes on fire-induced atmospheric carbon emissions: a model based on paleodata. *International Journal of Wildland Fire, 19*(8), 1015-1025. doi: Doi 10.1071/Wf09096

Brett, M.T. (2004). When is a correlation between non-independent variables "spurious"? *Oikos, 105*(3), 647-656. doi: 10.1111/j.0030-1299.2004.12777.x

Buma, B., Poore, R.E. et Wessman, C.A. (2014). Disturbances, their interactions, and cumulative effects on carbon and charcoal stocks in a forested ecosystem. *Ecosystems, 17*(6), 947-959. doi: 10.1007/s10021-014-9770-8

Bureau du forestier en chef. (2015). *Etat de la forêt publique du Québec et de son aménagement durable - Bilan 2008-2013*. Gouvernement du Québec, Roberval, Québec.

Burton, P.J., Messier, C., Adamowicz, W.L. et Kuuluvainen, T. (2006). Sustainable management of Canada's boreal forests: Progress and prospects. *Ecoscience, 13*(2), 234-248.

Buurman, P. et Jongmans, A.G. (2005). Podzolisation and soil organic matter dynamics. *Geoderma, 125*(1-2), 71-83. doi: 10.1016/j.geoderma.2004.07.006

Callesen, I., Liski, J., Raulund-Rasmussen, K., Olsson, M.T., Tau-Strand, L., Vesterdal, L. et Westman, C.J. (2003). Soil carbon stores in Nordic well-drained forest soils-relationships with climate and texture class. *Global Change Biology, 9*(3), 358-370. doi: 10.1046/j.1365-2486.2003.00587.x

Cardenas, E., Kranabetter, J.M., Hope, G., Maas, K.R., Hallam, S. et Mohn, W.W. (2015). Forest harvesting reduces the soil metagenomic potential for biomass decomposition. [Research Support, Non-U.S. Gov't]. *The ISME journal, 9*(11), 2465-2476. doi: 10.1038/ismej.2015.57 Récupéré de http://www.ncbi.nlm.nih.gov/pubmed/25909978

Carey, E.V., Sala, A., Keane, R. et Callaway, R.M. (2001). Are old forests underestimated as global carbon sinks? *Global Change Biology, 7*(4), 339-344. doi: 10.1046/j.1365-2486.2001.00418.x

Carey, J.C., Tang, J., Templer, P.H., Kroeger, K.D., Crowther, T.W., Burton, A.J., Dukes, J.S., Emmett, B., Frey, S.D., Heskel, M.A., Jiang, L., Machmuller, M.B., Mohan, J., Panetta, A.M., Reich, P.B., Reinsch, S., Wang, X., Allison, S.D., Bamminger, C., Bridgham, S., Collins, S.L., de Dato, G., Eddy, W.C.,

Enquist, B.J., Estiarte, M., Harte, J., Henderson, A., Johnson, B.R., Larsen, K.S., Luo, Y., Marhan, S., Melillo, J.M., Penuelas, J., Pfeifer-Meister, L., Poll, C., Rastetter, E., Reinmann, A.B., Reynolds, L.L., Schmidt, I.K., Shaver, G.R., Strong, A.L., Suseela, V. et Tietema, A. (2016). Temperature response of soil respiration largely unaltered with experimental warming. *Proc Natl Acad Sci U S A, 113*(48), 13797-13802. doi: 10.1073/pnas.1605365113 Récupéré de https://www.ncbi.nlm.nih.gov/pubmed/27849609

Castellano, M.J., Mueller, K.E., Olk, D.C., Sawyer, J.E. et Six, J. (2015). Integrating plant litter quality, soil organic matter stabilization, and the carbon saturation concept. *Global Change Biology, 21*(9), 3200-3209. doi: 10.1111/gcb.12982

Certini, G. (2005). Effects of fire on properties of forest soils: a review. *Oecologia, 143*(1), 1-10. doi: 10.1007/s00442-004-1788-8 Récupéré de http://www.ncbi.nlm.nih.gov/pubmed/15688212

Chapin, F.S., Woodwell, G.M., Randerson, J.T., Rastetter, E.B., Lovett, G.M., Baldocchi, D.D., Clark, D.A., Harmon, M.E., Schimel, D.S., Valentini, R., Wirth, C., Aber, J.D., Cole, J.J., Goulden, M.L., Harden, J.W., Heimann, M., Howarth, R.W., Matson, P.A., McGuire, A.D., Melillo, J.M., Mooney, H.A., Neff, J.C., Houghton, R.A., Pace, M.L., Ryan, M.G., Running, S.W., Sala, O.E., Schlesinger, W.H. et Schulze, E.D. (2006). Reconciling Carbon-cycle Concepts, Terminology, and Methods. *Ecosystems, 9*(7), 1041-1050. doi: 10.1007/s10021-005-0105-7

Chaste, E., Girardin, M.P., Kaplan, J.O., Portier, J., Bergeron, Y. et Hély, C. (2018). The pyrogeography of eastern boreal Canada from 1901 to 2012 simulated with the LPJ-LMfire model. *Biogeosciences, 15*(5), 1273-1292. doi: 10.5194/bg-15-1273-2018

Ciais, P., Sabine, C., Bala, G., Bopp, L., Brovkin, V., Canadell, J., Chhabra, A., DeFries, R., Galloway, J., Heimann, M., Jones, C., Le Quéré, C., Myneni, R.B., Piao, S. et Thornton, P. (2013). Carbon and Other Biogeochemical Cycles. Dans Stocker, T. F., Qin, D., Plattner, G.-K., Tignor, M., Allen, S. K., Boschung, J., Nauels, A., Xia, Y., Bex, V. et Midgley, P. M. (dir.), *Climate Change 2013: The Physical Science Basis. Contribution of Working Group I to the Fifth Assessment Report of the Intergovernmental Panel on Climate Change* (p. 465–570). Cambridge, United Kingdom and New York, NY, USA : Cambridge University Press.

Clarke, N., Gundersen, P., Jönsson-Belyazid, U., Kjønaas, O.J., Persson, T., Sigurdsson, B.D., Stupak, I. et Vesterdal, L. (2015). Influence of different tree-harvesting intensities on forest soil carbon stocks in boreal and northern temperate forest ecosystems. *Forest Ecology and Management, 351*, 9-19. doi: 10.1016/j.foreco.2015.04.034

Clemmensen, K.E., Bahr, A., Ovaskainen, O., Dahlberg, A., Ekblad, A., Wallander, H., Stenlid, J., Finlay, R.D., Wardle, D.A. et Lindahl, B.D. (2013). Roots and associated fungi drive long-term carbon sequestration in boreal forest. *Science, 339*(6127), 1615-1618. doi: 10.1126/science.1231923 Récupéré de http://www.ncbi.nlm.nih.gov/pubmed/23539604

Conant, R.T., Ryan, M.G., Ågren, G.I., Birge, H.E., Davidson, E.A., Eliasson, P.E., Evans, S.E., Frey, S.D., Giardina, C.P., Hopkins, F.M., Hyvönen, R., Kirschbaum, M.U.F., Lavallee, J.M., Leifeld, J., Parton, W.J., Megan Steinweg, J., Wallenstein, M.D., Martin Wetterstedt, J.Å. et Bradford, M.A. (2011). Temperature and soil organic matter decomposition rates - synthesis of current knowledge and a way forward. *Global Change Biology, 17*(11), 3392-3404. doi: 10.1111/j.1365-2486.2011.02496.x

Conseil canadien des ministres des forêts. (2018) *Base de données nationale sur les forêts*. de http://nfdp.ccfm.org

Cook, J., Oreskes, N., Doran, P.T., Anderegg, W.R.L., Verheggen, B., Maibach, E.W., Carlton, J.S., Lewandowsky, S., Skuce, A.G., Green, S.A., Nuccitelli, D., Jacobs, P., Richardson, M., Winkler, B., Painting, R. et Rice, K. (2016). Consensus on consensus: a synthesis of consensus estimates on human-caused global warming. *Environmental Research Letters, 11*(4), 048002. doi: 10.1088/1748-9326/11/4/048002

Cotrufo, M.F., Wallenstein, M.D., Boot, C.M., Denef, K. et Paul, E. (2013). The Microbial Efficiency-Matrix Stabilization (MEMS) framework integrates plant litter decomposition with soil organic matter stabilization: do labile plant inputs form stable soil organic matter? *Global change biology, 19*(4), 988-995. doi: 10.1111/gcb.12113 Récupéré de http://www.ncbi.nlm.nih.gov/pubmed/23504877

Courchesne, F. et Turmel, M.-C. (2007). Extractable Al, Fe, Mn, and Si. Dans Carter M. R. et Gregorich, E. G. (dir.), *Soil Sampling and Methods of Analysis, Second Edition.* Boca Raton, FL : CRC Press.

Cragg, S.M., Beckham, G.T., Bruce, N.C., Bugg, T.D., Distel, D.L., Dupree, P., Etxabe, A.G., Goodell, B.S., Jellison, J., McGeehan, J.E., McQueen-Mason, S.J., Schnorr, K., Walton, P.H., Watts, J.E. et Zimmer, M. (2015). Lignocellulose degradation mechanisms across the Tree of Life. *Curr Opin Chem Biol, 29*, 108-119. doi: 10.1016/j.cbpa.2015.10.018 Récupéré de https://www.ncbi.nlm.nih.gov/pubmed/26583519

Craine, J.M., Fierer, N. et McLauchlan, K.K. (2010). Widespread coupling between the rate and temperature sensitivity of organic matter decay. *Nature Geoscience, 3*(12), 854-857. doi: 10.1038/ngeo1009

Crowther, T.W., Todd-Brown, K.E., Rowe, C.W., Wieder, W.R., Carey, J.C., Machmuller, M.B., Snoek, B.L., Fang, S., Zhou, G., Allison, S.D., Blair, J.M., Bridgham, S.D., Burton, A.J., Carrillo, Y., Reich, P.B., Clark, J.S., Classen, A.T., Dijkstra, F.A., Elberling, B., Emmett, B.A., Estiarte, M., Frey, S.D., Guo, J., Harte, J., Jiang, L., Johnson, B.R., Kroel-Dulay, G., Larsen, K.S., Laudon, H., Lavallee, J.M., Luo, Y., Lupascu, M., Ma, L.N., Marhan, S., Michelsen, A., Mohan, J., Niu, S., Pendall, E., Penuelas, J., Pfeifer-Meister, L., Poll, C., Reinsch, S., Reynolds, L.L., Schmidt, I.K., Sistla, S., Sokol, N.W., Templer, P.H., Treseder, K.K., Welker, J.M. et Bradford, M.A. (2016). Quantifying global soil carbon losses in response to warming. *Nature, 540*(7631), 104-108. doi: 10.1038/nature20150 Récupéré de http://www.ncbi.nlm.nih.gov/pubmed/27905442

Crutzen, P.J. (2002). Geology of mankind. *Nature, 415*(6867), 23. doi: 10.1038/415023a Récupéré de https://www.ncbi.nlm.nih.gov/pubmed/11780095

Curtis, P.S. et Gough, C.M. (2018). Forest aging, disturbance and the carbon cycle. *New Phytol.* doi: 10.1111/nph.15227 Récupéré de https://www.ncbi.nlm.nih.gov/pubmed/29767850

Cyr, D., Gauthier, S. et Bergeron, Y. (2012). The influence of landscape-level heterogeneity in fire frequency on canopy composition in the boreal forest of

eastern Canada. *Journal of Vegetation Science, 23*(1), 140-150. doi: DOI 10.1111/j.1654-1103.2011.01338.x

Cyr, D., Gauthier, S., Bergeron, Y. et Carcaillet, C. (2009). Forest management is driving the eastern North American boreal forest outside its natural range of variability. *Frontiers in Ecology and the Environment, 7*(10), 519-524. doi: 10.1890/080088

Czimczik, C.I., Schmidt, M.W.I. et Schulze, E.D. (2005). Effects of increasing fire frequency on black carbon and organic matter in Podzols of Siberian Scots pine forests. *European Journal of Soil Science, 56*(3), 417-428. doi: 10.1111/j.1365-2389.2004.00665.x

Davidson, E.A. (2015). Soil carbon in a beer can. *Nature Geoscience, 8*(10), 748-749. doi: 10.1038/ngeo2522

Davidson, E.A. (2016). Projections of the soil-carbon deficit. *Nature, 540*(7631), 47-48. doi: 10.1038/540047a

Davidson, E.A. et Janssens, I.A. (2006). Temperature sensitivity of soil carbon decomposition and feedbacks to climate change. *Nature, 440*(7081), 165-173. doi: 10.1038/nature04514 Récupéré de http://www.ncbi.nlm.nih.gov/pubmed/16525463

De Deyn, G.B., Cornelissen, J.H. et Bardgett, R.D. (2008). Plant functional traits and soil carbon sequestration in contrasting biomes. *Ecol Lett, 11*(5), 516-531. doi: 10.1111/j.1461-0248.2008.01164.x Récupéré de http://www.ncbi.nlm.nih.gov/pubmed/18279352

de Gonzalo, G., Colpa, D.I., Habib, M.H. et Fraaije, M.W. (2016). Bacterial enzymes involved in lignin degradation. [Review]. *J Biotechnol, 236*, 110-119. doi: 10.1016/j.jbiotec.2016.08.011 Récupéré de https://www.ncbi.nlm.nih.gov/pubmed/27544286

de Lafontaine, G. et Payette, S. (2011). Shifting zonal patterns of the southern boreal forest in eastern Canada associated with changing fire regime during the Holocene. *Quaternary Science Reviews, 30*(7-8), 867-875. doi: 10.1016/j.quascirev.2011.01.002

Deluca, T.H. et Boisvenue, C. (2012). Boreal forest soil carbon: distribution, function and modelling. *Forestry, 85*(2), 161-184. doi: 10.1093/forestry/cps003

Dixon, R.K., Brown, S., Houghton, R.A., Solomon, A.M., Trexler, M.C. et Wisniewski, J. (1994). Carbon pools and flux of global forest ecosystems. *Science, 263*, 185-191.

Doetterl, S., Stevens, A., Six, J., Merckx, R., Van Oost, K., Casanova Pinto, M., Casanova-Katny, A., Muñoz, C., Boudin, M., Zagal Venegas, E. et Boeckx, P. (2015). Soil carbon storage controlled by interactions between geochemistry and climate. *Nature Geoscience, 8*(10), 780-783. doi: 10.1038/ngeo2516

Don, A., Rödenbeck, C. et Gleixner, G. (2013). Unexpected control of soil carbon turnover by soil carbon concentration. *Environmental Chemistry Letters, 11*(4), 407-413. doi: 10.1007/s10311-013-0433-3

Drever, J.I. (1994). The effect of land plants on weathering rates of silicate minerals. *Geochimica et Cosmochimica Acta, 58*(10), 2325-2332. doi: 10.1016/0016-7037(94)90013-2

Drever, J.I. et Stillings, L.L. (1997). The role of organic acids in mineral weathering. *Colloids and Surfaces A: Physicochemical and Engineering Aspects, 120*(1-3), 167-181. doi: 10.1016/s0927-7757(96)03720-x

Driscoll, C.T. et Likens, G.E. (1982). Hydrogen ion budget of an aggrading forested ecosystem. *Tellus, 34*(3), 283-292. doi: 10.1111/j.2153-3490.1982.tb01817.x

Dungait, J.A.J., Hopkins, D.W., Gregory, A.S. et Whitmore, A.P. (2012). Soil organic matter turnover is governed by accessibility not recalcitrance. *Global Change Biology, 18*(6), 1781-1796. doi: 10.1111/j.1365-2486.2012.02665.x

Ecological Stratification Working Group. (1996). *A national ecological framework for Canada*. Ottawa/Hull, Canada : Agriculture and Agri-Food Canada and Environment Canada.

Egli, M., Sartori, G., Mirabella, A., Favilli, F., Giaccai, D. et Delbos, E. (2009). Effect of north and south exposure on organic matter in high Alpine soils. *Geoderma, 149*(1-2), 124-136. doi: 10.1016/j.geoderma.2008.11.027

Ekschmitt, K., Kandeler, E., Poll, C., Brune, A., Buscot, F., Friedrich, M., Gleixner, G., Hartmann, A., Kästner, M., Marhan, S., Miltner, A., Scheu, S. et Wolters, V. (2008). Soil-carbon preservation through habitat constraints and biological limitations on decomposer activity. *Journal of Plant Nutrition and Soil Science, 171*(1), 27-35. doi: 10.1002/jpln.200700051

Ellis, E.C. et Haff, P.K. (2009). Earth Science in the Anthropocene: New Epoch, New Paradigm, New Responsibilities. *Eos, Transactions American Geophysical Union, 90*(49), 473. doi: 10.1029/2009eo490006

Federer, C.A., Turcotte, D.E. et Smith, C.T. (1993). The organic fraction–bulk density relationship and the expression of nutrient content in forest soils. *Canadian Journal of Forest Research, 23*(6), 1026-1032. doi: 10.1139/x93-131

Fenton, N.J. et Bergeron, Y. (2008). Does time or habitat make old-growth forests species rich? Bryophyte richness in boreal *Picea mariana* forests. *Biological Conservation, 141*(5), 1389-1399. doi: 10.1016/j.biocon.2008.03.019

Fenton, N.J., Bergeron, Y. et Paré, D. (2010). Decomposition rates of bryophytes in managed boreal forests: influence of bryophyte species and forest harvesting. *Plant and Soil, 336*(1-2), 499-508. doi: 10.1007/s11104-010-0506-z

Fenton, N.J., Lecomte, N., Légaré, S. et Bergeron, Y. (2005). Paludification in black spruce (Picea mariana) forests of eastern Canada: Potential factors and management implications. *Forest Ecology and Management, 213*(1-3), 151-159. doi: 10.1016/j.foreco.2005.03.017

Fernández, I., Cabaneiro, A. et Carballas, T. (1997). Organic matter changes immediately after a wildfire in an atlantic forest soil and comparison with laboratory soil heating. *Soil Biology and Biochemistry, 29*(1), 1-11. doi: 10.1016/s0038-0717(96)00289-1

Fierer, N., Allen, A.S., Schimel, J.P. et Holden, P.A. (2003). Controls on microbial CO_2 production: a comparison of surface and subsurface soil horizons. *Global Change Biology, 9*(9), 1322-1332. doi: 10.1046/j.1365-2486.2003.00663.x

Fierer, N., Craine, J.M., McLauchlan, K. et Schimel, J.P. (2005). Litter Quality and the Temperature Sensitivity of Decomposition. *Ecology, 86*(2), 320-326. doi: 10.1890/04-1254

Fierer, N. et Jackson, R.B. (2006). The diversity and biogeography of soil bacterial communities. *Proc Natl Acad Sci U S A, 103*(3), 626-631. doi: 10.1073/pnas.0507535103 Récupéré de https://www.ncbi.nlm.nih.gov/pubmed/16407148

Frégeau, M., Payette, S. et Grondin, P. (2015). Fire history of the central boreal forest in eastern North America reveals stability since the mid-Holocene. *The Holocene, 25*(12), 1912-1922. doi: 10.1177/0959683615591361

Frey, S.D., Lee, J., Melillo, J.M. et Six, J. (2013). The temperature response of soil microbial efficiency and its feedback to climate. *Nature Climate Change, 3*(4), 395-398. doi: 10.1038/nclimate1796

Frontier, S., Pichod-Vidal, D., Leprêtre, A., Davoult, D. et Luczak, C. (2008). Coopération entre de nombreuses espèces interactives : les recyclages de matière. Dans *Ecosystèmes : structure, fonctionnement, évolution* (p. 259-288). Paris, France : Dunod.

Fu, Z., Li, D., Hararuk, O., Schwalm, C., Luo, Y., Yan, L. et Niu, S. (2017a). Recovery time and state change of terrestrial carbon cycle after disturbance. *Environmental Research Letters, 12*(10), 104004. doi: 10.1088/1748-9326/aa8a5c

Fu, Z., Li, D.J., Hararuk, O., Schwalm, C., Luo, Y.Q., Yan, L.M. et Niu, S.L. (2017b). Recovery time and state change of terrestrial carbon cycle after disturbance. *Environmental Research Letters, 12*(10). doi: 10.1088/1748-9326/aa8a5c

Games, P.A. et Howell, F. (1976). Pairwise multiple comparison procedures with unequal N's and/or variances: a monte carlo study. *Journal of Educational Statistics, 1*(2), 113-125. doi: 10.2307/1164979

Gao, B., Taylor, A.R., Searle, E.B., Kumar, P., Ma, Z., Hume, A.M. et Chen, H.Y.H. (2017). Carbon storage declines in old boreal forests irrespective of succession pathway. *Ecosystems*. doi: 10.1007/s10021-017-0210-4

Gauthier, S., Bernier, P., Kuuluvainen, T., Shvidenko, A.Z. et Schepaschenko, D.G. (2015). Boreal forest health and global change. *Science, 349*(6250), 819-822. doi: 10.1126/science.aaa9092

Gelman, V., Hulkkonen, V., Kantola, R., Nousiainen, M., Nousiainen, V. et Poku-Marboah, M. (2013). Impacts of forest management practices on forest carbon. *Helsinki University Centre for Environment, Helsinki*.

Genet, H., He, Y., Lyu, Z., McGuire, A.D., Zhuang, Q., Clein, J., D'Amore, D., Bennett, A., Breen, A., Biles, F., Euskirchen, E.S., Johnson, K., Kurkowski, T., Kushch Schroder, S., Pastick, N., Rupp, T.S., Wylie, B., Zhang, Y., Zhou, X. et Zhu, Z. (2018). The role of driving factors in historical and projected carbon dynamics of upland ecosystems in Alaska. *Ecological Applications, 28*(1), 5-27. doi: 10.1002/eap.1641 Récupéré de https://www.ncbi.nlm.nih.gov/pubmed/29044791

Gignac, L.D. (2001). Bryophytes as indicators of climate change. *The Bryologist, 104*(3), 410-420. doi: 10.1639/0007-2745(2001)104[0410:Baiocc]2.0.Co;2

Girardin, M.P., Bouriaud, O., Hogg, E.H., Kurz, W., Zimmermann, N.E., Metsaranta, J.M., de Jong, R., Frank, D.C., Esper, J., Buntgen, U., Guo, X.J. et Bhatti, J. (2016). No growth stimulation of Canada's boreal forest under half-century of combined warming and CO2 fertilization. *Proc Natl Acad Sci U S A, 113*(52), E8406-E8414. doi: 10.1073/pnas.1610156113 Récupéré de http://www.ncbi.nlm.nih.gov/pubmed/27956624

Girardin, M.P. et Terrier, A. (2015). Mitigating risks of future wildfires by management of the forest composition: an analysis of the offsetting potential through boreal Canada. *Climatic Change, 130*(4), 587-601. doi: 10.1007/s10584-015-1373-7

Gobat, J.-M., Aragno, M. et Matthey, W. (2010). *Le sol vivant: bases de pédologie, biologie des sols*. (Vol. 14) : PPUR Presses polytechniques.

Gonzalez-Perez, J.A., Gonzalez-Vila, F.J., Almendros, G. et Knicker, H. (2004). The effect of fire on soil organic matter--a review. *Environment International, 30*(6), 855-870. doi: 10.1016/j.envint.2004.02.003 Récupéré de http://www.ncbi.nlm.nih.gov/pubmed/15120204

Gouvernement du Québec. (2018) *Registre des aires protégées*. de http://www.mddelcc.gouv.qc.ca/biodiversite/aires_protegees/registre/

Greene, D.F., Macdonald, S.E., Haeussler, S., Domenicano, S., Noël, J., Jayen, K., Charron, I., Gauthier, S., Hunt, S., Gielau, E.T., Bergeron, Y. et Swift, L. (2007). The reduction of organic-layer depth by wildfire in the North American boreal forest and its effect on tree recruitment by seed. *Canadian Journal of Forest Research, 37*(6), 1012-1023. doi: 10.1139/x06-245

Griscom, B.W., Adams, J., Ellis, P.W., Houghton, R.A., Lomax, G., Miteva, D.A., Schlesinger, W.H., Shoch, D., Siikamaki, J.V., Smith, P., Woodbury, P., Zganjar, C., Blackman, A., Campari, J., Conant, R.T., Delgado, C., Elias, P., Gopalakrishna, T., Hamsik, M.R., Herrero, M., Kiesecker, J., Landis, E., Laestadius, L., Leavitt, S.M., Minnemeyer, S., Polasky, S., Potapov, P., Putz, F.E., Sanderman, J., Silvius, M., Wollenberg, E. et Fargione, J. (2017). Natural climate solutions. *Proc Natl Acad Sci U S A, 114*(44), 11645-11650. doi: 10.1073/pnas.1710465114 Récupéré de https://www.ncbi.nlm.nih.gov/pubmed/29078344

Han, L., Sun, K., Jin, J. et Xing, B. (2016). Some concepts of soil organic carbon characteristics and mineral interaction from a review of literature. *Soil Biology and Biochemistry, 94*, 107-121. doi: 10.1016/j.soilbio.2015.11.023

Harden, J.W., Manies, K.L., O'Donnell, J., Johnson, K., Frolking, S. et Fan, Z. (2012). Spatiotemporal analysis of black spruce forest soils and implications for the fate of C. *Journal of Geophysical Research, 117*(G1). doi: 10.1029/2011jg001826

Harden, J.W., Mark, R.K., Sundquist, E.T. et Stallard, R.F. (1992). Dynamics of soil carbon during deglaciation of the Laurentide ice sheet. *Science, 258*(5090), 1921-1924. doi: 10.1126/science.258.5090.1921 Récupéré de http://www.ncbi.nlm.nih.gov/pubmed/17836185

Harlos, C., Edgell, T.C. et Hollander, J. (2016). No evidence of publication bias in climate change science. *Climatic Change, 140*(3-4), 375-385. doi: 10.1007/s10584-016-1880-1

Harper, K., Boudreault, C., DeGrandpré, L., Drapeau, P., Gauthier, S. et Bergeron, Y. (2003). Structure, composition, and diversity of old-growth black spruce boreal forest of the Clay Belt region in Quebec and Ontario. *Environmental Reviews, 11*(S1), S79-S98. doi: 10.1139/a03-013

Harvey, B.D., Leduc, A., Gauthier, S. et Bergeron, Y. (2002). Stand-landscape integration in natural disturbance-based management of the southern boreal forest. *Forest Ecology and Management, 155*(1-3), 369-385. doi: 10.1016/s0378-1127(01)00573-4

Heckman, K., Welty-Bernard, A., Rasmussen, C. et Schwartz, E. (2009). Geologic controls of soil carbon cycling and microbial dynamics in temperate conifer forests. *Chemical Geology, 267*(1-2), 12-23. doi: 10.1016/j.chemgeo.2009.01.004

Hendershot, W.H. et Lalande, H. (2007). Soil Reaction and Exchangeable Acidity. Dans Carter M. R. et Gregorich, E. G. (dir.), *Soil Sampling and Methods of Analysis, Second Edition.* Boca Raton, FL : CRC Press.

Hobbie, S.E., Schimel, J.P., Trumbore, S.E. et Randerson, J.R. (2000). Controls over carbon storage and turnover in high-latitude soils. *Global Change Biology, 6*, 196-210. doi: 10.1046/j.1365-2486.2000.06021.x

Houghton, R.A., Davidson, E.A. et Woodwell, G.M. (1998). Missing sinks, feedbacks, and understanding the role of terrestrial ecosystems in the global carbon balance. *Global Biogeochemical Cycles, 12*(1), 25-34. doi: 10.1029/97gb02729

Hudiburg, T.W., Higuera, P.E. et Hicke, J.A. (2017). Fire-regime variability impacts forest carbon dynamics for centuries to millennia. *Biogeosciences, 14*(17), 3873-3882. doi: 10.5194/bg-14-3873-2017

Hui, D., Deng, Q., Tian, H. et Luo, Y. (2017). Climate Change and Carbon Sequestration in Forest Ecosystems. Dans Chen, W.-Y., Suzuki, T. et Lackner,

M. (dir.), *Handbook of Climate Change Mitigation and Adaptation* (p. 555-594) : Springer International Publishing.

Hynes, H.M. et Germida, J.J. (2013). Impact of clear cutting on soil microbial communities and bioavailable nutrients in the LFH and Ae horizons of Boreal Plain forest soils. *Forest Ecology and Management, 306*, 88-95. doi: 10.1016/j.foreco.2013.06.006

IPCC. (2013). *Climate change 2013: the physical science basis. Contribution of working group I to the fifth assessment report of the intergovernmental panel on climate change*. Cambridge, UK and New York, NY : Cambridge University Press.

Irulappa Pillai Vijayakumar, D.B., Raulier, F., Bernier, P., Paré, D., Gauthier, S., Bergeron, Y. et Pothier, D. (2016). Cover density recovery after fire disturbance controls landscape aboveground biomass carbon in the boreal forest of eastern Canada. *Forest Ecology and Management, 360*, 170-180. doi: 10.1016/j.foreco.2015.10.035

IUSS Working Group WRB. (2015). *World reference base for soil ressources 2014, update 2015. International soil classification system for naming soils and creating legends for soil maps.* (Vol. 106). Rome : FAO.

James, J. et Harrison, R. (2016). The Effect of Harvest on Forest Soil Carbon: A Meta-Analysis. *Forests, 7*(12). doi: 10.3390/f7120308

Jandl, R., Lindner, M., Vesterdal, L., Bauwens, B., Baritz, R., Hagedorn, F., Johnson, D.W., Minkkinen, K. et Byrne, K.A. (2007). How strongly can forest management influence soil carbon sequestration? *Geoderma, 137*(3-4), 253-268. doi: 10.1016/j.geoderma.2006.09.003

Jenkinson, D.S., Andrew, S.P.S., Lynch, J.M., Goss, M.J. et Tinker, P.B. (1990). The Turnover of Organic Carbon and Nitrogen in Soil [and Discussion]. *Philosophical Transactions of the Royal Society B: Biological Sciences, 329*(1255), 361-368. doi: 10.1098/rstb.1990.0177

Jenny, H. (1994). *Factors of soil formation: a system of quantitative pedology*. New York, NY : Dover Publications Inc.

Jobbagy, E.G. et Jackson, R.B. (2000). The vertical distribution of soil organic carbon and its relation to climate and vegetation. *Ecological Applications, 10*(2), 423-436. doi: 10.2307/2641104

Johnson, D.W. et Curtis, P.S. (2001). Effects of forest management on soil C and N storage: meta analysis. *Forest Ecology and Management, 140*(2-3), 227-238. doi: 10.1016/S0378-1127(00)00282-6

Kafka, V., Gauthier, S. et Bergeron, Y. (2001). Fire impacts and crowning in the boreal forest: study of a large wildfire in western Quebec. *International Journal of Wildland Fire, 10*(2), 119-127. doi: Doi 10.1071/Wf01012

Kaiser, K., Eusterhues, K., Rumpel, C., Guggenberger, G. et Kögel-Knabner, I. (2002). Stabilization of organic matter by soil minerals — investigations of density and particle-size fractions from two acid forest soils. *Journal of Plant Nutrition and Soil Science, 165*(4), 451. doi: 10.1002/1522-2624(200208)165:4<451::aid-jpln451>3.0.co;2-b

Kane, E.S., Kasischke, E.S., Valentine, D.W., Turetsky, M.R. et McGuire, A.D. (2007). Topographic influences on wildfire consumption of soil organic carbon in interior Alaska: Implications for black carbon accumulation. *Journal of Geophysical Research: Biogeosciences, 112*(G3). doi: 10.1029/2007jg000458

Kane, E.S., Valentine, D.W., Schuur, E.A. et Dutta, K. (2005). Soil carbon stabilization along climate and stand productivity gradients in black spruce forests of interior Alaska. *Canadian Journal of Forest Research, 35*(9), 2118-2129. doi: 10.1139/x05-093

Keenan, R.J. et Kimmins, J. (1993). The ecological effects of clear-cutting. *Environmental Reviews, 1*(2), 121-144.

Kelly, R., Genet, H., McGuire, A.D. et Hu, F.S. (2015). Palaeodata-informed modelling of large carbon losses from recent burning of boreal forests. *Nature Climate Change, 6*(1), 79-82. doi: 10.1038/nclimate2832

Kenkel, N.C., Walker, D.J., Watson, P.R., Caners, R.T. et Lastra, R.A. (1997). Vegetation dynamics in boreal forest ecosystems. *Coenoses, 12*(2-3), 97-108.

Kirschbaum, M. (2006). The temperature dependence of organic-matter decomposition—still a topic of debate. *Soil Biology and Biochemistry, 38*(9), 2510-2518. doi: 10.1016/j.soilbio.2006.01.030

Kleber, M. (2010). What is recalcitrant soil organic matter? *Environmental Chemistry, 7*(4), 320. doi: 10.1071/en10006

Kloster, S. et Lasslop, G. (2017). Historical and future fire occurrence (1850 to 2100) simulated in CMIP5 Earth System Models. *Global and Planetary Change, 150*, 58-69. doi: 10.1016/j.gloplacha.2016.12.017

Knicker, H. (2007). How does fire affect the nature and stability of soil organic nitrogen and carbon? A review. *Biogeochemistry, 85*(1), 91-118. doi: 10.1007/s10533-007-9104-4

Kramer, M.G., Sanderman, J., Chadwick, O.A., Chorover, J. et Vitousek, P.M. (2012). Long-term carbon storage through retention of dissolved aromatic acids by reactive particles in soil. *Global Change Biology, 18*(8), 2594-2605. doi: 10.1111/j.1365-2486.2012.02681.x

Kroetsch, D. et Wang, C. (2007). Particle Size Distribution. Dans Carter M. R. et Gregorich, E. G. (dir.), *Soil Sampling and Methods of Analysis, Second Edition*. Boca Raton, FL : CRC Press.

Kunito, T., Isomura, I., Sumi, H., Park, H.-D., Toda, H., Otsuka, S., Nagaoka, K., Saeki, K. et Senoo, K. (2016). Aluminum and acidity suppress microbial activity and biomass in acidic forest soils. *Soil Biology and Biochemistry, 97*, 23-30. doi: 10.1016/j.soilbio.2016.02.019

Kurz, W.A., Shaw, C.H., Boisvenue, C., Stinson, G., Metsaranta, J., Leckie, D., Dyk, A., Smyth, C. et Neilson, E.T. (2013). Carbon in Canada's boreal forest — A synthesis. *Environmental Reviews, 21*(4), 260-292. doi: 10.1139/er-2013-0041

Kurz, W.A., Stinson, G., Rampley, G.J., Dymond, C.C. et Neilson, E.T. (2008). Risk of natural disturbances makes future contribution of Canada's forests to the global carbon cycle highly uncertain. *Proc Natl Acad Sci U S A, 105*(5), 1551-

1555. doi: 10.1073/pnas.0708133105 Récupéré de http://www.ncbi.nlm.nih.gov/pubmed/18230736

Kuusela, K. (1992). The boreal forests: an overview. *Unasylva (FAO), 43*. Récupéré de http://www.fao.org/docrep/u6850f/u6850f00.htm

Laganière, J., Angers, D.A., Paré, D., Bergeron, Y. et Chen, H.Y.H. (2011). Black Spruce Soils Accumulate More Uncomplexed Organic Matter than Aspen Soils. *Soil Science Society of America Journal, 75*(3), 1125. doi: 10.2136/sssaj2010.0275

Laganière, J., Boča, A., Van Miegroet, H. et Paré, D. (2017). A tree species effect on soil that is consistent across the species' range: The case of aspen and soil carbon in North America. *Forests, 8*(12), 113. doi: 10.3390/f8040113

Laganière, J., Paré, D., Bergeron, Y., Chen, H., Y., H., Brassard, B., W. et Cavard, X. (2013). Stability of soil carbon stocks varies with composition in the canadian boreal biome. *Ecosystems, 16*(5), 852-865. doi: 10.1007/s10021-013-9658-z

Laganière, J., Paré, D., Bergeron, Y. et Chen, H.Y.H. (2012). The effect of boreal forest composition on soil respiration is mediated through variations in soil temperature and C quality. *Soil Biology and Biochemistry, 53*, 18-27. doi: 10.1016/j.soilbio.2012.04.024

Laganière, J., Podrebarac, F., Billings, S.A., Edwards, K.A. et Ziegler, S.E. (2015). A warmer climate reduces the bioreactivity of isolated boreal forest soil horizons without increasing the temperature sensitivity of respiratory CO2 loss. *Soil Biology and Biochemistry, 84*, 177-188. doi: 10.1016/j.soilbio.2015.02.025

Lal, R. (2005). Forest soils and carbon sequestration. *Forest Ecology and Management, 220*(1-3), 242-258. doi: 10.1016/j.foreco.2005.08.015

Lang, S.I., Cornelissen, J.H.C., Klahn, T., van Logtestijn, R.S.P., Broekman, R., Schweikert, W. et Aerts, R. (2009). An experimental comparison of chemical traits and litter decomposition rates in a diverse range of subarctic bryophyte, lichen and vascular plant species. *Journal of Ecology, 97*(5), 886-900. doi: 10.1111/j.1365-2745.2009.01538.x

Lavoie, M., Paré, D., Fenton, N., Groot, A. et Taylor, K. (2005). Paludification and management of forested peatlands in Canada: a literature review. *Environmental Reviews, 13*(2), 21-50. doi: 10.1139/a05-006

Le Goff, H., Flannigan, M.D. et Bergeron, Y. (2009). Potential changes in monthly fire risk in the eastern Canadian boreal forest under future climate change. *Canadian Journal of Forest Research, 39*(12), 2369-2380. doi: 10.1139/x09-153

Le Goff, H., Flannigan, M.D., Bergeron, Y. et Girardin, M.P. (2007). Historical fire regime shifts related to climate teleconnections in the Waswanipi area, central Quebec, Canada. *International Journal of Wildland Fire, 16*(5), 607-618. doi: 10.1071/Wf06151

Le Goff, H., Girardin, M.P., Flannigan, M. et Bergeron, Y. (2008). Dendroclimatic inference of wildfire activity in Quebec over the 20th century and implication for natural disturbance-based forest management at the northern limit of the commercial forest. *International Journal of Wildland Fire, 17*, 348-362.

Le Quéré, C., Andrew, R.M., Friedlingstein, P., Sitch, S., Pongratz, J., Manning, A.C., Korsbakken, J.I., Peters, G.P., Canadell, J.G., Jackson, R.B., Boden, T.A., Tans, P.P., Andrews, O.D., Arora, V.K., Bakker, D.C.E., Barbero, L., Becker, M., Betts, R.A., Bopp, L., Chevallier, F., Chini, L.P., Ciais, P., Cosca, C.E., Cross, J., Currie, K., Gasser, T., Harris, I., Hauck, J., Haverd, V., Houghton, R.A., Hunt, C.W., Hurtt, G., Ilyina, T., Jain, A.K., Kato, E., Kautz, M., Keeling, R.F., Klein Goldewijk, K., Körtzinger, A., Landschützer, P., Lefèvre, N., Lenton, A., Lienert, S., Lima, I., Lombardozzi, D., Metzl, N., Millero, F., Monteiro, P.M.S., Munro, D.R., Nabel, J.E.M.S., Nakaoka, S.-i., Nojiri, Y., Padin, X.A., Peregon, A., Pfeil, B., Pierrot, D., Poulter, B., Rehder, G., Reimer, J., Rödenbeck, C., Schwinger, J., Séférian, R., Skjelvan, I., Stocker, B.D., Tian, H., Tilbrook, B., Tubiello, F.N., van der Laan-Luijkx, I.T., van der Werf, G.R., van Heuven, S., Viovy, N., Vuichard, N., Walker, A.P., Watson, A.J., Wiltshire, A.J., Zaehle, S. et Zhu, D. (2018). Global Carbon Budget 2017. *Earth System Science Data, 10*(1), 405-448. doi: 10.5194/essd-10-405-2018

Lecomte, N., Simard, M., Fenton, N. et Bergeron, Y. (2006). Fire severity and long-term ecosystem biomass dynamics in coniferous boreal forests of eastern Canada. *Ecosystems, 9*(8), 1215-1230. doi: 10.1007/s10021-004-0168-x

Li, C. (2002). Estimation of fire frequency and fire cycle: a computational perspective. *Ecological Modelling, 154*(1-2), 103-120. doi: 10.1016/s0304-3800(02)00069-8

Liski, J. et Westman, C.J. (1997). Carbon storage in forest soil of Finland. *Biogeochemistry, 36*, 239-260.

Luo, Z., Feng, W., Luo, Y., Baldock, J. et Wang, E. (2017). Soil organic carbon dynamics jointly controlled by climate, carbon inputs, soil properties and soil carbon fractions. *Global Change Biology, 23*(10), 4430-4439. doi: 10.1111/gcb.13767

Luyssaert, S., Schulze, E.D., Borner, A., Knohl, A., Hessenmoller, D., Law, B.E., Ciais, P. et Grace, J. (2008). Old-growth forests as global carbon sinks. *Nature, 455*(7210), 213-215. doi: 10.1038/nature07276 Récupéré de http://www.ncbi.nlm.nih.gov/pubmed/18784722

Mansuy, N., Thiffault, E., Paré, D., Bernier, P., Guindon, L., Villemaire, P., Poirier, V. et Beaudoin, A. (2014). Digital mapping of soil properties in Canadian managed forests at 250m of resolution using the k-nearest neighbor method. *Geoderma, 235-236*, 59-73. doi: 10.1016/j.geoderma.2014.06.032

Marchetti, G.M., Drton, M. et Sadeghi, K. (2015). *ggm: Functions for graphical Markov models*. Récupéré de https://CRAN.R-project.org/package=ggm

Marchi, E., Chung, W., Visser, R., Abbas, D., Nordfjell, T., Mederski, P.S., McEwan, A., Brink, M. et Laschi, A. (2018). Sustainable Forest Operations (SFO): A new paradigm in a changing world and climate. [Review]. *Sci Total Environ, 634*, 1385-1397. doi: 10.1016/j.scitotenv.2018.04.084 Récupéré de https://www.ncbi.nlm.nih.gov/pubmed/29710638

Marschner, B., Brodowski, S., Dreves, A., Gleixner, G., Gude, A., Grootes, P.M., Hamer, U., Heim, A., Jandl, G., Ji, R., Kaiser, K., Kalbitz, K., Kramer, C., Leinweber, P., Rethemeyer, J., Schäffer, A., Schmidt, M.W.I., Schwark, L. et Wiesenberg, G.L.B. (2008). How relevant is recalcitrance for the stabilization of organic matter in soils? *Journal of Plant Nutrition and Soil Science, 171*(1), 91-110. doi: 10.1002/jpln.200700049

Marty, C., Houle, D. et Gagnon, C. (2015). Variation in stocks and distribution of organic C in soils across 21 eastern Canadian temperate and boreal forests. *Forest Ecology and Management, 345*, 29-38. doi: 10.1016/j.foreco.2015.02.024

Masiello, C.A., Chadwick, O.A., Southon, J., Torn, M.S. et Harden, J.W. (2004). Weathering controls on mechanisms of carbon storage in grassland soils. *Global Biogeochemical Cycles, 18*(4), n/a-n/a. doi: 10.1029/2004gb002219

McBratney, A.B., Mendonça Santos, M.L. et Minasny, B. (2003). On digital soil mapping. *Geoderma, 117*(1-2), 3-52. doi: 10.1016/s0016-7061(03)00223-4

McLauchlan, K.K., Higuera, P.E., Gavin, D.G., Perakis, S.S., Mack, M.C., Alexander, H., Battles, J., Biondi, F., Buma, B., Colombaroli, D., Enders, S.K., Engstrom, D.R., Hu, F.S., Marlon, J.R., Marshall, J., McGlone, M., Morris, J.L., Nave, L.E., Shuman, B., Smithwick, E.A.H., Urrego, D.H., Wardle, D.A., Williams, C.J. et Williams, J.J. (2014). Reconstructing Disturbances and Their Biogeochemical Consequences over Multiple Timescales. *BioScience, 64*(2), 105-116. doi: 10.1093/biosci/bit017

Mikutta, R., Kleber, M., Torn, M.S. et Jahn, R. (2006). Stabilization of soil organic matter: Association with minerals or chemical recalcitrance? *Biogeochemistry, 77*(1), 25-56. doi: 10.1007/s10533-005-0712-6

Minasny, B., McBratney, A.B. et Salvador-Blanes, S. (2008). Quantitative models for pedogenesis — A review. *Geoderma, 144*(1-2), 140-157. doi: 10.1016/j.geoderma.2007.12.013

Ministère des Ressources Naturelles du Québec. (2013). *Rapport du Comité scientifique chargé d'examiner la limite nordique des forêts attribuables.*

Miyanishi, K. et Johnson, E.A. (2002). Process and patterns of duff consumption in the mixedwood boreal forest. *Canadian Journal of Forest Research, 32*(7), 1285-1295. doi: 10.1139/x02-051

Muggeo, V.M.R. (2008). Segmented: an R package to fit regression models with broken-line relationships. *R News, 8*(1), 20-25. Récupéré de http://cran.r-project.org/doc/Rnews/

Muscolo, A., Bagnato, S., Sidari, M. et Mercurio, R. (2014). A review of the roles of forest canopy gaps. *Journal of Forestry Research, 25*(4), 725-736. doi: 10.1007/s11676-014-0521-7

Nalder, I.A. et Wein, R.W. (1999). Long-term forest floor carbon dynamics after fire in upland boreal forests of western Canada. *Global Biogeochemical Cycles, 13*(4), 951-968. doi: 10.1029/1999gb900056

Nations Unies. (1998). Protocole de Kyoto la convention-cadre des Nations Unies sur les changements climatiques. *Kyoto, Japon.*

Nave, L.E., Vance, E.D., Swanston, C.W. et Curtis, P.S. (2011). Fire effects on temperate forest soil C and N storage. *Ecological applications, 21*(4), 1189-1201.

NFI. (2016) *Canada's national forest inventory*. de nfi.nfis.org

Oris, F., Asselin, H., Ali, A.A., Finsinger, W. et Bergeron, Y. (2014). Effect of increased fire activity on global warming in the boreal forest. *Environmental Reviews, 22*(3), 206-219. doi: 10.1139/er-2013-0062

Pacé, M., Fenton, N.J., Paré, D. et Bergeron, Y. (2017). Ground-layer composition affects tree fine root biomass and soil nutrient availability in jack pine and black spruce forests under extreme drainage conditions. *Canadian Journal of Forest Research, 47*(4), 433-444. doi: 10.1139/cjfr-2016-0352

Pan, Y., Birdsey, R.A., Fang, J., Houghton, R., Kauppi, P.E., Kurz, W.A., Phillips, O.L., Shvidenko, A., Lewis, S.L., Canadell, J.G., Ciais, P., Jackson, R.B., Pacala, S.W., McGuire, A.D., Piao, S., Rautiainen, A., Sitch, S. et Hayes, D. (2011). A large and persistent carbon sink in the world's forests. *Science, 333*(6045), 988-993. doi: 10.1126/science.1201609 Récupéré de http://www.ncbi.nlm.nih.gov/pubmed/21764754

Paré, D., Banville, J.L., Garneau, M. et Bergeron, Y. (2011). Soil Carbon Stocks and Soil Carbon Quality in the Upland Portion of a Boreal Landscape, James Bay, Quebec. *Ecosystems, 14*(4), 533-546. doi: 10.1007/s10021-011-9429-7

Paré, D., Bernier, P., Lafleur, B., Titus, B.D., Thiffault, E., Maynard, D.G. et Guo, X. (2013). Estimating stand-scale biomass, nutrient contents, and associated uncertainties for tree species of Canadian forests. *Canadian Journal of Forest Research, 43*(7), 599-608. doi: 10.1139/cjfr-2012-0454

Paré, D., Boutin, R., Larocque, G.R. et Raulier, F. (2006). Effect of temperature on soil organic matter decomposition in three forest biomes of eastern Canada. *Canadian Journal of Soil Science, 86*(Special Issue), 247-256. doi: 10.4141/s05-084

Paul, E.A. (2016). The nature and dynamics of soil organic matter: Plant inputs, microbial transformations, and organic matter stabilization. *Soil Biology and Biochemistry, 98*, 109-126. doi: 10.1016/j.soilbio.2016.04.001

Paul, E.A., Follett, R.F., Leavitt, S.W., Halvorson, A., Peterson, G.A. et Lyon, D.J. (1997). Radiocarbon Dating for Determination of Soil Organic Matter Pool Sizes and Dynamics. *Soil Science Society of America Journal, 61*(4), 1058. doi: 10.2136/sssaj1997.03615995006100040011x

Paul, E.A., Morris, S.J., Conant, R.T. et Plante, A.F. (2006). Does the Acid Hydrolysis–Incubation Method Measure Meaningful Soil Organic Carbon Pools? *Soil Science Society of America Journal, 70*(3), 1023. doi: 10.2136/sssaj2005.0103

Payette, S., Delwaide, A., Schaffhauser, A. et Magnan, G. (2012). Calculating long-term fire frequency at the stand scale from charcoal data. *Ecosphere, 3*(7), art59. doi: 10.1890/es12-00026.1

Payette, S., Pilon, V., Couillard, P.-L. et Frégeau, M. (2016). Long-term fire history of maple (Acer) forest sites in the central St. Lawrence Lowland, Quebec. *Canadian Journal of Forest Research, 46*(6), 822-831. doi: 10.1139/cjfr-2015-0305

Pellegrini, A.F.A., Ahlstrom, A., Hobbie, S.E., Reich, P.B., Nieradzik, L.P., Staver, A.C., Scharenbroch, B.C., Jumpponen, A., Anderegg, W.R.L., Randerson, J.T.

et Jackson, R.B. (2018). Fire frequency drives decadal changes in soil carbon and nitrogen and ecosystem productivity. *Nature, 553*(7687), 194-198. doi: 10.1038/nature24668 Récupéré de https://www.ncbi.nlm.nih.gov/pubmed/29227988

Périé, C. et Ouimet, R. (2008). Organic carbon, organic matter and bulk density relationships in boreal forest soils. *Canadian Journal of Soil Science, 88*(3), 315-325. doi: 10.4141/cjss06008

Peters, G. (2018). *userfriendlyscience: Quantitative analysis made accessible* (Version R package version 0.7.1). Récupéré de https://userfriendlyscience.com

Peura, M., Burgas, D., Eyvindson, K., Repo, A. et Mönkkönen, M. (2018). Continuous cover forestry is a cost-efficient tool to increase multifunctionality of boreal production forests in Fennoscandia. *Biological Conservation, 217*, 104-112. doi: 10.1016/j.biocon.2017.10.018

Plante, A.F., Conant, R.T., Paul, E.A., Paustian, K. et Six, J. (2006). Acid hydrolysis of easily dispersed and microaggregate-derived silt- and clay-sized fractions to isolate resistant soil organic matter. *European Journal of Soil Science, 57*(4), 456-467. doi: 10.1111/j.1365-2389.2006.00792.x

Pollegioni, L., Tonin, F. et Rosini, E. (2015). Lignin-degrading enzymes. *FEBS J, 282*(7), 1190-1213. doi: 10.1111/febs.13224 Récupéré de https://www.ncbi.nlm.nih.gov/pubmed/25649492

Porras, R.C., Hicks Pries, C.E., McFarlane, K.J., Hanson, P.J. et Torn, M.S. (2017). Association with pedogenic iron and aluminum: effects on soil organic carbon storage and stability in four temperate forest soils. *Biogeochemistry, 133*(3), 333-345. doi: 10.1007/s10533-017-0337-6

Portier, J., Gauthier, S., Leduc, A., Arseneault, D. et Bergeron, Y. (2016). Fire regime along latitudinal gradients of continuous to discontinuous coniferous boreal forests in eastern Canada. *Forests, 7*(10), 211. doi: 10.3390/f7100211

Pregitzer, K.S. et Euskirchen, E.S. (2004). Carbon cycling and storage in world forests: biome patterns related to forest age. *Global Change Biology, 10*(12), 2052-2077. doi: 10.1111/j.1365-2486.2004.00866.x

Prescott, C.E. (1997). Effects of clearcutting and alternative silvicultural systems on rates of decomposition and nitrogen mineralization in a coastal montane coniferous forest. *Forest Ecology and Management, 95*(3), 253-260.

Prescott, C.E. (2010). Litter decomposition: what controls it and how can we alter it to sequester more carbon in forest soils? *Biogeochemistry, 101*(1-3), 133-149. doi: 10.1007/s10533-010-9439-0

Prescott, C.E., Maynard, D.G. et Laiho, R. (2000). Humus in northern forests: friend or foe? *Forest Ecology and Management, 133*(1-2), 23-36. doi: 10.1016/s0378-1127(99)00295-9

Preston, C.M., Bhatti, J.S., Flanagan, L.B. et Norris, C. (2006). Stocks, chemistry, and sensitivity to climate change of dead organic matter along the Canadian boreal forest transect case study. *Climatic Change, 74*(1-3), 223-251. doi: 10.1007/s10584-006-0466-8

Preston, C.M., Simard, M., Bergeron, Y., Bernard, G.M. et Wasylishen, R.E. (2017). Charcoal in Organic Horizon and Surface Mineral Soil in a Boreal Forest Fire Chronosequence of Western Quebec: Stocks, Depth Distribution, Chemical Properties and a Synthesis of Related Studies. *Frontiers in Earth Science, 5*. doi: 10.3389/feart.2017.00098

Prévost, M. et Raymond, P. (2012). Effect of gap size, aspect and slope on available light and soil temperature after patch-selection cutting in yellow birch–conifer stands, Quebec, Canada. *Forest Ecology and Management, 274*, 210-221. doi: 10.1016/j.foreco.2012.02.020

Pribyl, D.W. (2010). A critical review of the conventional SOC to SOM conversion factor. *Geoderma, 156*(3-4), 75-83. doi: 10.1016/j.geoderma.2010.02.003

Protz, R., Shipitalo, M.J., Ross, G.J. et Terasmae, J. (1988). Podzolic soil development in the Southern James Bay Lowlands, Ontario. *Canadian Journal of Soil Science, 68*(2), 287-305. doi: 10.4141/cjss88-028

R Core Team. (2017). *R: A language and environment for statistical computing*. Vienna, Austria : R Foundation for Statistical Computing. Récupéré de https://www.R-project.org/

Rasmussen, C., Heckman, K., Wieder, W.R., Keiluweit, M., Lawrence, C.R., Berhe, A.A., Blankinship, J.C., Crow, S.E., Druhan, J.L., Hicks Pries, C.E., Marin-Spiotta, E., Plante, A.F., Schädel, C., Schimel, J.P., Sierra, C.A., Thompson, A. et Wagai, R. (2018). Beyond clay: towards an improved set of variables for predicting soil organic matter content. *Biogeochemistry, 137*(3), 297-306. doi: 10.1007/s10533-018-0424-3

Rasse, D.P., Rumpel, C. et Dignac, M.-F. (2005). Is soil carbon mostly root carbon? Mechanisms for a specific stabilisation. *Plant and Soil, 269*(1-2), 341-356. doi: 10.1007/s11104-004-0907-y

Raymond, P., Bédard, S., Roy, V., Larouche, C. et Tremblay, S. (2009). The irregular shelterwood system: review, classification, and potential application to forests affected by partial disturbances. *Journal of Forestry, 107*(8), 405-413.

Régnière, J. (1996). Generalized Approach to Landscape-Wide Seasonal Forecasting with Temperature-Driven Simulation Models. *Environmental Entomology, 25*(5), 869-881. doi: 10.1093/ee/25.5.869

Régnière, J., Saint-Amant, R. et Béchard, A. (2013). *BioSIM 10 user's manual.* (Vol. Information Report LAU-X-137). Québec, QC : Natural Ressources Canada.

Reimer, P.J., Bard, E., Bayliss, A., Beck, J.W., Blackwell, P.G., Ramsey, C.B., Buck, C.E., Cheng, H., Edwards, R.L., Friedrich, M., Grootes, P.M., Guilderson, T.P., Haflidason, H., Hajdas, I., Hatté, C., Heaton, T.J., Hoffmann, D.L., Hogg, A.G., Hughen, K.A., Kaiser, K.F., Kromer, B., Manning, S.W., Niu, M., Reimer, R.W., Richards, D.A., Scott, E.M., Southon, J.R., Staff, R.A., Turney, C.S.M. et van der Plicht, J. (2016). IntCal13 and Marine13 Radiocarbon Age Calibration Curves 0–50,000 Years cal BP. *Radiocarbon, 55*(04), 1869-1887. doi: 10.2458/azu_js_rc.55.16947

Remy, C.C., Fouquemberg, C., Asselin, H., Andrieux, B., Magnan, G., Brossier, B., Grondin, P., Bergeron, Y., Talon, B., Girardin, M.P., Blarquez, O., Bajolle, L. et Ali, A.A. (2018). Guidelines for the use and interpretation of palaeofire

reconstructions based on various archives and proxies. *Quaternary Science Reviews, 193*, 312-322. doi: 10.1016/j.quascirev.2018.06.010

Robitaille, A. et Saucier, J. (1998). *Paysages régionaux du Québec méridional*. Québec, QC : Les Publications du Québec.

Rogers, B.M., Soja, A.J., Goulden, M.L. et Randerson, J.T. (2015). Influence of tree species on continental differences in boreal fires and climate feedbacks. *Nature Geoscience, 8*(3), 228-234. doi: 10.1038/Ngeo2352

Rowe, J.S. et Scotter, G.W. (1973). Fire in the boreal forest. *Quaternary Research, 3*, 444-464.

Ruddiman, W.F. (2007). The early anthropogenic hypothesis: Challenges and responses. *Reviews of Geophysics, 45*(4). doi: 10.1029/2006rg000207

Ruddiman, W.F., Crucifix, M.C., Oldfield, F.A., Kutzbach, J.E. et Vavrus, S.J. (2011). Can natural or anthropogenic explanations of late-Holocene CO2 and CH4 increases be falsified? *The Holocene, 21*(5), 865-8879. doi: 10.1177/0959683610387172

Rumpel, C. et Kögel-Knabner, I. (2011). Deep soil organic matter—a key but poorly understood component of terrestrial C cycle. *Plant and Soil, 338*(1-2), 143-158. doi: 10.1007/s11104-010-0391-5

Ryan, M.G., Harmon, M.E., Birdsey, R.A., Giardina, C.P., Heath, L.S., Houghton, R.A., Jackson, R.B., McKinley, D.C., Morrison, J.F. et Murray, B.C. (2010). A synthesis of the science on forests and carbon for US forests. *Ecological Society of America: Issues In Ecology. 13: 1-16.*, 1-16.

Salomé, C., Nunan, N., Pouteau, V., Lerch, T.Z. et Chenu, C. (2010). Carbon dynamics in topsoil and in subsoil may be controlled by different regulatory mechanisms. *Global Change Biology, 16*(1), 416-426. doi: 10.1111/j.1365-2486.2009.01884.x

Sanborn, P., Lamontagne, L. et Hendershot, W. (2011). Podzolic soils of Canada: Genesis, distribution, and classification. *Canadian Journal of Soil Science, 91*(5), 843-880. doi: 10.4141/Cjss10024

Sanderman, J., Hengl, T. et Fiske, G.J. (2017). Soil carbon debt of 12,000 years of human land use. *Proc Natl Acad Sci U S A, 114*(36), 9575-9580. doi: 10.1073/pnas.1706103114 Récupéré de https://www.ncbi.nlm.nih.gov/pubmed/28827323

Santin, C., Doerr, S.H., Kane, E.S., Masiello, C.A., Ohlson, M., de la Rosa, J.M., Preston, C.M. et Dittmar, T. (2016). Towards a global assessment of pyrogenic carbon from vegetation fires. *Glob Chang Biol, 22*(1), 76-91. doi: 10.1111/gcb.12985 Récupéré de http://www.ncbi.nlm.nih.gov/pubmed/26010729

Santín, C., Doerr, S.H., Preston, C. et Bryant, R. (2013). Consumption of residual pyrogenic carbon by wildfire. *International Journal of Wildland Fire, 22*(8), 1072. doi: 10.1071/wf12190

Saucier, J.-P., Bergeron, J.-F., Grondin, P. et Robitaille, A. (1998). Les régions écologiques du Québec méridional (3e version) : un des éléments du système hierarchique de classification du territoire mis au point par le ministère des Ressources naturelles du Québec. *L'Aubelle, 124*, 1-12.

Schaetzl, R. et Anderson, S. (2005). *Soils: genesis and geomorphology* (2éd.). New York : Cambridge University Press.

Scharlemann, J.P.W., Tanner, E.V.J., Hiederer, R. et Kapos, V. (2014). Global soil carbon: understanding and managing the largest terrestrial carbon pool. *Carbon Management, 5*(1), 81-91. doi: 10.4155/cmt.13.77

Schimel, D.S., House, J.I., Hibbard, K.A., Bousquet, P., Ciais, P., Peylin, P., Braswell, B.H., Apps, M.J., Baker, D., Bondeau, A., Canadell, J., Churkina, G., Cramer, W., Denning, A.S., Field, C.B., Friedlingstein, P., Goodale, C., Heimann, M., Houghton, R.A., Melillo, J.M., Moore, B., Murdiyarso, D., Noble, I., Pacala, S.W., Prentice, I.C., Raupach, M.R., Rayner, P.J., Scholes, R.J., Steffen, W.L. et Wirth, C. (2001). Recent patterns and mechanisms of carbon exchange by

terrestrial ecosystems. *Nature, 414*(6860), 169-172. doi: 10.1038/35102500 Récupéré de http://www.ncbi.nlm.nih.gov/pubmed/11700548

Schliemann, S.A. et Bockheim, J.G. (2014). Influence of gap size on carbon and nitrogen biogeochemical cycling in Northern hardwood forests of the Upper Peninsula, Michigan. *Plant and Soil, 377*(1-2), 323-335. doi: 10.1007/s11104-013-2005-5

Schmidt, M.W., Torn, M.S., Abiven, S., Dittmar, T., Guggenberger, G., Janssens, I.A., Kleber, M., Kogel-Knabner, I., Lehmann, J., Manning, D.A., Nannipieri, P., Rasse, D.P., Weiner, S. et Trumbore, S.E. (2011). Persistence of soil organic matter as an ecosystem property. *Nature, 478*(7367), 49-56. doi: 10.1038/nature10386 Récupéré de http://www.ncbi.nlm.nih.gov/pubmed/21979045

Seedre, M., Shrestha, B.M., Chen, H.Y.H., Colombo, S. et Jõgiste, K. (2011). Carbon dynamics of North American boreal forest after stand replacing wildfire and clearcut logging. *Journal of Forest Research, 16*(3), 168-183. doi: 10.1007/s10310-011-0264-7

Shaw, C.H., Bona, K.A., Kurz, W.A. et Fyles, J.W. (2015). The importance of tree species and soil taxonomy to modeling forest soil carbon stocks in Canada. *Geoderma Regional, 4*, 114-125. doi: 10.1016/j.geodrs.2015.01.001

Shaw, C.H., Hilger, A.B., Metsaranta, J., Kurz, W.A., Russo, G., Eichel, F., Stinson, G., Smyth, C. et Filiatrault, M. (2014). Evaluation of simulated estimates of forest ecosystem carbon stocks using ground plot data from Canada's National Forest Inventory. *Ecological Modelling, 272*, 323-347. doi: 10.1016/j.ecolmodel.2013.10.005

Shipley, B. (2000a). *Cause and correlation in biology: a user's guide to path analysis, structural equations and causal inference*. Cambridge, UK : Cambridge University Press.

Shipley, B. (2000b). A new inferential test for path models based on directed acyclic graphs. *Structural Equation Modeling, 7*(2), 206-218. doi: 10.1207/s15328007sem0702_4

Shipley, B. (2009). Confirmatory path analysis in a generalized multilevel context. *Ecology, 90*(2), 363-368. doi: 10.1890/08-1034.1

Shipley, B. (2013). The AIC model selection method applied to path analytic models compared using a d-separation test. *Ecology, 94*(3), 560-564. doi: 10.1890/12-0976.1

Siira-Pietikäinen, A., Pietikäinen, J., Fritze, H. et Haimi, J. (2001). Short-term responses of soil decomposer communities to forest management: clear felling versus alternative forest harvesting methods. *Canadian Journal of Forest Research, 31*(1), 88-99. doi: 10.1139/x00-148

Silveira, M.L., Comerford, N.B., Reddy, K.R., Cooper, W.T. et El-Rifai, H. (2008). Characterization of soil organic carbon pools by acid hydrolysis. *Geoderma, 144*(1-2), 405-414. doi: 10.1016/j.geoderma.2008.01.002

Simard, M., Lecomte, N., Bergeron, Y., Bernier, P.Y. et Paré, D. (2007). Forest productivity decline caused by successional paludification of boreal soils. *Ecological Applications, 17*(6), 1619-1637. doi: 10.1890/06-1795.1

Six, J., Conant, R.T., Paul, E.A. et Paustian, K. (2002). Stabilization mechanisms of soil organic matter: Implications for C-saturation of soils. *Plant and Soil, 241*(2), 155-176. doi: 10.1023/a:1016125726789

Skjemstad, J.O. et Baldock, J.A. (2007). Total and Organic Carbon. Dans Carter M. R. et Gregorich, E. G. (dir.), *Soil Sampling and Methods of Analysis, Second Edition.* Boca Raton, FL : CRC Press.

Smith, C.K., Coyea, M.R. et Munson, A.D. (2000). Soil carbon, nitrogen, and phosphorus stocks and dynamics under disturbed black spruce forests. *Ecological Applications, 10*(3), 775-788.

Soil Classification Working Group. (1998). *The Canadian System of Soil Classification, 3rd edition.* (NRC Research Press éd.). Ottawa (ON).

Soucémarianadin, L.N., Quideau, S.A. et MacKenzie, M.D. (2014). Pyrogenic carbon stocks and storage mechanisms in podzolic soils of fire-affected Quebec black

spruce forests. *Geoderma, 217-218*, 118-128. doi: 10.1016/j.geoderma.2013.11.010

Steffen, W., Rockstrom, J., Richardson, K., Lenton, T.M., Folke, C., Liverman, D., Summerhayes, C.P., Barnosky, A.D., Cornell, S.E., Crucifix, M., Donges, J.F., Fetzer, I., Lade, S.J., Scheffer, M., Winkelmann, R. et Schellnhuber, H.J. (2018). Trajectories of the Earth System in the Anthropocene. *Proc Natl Acad Sci U S A*. doi: 10.1073/pnas.1810141115 Récupéré de https://www.ncbi.nlm.nih.gov/pubmed/30082409

Stendahl, J., Berg, B. et Lindahl, B.D. (2017). Manganese availability is negatively associated with carbon storage in northern coniferous forest humus layers. *Sci Rep, 7*(1), 15487. doi: 10.1038/s41598-017-15801-y Récupéré de https://www.ncbi.nlm.nih.gov/pubmed/29138466

Stockmann, U., Padarian, J., McBratney, A., Minasny, B., de Brogniez, D., Montanarella, L., Hong, S.Y., Rawlins, B.G. et Field, D.J. (2015). Global soil organic carbon assessment. *Global Food Security, 6*, 9-16. doi: 10.1016/j.gfs.2015.07.001

Stocks, B.J., Mason, J.A., Todd, J.B., Bosch, E.M., Wotton, B.M., Amiro, B.D., Flannigan, M.D., Hirsch, K.G., Logan, K.A., Martell, D.L. et Skinner, W.R. (2002). Large forest fires in Canada, 1959–1997. *Journal of Geophysical Research, 108*(D1). doi: 10.1029/2001jd000484

Strand, L.T., Callesen, I., Dalsgaard, L. et de Wit, H.A. (2016). Carbon and nitrogen stocks in Norwegian forest soils — the importance of soil formation, climate, and vegetation type for organic matter accumulation. *Canadian Journal of Forest Research, 46*(12), 1459-1473. doi: 10.1139/cjfr-2015-0467

Sturtevant, B.R., Bissonette, J.A., Long, J.N. et Roberts, D.W. (1997). Coarse woody debris as a function of age, stand structure, and disturbance in boreal Newfoundland. *Ecological Applications, 7*(2), 702-712. doi: 10.1890/1051-0761(1997)007[0702:cwdaaf]2.0.co;2

Symonds, M.R.E. et Moussalli, A. (2010). A brief guide to model selection, multimodel inference and model averaging in behavioural ecology using

Akaike's information criterion. *Behavioral Ecology and Sociobiology, 65*(1), 13-21. doi: 10.1007/s00265-010-1037-6

Taylor, A.R., Seedre, M., Brassard, B.W. et Chen, H.Y.H. (2014). Decline in Net Ecosystem Productivity Following Canopy Transition to Late-Succession Forests. *Ecosystems, 17*(5), 778-791. doi: 10.1007/s10021-014-9759-3

Thornley, J.H.M. et Canell, M.G.R. (2001). Soil carbon storage response to temperature: an hypothseis. *Annals of Botany, 87*(5), 591-598. doi: 10.1006/anbo.2001.1372

Torn, M.S., Trumbore, S.E., Chadwick, O.A., Vitousek, P.M. et Hendricks, D.M. (1997). Mineral control of soil organic carbon storage and turnover. *Nature, 389*(6647), 170-173. doi: 10.1038/38260

Tremblay, S., Ouimet, R. et Houle, D. (2002). Prediction of organic carbon content in upland forest soils of Quebec, Canada. *Canadian Journal of Forest Research, 32*(5), 903-914. doi: 10.1139/x02-023

Triviño, M., Pohjanmies, T., Mazziotta, A., Juutinen, A., Podkopaev, D., Le Tortorec, E., Mönkkönen, M. et Mori, A. (2017). Optimizing management to enhance multifunctionality in a boreal forest landscape. *Journal of Applied Ecology, 54*(1), 61-70. doi: 10.1111/1365-2664.12790

Trumbore, S.E. et Harden, J.W. (1997). Accumulation and turnover of carbon in organic and mineral soils of the BOREAS northern study area. *Journal of Geophysical Research: Atmospheres, 102*(D24), 28817-28830. doi: 10.1029/97jd02231

van Bellen, S., Garneau, M. et Bergeron, Y. (2010). Impact of Climate Change on Forest Fire Severity and Consequences for Carbon Stocks in Boreal Forest Stands of Quebec, Canada: A Synthesis. *Fire Ecology, 6*(3), 16-44. doi: 10.4996/fireecology.0603016

van Gestel, N., Shi, Z., van Groenigen, K.J., Osenberg, C.W., Andresen, L.C., Dukes, J.S., Hovenden, M.J., Luo, Y., Michelsen, A., Pendall, E., Reich, P.B., Schuur, E.A.G. et Hungate, B.A. (2018). Predicting soil carbon loss with warming.

Nature, 554(7693), E4-E5. doi: 10.1038/nature25745 Récupéré de http://www.ncbi.nlm.nih.gov/pubmed/29469098

Van Wagner, C.E. (1968). The line intersect method in forest fuel sampling. *Forest Science, 14*(1), 20-26.

Van Wagner, C.E. (1978). Age-class distribution and the forest fire cycle. *Canadian Journal of Forest Research, 8*, 220-227.

Vesala, T., Suni, T., Rannik, Ü., Keronen, P., Markkanen, T., Sevanto, S., Grönholm, T., Smolander, S., Kulmala, M., Ilvesniemi, H., Ojansuu, R., Uotila, A., Levula, J., Mäkelä, A., Pumpanen, J., Kolari, P., Kulmala, L., Altimir, N., Berninger, F., Nikinmaa, E. et Hari, P. (2005). Effect of thinning on surface fluxes in a boreal forest. *Global Biogeochemical Cycles, 19*(2). doi: 10.1029/2004GB002316

Vesterdal, L., Clarke, N., Sigurdsson, B.D. et Gundersen, P. (2013). Do tree species influence soil carbon stocks in temperate and boreal forests? *Forest Ecology and Management, 309*, 4-18. doi: 10.1016/j.foreco.2013.01.017

von Lützow, M. et Kögel-Knabner, I. (2009). Temperature sensitivity of soil organic matter decomposition—what do we know? *Biology and Fertility of Soils, 46*(1), 1-15. doi: 10.1007/s00374-009-0413-8

von Lützow, M., Kögel-Knabner, I., Ekschmitt, K., Flessa, H., Guggenberger, G., Matzner, E. et Marschner, B. (2007). SOM fractionation methods: Relevance to functional pools and to stabilization mechanisms. *Soil Biology and Biochemistry, 39*(9), 2183-2207. doi: 10.1016/j.soilbio.2007.03.007

Walker, L.R., Wardle, D.A., Bardgett, R.D. et Clarkson, B.D. (2010). The use of chronosequences in studies of ecological succession and soil development. *Journal of Ecology, 98*(4), 725-736. doi: 10.1111/j.1365-2745.2010.01664.x

Wang, C., Bond-Lamberty, B. et Gower, S.T. (2003). Carbon distribution of a well- and poorly-drained black spruce fire chronosequence. *Global Change Biology, 9*(7), 1066-1079. doi: 10.1046/j.1365-2486.2003.00645.x

Wang, X., Parisien, M.-A., Taylor, S.W., Candau, J.-N., Stralberg, D., Marshall, G.A., Little, J.M. et Flannigan, M.D. (2017). Projected changes in daily fire spread across Canada over the next century. *Environmental Research Letters, 12*(2), 025005. doi: 10.1088/1748-9326/aa5835

Ward, C., Pothier, D. et Paré, D. (2014). Do boreal forests need fire disturbance to maintain productivity? *Ecosystems, 17*(6), 1053-1067. doi: 10.1007/s10021-014-9782-4

Wardle, D.A., Bardgett, R.D., Klironomos, J.N., Setala, H., van der Putten, W.H. et Wall, D.H. (2004). Ecological linkages between aboveground and belowground biota. [Review]. *Science, 304*(5677), 1629-1633. doi: 10.1126/science.1094875 Récupéré de https://www.ncbi.nlm.nih.gov/pubmed/15192218

Wardle, D.A., Walker, L.R. et Bardgett, R.D. (2004). Ecosystem properties and forest decline in contrasting long-term chronosequences. *Science, 305*(5683), 509-513. doi: 10.1126/science.1098778 Récupéré de https://www.ncbi.nlm.nih.gov/pubmed/15205475

Weber, M.G. et Stocks, B.J. (1998). Forest fires and sustainability in the boreal forests of Canada. *Ambio, 27*(7), 545-550.

Weetman, G. (1980). The importance of raw humus accumulation in boreal forest management. *Forest regeneration at high latitudes. USDA, Pac. Northwest For. and Range Expt. Stn., Gen. Tech. Rep. PNW-107*, 7-10.

Wood, M. (1995). A mechanism of aluminium toxicity to soil bacteria and possible ecological implications. *Plant and Soil, 171*(1), 63-69. doi: 10.1007/bf00009566

Wotton, B.M., Flannigan, M.D. et Marshall, G.A. (2017). Potential climate change impacts on fire intensity and key wildfire suppression thresholds in Canada. *Environmental Research Letters, 12*(9), 095003. doi: 10.1088/1748-9326/aa7e6e

Xu, J.M., Cheng, H.H., Koskinen, W.C. et Molina, J.A.E. (1997). Characterization of potentially bioreactive soil organic carbon and nitrogen by acid hydrolysis.

Nutrient Cycling in Agroecosystems, 49(1/3), 267-271. doi: 10.1023/a:1009763023828

Yu, Z.C. (2012). Northern peatland carbon stocks and dynamics: a review. *Biogeosciences, 9*(10), 4071-4085. doi: 10.5194/bg-9-4071-2012

Zalasiewicz, J., Williams, M., Haywood, A. et Ellis, M. (2011). The Anthropocene: a new epoch of geological time? *Philos Trans A Math Phys Eng Sci, 369*(1938), 835-841. doi: 10.1098/rsta.2010.0339 Récupéré de https://www.ncbi.nlm.nih.gov/pubmed/21282149

Zhang, D., Hui, D., Luo, Y. et Zhou, G. (2008). Rates of litter decomposition in terrestrial ecosystems: global patterns and controlling factors. *Journal of Plant Ecology, 1*(2), 85-93. doi: 10.1093/jpe/rtn002

Zhou, G., Liu, S., Li, Z., Zhang, D., Tang, X., Zhou, C., Yan, J. et Mo, J. (2006). Old-growth forests can accumulate carbon in soils. *Science, 314*(5804), 1417. doi: 10.1126/science.1130168 Récupéré de http://www.ncbi.nlm.nih.gov/pubmed/17138894

Ziadi, N. et Sen Tran, T. (2007). Mehlich 3-Extractable Elements. Dans Carter M. R. et Gregorich, E. G. (dir.), *Soil Sampling and Methods of Analysis, Second Edition.* Boca Raton, FL : CRC Press.

Ziegler, S.E., Benner, R., Billings, S.A., Edwards, K.A., Philben, M., Zhu, X. et Laganière, J. (2017). Climate warming can accelerate carbon fluxes without changing soil carbon stocks. *Frontiers in Earth Science, 5*(2). doi: 10.3389/feart.2017.00002